CENTRO DE INVESTIGACIÓN Y DE ESTUDIOS AVANZADOS DEL INSTITUTO POLITÉCNICO NACIONAL

Unidad Zacatenco

# Analysis, Modeling and Control of an Oilwell Drilling System

## THESIS REPORT

**Submitted to Obtain the Degree of Doctor (Ph.D.) in Sciences: Automatic Control by**

**Martha Belem Saldivar Márquez**

Thesis Supervisors:

Dr. Sabine Mondié Cuzange

Dr. Jean Jacques Loiseau

México Distrito Federal, April, 2013

# *Agradecimientos*

Me siento honrada y afortunada de haber trabajado bajo la supervisión de la doctora **Sabine Mondié**, le reitero mi admiración por su profesionalismo y dedicación. Muchas gracias por el tiempo invertido en la dirección de este proyecto.

Agradezco enormemente al doctor **Jean Jacques Loiseau** por su completa disponibilidad y por la supervisión del trabajo de tesis, aprecio el acogimiento brindado durante mi estancia en la bella cuidad de Nantes en Francia. Gracias también por su honrosa asistencia a mi examen doctoral.

Muchas gracias a los doctores **Hugues Mounier** y **Vladimir Rasvan** por la lectura y revisión de esta memoria de tesis, sin duda alguna sus comentarios y sugerencias contribuyeron a mejorar la calidad del presente documento. Aprecio bastante que hayan atravesado el Atlántico para presenciar la defensa de tesis.

A los doctores **Alexander Poznyak** y **Moisés Bonilla** les reitero mi más sincero agradecimiento por el todo el apoyo brindado y por su participación como miembros del jurado del examen doctoral.

Reconozco y agradezco la valiosa participación de los doctores **Alexandre Seuret**, **Raúl Villafuerte** y **Emilia Fridman** en el desarrollo de algunos resultados presentados en esta tesis.

Muchas gracias a las instituciones a las que debo mi formación, el **Centro de Investigación y de Estudios Avanzados del Instituto Politécnico Nacional**, el **Institut de Recherche en Communication et Cybernétique de Nantes**.

Gracias al **Consejo Nacional de Ciencia y Tecnología** por la beca doctoral y los apoyos otorgados para hacer posible la asistencia a diversos congresos nacionales e internacionales.

Deseo también expresar todo mi agradecimiento a mi familia, por su apoyo incondicional a lo largo de este trayecto. Por último, dar las gracias a mis amigos y compañeros que, de un modo u otro, han respaldado este esfuerzo.

# Notation

## List of mathematical symbols

In this text, the following mathematical symbols are used.

| | |
|---|---|
| $\mathcal{R}$ | Real numbers. |
| $\mathcal{R}^n$ | $n$-dimensional Euclidean space. |
| $\mathcal{R}^{n\times m}$ | Set of $n \times m$ real matrices. |
| $\mathcal{R}^+$ | Positive real numbers. |
| $\mathcal{C}^1([-h, 0], \mathcal{R}^n)$ | Set of continuously differentiable functions on the interval $[-h, 0]$. |
| $x(t, \phi)$ or $x(t)$ | Solution of the system with initial conditions $\phi$. |
| $x_t(\phi)$ | System state. |
| $T$ | Matrix transposition. |
| $\lambda_{\min}(A)$, $(\lambda_{\max}(A))$ | Smallest (largest) eigenvalue of a symmetric matrix $A$. |
| $P > 0$, $(P < 0)$ | Symmetric positive (negative) definite matrix $P \in \mathcal{R}^{n\times n}$. |
| $Q^T$ | Transpose of the matrix $Q \in \mathcal{R}^{n\times m}$. |
| $\rightarrow$ | Mapping of the elements of the domain to the elements of the range. |
| $\Rightarrow$ | Implies. |
| $\forall$ | For all. |
| $\exists$ | Exists. |
| $\in$ | Belongs to. |
| $(\cdot)^{-1}$ | Inverse operator. |
| $\mathrm{tr}(\cdot)$ | Trace operator. |
| $\lvert\cdot\rvert$ | Euclidean norm for vectors. |
| $\lVert\cdot\rVert$ | Induced norm for matrices. |

The notation $|\cdot|_h$ for any function $\phi$ from $\mathcal{C}^1\left([-h; 0], \mathcal{R}^n\right)$ is $\sup_{s\in[-h;0]}\left(|\phi\left(s\right)|\right)$ and $\|\phi\|_h = \max\left(|\phi\left(s\right)|_h, |\dot{\phi}\left(s\right)|_h\right)$.

# Acronyms list

| | |
|---|---|
| **ADAMS** | Advanced Drillstring Analysis and Measurement System. |
| **AIC** | Active Isolation Control. |
| **ANC** | Active Noise Control. |
| **ASC** | Active Structural Control. |
| **BHA** | Bottom Hole Assembly. |
| **BMI** | Bilinear Matrix Inequality. |
| **DOF** | Degree Of Freedom. |
| **LMI** | Linear Matrix Inequality. |
| **MWD** | Measure While Drilling. |
| **ODE** | Ordinary Differential Equation. |
| **PDC** | Polycrystalline Diamond Compact. |
| **PDE** | Partial Differential Equation. |
| **PID** | Proportional–Integral–Derivative. |
| **RMS** | Root Mean Square. |
| **ROP** | Rate of Penetration. |
| **STRS** | Soft Torque Rotary System. |
| **TOB** | Torque on the bit. |
| **TVA** | Tuned Vibration Absorbers. |
| **WOB** | Weight On Bit. |

# Contents

## Analysis, Modeling and Control of an Oilwell Drilling System

**Abstract:** In drilling operations, the drillstring interaction with the borehole gives rise to a wide variety of non-desired oscillations. The main types of drilling vibrations are torsional (stick-slip), axial (bit-bounce) and lateral (whirling). The analysis and modeling of rotary drilling vibrations is a topic whose economical interest has been renewed by recent oilfields discoveries leading to a growing literature. The first part of this work concerns the modeling problem of a vertical oilwell drilling system. The wave equation subject to mixed boundary conditions is used to reproduce torsional oscillations of the drill string. By means of a direct transformation we derive an input-output model described by a neutral-type time-delay equation which clearly simplifies the simulation of the torsional dynamics. Axial vibrations are modeled by an ordinary differential equation describing a damped harmonic oscillator. The proposed modeling strategies are validated via simulations by testing known experience-based techniques to reduce drilling vibrations. In the second part of the work, based on the different modeling approaches, we develop effective control strategies to suppress drilling oscillations. Lyapunov techniques allow us to analyze the system stability and lead the synthesis of stabilizing feedback controllers by means of the solution of linear and bilinear matrix inequalities. The performance of the proposed approaches is highlighted through simulations showing an effective suppression of the undesirable phenomena stick-slip and bit-bounce. The special significance of this research project lies in the fact that the proposed control techniques can be easily extended to be applied to more general systems.

# Résumé

## Introduction Générale

La présence d'intenses vibrations dans les tiges de forage a été considérée pendant de nombreuses années comme l'une des causes les plus importantes de la mauvaise performance du processus de forage. Pour le secteur pétrolier, l'amélioration des opérations de forage est une question cruciale d'intérêt économique.

Malgré le progrès technologique, les phénomènes vibratoires qui augmentent considérablement les coûts de forage continuent à se produire. Avant 1960, les analyses effectuées pour résoudre le problème ont porté sur le type et la résistance du matériau utilisé pour la construction du train de tiges, cependant, les tendances ont changé, les analyses récentes étudient le comportement dynamique de la tige de forage [54].

Les différents types de vibrations qui affectent le taux de pénétration et provoquent la détérioration prématurée des composants du système peuvent être classés en trois catégories en fonction de la direction dans laquelle les oscillations se produisent, ceux-ci sont :

- de torsion ou de rotation, également connus comme phénomène de coller-glisser (stick-slip),

- axial ou longitudinal, caractérisés par le rebond du trépan (bit-bounce),

- latérale ou transversale, mouvement rotatif irrégulier qui se produit lorsque la tige de forage opère hors de l'équilibre (whirling).

La présence de vibrations empêche l'exécution efficace du processus de forage, car elle provoque une détérioration prématurée des mécanismes [79], cause une utilisation excessive d'énergie [78] et peut induire une instabilité dans le puit en réduisant le contrôle directionnel [37].

Ci-dessous une brève description des causes et conséquences possibles des modes de vibration mentionnés.

**- Vibrations de Torsion.** L'application d'une vitesse constante à l'extrémité supérieure de la tige ne se traduit pas nécessairement par un mouvement

régulier de rotation du trépan, en fait, la vitesse angulaire à l'extrémité inférieure présente habituellement des fluctuations de grande amplitude pendant une fraction significative du temps de forage. Cette vitesse de rotation non uniforme est principalement due à la flexibilité de torsion de la tige [105]. Les vibrations de torsion provoquent une rotation irrégulière qui endommage les connexions des segments de tige de forage et le trépan. De plus, le processus de forage est prolongé car les vibrations réduisent le taux de pénétration. Les oscillations de torsion sont détectées par les fluctuations de la puissance nécessaire pour maintenir une vitesse de rotation constante.

**- Vibrations Axiales.** Les oscillations longitudinales impliquent un mouvement de la tige le long de l'axe, en raison de l'accouplement des éléments du mécanisme, la présence de ceux-ci peuvent provoquer indirectement le déplacement latéral de l'arbre [104]. Les vibrations axiales causent des collisions répétées entre l'outil de forage et la roche, ce qui conduit à la destruction du trépan. Le rebondissement du dispositif de forage est lié à l'utilisation d'un type spécifique de outil de forage appelé trépan "tricône" ou à rouleaux coniques qui est composé des lobes multiples, cela entraîne une interaction irrégulière avec le fond du puit en perdant le contact avec la formation rocheuse.

**- Vibrations Latérales.** Les oscillations transversales peuvent se produire sans être détectées à la surface. A l'extrémité inférieure, l'arbre entre en collision avec les parois du puit, ce qui provoque la création d'un orifice excentrique et endommage gravement les composants du système [83]. Les vibrations latérales perturbent gravement la structure du puit et modifient la direction du forage [54]. La rotation irrégulière est induite par centrifugation lorsque le centre de gravité du collier de forage n'est pas situé exactement dans la ligne centrale du puit provoquant un inclinaison de la tige [116]. Ce comportement est intensifié en raison de l'effet combiné du fluide d'amortissement, le retrait de dispositifs stabilisants, et le frottement de la chaîne contre les parois du puit [115].

Compte tenu de tous les problèmes liés au phénomène vibratoire, diverses méthodes ont été proposées au cours des années pour éliminer ou au moins réduire le problème. Les ingénieurs pétroliers et les experts ont développé des méthodes empiriques basées sur l'expérience. Les plus courantes sont la réduction du poids sur le trépan et l'augmentation de la vitesse angulaire à l'extrémité supérieure. Ces solutions sont utiles pour prévenir l'apparition de vibrations, toutefois, elles impliquent une diminution du taux de pénétration. Il existe des solutions plus sophistiquées pour réduire le phénomène de coller-glisser, nous énonçons ci-dessous quelques-unes.

### Commande par retour du couple

Avec la méthode de commande par retour du couple, les oscillations de torsion peuvent être évitées si la vitesse de la table tournante est modifiée en fonction des variations de torsion. La vitesse à la surface est ajustée de telle sorte que l'onde de torsion qui se propage le long de la tige est amortie, au lieu d'être réfléchie en retour vers le bas de la colonne de forage. L'inconvénient de cette méthode est qu'elle requiert une mesure précise du couple, qui, dans un processus réel est difficile à obtenir [51], [67].

### Système rotatif de couple souple (Soft Torque Rotary System STRS)

La compagnie hollandaise Shell, conscient du problème qu'implique une mesure précise du couple, a concentré ses recherches sur l'amélioration de commande de vibrations par retour du couple durant la décennie 1990 [54], [55]. La méthode développée consiste à calculer le couple sur l'extrémité inférieure en mesurant le courant du moteur, et à l'utiliser dans la boucle de retour. Les oscillations sont réduites par un réglage approprié de la commande, de sorte que le système se comporte comme un amortisseur règlé actif, similaire aux amortisseurs que l'on utilise pour éviter des oscillations induites par le vent dans les lignes de transmission d'énergie. Ce système a été appelé système rotatif de couple souple. Des essais expérimentaux ont montré une amélioration de la performance du processus de forage et une réduction considérable des défaillances du mécanisme. Le système rotatif de couple souple est disponible commercialement depuis plusieurs années et est utilisé dans différents endroits à travers le monde.

### Commande Proportionnel-Intégral-Dérivé (PID)

Une méthode simple pour traiter le problème de coller-glisser a été présentée par Pavone et Desplans en 1994 [89]. Ils ont trouvé que grâce à une analyse de stabilité on peut déterminer les paramètres d'un contrôleur Proportionnel-Intégral-Dérivé qui élimine les oscillations de torsion. Les données analysées ont été obtenues sur le système TRAFOR qui est un mécanisme de mesure développé par l'Institut Français du Pétrole. Un résultat important de cette recherche est la relation trouvée entre le couple et la vitesse à l'extrémité inférieure.

### Commande $\mathcal{H}_\infty$

En 1998 Serrarens, van de Molengraft et van den Steen ont proposé une méthode de commande $\mathcal{H}_\infty$ pour supprimer les oscillations de coller-glisser [107]. Le commande $\mathcal{H}_\infty$ a été largement utilisée pour traiter les problèmes de

vibrations, comme par exemple dans les processus de coupure où il s'emploie à éliminer les oscillations (chattering) dans les machines. Le contrôleur $\mathcal{H}_\infty$ supprime les vibrations malgré le fait qu'il est linéaire et invariant dans le temps et le frottement sur le trépan est fortement non linéaire. Cette méthode n'a pas été essayée dans le cadre des plates-formes réelles, cependant les résultats de prototypes expérimentaux montrent une bonne performance.

### D-OSKIL

Une méthode alternative pour éliminer les oscillations de torsion consiste à utiliser le poids sur l'outil de forage comme entrée de commande supplémentaire. La méthode appelée *Drilling OScillation KILler* (D-OSKIL) a été introduite par Canudas-de-Wit et al. en 2005 [26], [27]. Afin de garantir un taux de forage adéquat, il est nécessaire de maintenir un certain poids sur le trépan, cependant l'augmentation de cette variable conduit à des oscillations de torsion. L'objectif de la méthode proposée est de trouver une relation optimale entre le taux de forage et de poids sur le trépan. Quand les oscillations de torsion sont détectées, cette méthode permet une réduction du poids sur le dispositif de coupure à travers la manipulation de la force sur le crochet de levage du train de tiges, l'arbre est tiré vers le haut pour réduire le poids sur le trépan. Les résultats expérimentaux obtenus avec un prototype de laboratoire montrent une réduction substantielle des oscillations de torsion.

### Amortisseur de vibrations actif

En 2007, Zamanian, Khadem et Ghazavi ont étudié les vibrations de coller-glisser pour une tige de forage avec un trépan de traînage [122]. Cette recherche a montré que les vibrations de torsion peuvent être évitées en augmentant l'amortissement du fluide ou boue de forage et en sélectionnant convenablement le taux d'amortissement actif. Les mesures du mouvement relatif de l'outil de forage et le train de tiges sont prises en temps réel durant le processus, de façon que les propriétés d'amortissement sont constamment modifiées.

### Compensation des erreurs de modélisation

En 2008, Puebla et Álvarez-Ramírez ont introduit une approche de commande basé sur la compensation des erreurs de modélisation pour éliminer le phénomène de coller-glisser. Le schéma de commande de retour suggéré permet de faire face aux incertitudes du modèle de frottement et des paramètres du système. La tige de forage est modélisée comme un pendule de torsion, actionné par un moteur électrique, qui comprend des inerties amorties assemblées mécaniquement par un axe élastique. Dans [93] deux schémas de commande sont présentés : la commande en cascade, qui utilise comme

entrée unique de commande les propriétés électriques du moteur, et le schéma de commande décentralisée, qui règle les oscillations dans la table tournante à travers le moteur et les vibrations dans l'extrémité inférieure au moyen du poids sur le trépan. Les simulations numériques présentées montrent une suppression satisfaisante de vibrations, bien qu'il n'y ait pas actuellement de système disponible commercialement basé sur cette méthode de commande.

**Commande pour l'atténuation des vibrations avec stabilité garantie**

Nos contributions à la conception de lois de commande pour l'élimination d'oscillations dans un système de perforation vertical sont basés sur différentes approches de modélisation. Dans [46], nous présentons un modèle à paramètres distribués qui décrit la dynamique de torsion de la colonne de forage. L'equation des ondes à une dimension couplée à des conditions mixtes aux frontières décrit le comportement rotatif le long de l'arbre. Dans cet article, des bornes sur les solutions du système ont été présentés. Dans [99], sur la base de cette stratégie de modélisation, nous proposons une fonction d'énergie, qui en permettant une analyse de la dissipativité du système, conduit à la conception d'un contrôleur pour la suppression du phénomène de coller-glisser. Dans ce travail, nous dérivons un modèle simplifié représenté par une équation à retards de type neutre obtenu à travers de la transformation de D'Alembert qui simplifie l'analyse et facilite le calcul de simulations du système. Pour la validation du modèle proposé, nous avons examiné les stratégies pratiques pour éliminer les oscillations de torsion utilisées sur les plates-formes réelles. Le modèle du couple sur le dispositif de coupe qui représente l'interaction entre la formation rocheuse et le trépan est décrit par une fonction non linéaire qui dépend de la vitesse angulaire à l'extrémité inférieure et comprend la fonction signe. Dans [100], on présente une analyse de la stabilité exponentielle du système de forage en utilisant la théorie de systèmes à commutation. Dans [101], on conçoit une loi de commande non linéaire pour supprimer les oscillations de torsion à travers d'une représentation polytopique du modèle à retards. Dans [102], a partir d'un modèle couplé des oscillations axiales et de torsion, nous avons conçu, au moyen de la méthode de l'ellipsoïde attractif, deux contrôleurs linéaires pour éliminer simultanément le phénomène de coller-glisser et de rebond du trépan. Les entrées de commande correspondent à la vitesse angulaire fournie par le table tournante pour éliminer les vibrations de torsion et au taux de perforation pour supprimer les oscillations axiales. Puisque toutes les approches présentées sont basés sur la théorie de Lyapunov, la stabilité du système, dans tout cas, est garantie. Tout au long de ce document, on explique en détail les méthodologies proposées qui s'attaquent au problème de vibration.

## Motivation et objectifs

Alors que la technologie évolue, de nouveaux défis sont posés et la complexité dans le forage des puits de pétrole augmente. Les nouvelles technologies ont permis l'exploration pétrolière dans des eaux toujours plus profondes ce qui requiert des analyses de plus en plus sophistiquées pour assurer la suppression intégrale des oscillations indésirables. Les chercheurs ont généralement étudié chaque mode de vibration individuellement, puis, il ya surtout des solutions individuelles pour chacun des problèmes de vibrations. Par ailleurs, très peu de travaux ont fourni une analyse de stabilité propre des stratégies de commande proposées.

Dans cette thèse, nous développons une analyse exhaustive des oscillations de torsion et axiales couplées qui se produisent au cours du processus de forage, permettant de concevoir des contrôleurs stabilisants pour supprimer simultanément le phénomène de coller-glisser et le rebond du trépan. Nous visons à développer une analyse de stabilité du système de forage basée sur la théorie de Lyapunov.

Le premier objectif de cette thèse est de trouver une description mathématique précise du comportement mécanique du système de forage. Le modèle de forage doit reproduire de manière efficace le couplage mutuel entre les modes de vibration observés dans les plates-formes réels.

Le deuxième objectif de nos recherches concerne l'analyse de la stabilité et la conception de lois de commande pour supprimer ou au moins réduire à des niveaux acceptables, les oscillations de forage les plus critiques.

# Chapitre 2

Dans le processus de forage pour l'extraction du pétrole, le puit est créé par un dispositif de coupe appelé trépan ou fraise. La tige de forage est composée du mécanisme inférieur de perforation (BHA, par ses sigles en anglais Bottom Hole Assembly) et des segments tubulaires assemblés pour former le train de tiges. Le mécanisme inférieur de perforation comprend le trépan, deux ou plusieurs dispositifs stabilisants qui empêchent le déséquilibre de la colonne et une série des lourds tronçons tubulaires connus comme colliers de forage. Au fur et à mesure du forage, la longueur de la colonne doit être augmentée en ajoutant des tronçons. Un élément important du processus de forage est la boue ou fluide de perforation qui a la fonction de nettoyer, de refroidir et de lubrifier le trépan. La colonne de perforation est mise en rotation depuis la surface au moyen d'un moteur électrique actionnant une table tournante.

La complexité du système de forage pose des défis de modélisation et de commande. Le modèle doit décrire avec précision les phénomènes les plus

importants qui se produisent dans des plates-formes réelles et doit être suffisamment simple pour des fins d'analyse.

L'équation d'onde est largement utilisée pour reproduire le comportement oscillatoire des systèmes physiques. Dans les années soixante, quelques analyses ont été réalisées en utilisant cette équation pour décrire le comportement de torsion du train de tiges [6], [39]. Cette stratégie de modélisation a également été adoptée en [28], [111], [112] et [113].

Normalement, quand un modèle à paramètres distribués est soumis à des non-linéarités et à des incertitudes, l'analyse et les simulations ne sont pas des tâches faciles. Il est donc souhaitable d'obtenir un modèle plus simple impliquant uniquement les variables d'intérêt principal. Grâce à une transformation directe, il est possible de dériver un modèle d'entrée-sortie décrit par une équation à retards de type neutre qui simplifie clairement l'analyse et les simulations. La procédure qui permet de transformer une équation différentielle partielle en système à retards de type neutre a été présentée pour la première fois dans [3], voir aussi [5], [10], [19], [21], [22], [30], [40], [49] et [99].

Ce chapitre présente l'équation d'onde à une dimension décrivant le comportement en torsion de la tige. Le modèle à paramètres distribués est soumis à des conditions aux frontières mixtes sélectionnées en fonction du comportement observé aux deux extrémités de la tige. On présente aussi l'équation de type neutre qui rattache des variables aux limites supérieure et inférieure de la tige.

## Modèle à paramètres distribués

Le comportement de torsion d'une tige de perforation de longueur $L$, décrit par l'angle de rotation $\theta(\xi,t)$ peut être modélisé par l'équation d'onde [21], [22], [28], [46], [111], [112], [113] :

$$GJ\frac{\partial^2\theta}{\partial\xi^2}(\xi,t) - I\frac{\partial^2\theta}{\partial t^2}(\xi,t) - \beta\frac{\partial\theta}{\partial t}(\xi,t) = 0, \qquad \xi\in(0,L), \qquad t>0. \tag{1}$$

L'angle de torsion $\theta$ dépend de la coordonnée longitudinale $\xi$ et du temps $t$, $\beta\geq 0$ est l'amortissement visqueux et structurel considéré le long de la tige, les paramètres $I$, $G$ et $J$ correspondent à l'inertie, le module de rigidité et le moment d'inertie géométrique respectivement.

Les conditions aux frontières sont [99] :

$$GJ\frac{\partial\theta}{\partial\xi}(L,t) + I_B\frac{\partial^2\theta}{\partial t^2}(L,t) = -T\left(\frac{\partial\theta}{\partial t}(L,t)\right), \tag{2}$$

$$GJ\frac{\partial\theta}{\partial\xi}(0,t) = c_{\mathrm{a}}\left(\frac{\partial\theta}{\partial t}(0,t) - \Omega(t)\right), \tag{3}$$

ou $I_B$ représente l'inertie concentré à l'extrémité inférieure ($\xi = L$). Le couple $T$, qui décrit l'interaction du trépan avec la roche, est une fonction de la vitesse angulaire de l'outil de forage. À la frontière supérieure ($\xi = L$), on considère que la vitesse angulaire du moteur $\Omega$ ne correspond pas à la vitesse de rotation de l'extrémité supérieure de la tige $\frac{\partial\theta}{\partial t}(0,t)$, ce qui occasionne une torsion locale.

## Modèle à retards de type neutre

Comme la plupart de la dissipation d'énergie dans le processus de forage est effectuée dans l'interface trépan-roche, on peut considérer que l'amortissement le long de la structure est faible, soit $\beta = 0$, donc le modèle à paramètres distribués (1) est réduit à l'équation d'onde à une dimension :

$$\frac{\partial^2\theta}{\partial\xi^2}(\xi,t) = p^2\frac{\partial^2\theta}{\partial t^2}(\xi,t), \qquad \xi \in (0,L), \qquad p = \sqrt{\frac{I}{GJ}}. \tag{4}$$

Une conversion directe de l'équation d'onde (4) avec des conditions aux frontières (2-3) conduit au modèle à retards de type neutre suivant qui décrit le comportement de la colonne de forage [99] :

$$\begin{aligned} \dot{z}(t) - \Upsilon\dot{z}(t-2\Gamma) &= -\Psi z(t) - \Upsilon\Psi z(t-2\Gamma) \\ &\quad -\frac{1}{I_{\mathrm{B}}}T\left(z(t)\right) + \frac{1}{I_{\mathrm{B}}}\Upsilon T\left(z(t-2\Gamma)\right) + \Pi\Omega(t-\Gamma), \end{aligned} \tag{5}$$

où $z(t)$ est la vitesse angulaire à l'extrémité inférieure. Les constantes impliquées sont données par :

$$\Pi = \frac{2\Psi c_{\mathrm{a}}}{c_{\mathrm{a}} + \sqrt{IGJ}}, \ \Upsilon = \frac{c_{\mathrm{a}} - \sqrt{IGJ}}{c_{\mathrm{a}} + \sqrt{IGJ}}, \ \Psi = \frac{\sqrt{IGJ}}{I_{\mathrm{B}}}, \ \Gamma = \sqrt{\frac{I}{GJ}}L. \tag{6}$$

De la même manière on peut obtenir une expression à retards qui décrit le comportement à la partie supérieure :

$$\dot{v}(t)+\Upsilon\dot{v}(t-2\Gamma) = (c_a/\Lambda)\left[\Omega(t)+\Omega(t-2\Gamma)\right]-(2/\Lambda)\left[I_B\dot{z}(t-\Gamma)+T\left(z(t-\Gamma)\right)\right] \tag{7}$$

où $\dot{v}(t)$ est la vitesse angulaire à l'extrémité supérieure et $\Lambda = c_a+\sqrt{IGJ}$.

La transformation du modèle est réalisée au moyen de la méthode de D'Alembert qui propose une solution générale de l'équation d'onde. Alternativement, elle peut être effectuée en utilisant des techniques du domaine fréquentiel (transformée de Laplace).

# Chapitre 3

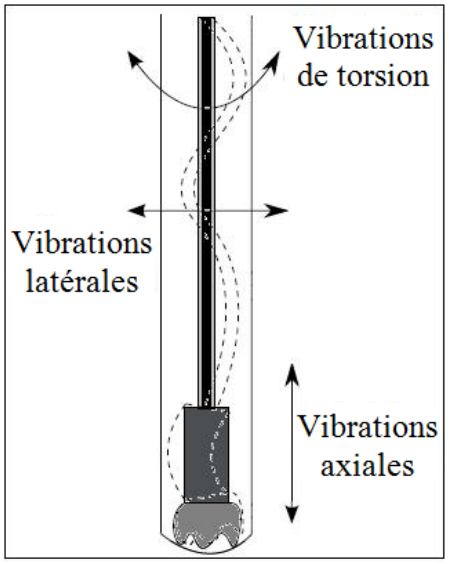


FIGURE 1 – Vibrations dans la tige de forage.

L'interaction de la colonne de perforation avec le puit donne lieu à trois types d'oscillations qui peuvent être classifiés conformément à la direction dans laquelle elles apparaissent : de torsion (oscillations de coller-glisser), axiales (phénomène de rebond du trépan) et latérales (mouvement tournant irrégulier occasionné par le déséquilibre de la colonne de perforation).

Ce travail se concentre sur l'étude du mode le plus critique des vibrations, le phénomène de coller-glisser. Cependant, puisque la présence de vibrations de torsion contribue à l'apparition d'oscillations axiales, des analyses sur le phénomène de rebond du trépan seront aussi présentées.

Ce chapitre aborde le problème de la modélisation des phénomènes de coller-glisser et de rebond du trépan. Il pose aussi une approche empirique de réduction des vibrations de torsion. Les stratégies pratiques, qui reflètent l'expérience des ingénieurs pétroliers et des experts qualitativement, consistent à manipuler convenablement certains paramètres du système tels que la vitesse de rotation, le poids sur le trépan et les caractéristiques du fluide de perforation.

## Dynamiques de torsion

En général on suppose que les instabilités qui conduisent éventuellement au phénomène de coller-glisser découlent du modèle de frottement qui décrit empiriquement l'interaction entre la roche et le trépan.

L'équation non-linéaire suivante, introduite dans [85], permet de modéliser le phénomène physique qui se produit au niveau du trépan

$$T\left(z(t)\right) = c_{\mathrm{b}} z(t) + W_{\mathrm{ob}} R_{\mathrm{b}} \mu_{\mathrm{b}}\left(z(t)\right) \operatorname{sign}\left(z(t)\right). \tag{8}$$

Le terme $c_{\mathrm{b}} z(t)$ correspond à un amortissement visqueux qui modélise l'influence de la boue ou fluide de forage. Le terme $W_{\mathrm{ob}} R_{\mathrm{b}} \mu_{\mathrm{b}}\left(z(t)\right)\mathrm{sign}(z(t))$ est un couple de frottement sec qui représente le contact fraise-roche. $R_{\mathrm{b}} > 0$ et $W_{\mathrm{ob}} > 0$ sont le rayon et le poids sur le trépan respectivement. Le coefficient de frottement sec $\mu_{\mathrm{b}}(z(t))$ est décrit par

$$\mu_{\mathrm{b}}\left(z(t)\right) = \mu_{\mathrm{cb}} + (\mu_{\mathrm{sb}} - \mu_{\mathrm{cb}})\mathrm{e}^{-\frac{\gamma_{\mathrm{b}}}{v_{\mathrm{f}}}|z(t)|}, \tag{9}$$

où $\mu_{\mathrm{sb}}$, $\mu_{\mathrm{cb}} \in (0, 1)$ sont les coefficients de frottement statique et de Coulomb et $0 < \gamma_{\mathrm{b}} < 1$ est une constante qui définit la vitesse de décroissance.

## Dynamiques axiales

Les modes de vibrations axiales et de torsion sont couplés et se produisent simultanément. La grande vitesse du trépan causée par le phénomène de coller-glisser peut induire des vibrations axiales de grande amplitude en causant le rebond du trépan.

Le modèle de l'oscillateur harmonique amorti peut être utilisé pour décrire les dynamiques axiales de la tige de perforation [28] :

$$m_0 \ddot{Y} + c_0 \dot{Y} + k_0 (Y - \mathrm{ROP}t) = -\mu_1 T\left(z(t)\right), \tag{10}$$

où les notations $Y$, $\dot{Y}$ et $\ddot{Y}$ représentent les variables axiales de position, vitesse et accélération respectivement, la vitesse de perforation ROP (par ses sigles en anglais Rate Of Penetration) est une vitesse axial imposée à la surface, $m_0$, $c_0$, et $k_0$ symbolisent la masse, l'amortissement et la constante du ressort. La constante $\mu_1$ dépend de la géométrie du trépan [28].

L'accouplement entre le modèle de torsion (5) et axial (10) découle du couple sur le trépan qui influe sur les deux dynamiques.

Le changement de variable $y = Y - \mathrm{ROP}t$ conduit au modèle équivalent suivant :

$$m_0 \ddot{y} + c_0 \left(\dot{y} + \mathrm{ROP}\right) + k_0 y = -\mu_1 T\left(z(t)\right). \tag{11}$$

## Résultats des simulations

Les paramètres du modèle utilisés dans les simulations sont les suivants [28], [84] :

$$\begin{array}{lll} G = 79.3x10^{9}\text{N m}^{-2}, & I = 0.095\text{Kg m}, & L = 1172\text{m}, \\ J = 1.19x10^{-5}\text{m}^{4}, & R_{\text{b}} = 0.155575\text{m}, & v_{\text{f}} = 1, \\ W_{\text{ob}} = 97347\text{N}, & I_{\text{B}} = 89\text{Kg m}^{2}, & c_{\text{a}} = 2000\text{N m s}, \\ \mu_{\text{cb}} = 0.5, & \mu_{\text{sb}} = 0.8, & \gamma_{\text{b}} = 0.9, \\ c_{\text{b}} = 0.03\text{N m s rad}^{-1}, & m_0 = 37278\text{Kg}, & c_0 = 16100\text{kg s}^{-1}, \\ k_0 = 1.55 \times 10^{6}\text{Kg s}^{-2}, & \text{ROP} = 0.01\text{m s}^{-1}, & \mu_1 = 257\text{m}^{-1}. \end{array} \tag{12}$$

Les Figures 2 et 3 montrent la réponse du système en boucle ouverte. La simulation du système (5), (8-9) montrée dans la Figure 2 illustre la présence du phénomène de coller-glisser.

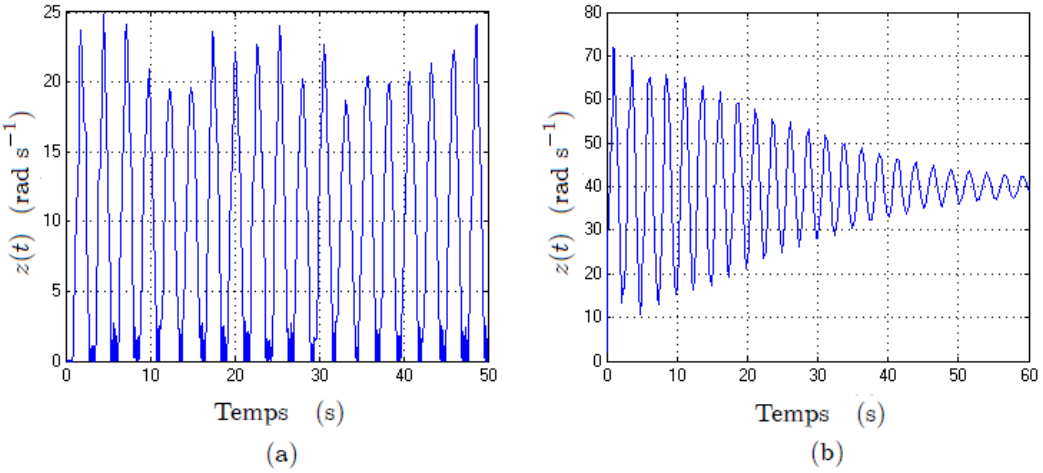


FIGURE 2 – Vitesse angulaire à l'extrémité inférieure $z(t)$ pour : (a) $\Omega(t) = 10\text{rad s}^{-1}$ (phénomène de coller-glisser), (b) $\Omega(t) = 40\text{rad s}^{-1}$.

On suppose que lorsque la tige de perforation n'est pas en contact avec le fond du puit, la vitesse angulaire est la même aux deux extrémités. Lorsque le trépan commence à interagir avec la formation de roche le système est inévitablement perturbé et des vibrations axiales et de torsion peuvent se produire simultanément.

La présence de fluctuations de la vitesse angulaire du trépan induit l'apparition des vibrations axiales comme le montre la Figure 3.

Il est clair que, pour un contrôle efficace des vibrations de la colonne, découlant de l'interaction du trépan avec le puit à l'extrémité inférieure, la

mesure et la rétroaction de certaines variables au niveau du trépan sont requises.

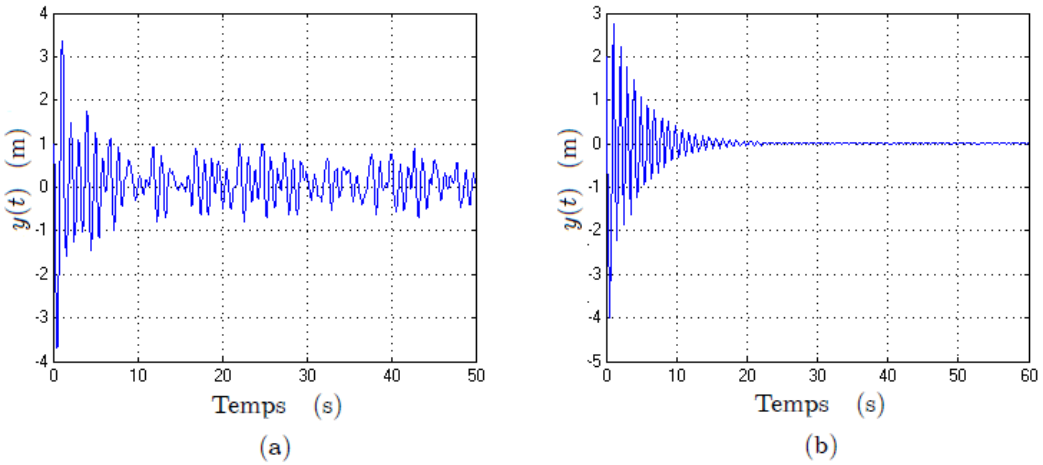


FIGURE 3 – Variable $y = Y - \mathrm{ROP}t$ pour : (a) $\Omega(t) = 10\mathrm{rad\ s}^{-1}$ (rebond du trépan), (b) $\Omega(t) = 40\mathrm{rad\ s}^{-1}$.

## Stratégies empiriques pour réduire le problème de coller-glisser

Dans la pratique, l'opérateur du processus de forage commande, depuis la surface, certains paramètres du système tels que le poids sur le trépan, les caractéristiques du fluide de perforation et la vitesse angulaire fournie par la table tournante pour optimiser l'opération de perforation.

Nous présentons les principales stratégies empiriques utilisées pour prévenir ou réduire les oscillations de torsion.

### Réduction du poids sur le trépan

L'expérience dans l'industrie du forage montre qu'en considérant une vitesse angulaire $\Omega$ fixe à la surface, la réduction du poids sur le trépan induit l'élimination du phénomène de coller-glisser.

### Augmentation de la vitesse angulaire fournie par la table tournante

Des preuves expérimentales indiquent une atténuation du phénomène de coller-glisser par augmentation de la vitesse angulaire à l'extrémité supérieure.

### Introduction d'une loi de variation du poids sur le trépan

Une solution alternative pour éliminer les vibrations de coller-glisser est la manipulation du poids sur le trépan. La loi de variation suivante est proposée dans [84].

$$W_{\mathrm{ob}}(z(t)) = K_{\mathrm{w}} \left| z(t) \right| + W_{\mathrm{ob0}}, \tag{13}$$

où $W_{\mathrm{ob0}} > 0$ et $W_{\mathrm{ob}} > W_{\mathrm{ob0}}$. L'expression (13) implique une réduction du poids sur le trépan lorsque la vitesse angulaire à l'extrémité inférieure $z(t)$ diminue et une valeur minimale du poids sur le trépan $W_{\mathrm{ob0}}$ pour garantir une vitesse de perforation adéquate.

### Augmentation de l'amortissement à l'extrémité inférieure

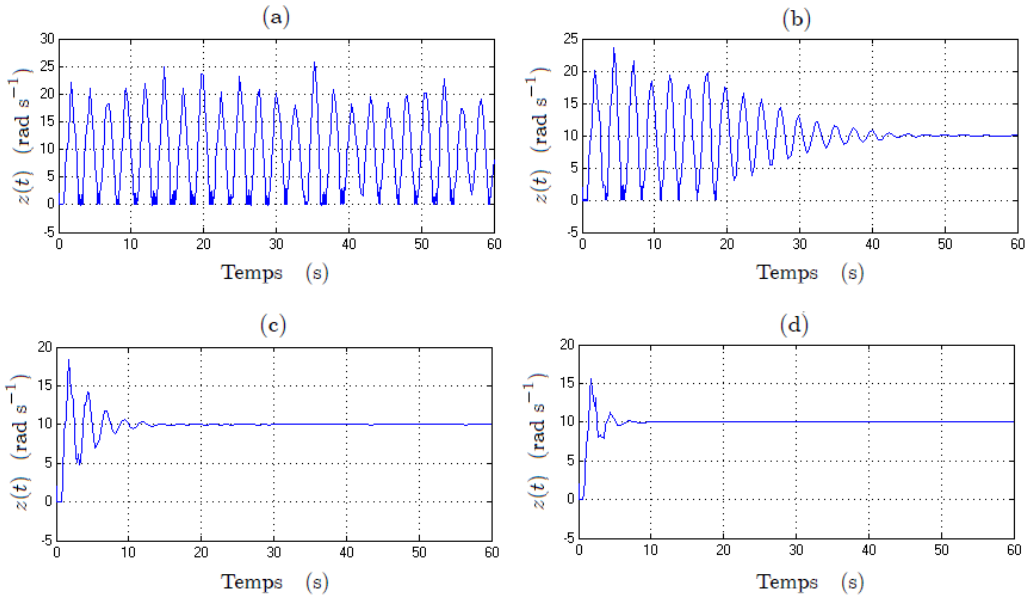


FIGURE 4 – Vitesse angulaire à l'extrémité inférieure pour différentes valeurs de $c_{\mathrm{b}}$ (N m s rad$^{-1}$) : (a) 0.8, (b) 15, (c) 65, (d) 150.

Une autre stratégie pour l'atténuation des oscillations de torsion consiste à augmenter l'amortissement au niveau du trépan. Cela peut être fait, dans la pratique, au moyen de la manipulation des caractéristiques du fluide de forage.

La Figure 4 montre les trajectoires de la vitesse angulaire à l'extrémité inférieure du système (5) sujet au modèle de couple (8-9) pour différentes valeurs du coefficient d'amortissement $c_{\mathrm{b}}$, indiquant que l'augmentation de ce coefficient réduit le phénomène de coller-glisser.

On conclut que ces stratégies empiriques réduisent d'une manière satisfaisante l'amplitude des oscillations de perforation, cependant, celles-ci ne peuvent pas garantir une performance optimale du processus. L'augmentation de la vitesse de rotation peut causer des problèmes de vibration latérale, et de plus, une réduction substantielle du poids sur le trépan pourrait arrêter la perforation. Ces lignes directrices opérationnelles ne sont pas suffisantes pour éliminer les vibrations de perforation, demandant l'introduction d'actions de commande. Les deux chapitres suivants abordent la conception de lois de commande pour éliminer ces vibrations indésirables dans le train de tiges.

# Chapitre 4

Ce chapitre aborde le problème d'analyse de la stabilité et la réduction des vibrations de perforation dans le cadre des systèmes à paramètres distribués.

Une fonction d'énergie permet d'analyser la dissipativité du système et conduit à concevoir une loi de commande qui garantit la suppression du phénomène de coller-glisser. Cette approche est basée sur l'équation d'onde décrivant le comportement en torsion de la tige de forage.

Ce chapitre aborde également le problème des vibrations couplées. On développe une approche d'inégalités matricielles pour une classe des systèmes dans lesquels l'équation d'onde est couplée à l'équation différentielle ordinaire. Cette approche permet la synthèse de contrôleurs stabilisants qui garantissent l'élimination simultanée des phénomènes de coller-glisser et de rebond du trépan.

## Analyse de la dissipation d'énergie

L'équation suivante correspond au modèle normalisé du système de forage

$$z_{tt}(\sigma,t) = az_{\sigma\sigma}(\sigma,t) - dz_t(\sigma,t), \quad t>0, \quad 0<\sigma<1, \tag{14}$$

où $a=\frac{GJ}{IL^2}$ et $d=\frac{\beta}{I}$, avec conditions aux frontières mixtes

$$\begin{aligned} z_\sigma(0,t) &= g\left(z_t(0,t)-u_1(t)\right), \qquad \sigma\in(0,1), \qquad t>0, \\ z_\sigma(1,t) &= -kz_t(1,t) - q\mu_{\mathrm{b}}(z_t(1,t))\mathrm{sign}(z_t(1,t)) - hz_{tt}(1,t), \end{aligned} \tag{15}$$

$u_1(t)$ est la vitesse angulaire fournie par la table tournante et $g=\frac{c_aL}{GJ}$, $k=\frac{c_bL}{GJ}$, $q=\frac{W_{ob}R_bL}{GJ}$, $h=\frac{I_BL}{GJ}$.

On considère la fonction d'énergie suivante

$$E(t) = \int_0^1 az_\sigma^2(\sigma,t)d\sigma + \int_0^1 z_t^2(\sigma,t)d\sigma + ahz_t^2(1,t). \tag{16}$$

Sa dérivée par rapport au temps le long des trajectoires de (14-15) est :

$$\begin{aligned}\frac{d}{dt}E(t) &= 2a\int_0^1 z_\sigma(\sigma,t)z_{t\sigma}(\sigma,t)d\sigma + 2az_t(1,t)(-kz_t(1,t)\\ &\quad -q\mu_{\mathrm{b}}(z_t(1,t))\mathrm{sign}(z_t(1,t)) - hz_{tt}(1,t))\\ &\quad -2agz_t(0,t)\left(z_t(0,t)-u_1(t)\right)\\ &\quad -2a\int_0^1 z_\sigma(\sigma,t)z_{t\sigma}(\sigma,t)d\sigma - 2d\int_0^1 z_t(\sigma,t)z_t(\sigma,t)d\sigma\\ &\quad +2ahz_t(1,t)z_{tt}(1,t),\end{aligned}$$

puisque

$$\mu_{\mathrm{b}}(z_t(1,t))\mathrm{sign}(z_t(1,t))z_t(1,t) = \mu_{\mathrm{b}}(z_t(1,t))\left|z_t(1,t)\right|,$$

on obtient,

$$\begin{aligned}\tfrac{d}{dt}E(t) = &-2aq\mu_{\mathrm{b}}(z_t(1,t))\left|z_t(1,t)\right| - 2d\textstyle\int_0^1 z_t^2(\sigma,t)d\sigma\\ &- 2agz_t(0,t)\left(z_t(0,t)-u_1(t)\right) - 2akz_t^2(1,t).\end{aligned} \tag{17}$$

Pour assurer la dissipation d'énergie, la loi de commande $u_1(t)$ doit garantir la négativité de (17).

En choisissant la structure suivante pour $u_1(t)$,

$$u_1(t) = (1-c_1)z_t(0,t) + 2c_1z_t(1,t) - c_1\frac{\left(z_t(1,t)\right)^2}{z_t(0,t)}, \tag{18}$$

avec $c_1 > 0$, on obtient

$$\begin{aligned}\tfrac{d}{dt}E(t) = &-2aq\mu_b(z_t(1,t))\left|z_t(1,t)\right| - 2d\textstyle\int_0^1 z_t^2(\zeta,t)d\zeta\\ &- 2agc_1\left(z_t(1,t)-z_t(0,t)\right)^2\\ &- 2akz_t^2(1,t).\end{aligned}$$

Puisque $\mu_b(z_t(1,t)) > 0$ et $a$, $q$, $k$, $d$, $g$ sont des constantes positives, donc $\frac{d}{dt}E(t) \leq 0$ et la dissipation d'énergie du système est assurée. Intuitivement, la dissipation d'énergie pourrait correspondre à l'atténuation des oscillations de torsion, ce qui serait confirmé par une simulation du système en boucle fermée avec la loi de commande (18).

La Figure 5 montre le résultat de la simulation du modèle (5), (8-9) en boucle fermée avec le contrôleur (18). Il est clair que, la loi de commande proposée conduit à la réduction des vibrations de coller-glisser.

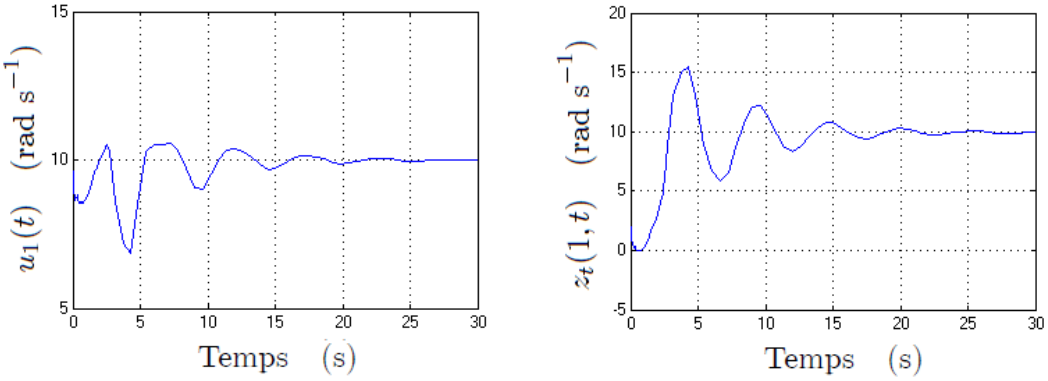


FIGURE 5 – Suppression du phénomène de coller-glisser au moyen de l'application de la loi de commande (18) avec $c_1 = 0.3$.

La Figure 6 montre la trajectoire de la variable longitudinale $y(t)$ après l'application de la commande proposée (18). On observe donc que l'élimination du phénomène de coller-glisser induit la réduction des vibrations axiales.

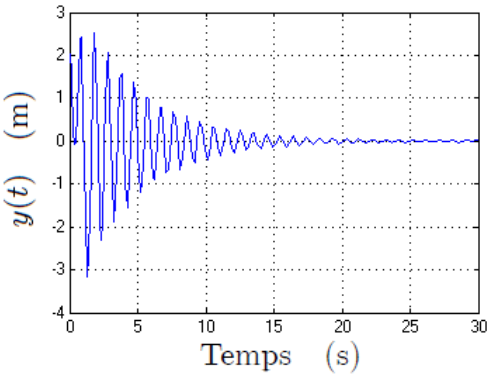


FIGURE 6 – Réduction des vibrations axiales en appliquant la loi de commande (18) avec $c_1 = 0.3$.

## Commande pour la suppression des vibrations couplées

Le système suivant correspond au modèle de torsion normalisé (1) avec des conditions aux frontières (2-3) sujet au modèle de couple sur le trépan (8-9) lié au modèle axial (11). Ce système décrit le couplage des dynamiques de torsion décrites par l'équation d'onde avec le comportement longitudinal de la tige de forage représenté par une équation différentielle ordinaire.

$$
\begin{aligned}
z_{tt}(\zeta,t) &= a z_{\zeta\zeta}(\zeta,t) - d z_t(\zeta,t), \quad \zeta \in (0,1), \quad t>0, && (19)\\
z_\zeta(0,t) &= g\left(z_t(0,t) - u_1(t)\right), && (20)\\
z_\zeta(1,t) &= -h z_{tt}(1,t) - k z_t(1,t) - q T_{\mathrm{nl}}(z_t(1,t)) + \omega, && (21)
\end{aligned}
$$

$$
\dot{x}(t) = Ax(t) + Bu_2(t) + E_1 z_t(1,t) + E_2 T_{\mathrm{nl}}(z_t(1,t)). \qquad (22)
$$

Les entrées de commande $u_1$, $u_2$ correspondent à la vitesse angulaire $\Omega$ fournie par la table tournante et à la vitesse de forage ROP respectivement. Le vecteur $x(t)$ et les paramètres du modèle sont définis comme suit :

$$
x(t) = [y(t)\ \dot{y}(t)]^T, \quad a = \frac{GJ}{IL^2}, \quad d = \frac{\beta}{I}, \quad g = \frac{c_a L}{GJ},
$$
$$
h = \frac{I_B L}{GJ}, \quad k = \frac{c_b L}{GJ}, \quad q = \frac{W_{\mathrm{ob}} R_{\mathrm{b}} L}{GJ}.
$$

Les matrices constantes sont définies par :

$$
A = \begin{bmatrix} 0 & 1 \\ -\frac{k_0}{m_0} & -\frac{c_0}{m_0} \end{bmatrix},\ B = \begin{bmatrix} 0 \\ -\frac{c_0}{m_0} \end{bmatrix},\ E_1 = \begin{bmatrix} 0 \\ -\frac{\mu_1 c_{\mathrm{b}}}{m_0} \end{bmatrix},\ E_2 = \begin{bmatrix} 0 \\ -\frac{\mu_1 W_{\mathrm{ob}} R_{\mathrm{b}}}{m_0} \end{bmatrix}.
$$

Le terme non linéaire $T_{\mathrm{nl}}$ est défini comme suit :

$$
T_{\mathrm{nl}}(z_t(1,t)) = \left(\mu_{\mathrm{cb}} + (\mu_{\mathrm{sb}} - \mu_{\mathrm{cb}}) \mathrm{e}^{-\frac{\gamma_{\mathrm{b}}}{v_{\mathrm{f}}}|z_t(1,t)|}\right) \mathrm{sign}\left(z_t(1,t)\right).
$$

La variable bornée $\omega$ représente la présence des incertitudes, des perturbations et(ou) des erreurs de modélisation ; on suppose qu'elle satisfait :

$$
\omega^2 \leq \varepsilon. \qquad (23)
$$

**Lemme 1** *On considère une fonctionnelle* $V(z_\zeta(\cdot,t), z_t(\cdot,t),\ x_t)$ *telle que*

$$
\int_0^1 \tilde{z}^T(\zeta,t) P \tilde{z}(\zeta,t) d\zeta \leq V(z_\zeta(\cdot,t), z_t(\cdot,t),\ x_t) \leq \bar{V}(z_\zeta(\cdot,t), z_t(\cdot,t),\ x_t) \qquad (24)
$$

$$
\frac{d}{dt} V(z_\zeta(\cdot,t), z_t(\cdot,t),\ x_t) + \sigma V(z_\zeta(\cdot,t), z_t(\cdot,t),\ x_t) \leq \beta\varepsilon \quad \forall t \geq 0,\ \sigma > 0,\ \beta > 0, \qquad (25)
$$

*où* $\tilde{z}(\zeta,t) = [z_\zeta(\zeta,t) \quad z_t(\zeta,t) \quad x_t]^T$ *et* $P$ *est une matrice symétrique définie positive. Alors, pour toute fonction initiale* $\tilde{\phi}(\zeta,t) = [\phi_\zeta(\zeta) \quad \phi_1(\zeta) \quad x_0]^T$, *le problème de valeurs aux frontières (19-22) satisfait la borne suivante*

$$
\int_0^1 \tilde{z}^T(\zeta,t) P \tilde{z}(\zeta,t) d\zeta \leq e^{-\sigma t} \bar{V}(\phi_\zeta(\zeta),\ \phi_1(\zeta),\ x_0) + \frac{\beta\varepsilon}{\sigma}, \qquad (26)
$$

*pour* $t \geq T_a(\phi,\varsigma) > 0$ *où*

$$T_a(\tilde{\phi},\varsigma) = \frac{1}{\sigma}\ln\left(\frac{1}{\varsigma}\bar{V}(\phi_\varsigma(\zeta),\ \phi_1(\zeta),\ x_0)\right).$$

Compte tenu du résultat antérieur, nous cherchons une fonction qui satisfait les conditions du Lemme 1. Soit la fonctionnelle de Lyapunov-Krasovskii suivante

$$\begin{aligned} V(z_\varsigma(\cdot,t),z_t(\cdot,t),\ x_t) &= V_1(z_\varsigma(\zeta,t)) + V_2(z_t(\zeta,t)) \\ &\quad + V_3(z_\varsigma(\zeta,t),z_t(\zeta,t)) + V_4(x_t), \end{aligned}$$

où

$$\begin{aligned} V_1(z_\varsigma(\zeta,t)) &= pa\int_0^1 z_\zeta^2(\zeta,t)d\zeta, \\ V_2(z_t(\zeta,t)) &= p\int_0^1 z_t^2(\zeta,t)d\zeta, \\ V_3(z_\varsigma(\zeta,t),z_t(\zeta,t)) &= 2\chi\int_0^1 (\zeta+1)\, z_\varsigma(\zeta,t)z_t(\zeta,t)d\zeta, \\ V_4(x_t) &= x^T(t)Rx(t). \end{aligned}$$

La fonctionnelle proposée peut s'écrire comme

$$V(z_\varsigma(\cdot,t),z_t(\cdot,t),\ x_t) = \int_0^1 \tilde{z}^T(\zeta,t)P\tilde{z}(\zeta,t)d\zeta, \quad \tilde{z}(\zeta,t) = [z_\varsigma(\zeta,t)\ z_t(\zeta,t)\ x(t)]^T,$$

$$P = \begin{bmatrix} ap & \chi(\zeta+1) & 0 \\ \chi(\zeta+1) & p & 0 \\ 0 & 0 & R \end{bmatrix} > 0,\ p>0,\ a>0,\ R>0.$$

En prenant la dérivée par rapport au temps de $V(z_\varsigma(\cdot,t), z_t(\cdot,t), x_t)$ le long des trajectoires du système (19-22) en boucle fermée avec les lois de commande de la forme

$$u_1(t) = c_{11}z_{tt}(1,t) + c_{12}z_t(1,t) + c_{13}T_{\mathrm{nl}}(z_t(1,t)) + c_{14}z_t(0,t), \tag{27}$$

$$u_2(t) = c_2x(t), \tag{28}$$

et en considérant le terme positif $-\beta(\omega^2-\varepsilon)$ résultant de la condition (23), l'inégalité suivante est satisfaite

$$\frac{d}{dt}V(\cdot) + \sigma V(\cdot) - \beta\varepsilon \leq \int_0^1 \eta_1^T\Psi\eta_1 d\zeta + \eta_2^T\Phi\eta_2,$$

où

$$\begin{aligned}\eta_1 &= (\ z_t(\zeta,t)\ z_\zeta(\zeta,t)\ )^T,\\ \eta_2 &= (\ z_{tt}(1,t)\ z_t(1,t)\ T_{\rm nl}(z_t(1,t))\ z_t(0,t)\ x(t)\ \omega\ )^T,\end{aligned}$$

et

$$\Psi = \begin{bmatrix} -2pd-\chi+\sigma p & -d\chi(\zeta+1)+\sigma\chi(\zeta+1) \\ * & -a\chi+\sigma pa \end{bmatrix}, \tag{29}$$

$$\Phi = \begin{bmatrix} 2a\chi h^2 - a\chi g^2 c_{11}^2 & \Phi_{12} & \Phi_{13} & \Phi_{14} & 0 & -2a\chi h \\ * & \Phi_{22} & \Phi_{23} & \Phi_{24} & {E_1}^T R & -2a\chi k+pa \\ * & * & \Phi_{33} & \Phi_{34} & E_2^T R & -2a\chi q \\ * & * & * & \Phi_{44} & 0 & 0 \\ * & * & * & * & \Upsilon_1+\sigma R & 0 \\ * & * & * & * & * & 2a\chi-\beta \end{bmatrix}, \tag{30}$$

où

$$\begin{aligned}
\Phi_{12} &= 2a\chi hk - pah - a\chi g^2 c_{11}c_{12} & \Phi_{24} &= a\chi g^2 c_{12}(1-c_{14}) + pagc_{12}\\
\Phi_{13} &= 2a\chi hq - a\chi g^2 c_{11}c_{13} & \Phi_{33} &= 2a\chi q^2 - a\chi g^2 c_{13}^2\\
\Phi_{14} &= a\chi g^2 c_{11}(1-c_{14}) + pagc_{11} & \Phi_{34} &= a\chi g^2 c_{13}(1-c_{14}) + pagc_{13}\\
\Phi_{22} &= 2a\chi k^2 + 2\chi - 2pak - a\chi g^2 c_{12}^2 & \Phi_{44} &= -a\chi g^2(1-c_{14})^2 - \chi\\
\Phi_{23} &= 2a\chi kq - paq - a\chi g^2 c_{12}c_{13} & & \quad - 2pag + pagc_{14}\\
\Upsilon_1 &= A^T R + RA + c_2^T B^T R + RBc_2.
\end{aligned}$$

Le théorème suivant stipule le résultat de stabilisation du système (19-22).

**Théorème 1** *Les trajectoires du système de perforation décrit par le modèle couplé (19-22) en boucle fermée avec les lois de commande (27) et (28) admettent la borne (26) si les inégalités matricielles* $P>0$, $\Psi<0$ *et* $\Phi<0$ *sont satisfaites pour* $p>0$, $\chi>0$, $\beta>0$, $R>0$ *et quelconques* $c_{11}$, $c_{12}$, $c_{13}$, $c_{14}$, $c_2$.

Les paramètres utilisés dans les simulations suivantes sont ceux indiqués dans (12). Le taux maximal de décroissance exponentielle pour laquelle les conditions du Théorème 1 sont satisfaites est $\sigma = 0.8$. Un résultat de l'inégalité matricielle linéaire $\Psi<0$ avec $\Psi$ définie dans (29) est :

$$p = 0.7406, \qquad \chi = 0.9559.$$

Sur la base des valeurs précédentes, on trouve pour l'inégalité matricielle bilinéaire $\Phi<0$ avec $\Phi$ définie dans (30), la solution suivante :

$$\begin{aligned} &c_{11} = -0.0067, \quad c_{12} = -0.04699, \quad c_{13} = -0.0548,\\ &c_{14} = 0.6642, \qquad c_2 = [0 \quad 2.0234], \quad \beta = 16.8149, \end{aligned} \tag{31}$$

$$R = \begin{bmatrix} 551.7373 & 11.7383 \\ 11.7383 & 13.4465 \end{bmatrix}.$$

Une simulation du modèle (5) sujet à la fonction du couple sur le trépan (8-9) en boucle fermée avec la loi de commande (27) et du modèle (11) en boucle fermée avec le contrôleur (28) illustre la performance de la stratégie proposée. La Figure 7 montre l'élimination des phénomènes de coller-glisser et de rebond du trépan.

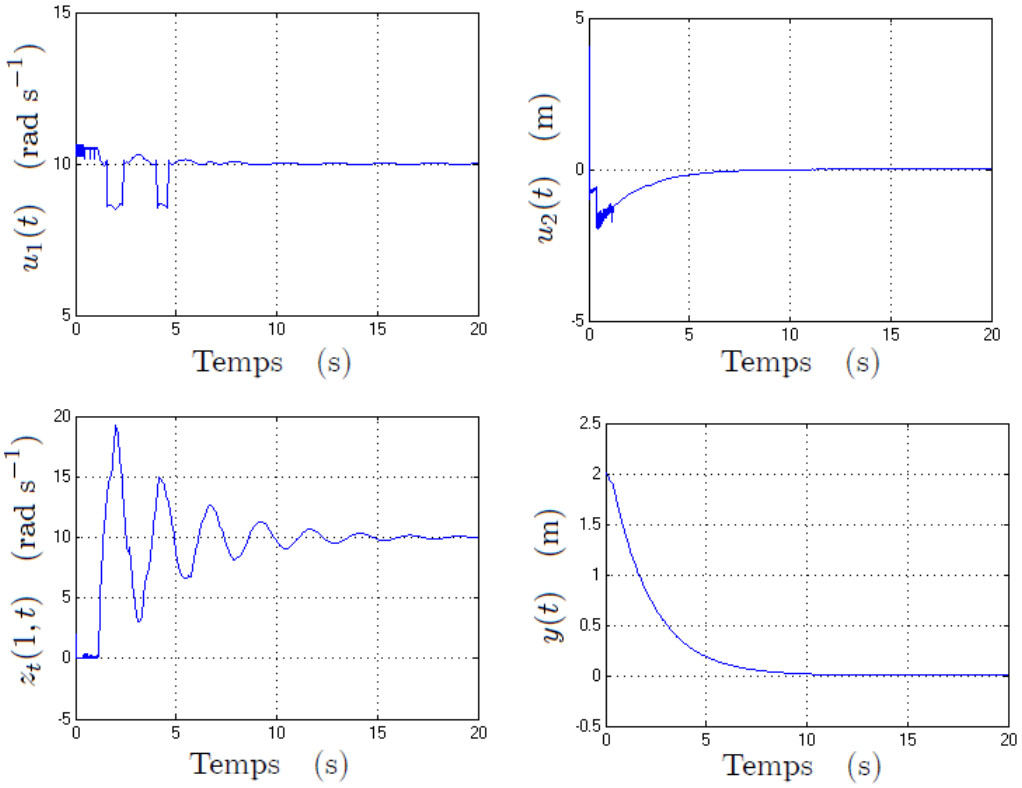


FIGURE 7 – Trajectoires de torsion et axiales du système de perforation en boucle fermée avec les contrôleurs $u_1$ et $u_2$ indiqués dans (27) et (28).

Nous pouvons conclure que la méthodologie de commande basée sur l'analyse de dissipation d'énergie est réalisée d'une manière plus simple et directe par rapport à l'approche d'inégalités matricielles, cependant, celle-ci offre une élimination intégrale des vibrations couplées dans la tige de forage. En ce qui concerne la taille de la commande, on peut observer que la trajectoire du contrôleur (27) est plus proche de la trajectoire la référence, ce qui semble assez convenable en considérant la présence de restrictions de saturation sur les entrées de commande. Ce problème particulier sera abordé dans le chapitre

suivant. Il est bien connu que les modèles à paramètres distribués constituent une description proche de la réalité, cependant, le manque d'outils numériques pour la simulation des systèmes de dimension infinie sujets à des non-linéarités et à des incertitudes conduit à l'idée d'aborder le problème depuis une perspective différente. Le chapitre suivant attaque le problème de commande des vibrations à partir du modèle à retards de type neutre qui décrit le comportement du système de forage vertical considéré.

# Chapitre 5

Ce chapitre aborde le problème de l'analyse de stabilité et de commande des vibrations du train de tiges dans le cadre de systèmes à retards.

Comme nous l'avons déjà expliqué, le comportement en torsion de la tige de forage peut être modélisé par une équation non-linéaire à retards de type neutre qui représente la relation entrée-sortie du système. Dans ce chapitre, ce modèle est transformé en un ensemble de modèles linéaires, non-linéairement pondérés, ce qui permet de mettre à profit les outils pour l'analyse et la commande des systèmes linéaires. Au moyen d'une analyse de stabilité de Lyapunov, on obtient des conditions de stabilité et de stabilisation en termes d'inégalités matricielles linéaires. La loi de commande proposée garantit la stabilité en boucle fermée du système et élimine efficacement les oscillations de torsion. Par la suite, on aborde le problème de vibrations axiales et de torsion couplées. On obtient, au moyen de la méthode de l'ellipsoïde attractif, la synthèse de commandes stabilisants qui garantissent une élimination intégrale des vibrations de perforation. Cette approche soulève un problème d'optimisation soumis aux conditions de stabilisation pratique en termes d'inégalités matricielles bilinéaires.

## Commande des vibrations de torsion : approche multimodèle

On examine dans cette section la stabilisation des systèmes non linéaires à retards de type neutre qui peuvent se transformer en un système multimodèle, c'est à dire, un ensemble de modèles linéaires non-linéairement pondérés représentés par :

$$\dot{x}(t) - D\dot{x}(t-\tau_1) = \sum_{i \in I^r} h_i(x_t) \left\{ A_i x(t) + A_{i\tau_1} x(t-\tau_1) + Bu(t) \right\}, \qquad (32)$$

où $\tau_1 > 0$ est le retard constant, $I^r$ est l'ensemble des nombres entiers $\{1, ..., r\}$, et $r$ est le nombre de sous-systèmes nécessaires pour décrire le système multimodèle. Les $h_i(\cdot)$ sont des fonctions scalaires de pondération qui

remplissent les conditions de convexité suivantes :

$$\sum_{i\in I^r} h_i(x_t) = 1 \quad \forall i = 1, ..., r, \quad h_i(x_t) \geq 0. \tag{33}$$

Afin de garantir la stabilité de l'opérateur de différence on considère que $|D| < 1$.

Le théorème suivant présente un algorithme qui permet la synthèse d'un gain $K$ tel que la loi de commande $u(t) = Kx(t - \tau_1)$ stabilise exponentiellement le système en boucle fermée

$$\dot{x}(t) - D\dot{x}(t - \tau_1) = \sum_{i\in I^r} h_i(x_t) \left\{ A_i x(t) + (A_{i\tau_1} + BK)\, x(t - \tau_1) \right\}, \tag{34}$$

avec un taux de décroissance garanti $\alpha$.

**Théorème 2** *Le système en boucle fermée (34) est $\alpha$-stable s'il existe un nombre réel $\varepsilon > 0$ et des matrices $\bar{P}_1 > 0$, $\bar{P}$, $\bar{Q} = \bar{Q}^T$, $\bar{R} = \bar{R}^T$, et $Y$ de dimension $n \times n$, telles que pour tout $i \in I^r$ l'inégalité matricielle linéaire suivante est satisfaite*

$$\begin{pmatrix} \Phi_i & \begin{pmatrix} e^{\alpha\tau_1}\vartheta \end{pmatrix} & \begin{pmatrix} e^{\alpha\tau_1} D\bar{P} \end{pmatrix} \\ \begin{pmatrix} e^{\alpha\tau_1}\vartheta \end{pmatrix}^T & -\bar{R}/\tau_1 & 0 \\ \begin{pmatrix} e^{\alpha\tau_1} D\bar{P} \end{pmatrix}^T & 0 & -\bar{Q} \end{pmatrix} < 0, \qquad \Phi_i = \begin{pmatrix} \Phi_{11} & \Phi_{12} \\ * & \Phi_{22} \end{pmatrix},$$

$$\begin{aligned} \vartheta &= (A_{i\tau_1} - \alpha D)\, \bar{P} + BY, \\ \Phi_{11} &= (A_i + \alpha I_n + e^{\alpha\tau_1} (A_{i\tau_1} - \alpha D))\, \bar{P} \\ &\quad + \bar{P}^T (A_i + \alpha I_n + e^{\alpha\tau_1} (A_{i\tau_1} - \alpha D))^T + BY + Y^T B^T, \\ \Phi_{12} &= \bar{P}_1^T - \bar{P} + \varepsilon \bar{P}^T (A_i + \alpha I_n + e^{\alpha\tau_1} (A_{i\tau_1} - \alpha D))^T + \varepsilon Y^T B^T, \\ \Phi_{22} &= -\varepsilon \left( \bar{P} + \bar{P}^T \right) + \tau_1 \bar{R} + \bar{Q}. \end{aligned}$$

*De plus, le gain de retour est donné par $K = Y\bar{P}^{-1}$.*

Pour appliquer le résultat antérieur au système de perforation, on doit obtenir une représentation polytopique du modèle non linéaire (5), (8-9).

En considérant $\mu_{\text{cb}} = 0$, et le changement de variable suivant

$$x_1(t) = z(t) - \Omega_0, \tag{35}$$

on obtient l'expression non linéaire suivante qui décrit le comportement du système à l'extrémité inférieure :

$$\begin{aligned}\dot{x}_1(t)+d\dot{x}_1(t-2\Gamma) &= a_0x_1(t)+a_1x_1(t-2\Gamma)+bu(t-\Gamma)\\ &\quad -c_2\mathrm{e}^{-\frac{\gamma_\mathrm{b}}{v_\mathrm{f}}(x_1(t)+\Omega_0)}\mathrm{sign}\left(x_1(t)+\Omega_0\right)\\ &\quad +c_2\Upsilon\mathrm{e}^{-\frac{\gamma_\mathrm{b}}{v_\mathrm{f}}(x_1(t-2\Gamma)+\Omega_0)}\mathrm{sign}\left(x_1(t-2\Gamma)+\Omega_0\right),\end{aligned} \tag{36}$$

où $a_0=-\Psi-\frac{c_\mathrm{b}}{I_\mathrm{B}}$, $a_1=\frac{\Upsilon c_\mathrm{b}}{I_\mathrm{B}}-\Upsilon\Psi$, $d=-\Upsilon$, $b=\Pi$ et $c_2=\frac{W_{\mathrm{ob}}R_\mathrm{b}\mu_{\mathrm{sb}}}{I_\mathrm{B}}$. Nous proposons le changement de variables suivant :

$$\left\{\begin{array}{l}\varkappa_1(t)=x_1(t),\\ \varkappa_2(t)=\mathrm{e}^{-\frac{\gamma_\mathrm{b}}{v_\mathrm{f}}\varkappa_1(t)+\Omega_0},\end{array}\right. \quad \text{alors, on a} \quad \left\{\begin{array}{l}\dot{\varkappa}_1(t)=\dot{x}_1(t),\\ \dot{\varkappa}_2(t)=-\frac{\gamma_\mathrm{b}}{v_\mathrm{f}}\dot{\varkappa}_1(t)\varkappa_2(t).\end{array}\right.$$

Le système (36) peut s'écrire comme

$$\dot{x}(t)-D\dot{x}(t-2\Gamma)=A(x)x(t)+A_{2\Gamma}(x)x(t-2\Gamma)+B_\Gamma u(t-\Gamma), \tag{37}$$

où l'entrée de commande $u(t)$ correspond à la vitesse angulaire fournie par la table tournante, et où :

$$x(t)=\left[\varkappa_1(t)\ \ \varkappa_2(t)\right]^T,\quad D=\begin{pmatrix}\Upsilon & 0\\ 0 & 0\end{pmatrix},\quad B_\Gamma=\begin{pmatrix}\Pi\\ 0\end{pmatrix},$$

$$A_{2\Gamma}(x)=\begin{pmatrix}\Upsilon\left(\frac{c_\mathrm{b}}{I_\mathrm{B}}-\Psi\right) & c_2\Upsilon\mathrm{sign}(\varkappa_1(t-2\Gamma)+\Omega_0)\\ 0 & 0\end{pmatrix},$$

$$A(x)=\begin{pmatrix}-\left(\Psi+\frac{c_\mathrm{b}}{I_\mathrm{B}}\right) & -c_2\mathrm{sign}(\varkappa_1(t)+\Omega_0)\\ 0 & -\frac{\gamma_\mathrm{b}}{v_\mathrm{f}}\dot{\varkappa}_1(t)\end{pmatrix}.$$

On observe que les éléments des matrices $D$ et $B_\Gamma$ sont constants, et que le terme $c_2\Upsilon\mathrm{sign}(\varkappa_1(t-2\Gamma)+\Omega_0)$ de la matrice $A_{2\Gamma}(x)$ est borné. Puisque $\dot{\varkappa}_1(t)$ est une variable bornée, alors la matrice $A(x)$ l'est aussi.

La représentation polytopique suivante est obtenue,

$$A(x)x(t)+A_{2\Gamma}(x)x(t-2\Gamma)=\sum_{i\in I^r}h_i(x_t)\left(A_ix(t)+A_{i2\Gamma}x(t-2\Gamma)\right), \tag{38}$$

où les matrices $A_i$ et $A_{i2\Gamma}$ ont seulement des coefficients constants [108].

En utilisant les paramètres donnés dans (12), les matrices $A(x)$, $A_{2\Gamma}(x)$, $B_\Gamma$ et $D$ du système (37) prennent les valeurs suivantes :

$$\begin{aligned}D &= \begin{pmatrix}0.7396 & 0\\ 0 & 0\end{pmatrix},\ B_\Gamma=\begin{pmatrix}5.8523\\ 0\end{pmatrix},\\ A(x) &= \begin{pmatrix}-3.3645 & -136.1327\mathrm{sign}(\varkappa_1(t)+\Omega_0)\\ 0 & -0.9\dot{\varkappa}_1(t)\end{pmatrix},\\ A_{2\Gamma}(x) &= \begin{pmatrix}-2.4878 & 100.6802\mathrm{sign}(\varkappa_1(t-2\Gamma)+\Omega_0)\\ 0 & 0\end{pmatrix}.\end{aligned}$$

Pour obtenir une représentation polytopique du système, les matrices $A(x)$ et $A_{2\Gamma}(x)$ doivent être bornées, celles-ci dépendent de trois fonctions indépendantes : $\dot{\varkappa}_1(t)$, $\text{sign}(\varkappa_1(t)+\Omega_0)$ et $\text{sign}(\varkappa_1(t-2\Gamma)+\Omega_0)$.

Pour la matrice $A$ nous avons :

$$A_i(x) = \begin{pmatrix} -3.3645 & a^i_{23}(x) \\ 0 & a^i_{33}(x) \end{pmatrix},$$

$$\begin{aligned} -136.1327 &= a^1_{23} \leq a^i_{23}(x) \leq a^2_{23} = 0, \\ -0.9Acc_{\max} &= a^1_{33} \leq a^i_{33}(x) \leq a^2_{33} = -0.9Dec_{\max}, \end{aligned}$$

$Acc_{\max}$ et $Dec_{\max}$ correspondent à l'accélération et à la décélération maximales respectivement. Pour la matrice $A_{2\Gamma}(x)$ nous avons :

$$A_{i2\Gamma}(x) = \begin{pmatrix} -2.4878 & a^i_{2\Gamma 23}(x) \\ 0 & 0 \end{pmatrix},$$

$$0 = a^1_{2\Gamma 23}(x) \leq a^i_{2\Gamma 23}(x) \leq a^2_{2\Gamma 23}(x) = 100.6802.$$

En appliquant le résultat du Théorème 2 au système de forage en boucle fermée avec la loi de commande $u(t) = Kx(t-\Gamma)$, la solution suivante est obtenue :

$$K = Y\bar{P}^{-1} = \begin{pmatrix} 0.44 & -4.25 \end{pmatrix}.$$

En considérant le changement de variable (35), la loi de commande stabilisante pour le système (36) est donnée par

$$u(t) = 0.44z(t-\Gamma) - 4.25\text{e}^{-\frac{\gamma_b}{v_f}z(t-\Gamma)} - 0.44\Omega_0. \tag{39}$$

La Figure 8 montre une élimination efficace du phénomène de coller-glisser en appliquant la loi de commande (39).

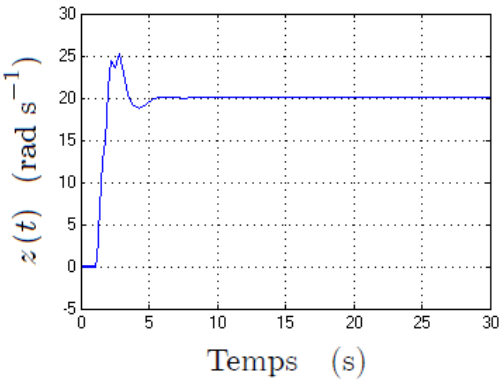


FIGURE 8 – Trajectoire $z(t)$ du modèle de torsion en boucle fermée avec la loi de commande (39) avec $\Omega_0 = 20\text{rad s}^{-1}$.

## Commande des vibrations couplées : méthode de l'ellipsoïde attractif

Cette section aborde le problème de commande des vibrations couplées dans le système de forage. On propose une méthodologie pour la synthèse de contrôleurs stabilisants basée sur une combinaison de la méthode de Lyapunov et le principe des ensembles attractifs qui pose un problème d'optimisation sujet aux restrictions matricielles bilinéaires. La stratégie proposée garantit l'élimination des oscillations axiales et de torsion couplées et permet de déterminer l'ellipsoïde minimal attractif pour les trajectoires du système en boucle fermée.

**Définition 1** *[66] Un ellipsoïde centré à l'origine est définie comme un ensemble de* $\mathcal{R}^n$ *tel que* $\mathcal{E}_M = \left\{x \in \mathcal{R}^n : x^T M x \leq 1\right\}$*, où* $M$ *est une matrice symétrique définie positive.*

**Définition 2 (Ellipsoïde attractif)** *[86] Un ellipsoïde* $\mathcal{E}$ *est un domaine attractif pour le système (42) si*
*1)* $\phi(\theta) \in \mathcal{E}$*,* $\theta \in [-h, 0]$ *implique que* $x(t, \phi) \in \mathcal{E}$*,* $t \geq 0$*,*
*2)*$\phi(\theta) \in \mathcal{R}^n \backslash \mathcal{E}$*, pour* $\theta \in [-h, 0]$ *implique qu'il existe* $T_a$*,* $0 \leq T_a < \infty$*, tel que* $x(t, \phi) \in \mathcal{E}$*,* $t \geq 0$*.*

**Lemme 2** *On considère une fonctionnelle* $V(x_t)$ *qui satisfait*

$$x^T(t) P x(t) \leq V(x_t) \leq \alpha \left\|x_t\right\|_h^2, \tag{40}$$

*où* $P$ *est une matrice symétrique définie positive et*

$$\frac{\mathsf{d}}{\mathsf{d}t} V(x_t) + \sigma V(x_t) \leq \beta, \quad \forall t \geq 0, \quad \sigma > 0, \quad \beta > 0. \tag{41}$$

*Alors, pour toute fonction initiale* $\phi \in \mathcal{PC}([-h, 0], \mathcal{R}^n)$*, la solution* $x(t, \phi)$ *est contenue dans l'ellipsoïde* $\mathcal{E}_{\tilde{P}} = \left\{x \in \mathcal{R}^n : x^T \tilde{P} x \leq 1\right\}$*,* $\tilde{P} = \left(\frac{\sigma}{\beta} + \varsigma\right) P$*,* $\varsigma > 0$ *pour* $t \geq T_a(\phi, \varsigma) > 0$ *où*

$$T_a(\phi, \varsigma) = \frac{1}{\sigma} \ln \left( \frac{\alpha \left\|\phi\right\|_h^2}{\varsigma} - \frac{\beta}{\varsigma \sigma} \right).$$

Considérons un système à retards de type neutre sous la forme :

$$\begin{aligned} \dot{x}(t) + D\dot{x}(t - 2\tau) \quad = \quad & A_0 x(t) + A_1 x(t - 2\tau) + B_1 u_1(t - \tau) \\ & + B_2 u_2(t) + C_0 f(x(t)) + C_1 f(x(t - 2\tau)) + \omega, \end{aligned} \tag{42}$$

où $\omega$ satisfait

$$\|\omega\|_{K_\omega} = \omega^T K_\omega \omega \leq 1, \qquad t \geq 0. \tag{43}$$

Conformément à l'application considérée, les structures suivantes pour $u_1$ et $u_2$ sont proposées

$$u_1(t-\tau) = K_0 \dot{x}(t-2\tau) + K_1 x(t-2\tau), \tag{44}$$

$$u_2(t) = K_2 x(t). \tag{45}$$

On considère que la loi de commande $u_2$ est soumise à la restriction :

$$|u_2(t)| \leq \bar{u}_2, \tag{46}$$

où $\bar{u}_2$ est le niveau de saturation, c'est à dire, le vecteur $u_2(t) = \text{col}\ \{u_2^1(t), ..., u_2^m(t)\}$ est soumis aux restrictions d'amplitude suivantes :

$$\left|u_2^j(t)\right| \leq \bar{u}_2^j, \quad 0 < \bar{u}_2^j, \quad j = 1, ..., m.$$

L'objectif est de trouver les conditions qui garantissent que l'ellipsoïde défini par $\mathcal{E}_{\tilde{P}} = \left\{x \in \mathcal{R}^n : x^T \tilde{P} x \leq 1\right\}$, soit un ensemble attractif pour les trajectoires du système (42) en boucle fermée avec (44-45), c'est à dire, $\overline{\lim}_{t\to\infty} x^T(t)\tilde{P}x(t) \leq 1$. De plus, les matrices $K_0$, $K_1$, $K_2 \in \mathcal{R}^{m\times n}$ et $\tilde{P}$ doivent garantir la minimisation de l'ellipsoïde $\mathcal{E}_{\tilde{P}}$. Étant donné que la matrice $\tilde{P}$ est inversement proportionnelle aux axes de l'ellipsoïde, se pose le problème d'optimisation suivant :

$$\begin{gathered} \min \text{tr}(\tilde{P}^{-1}) \\ \text{sujet à } \tilde{P} \in \Sigma_1, \quad K_0, K_1, K_2 \in \Sigma_2, \end{gathered} \tag{47}$$

où $\Sigma_1$, $\Sigma_2$, définissent l'ensemble de matrices admissibles, de dimensions $n \times n$ et $m \times n$ respectivement, qui garantissent la propriété d'invariance de l'ellipsoïde $\mathcal{E}_{\tilde{P}}$.

On considère la fonctionnelle

$$\begin{aligned} V(x_t) \;=\; & x^T(t)Px(t) + \int_{t-2\tau}^{t} \mathrm{e}^{\sigma(s-t)} x^T(s) S x(s) \mathrm{d}s \\ & + 2\tau \int_{-2\tau}^{0} \int_{t+\theta}^{t} \mathrm{e}^{\sigma(s-t)} \dot{x}^T(s) R \dot{x}(s) \mathrm{d}s \mathrm{d}\theta. \end{aligned} \tag{48}$$

En prenant la dérivée de $V(x_t)$ par rapport au temps et en suivant l'approche descripteur, on obtient :

$$\frac{\mathrm{d}V(x_t)}{\mathrm{d}t} + \sigma V(x_t) - \beta \leq \eta^T \Phi \eta,$$

où le vecteur $\eta$ est défini comme

$$\eta = (x(t)\ x(t-2\tau)\ \dot{x}(t)\ \dot{x}(t-2\tau)\ u_1(t-\tau)\ u_2(t)\ f(x(t))\ f(x(t-2\tau))\ \omega)^T,$$

et $\Phi$ est une matrice symétrique avec éléments $\Phi_{ij}$, $i = 1, .., 9$, $j = 1, ..., 9$ définie comme :

$$\begin{bmatrix}
\Phi_{11} & \Phi_{12} & \Phi_{13} & \Phi_{14} & \Phi_{15} & \Phi_{16} & \Phi_{17} & P_2^T C_1 + A_0^T P_8 & P_2^T + A_0^T P_9 \\
* & \Phi_{22} & A_1^T P_3 & \Phi_{24} & \Phi_{25} & A_1^T P_6 & A_1^T P_7 & A_1^T P_8 & A_1^T P_9 \\
* & * & \Phi_{33} & \Phi_{34} & \Phi_{35} & \Phi_{36} & \Phi_{37} & P_3^T C_1 - P_8 & P_3^T - P_9 \\
* & * & * & \Phi_{44} & \Phi_{45} & \Phi_{46} & \Phi_{47} & P_4^T C_1 - D^T P_8 & P_4^T - D^T P_9 \\
* & * & * & * & \Phi_{55} & \Phi_{56} & \Phi_{57} & P_5^T C_1 + B_1^T P_8 & P_5^T + B_1^T P_9 \\
* & * & * & * & * & \Phi_{66} & \Phi_{67} & P_6^T C_1 + B_2^T P_8 & P_6^T + B_2^T P_9 \\
* & * & * & * & * & * & \Phi_{77} & P_7^T C_1 + C_0^T P_8 & P_7^T + C_0^T P_9 \\
* & * & * & * & * & * & * & P_8^T C_1 + C_1^T P_8 & P_8^T + C_1^T P_9 \\
* & * & * & * & * & * & * & * & \Phi_{99}
\end{bmatrix},$$

où :

$$\begin{aligned}
\Phi_{11} &= A_0^T P_2 + P_2^T A_0 \\
&\quad + S + \sigma P - \mathrm{e}^{-\sigma 2\tau} R \\
&\quad + P_{14} K_2 + K_2^T P_{14} \\
\Phi_{12} &= \mathrm{e}^{-\sigma 2\tau} R + P_2^T A_1 \\
\Phi_{13} &= P - P_2^T + A_0^T P_3 \\
\Phi_{14} &= -P_2^T D + A_0^T P_4 \\
\Phi_{15} &= P_2^T B_1 + A_0^T P_5 \\
\Phi_{16} &= P_2^T B_2 + A_0^T P_6 \\
&\quad + K_2^T P_{13} - P_{14}^T \\
\Phi_{17} &= P_2^T C_0 + A_0^T P_7 \\
\Phi_{22} &= -\mathrm{e}^{-\sigma 2\tau}(S + R) \\
&\quad + P_{12}^T K_1 + K_1^T P_{12} \\
\Phi_{23} &= A_1^T P_3 \\
\Phi_{24} &= A_1^T P_4 + K_1^T P_{11} \\
&\quad + P_{12}^T K_0 \\
\Phi_{25} &= A_1^T P_5 + K_1^T P_{10} \\
&\quad - P_{12}^T \\
\Phi_{33} &= 4\tau^2 R - P_3 - P_3^T \\
\Phi_{34} &= -P_3^T D - P_4 \\
\Phi_{35} &= P_3^T B_1 - P_5 \\
\Phi_{36} &= P_3^T B_2 - P_6 \\
\Phi_{37} &= P_3^T C_0 - P_7 \\
\Phi_{44} &= -P_4^T D - D^T P_4 \\
&\quad + P_{11}^T K_0 + K_0^T P_{11} \\
\Phi_{45} &= P_4^T B - D^T P_5 \\
&\quad + K_0^T P_{10} - P_{11}^T \\
\Phi_{46} &= P_4^T B_2 - D^T P_6 \\
\Phi_{47} &= P_4^T C_0 - D^T P_7 \\
\Phi_{55} &= P_5^T B_1 + B_1^T P_5 \\
&\quad - P_{10}^T - P_{10} \\
\Phi_{56} &= P_5^T B_2 + B_1^T P_6 \\
\Phi_{57} &= P_5^T C_0 + B_1^T P_7 \\
\Phi_{66} &= P_6^T B_2 + B_2^T P_6 \\
&\quad - P_{13}^T - P_{13} \\
\Phi_{67} &= P_6^T C_0 + B_2^T P_7 \\
\Phi_{77} &= P_7^T C_0 + C_0^T P_7 \\
\Phi_{99} &= P_9^T + P_9 - \beta K_\omega.
\end{aligned}$$

Il est clair que si $\Phi < 0$, la condition (41) du Lemme 2 est satisfaite.

L'introduction de l'inégalité supplémentaire :

$$\mathcal{H} := \begin{bmatrix} H & I_n \\ I_n & P \end{bmatrix} > 0,\ H \geq P^{-1}$$

permet de réduire le problème d'optimisation non linéaire (47) au problème linéaire min $\mathrm{tr}(H)$. En utilisant la propriété du complément de Schur, on peut démontrer que la minimisation de la trace de $H$ implique la minimisation de la trace de $P^{-1}$ [48].

Pour prendre en compte les restrictions physiques sur les entrées de commande, on considére l'inégalité suivante :

$$\mathcal{I}_j := \begin{pmatrix} \left(\frac{\sigma}{\beta}+\varsigma\right)\bar{u}_2^j P & k_2^{jT} \\ * & \bar{u}_2^j \end{pmatrix} \geq 0 \qquad j=1,...,m,$$

où $k_2^j$ est la ligne $j$ de la matrice $K_2$.

Le résultat sur l'ellipsoïde minimal attractif pour le système (42) est énoncé dans le théorème suivant.

**Théorème 3** *Considérons le problème d'optimisation suivant*

$$\min \ tr(H)$$

*sujet à*

$$\begin{cases} \Lambda := \{H, P, S, R, K_0, K_1, K_2, P_k, \beta\}, \quad k=1,...,14, \\ \Phi < 0, \\ \mathcal{H} > 0, \\ \mathcal{I}_j \geq 0 \quad j=1,...,m, \\ P>0, \ S>0, \ R>0, \ \beta>0, \ \sigma>0, \ \varsigma>0, \end{cases}$$

*avec une solution optimale* $\hat{\Lambda} := \left\{\hat{H}, \hat{P}, \hat{S}, \hat{R}, \hat{K}_0, \hat{K}_1, \hat{K}_2, \hat{P}_k, \hat{\beta}\right\}, k=1,...,14.$ *L'ellipsoïde* $\mathcal{E}(0,\tilde{P})$ *déterminé par la matrice* $\left(\frac{\sigma}{\hat{\beta}}+\varsigma\right)\hat{P}$*, est un ensemble minimal attractif pour les trajectoires du système (42) en boucle fermée avec les contrôleurs (44-46) pour* $t \geq T_a(\phi,\varsigma) = \frac{1}{\sigma}\ln\left(\frac{\alpha\|\phi\|_h^2}{\varsigma} - \frac{\beta}{\varsigma\sigma}\right)$.

Les dynamiques axiales et de torsion couplées de la tige de perforation sont décrites au moyen de l'équation suivante :

$$\begin{aligned} \dot{x}(t) + D\dot{x}(t-2\Gamma) = A_0x(t) + A_1x(t-2\Gamma) + B_1u_1(t-\Gamma) + B_2u_2(t) \\ + C_0f(x_1(t)+\Omega_0) + C_1f(x_1(t-2\Gamma)+\Omega_0) + \omega, \end{aligned} \tag{49}$$

où $x(t) = \begin{bmatrix} x_1(t) & x_2(t) & x_3(t) \end{bmatrix}^T$,

$$x_1(t) = z(t) - \Omega_0, \qquad x_2(t) = y(t) = Y(t) - \mathrm{ROP}t, \qquad x_3(t) = \dot{y}(t),$$

$$A_0 = \begin{bmatrix} -\Psi - \frac{c_\mathrm{b}}{I_\mathrm{B}} & 0 & 0 \\ 0 & 0 & 1 \\ -\frac{\mu_1 c_\mathrm{b}}{m_0} & -\frac{k_0}{m_0} & -\frac{c_0}{m_0} \end{bmatrix}, \ A_1 = \begin{bmatrix} \frac{\Upsilon c_\mathrm{b}}{I_\mathrm{B}} - \Upsilon\Psi & 0 & 0 \\ 0 & 0 & 0 \\ \frac{\mu_1 c_\mathrm{b}}{m_0} & 0 & 0 \end{bmatrix}, \ B_1 = \begin{bmatrix} \Pi \\ 0 \\ 0 \end{bmatrix}$$

$$B_2 = \begin{bmatrix} 0 \\ 0 \\ -\frac{c_0}{m_0} \end{bmatrix}, \ C_0 = \begin{bmatrix} -\frac{1}{I_\mathrm{B}} \\ 0 \\ -\frac{\mu_1}{m_0} \end{bmatrix}, \ C_1 = \begin{bmatrix} \frac{\Upsilon}{I_\mathrm{B}} \\ 0 \\ 0 \end{bmatrix}, \ D = \begin{bmatrix} -\Upsilon & 0 & 0 \\ 0 & 0 & 0 \\ 0 & 0 & 0 \end{bmatrix},$$

le retard est donné par $\Gamma = \sqrt{\frac{I}{GJ}}L$, les entrées de commande $u_1$ et $u_2$ correspondent à la vitesse angulaire $\Omega(t)$ fournie par le moteur et au taux de perforation ROP, respectivement, $f(\cdot)$ correspond au terme non linéaire du modèle du couple sur le trépan :

$$T_{\text{nl}}\left(z(t)\right) = W_{\text{ob}} R_{\text{b}} \left(\mu_{\text{cb}} + (\mu_{\text{sb}} - \mu_{\text{cb}}) \text{e}^{-\frac{\gamma_{\text{b}}}{v_{\text{f}}}|z(t)|}\right) \text{sign}\left(z(t)\right). \tag{50}$$

Les paramètres utilisés dans les simulations suivantes sont donnés dans (12). Nous considérons qu'à cause des conditions physiques du système, l'entrée de commande $u_2(t)$ est soumise à la restriction $|u_2(t)| \leq \bar{u}_2$ où $\bar{u}_2 = 100$, et que la condition initiale $\phi$ satisfait $\|\phi\|_h = 2$. Pour obtenir la synthèse des contrôleurs (44-45) en utilisant le Théorème 3, un outil numérique approprié pour résoudre les problèmes qui impliquent des restrictions bilinéaires, comme le paquet "PENBMI" de MATLAB, est requis.

Le taux maximum de décroissance exponentielle pour laquelle les conditions du Théorème 3 sont satisfaites est $\sigma = 1.5$. La solution au problème d'optimisation est donnée par :

$$P = \begin{bmatrix} 6.1522 & 2.5914 & 0.2713 \\ 2.5914 & 13.0989 & 3.4865 \\ 0.2713 & 3.4865 & 1.4203 \end{bmatrix}, \quad \text{eig}(P) = \begin{Bmatrix} 0.4238 \\ 5.4240 \\ 14.8236 \end{Bmatrix},$$

$$\lambda_{\max}(S) = 318.9226, \ \lambda_{\max}(R) = 3.9407, \ \beta = 1.3620, \ \alpha = 254.1923,$$

$$K_0 = \begin{bmatrix} -0.1272 & 0 & 0 \end{bmatrix}, \quad K_1 = \begin{bmatrix} 0.4429 & 0.0196 & 0.0088 \end{bmatrix},$$

$$K_2 = \begin{bmatrix} 24.3378 & 305.7411 & 120.3589 \end{bmatrix}.$$

En choisissant $\varsigma = 0.1$ on observe que les trajectoires du système de perforation sont contenues dans l'ellipsoïde $\mathcal{E}_{\tilde{P}} = \left\{x \in \mathcal{R}^n : x^T \tilde{P} x \leq 1\right\}$, pour $t \geq T_a(\phi, \varsigma) = 0.6667 \ln\left(2541.9 \|\phi\|_h^2 - 9.0800\right) = 6.1510\text{s}$. La Figure 9 montre l'ellipsoïde minimal attractif pour les trajectoires du système (49).

Les résultats de simulation montrent une performance satisfaisante des contrôleurs proposés, cependant, en vue de la réponse oscillatoire des trajectoires dans le cas de boucle fermée, le temps dans lequel les vibrations de torsion sont éliminées et la complexité de la solution des inégalités matricielles, nous pouvons conclure que le contrôleur non-linéaire (39) qui est dérivé de l'approche multimodèle est la meilleure solution pour éliminer le phénomène de coller-glisser. Cependant, la méthode de l'ellipsoïde attractif, bien qu'elle implique certain conservatisme dérivé de l'introduction des variables de pondération libre de l'approche descripteur, fournit une solution

intégrale au problème des vibrations couplées. Cette stratégie permet d'obtenir la synthèse de contrôleurs stabilisants qui garantissent l'élimination des vibrations axiales et de torsion même en présence de restrictions de saturation dans l'entrée de commande.

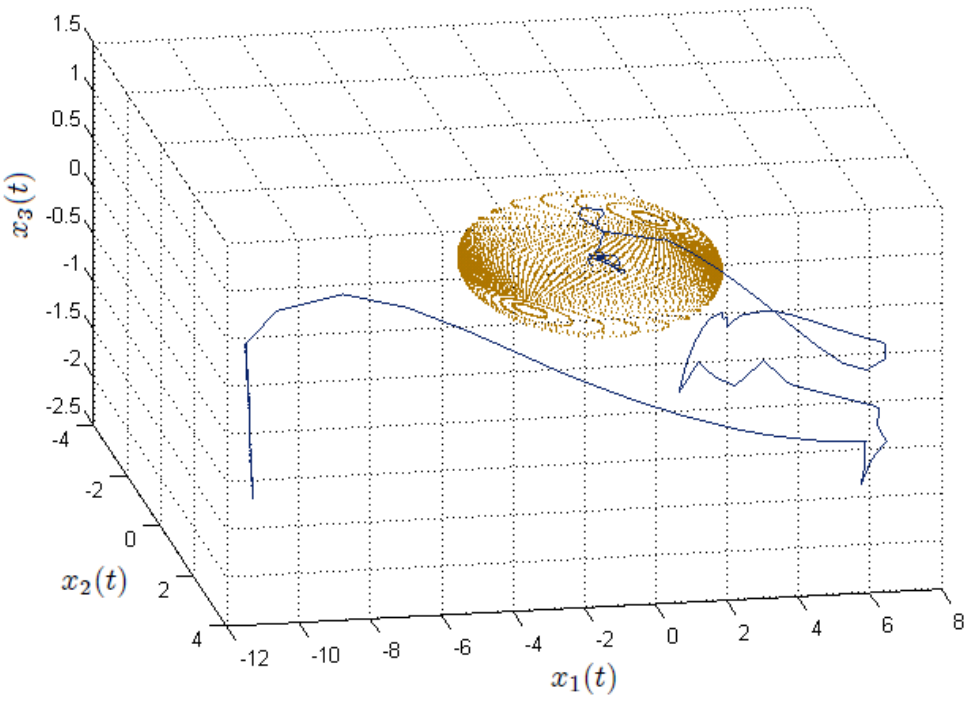


FIGURE 9 – $x_1(t)$ vs. $x_2(t)$ vs. $x_3(t)$ en convergeant à l'ellipsoïde $\mathcal{E}(0, \tilde{P})$.

# Conclusions générales et perspectives

Le document présent résume les contributions principales dérivées d'une recherche exhaustive sur la modélisation, l'analyse et la commande des vibrations qui se produisent dans le processus de perforation.

Le phénomène de coller-glisser, qui constitue la source principale de défaillances dans les opérations de forage, est le point focal de ce projet de thèse, cependant, puisque l'apparition de vibrations de torsion contribue à l'excitation des oscillations axiales, une attention particulière a été portée au couplage des vibrations.

Sur la base des différentes stratégies de modélisation proposées pour décrire la dynamique de la tige de forage, des analyses de stabilité et stabilisabilité ont été réalisées. Certes, l'équation d'onde est la description la plus proche de la réalité, car elle reproduit le comportement distribuée du système, mais

la complexité des simulations nous conduit à dériver un modèle simplifié qui représente raisonnablement le comportement du système et qui permet d'exploiter les techniques de la théorie de commande pour systèmes à retards.

L'approche des inégalités matricielles dérivé de la théorie de Lyapunov est un outil efficace pour l'analyse de stabilité et pour la commande des systèmes dynamiques. Grâce à cet outil le système de perforation a été analysé en utilisant les différentes stratégies de modélisation proposées.

Nous avons conçu des contrôleurs stabilisants linéaires et non linéaires pour l'élimination des vibrations couplées impliquant la mesure de certaines variables à l'extrémité inférieure de la tige.

Nous pouvons conclure que le modèle à retards de type neutre constitue une représentation simple et fiable de la dynamique de forage. Par ailleurs, les techniques de commande proposées pour supprimer les oscillations de forage sont nouvelles, simples et efficaces par rapport à celles déjà existantes. Ils permettent l'opération de forage à faible vitesse, ce qui est impossible sans une loi de commande. Les stratégies présentées ont un large domaine d'application puisque elles peuvent être généralisées pour traiter de nombreux autres problèmes d'ingénierie, physiques, biologiques, etc.

## Perspectives

Pour décrire complètement le comportement de la tige de perforation pendant le processus de forage, les travaux futurs, doivent inclure un modèle approprié pour les dynamiques des vibrations latérales. De plus, des paramètres inconnus et variants dans le temps du système et des entrées de commande supplémentaires pourraient être pris en considération.

Il serait aussi intéressant d'analyser le comportement de la tige de forage dans différents environnements opérationnels, par exemple, le forage offshore, dans lequel le procédé est effectué par une plate-forme située en mer.

Un large éventail de lignes de recherche peut émerger de ce projet de thèse, puisque les phénomènes vibratoires qui se produisent fréquemment dans les différents types de dispositifs et de machines représentent une source majeure d'échec, de mauvaises performances et de problèmes de sécurité.

# Resumen

## Introducción General

La presencia de intensas vibraciones en la sarta de perforación ha sido considerada por muchos años como una de las más relevantes causas del bajo rendimiento en el proceso de perforación. En la industria del petróleo, la mejora del desempeño en las operaciones de perforación es una cuestión crucial de interés económico.

A pesar del avance tecnológico, los fenómenos vibracionales que afectan considerablemente los costos de perforación siguen ocurriendo. Antes de 1960 los estudios realizados para resolver el problema se enfocaron en el tipo y resistencia del material usado para la construcción de la sarta de perforación, sin embargo las tendencias cambiaron, los análisis recientes estudian el comportamiento dinámico de la barra [54].

Los diferentes tipos de vibración que afectan la tasa de penetración y causan el deterioro prematuro de los componentes del sistema pueden clasificarse en tres categorías que dependen de la dirección en la que las oscilaciones se producen, estas son:

- torsionales o rotacionales, también conocidas como fenómeno atore-deslizamiento (stick-slip),

- axiales o longitudinales, caracterizadas por el rebote del dispositivo de corte (bit-bounce),

- laterales o transversales, movimiento giratorio irregular que ocurre cuando la barra opera fuera de balance (whirling).

La presencia de vibraciones impide un desempeño eficiente del proceso de perforación, puesto que causa un deterioro prematuro del equipo [79], ocasiona un uso excesivo de energía [78] y puede inducir inestabilidad en el pozo reduciendo el control direccional [37].

A continuación se presenta una breve descripción de las causas y consecuencias posibles de los tipos de vibración mencionados.

**- Vibración Torsional.** La aplicación de una velocidad constante en el extremo superior de la barra no necesariamente se traduce en un movimiento de rotación constante del dispositivo de corte, de hecho, la velocidad angular en el extremo inferior exhibe comúnmente grandes fluctuaciones de amplitud durante una fracción significativa del tiempo de perforación. Esta velocidad rotacional no uniforme se debe principalmente a la gran flexibilidad torsional de la barra [105]. Las vibraciones torsionales causan una rotación irregular que daña las conexiones de los segmentos de tubería que conforman la sarta y el dispositivo de corte. Además el proceso de perforación se prolonga puesto que las vibraciones reducen la tasa de penetración. Las oscilaciones torsionales se detectan por las fluctuaciones en la potencia necesaria para mantener una velocidad constante de rotación.

**- Vibración Axial**. Las oscilaciones longitudinales involucran el movimiento de la barra a lo largo del eje, debido al acoplamiento de los componentes del mecanismo, la presencia de éstas puede indirectamente inducir desplazamientos laterales de la barra [104]. Las vibraciones axiales causan que el dispositivo de corte (broca) colisione contra el suelo repetidamente lo que puede ocasionar su destrucción. El patrón de rebote del dispositivo de corte está relacionado con el uso de un específico tipo de broca conocida como broca "tricone.º de rodillo cónico que está formada por múltiples lóbulos, lo que conduce a una interacción irregular con el fondo del pozo.

**- Vibración Lateral.** Las oscilaciones longitudinales pueden presentarse sin ser detectadas en la superficie. En el extremo inferior, la barra colisiona con las paredes del pozo creando un orificio excéntrico y dañando gravemente los componentes del sistema [83]. Las vibraciones laterales deterioran severamente la estructura del pozo y afectan el direccionamiento de la perforación [54]. El movimiento giratorio irregular se produce cuando el centro de gravedad de los collares de perforación no está situado exactamente en la línea central del pozo, ocasionando una inclinación de la barra [116]. Este comportamiento se intensifica debido al efecto combinado del fluido de amortiguación, la remoción de dispositivos estabilizadores, y el roce de la sarta contra las paredes del pozo [115].

Debido a todos los problemas que acarrea el fenómeno vibracional, se han propuesto diversos métodos para eliminar o al menos reducir las oscilaciones en la sarta. Los ingenieros petroleros y expertos han desarrollado algunos métodos empíricos. Los más comunes son la reducción en el peso que soporta la broca y el incremento de la velocidad angular en el extremo superior. Estas soluciones han demostrado ser útiles para prevenir la ocurrencia de vibraciones, sin embargo, implican un bajo desempeño en la tasa de perforación.

Existen algunas soluciones más sofisticadas para reducir el fenómeno de atore-deslizamiento, a continuación enlistamos algunas de estas.

### Realimentación del torque

Con el método de control por realimentación del torque, la velocidad de la mesa giratoria se modifica en función de las variaciones de torsión para evitar oscilaciones de atore-deslizamiento. La velocidad en la superficie se ajusta de tal modo que las ondas torsionales que viajan a lo largo de la barra sean amortiguadas en vez de reflejarse nuevamente hacia abajo de la sarta. Un inconveniente de este método es que necesita una medición precisa del torque, que en la práctica es difícil de obtener [51], [67].

### Sistema rotatorio de torque suave (Soft Torque Rotary System STRS)

La compañía holandesa *Shell*, consciente del problema que implica una medición precisa del torque, centró su investigación en la mejora del control de vibraciones por realimentación del torque durante la década de 1990 [54], [55]. El método desarrollado consiste en calcular el torque en el extremo inferior mediante el uso de la corriente del motor, y usarlo en el lazo de realimentación. Las oscilaciones se reducen mediante una sintonización adecuada del controlador, lo que hace que el sistema se comporte como un amortiguador sintonizado activo, similar a los amortiguadores que se utilizan para evitar oscilaciones inducidas por el viento en las líneas de transmisión de energía. Este sistema fue nombrado sistema rotatorio de torque suave. Pruebas experimentales muestran una mejora del desempeño de la perforación y una reducción considerable de fallas en el mecanismo. El sistema rotatorio de torque suave ha estado disponible comercialmente por muchos años y es usado en diferentes lugares al rededor del mundo.

### Control Proporcional-Integral-Derivativo (PID)

Un método simple para tratar el problema de atore-deslizamiento fue presentado por Pavone y Desplans en 1994 [89]. Ellos encontraron que a través de un análisis de estabilidad se pueden determinar los parámetros de un controlador Proporcional-Integral-Derivativo que elimina las oscilaciones torsionales. Los datos analizados se obtuvieron del sistema TRAFOR que es un mecanismo de medición desarrollado por el Institut Français du Pétrole. Un resultado importante de esta investigación fue la relación encontrada entre el torque y la velocidad en el extremo inferior.

### Control $\mathcal{H}_\infty$

En 1998 Serrarens, van de Molengraft y van den Steen propusieron un método de control $\mathcal{H}_\infty$ para suprimir las oscilaciones de atore-deslizamiento [107]. El control $\mathcal{H}_\infty$ se ha usado ampliamente para tratar problemas vibracionales, como por ejemplo en los procesos de corte donde se usa para eliminar las oscilaciones (chattering) en la maquinaria. El controlador $\mathcal{H}_\infty$ suprime las vibraciones a pesar de que es lineal e invariante en el tiempo y la fricción sobre la broca es fuertemente no lineal. Este método no ha sido probado en plataformas reales, sin embargo, los resultados obtenidos en prototipos experimentales muestran un buen desempeño.

### D-OSKIL

Un método alternativo para eliminar las oscilaciones torsionales consiste en usar el peso sobre la broca como entrada de control adicional. El método llamado *Drilling OScillation KILler* (D-OSKIL) fue introducido por Canudas-de-Wit et al. en 2005 [26], [27]. Para asegurar una tasa de perforación adecuada, es necesario mantener cierto peso sobre la broca, sin embargo, el incremento de esta variable conduce a oscilaciones torsionales. El objetivo del método propuesto es encontrar una relación óptima entre la tasa de perforación y el peso sobre la broca. Cuando las oscilaciones torsionales se detectan, el método permite una reducción del peso sobre el dispositivo de corte a través de la manipulación de la fuerza en el gancho de elevación de la sarta de perforación en la plataforma, la barra de perforación se eleva ligeramente para reducir el peso sobre la broca. Los resultados obtenidos mediante pruebas experimentales en un prototipo de laboratorio muestran una reducción considerable de las oscilaciones torsionales.

### Amortiguador de vibraciones activo

En 2007, Zamanian, Khadem and Ghazavi estudiaron las vibraciones de atore-deslizamiento en una barra de perforación con una broca de arrastre [122]. Esta investigación mostró que las vibraciones torsionales pueden evitarse incrementando el amortiguamiento del fluido o lodo de perforación y seleccionando adecuadamente la tasa de amortiguamiento activo. Las mediciones del movimiento relativo de la broca y la sarta de perforación son tomadas en tiempo real durante el proceso, de esta manera las propiedades de amortiguación se modifican constantemente.

### Compensación del error de modelado

En 2008, Puebla y Álvarez-Ramírez introdujeron un enfoque de control basado en compensación del error de modelado para eliminar el fenómeno

atore-deslizamiento. El esquema de control de realimentación sugerido permite lidiar con las incertidumbres en el modelo de fricción y en los parámetros del sistema. La barra de perforación se modela como un péndulo torsional, accionado por un motor eléctrico, que consta de inercias amortiguadas acopladas mecánicamente por un eje elástico. En [93] se exponen dos esquemas de control: el esquema de control en cascada, que usa las propiedades eléctricas del motor como única entrada de control, y el esquema de control descentralizado, que regula las vibraciones en la mesa giratoria a través del motor y las vibraciones en el extremo inferior de la barra mediante el peso sobre la broca. Las simulaciones numéricas presentadas muestran que el método elimina satisfactoriamente las vibraciones. No existen sistemas basados en este método de control disponibles comercialmente.

### Controladores de vibración con estabilidad garantizada

Nuestras contribuciones al diseño de control para la eliminación de oscilaciones en un sistema de perforación están basadas en diferentes enfoques de modelado. En [46] presentamos un modelo de parámetros distribuidos que describe la dinámica torsional de la sarta. La ecuación de onda unidimensional acoplada a condiciones mixtas en las fronteras describe el comportamiento oscilatorio a lo largo de la barra. En este trabajo se presentaron cotas de las soluciones del sistema. En [99], con base en esta estrategia de modelado, se propone una función de energía, que permitiendo un análisis de disipatividad del sistema, conduce al diseño de un controlador para la eliminación del fenómeno atore-deslizamiento. En este trabajo, derivamos un modelo simplificado representado por una ecuación con retardos de tipo neutral obtenido a través de la transformación de D'Alembert que simplifica el análisis y facilita el cómputo de simulaciones del sistema. Para la validación del modelo propuesto, hemos examinado algunas estrategias prácticas para eliminar las oscilaciones torsionales utilizadas en plataformas reales. El modelo del torque sobre el dispositivo de corte, que representa la interacción entre la formación de roca y la broca, es descrito por una función no lineal que depende de la velocidad angular en el extremo inferior y está sujeta a la función signo. En [100], se presenta un análisis de estabilidad exponencial del sistema de perforación utilizando la teoría de sistemas conmutados. En [101], diseñamos una ley de control no lineal para eliminar las oscilaciones torsionales a través de una representación politópica del modelo con retardos. En [102], con base en un modelo que describe el acoplamiento entre las vibraciones torsionales y axiales, se diseñaron dos controladores lineales para eliminar simultáneamente el fenómeno de atore-deslizamiento y el de rebote de la broca, mediante el método del elipsoide atractivo. Las entradas de control corresponden a la velocidad angular provista por la mesa giratoria para eliminar las vibraciones torsio-

nales, y la tasa de perforación para suprimir las oscilaciones axiales. Puesto que todos los enfoques presentados están basados en la teoría de Lyapunov, la estabilidad del sistema, en cualquier caso, está garantizada. A lo largo de este trabajo se explican de forma detallada las metodologías propuestas que atacan el problema vibracional.

### Motivación y Objetivos

Conforme la tecnología evoluciona, se plantean nuevos desafíos y la complejidad del proceso de perforación de pozos aumenta. El desarrollo de nuevas tecnologías ha permitido la exploración petrolera en aguas profundas, lo que exige soluciones de control cada vez más sofisticadas para la eliminación integral de oscilaciones no deseadas. Los trabajos que abordan el problema vibracional en la barra de perforación, por lo regular, han analizado de manera individual cada uno de los modos de oscilación, por lo que existen principalmente soluciones particulares a cada problema de vibración. Además, sólo algunos trabajos proveen un análisis de estabilidad de las estrategias de control propuestas.

En esta tesis, desarrollamos un análisis de las oscilaciones acopladas que ocurren durante el proceso de perforación que permite el diseño de controladores estabilizantes para eliminar simultáneamente los fenómenos de atore-deslizamiento y de rebote de la broca. Los análisis de estabilidad del sistema de perforación presentados están basados en la teoría de Lyapunov.

El primer objetivo de la tesis consiste en encontrar una descripción matemática precisa del comportamiento mecánico del sistema de perforación. El modelo debe reproducir eficazmente el acoplamiento entre los modos de vibración observados en las plataformas reales.

El segundo objetivo de la investigación es el desarrollo de un análisis de estabilidad y el diseño de leyes de control para eliminar, o al menos reducir a niveles aceptables, la amplitud de las oscilaciones de perforación más críticas.

## Capítulo 2

En el proceso de perforación para extracción de petróleo, el pozo se crea mediante un dispositivo de corte llamado broca o barrena. La columna de perforación consta del mecanismo inferior de perforación (BHA, por sus siglas en inglés Bottom Hole Assembly) y de segmentos tubulares unidos para formar la sarta de perforación. El mecanismo inferior de perforación consta de la broca, dos o más estabilizadores que impiden el desbalance de la columna y una serie de secciones de tubo más pesados conocida como collares de perforación.

A medida que la perforación avanza en profundidad, la longitud de la columna debe aumentarse adicionando secciones de tubería. Un elemento importante del proceso es el lodo o fluido de perforación que tiene la función de limpiar, enfriar y lubricar la broca. La sarta de perforación se hace girar desde la superficie mediante un motor eléctrico que acciona la mesa giratoria.

La complejidad del sistema de perforación plantea desafíos de modelado y control. El modelo debe describir con precisión los fenómenos más importantes que ocurren en plataformas reales y tiene que ser lo suficientemente simple para propósitos de análisis.

La ecuación de onda es ampliamente utilizada para reproducir el comportamiento oscilatorio de los sistemas físicos. En los años sesenta, se llevaron a cabo algunos análisis utilizando la ecuación de onda para describir el comportamiento torsional de la sarta de perforación [6], [39]. Esta estrategia de modelado también se adoptó en [28], [111], [112] y [113].

Normalmente, cuando un modelo de parámetros distribuidos está sujeto a no linealidades e incertidumbres, el análisis y las simulaciones no son tareas fáciles. Es conveniente entonces, obtener un modelo más simple que involucre las variables de interés principal. Por medio de una transformación directa es posible derivar un modelo de entrada-salida descrito por una ecuación con retardos en el tiempo de tipo neutral que claramente simplifica el análisis y las simulaciones. El procedimiento que permite transformar una ecuación diferencial parcial en un sistema con retardos de tipo neutral se presentó por primera vez en [3], véase también en [5], [10], [19], [21], [22], [30], [40], [49] y [99].

En este capítulo se introduce la ecuación de onda unidimensional que describe el comportamiento torsional de la columna. El modelo de parámetros distribuidos está sujeto a condiciones de frontera mixtas escogidas de acuerdo al comportamiento observado en ambos extremos de la sarta. Se presenta también la ecuación de tipo neutral que relaciona las variables en ambos extremos de la columna.

## Modelo de parámetros distribuidos

El comportamiento torsional de una columna de perforación de longitud $L$, descrito por el ángulo de rotación $\theta(\xi,t)$, puede ser modelado a través de la ecuación de onda [21], [22], [28], [46], [111], [112], [113]:

$$GJ\frac{\partial^2\theta}{\partial\xi^2}(\xi,t) - I\frac{\partial^2\theta}{\partial t^2}(\xi,t) - \beta\frac{\partial\theta}{\partial t}(\xi,t) = 0, \qquad \xi\in(0,L), \qquad t>0. \tag{51}$$

El ángulo de torsión $\theta$ depende de la coordenada longitudinal $\xi$ y el tiempo $t$, $\beta \geq 0$ es el amortiguamiento viscoso y estructural considerado a lo largo de la

barra, los parámetros $I$, $G$ y $J$ corresponden a la inercia, el módulo de rigidez y el momento geométrico de inercia respectivamente.

Las condiciones en las fronteras son [99]:

$$GJ\frac{\partial\theta}{\partial\xi}(L,t)+I_B\frac{\partial^2\theta}{\partial t^2}(L,t) = -T\left(\frac{\partial\theta}{\partial t}(L,t)\right), \tag{52}$$

$$GJ\frac{\partial\theta}{\partial\xi}(0,t) = c_{\mathrm{a}}\left(\frac{\partial\theta}{\partial t}(0,t)-\Omega(t)\right), \tag{53}$$

donde $I_B$ representa la inercia concentrada en el extremo inferior ($\xi = L$). El torque $T$, que describe la interacción de la broca con la roca, está en función de la velocidad angular del dispositivo de corte. En la frontera superior ($\xi = L$), se considera que la velocidad angular proveniente del motor $\Omega$ no coincide con la velocidad rotacional del extremo superior de la barra $\frac{\partial\theta}{\partial t}(0,t)$, lo que ocasiona una torsión local.

## Modelo con retardos en el tiempo de tipo neutral

Dado que la mayor parte de la disipación de energía en el proceso de perforación se lleva a cabo en la interfaz broca-roca, puede considerarse que el amortiguamiento a lo largo de la estructura $\beta$ es nulo, así, el modelo de parámetros distribuidos (51) se reduce a la ecuación de onda unidimensional:

$$\frac{\partial^2\theta}{\partial\xi^2}(\xi,t)=p^2\frac{\partial^2\theta}{\partial t^2}(\xi,t), \qquad \xi\in(0,L), \qquad p=\sqrt{\frac{I}{GJ}}. \tag{54}$$

Una transformación directa de la ecuación de onda (54) con condiciones de frontera (52-53) permite obtener el siguiente modelo con retardos de tipo neutral que describe el comportamiento de la sarta de perforación [99]:

$$\begin{aligned}\dot{z}(t)-\Upsilon\dot{z}(t-2\Gamma) &= -\Psi z(t)-\Upsilon\Psi z(t-2\Gamma) \\ &\quad -\frac{1}{I_{\mathrm{B}}}T\left(z(t)\right)+\frac{1}{I_{\mathrm{B}}}\Upsilon T\left(z(t-2\Gamma)\right)+\Pi\Omega(t-\Gamma),\end{aligned} \tag{55}$$

donde $z(t)$ es la velocidad angular en el extremo inferior, las constantes involucradas están dadas por:

$$\Pi=\frac{2\Psi c_{\mathrm{a}}}{c_{\mathrm{a}}+\sqrt{IGJ}},\ \Upsilon=\frac{c_{\mathrm{a}}-\sqrt{IGJ}}{c_{\mathrm{a}}+\sqrt{IGJ}},\ \Psi=\frac{\sqrt{IGJ}}{I_{\mathrm{B}}},\ \Gamma=\sqrt{\frac{I}{GJ}}L. \tag{56}$$

Similarmente puede obtenerse una expresión con retardos que describe el comportamiento en el extremo superior:

$$\dot{v}(t)+\Upsilon\dot{v}(t-2\Gamma)=(c_a/\Lambda)\left[\Omega(t)+\Omega(t-2\Gamma)\right]-(2/\Lambda)\left[I_B\dot{z}(t-\Gamma)+T\left(z(t-\Gamma)\right)\right] \tag{57}$$

donde $\dot{v}(t)$ es la velocidad angular en el extremo superior y $\Lambda = c_a + \sqrt{IGJ}$.

La transformación del modelo se lleva a cabo mediante el método de D'Alembert que propone una solución general de la ecuación de onda. Alternativamente, puede hacerse también usando técnicas en el dominio de la frecuencia (transformada de Laplace).

# Capítulo 3

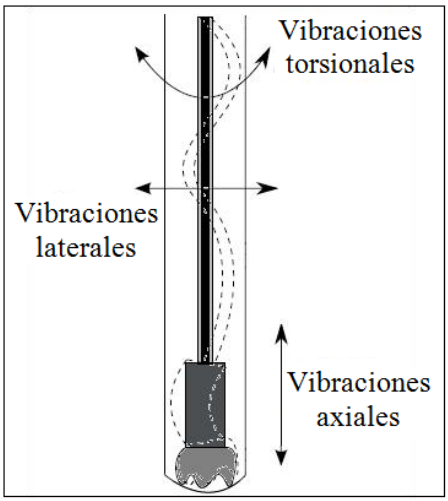


Figura 10: Vibraciones en la barra de perforación.

La interacción de la columna de perforación con el pozo da lugar a tres tipos de oscilaciones que pueden ser clasificarse de acuerdo con la dirección en la que aparecen: torsionales (oscilaciones de atore-deslizamiento), axiales (fenómeno de rebote de la broca) y laterales (movimiento giratorio irregular ocasionado por el desbalance de la barra de perforación).

Este trabajo se enfoca en el estudio del modo de vibración más crítico, el fenómeno atore-deslizamiento. Sin embargo, puesto que la presencia de vibraciones torsionales contribuye a la aparición de oscilaciones axiales, también serán presentados algunos análisis sobre el fenómeno de rebote de la broca.

Este capítulo aborda el problema de modelado de los fenómenos de atore-deslizamiento y de rebote de la broca. También se plantea un enfoque empírico para reducir las vibraciones torsionales. Las estrategias prácticas, que reflejan cualitativamente la experiencia de los ingenieros petroleros y expertos, consisten en manipular adecuadamente algunos parámetros del sistema tales como la velocidad de rotación, el peso sobre la broca y las características del fluido de perforación.

## Dinámicas Torsionales

Generalmente se asume que el incremento de inestabilidades que conducen eventualmente al fenómeno de atore-deslizamiento emerge del modelo friccional que empíricamente captura la interacción entre la roca y la broca.

La ecuación no-lineal siguiente, introducida en [85], permite modelar el fenómeno físico que se produce a nivel de la broca

$$T\left(z(t)\right) = c_{\mathrm{b}} z(t) + W_{\mathrm{ob}} R_{\mathrm{b}} \mu_{\mathrm{b}}\left(z(t)\right) \operatorname{sign}\left(z(t)\right). \tag{58}$$

El término $c_{\mathrm{b}} z(t)$ corresponde a un amortiguamiento viscoso que moela la influencia del lodo o fluido de perforación. El término $W_{\mathrm{ob}} R_{\mathrm{b}} \mu_{\mathrm{b}}\left(z(t)\right)\operatorname{sign}(z(t))$ es un torque de fricción seca que representa el contacto broca-roca. $R_{\mathrm{b}} > 0$ y $W_{\mathrm{ob}} > 0$ son el radio y el peso sobre la broca respectivamente. El coeficiente de fricción seca $\mu_{\mathrm{b}}(z(t))$ es descrito por

$$\mu_{\mathrm{b}}\left(z(t)\right) = \mu_{\mathrm{cb}} + (\mu_{\mathrm{sb}} - \mu_{\mathrm{cb}}) \mathrm{e}^{-\frac{\gamma_{\mathrm{b}}}{v_{\mathrm{f}}}|z(t)|}, \tag{59}$$

donde $\mu_{\mathrm{sb}}, \mu_{\mathrm{cb}} \in (0, 1)$ son los coeficientes de fricción estática y de Coulomb, $0 < \gamma_{\mathrm{b}} < 1$ es una constante que define la tasa de decaimiento.

## Dinámicas axiales

Las vibraciones torsionales están acopladas a las oscilaciones axiales y ocurren simultáneamente. La alta velocidad de la broca causada por el fenómeno atore-deslizamiento puede inducir vibraciones axiales de gran amplitud causando el rebote de la broca.

El modelo del oscilador armónico amortiguado puede utilizarse para describir las dinámicas axiales de la barra de perforación [28]:

$$m_0 \ddot{Y} + c_0 \dot{Y} + k_0 (Y - \mathrm{ROP}t) = -\mu_1 T\left(z(t)\right), \tag{60}$$

donde $Y$, $\dot{Y}$ y $\ddot{Y}$ representan las variables axiales de posición, velocidad y aceleración respectivamente, la tasa de perforación ROP (por sus siglas en inglés Rate Of Penetration) es una velocidad axial impuesta en la superficie , $m_0$, $c_0$, y $k_0$ simbolizan la masa, amortiguamiento y constante de resorte. La constante $\mu_1$ depende de la geometría de la broca [28].

El acoplamiento entre el modelo torsional (55) y el axial (60) se debe al torque sobre la broca que influye en ambas dinámicas.

El cambio de variable $y = Y - \mathrm{ROP}t$ da lugar al siguiente modelo equivalente:

$$m_0 \ddot{y} + c_0 \left(\dot{y} + \mathrm{ROP}\right) + k_0 y = -\mu_1 T\left(z(t)\right). \tag{61}$$

## Resultados de simulaciones

Los parámetros del modelo usados en las simulaciones son los siguientes [28], [84]:

$$\begin{array}{lll} G = 79.3x10^{9}\text{N m}^{-2}, & I = 0.095\text{Kg m}, & L = 1172\text{m}, \\ J = 1.19x10^{-5}\text{m}^{4}, & R_{\text{b}} = 0.155575\text{m}, & v_{\text{f}} = 1, \\ W_{\text{ob}} = 97347\text{N}, & I_{\text{B}} = 89\text{Kg m}^{2}, & c_{\text{a}} = 2000\text{N m s}, \\ \mu_{\text{cb}} = 0.5, & \mu_{\text{sb}} = 0.8, & \gamma_{\text{b}} = 0.9, \\ c_{\text{b}} = 0.03\text{N m s rad}^{-1}, & m_0 = 37278\text{Kg}, & c_0 = 16100\text{kg s}^{-1}, \\ k_0 = 1.55 \times 10^{6}\text{Kg s}^{-2}, & \text{ROP} = 0.01\text{m s}^{-1}, & \mu_1 = 257\text{m}^{-1}. \end{array} \tag{62}$$

Las Figuras 11 y 12 muestran la respuesta del sistema en lazo abierto. La simulación del sistema (55), (58-59) mostrada en la Figura 11 ilustra la presencia del fenómeno atore-deslizamiento.

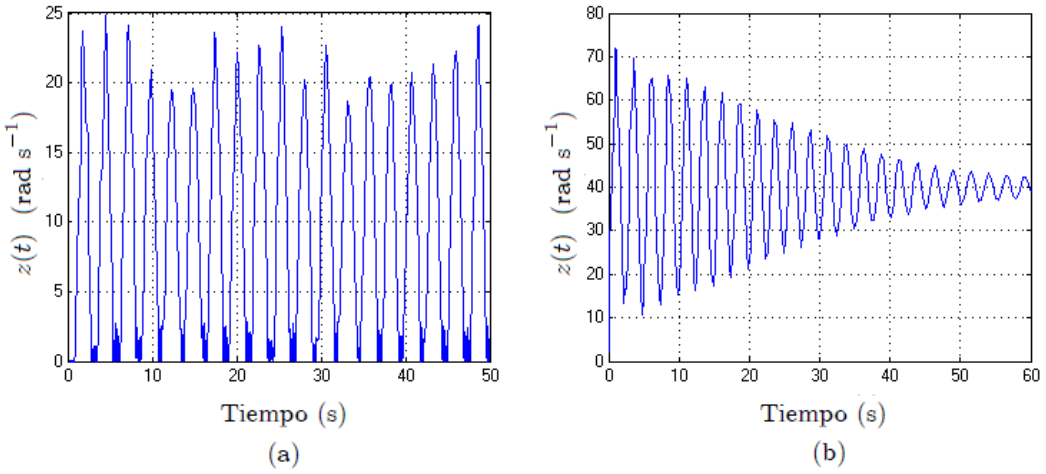


Figura 11: Velocidad angular en el extremo inferior $z(t)$ para: (a) $\Omega(t) = 10\text{rad s}^{-1}$ (fenómeno atore-deslizamiento), (b) $\Omega(t) = 40\text{rad s}^{-1}$.

Se asume que cuando la barra de perforación no está en contacto con el fondo del pozo, la velocidad angular es la misma en ambos extremos. Cuando la broca empieza a interactuar con la formación de roca el sistema es inevitablemente perturbado y las vibraciones axiales y torsionales pueden producirse simultáneamente.

La presencia de fluctuaciones en la velocidad angular en la broca induce la aparición de vibraciones axiales de gran magnitud, como se muestra en la Figura 12.

Está claro que las vibraciones de la columna se derivan de la interacción de la broca con el pozo en el extremo inferior, entonces, para un control eficaz de

vibraciones, se requiere de la medición y realimentación de algunas variables a nivel de la broca.

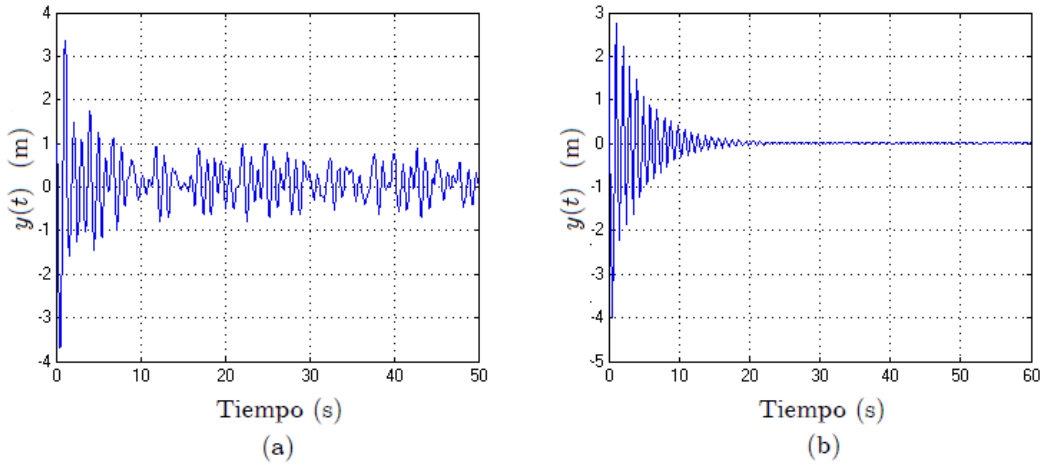


Figura 12: Variable $y = Y - \mathrm{ROP}t$ para: (a) $\Omega(t) = 10\mathrm{rad\ s}^{-1}$ (rebote de la broca), (b) $\Omega(t) = 40\mathrm{rad\ s}^{-1}$.

## Estrategias empíricas para reducir el problema de atore-deslizamiento

En la práctica, el operador del proceso controla desde la superficie parámetros como el peso sobre la broca, las características del fluido de perforación y la velocidad angular provista por la mesa giratoria para optimizar la operación de perforación.

A continuación presentamos las principales estrategias empíricas usadas para prevenir o reducir las oscilaciones torsionales.

### Reducción del peso sobre la broca

De acuerdo con la experiencia en la industria de perforación, considerando una velocidad angular fija en la superficie $\Omega$, la reducción del peso sobre la broca puede inducir la eliminación del fenómeno atore-deslizamiento.

### Incremento de la velocidad angular provista por la mesa giratoria

Pruebas experimentales indican una atenuación del fenómeno atore-deslizamiento por medio de un incremento en la velocidad del extremo superior.

### Introducción de una ley de variación del peso sobre la broca

Una solución alternativa para eliminar las vibraciones de atore-deslizamiento es la manipulación del peso sobre la broca. En [84] se propone la siguiente ley de variación:

$$W_{\mathrm{ob}}(z(t)) = K_{\mathrm{w}} \left| z(t) \right| + W_{\mathrm{ob0}}, \tag{63}$$

donde $W_{\mathrm{ob0}} > 0$ y $W_{\mathrm{ob}} > W_{\mathrm{ob0}}$. La expresión (63) implica una reducción del peso sobre la broca cuando disminuye la velocidad angular de la broca $z(t)$ y un valor mínimo del peso sobre la broca $W_{\mathrm{ob0}}$ para garantizar una tasa de perforación adecuada.

### Incremento del amortiguamiento en el extremo inferior

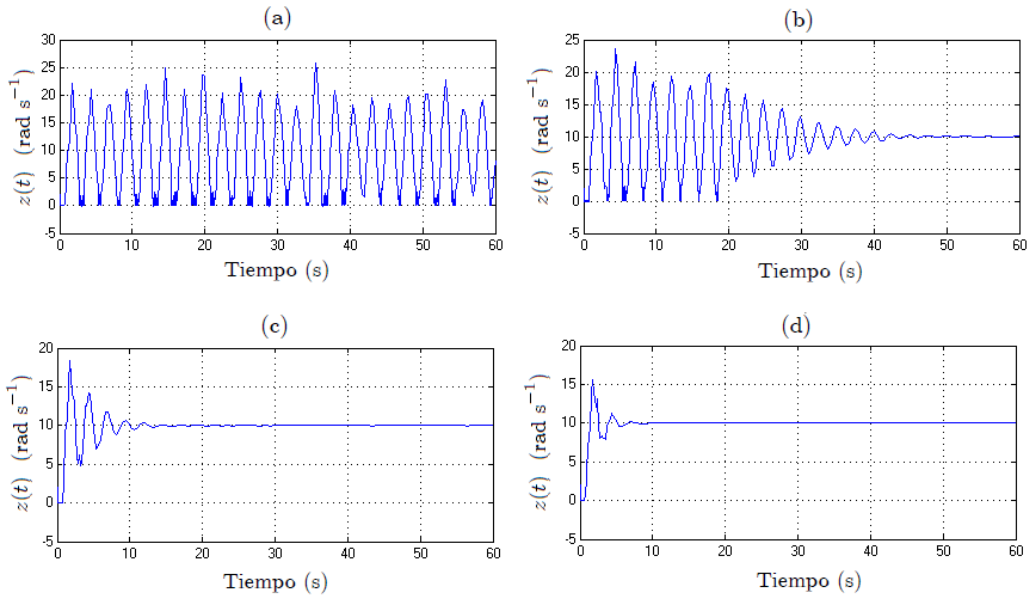


Figura 13: Velocidad angular en el extremo inferior para diferentes valores de $c_{\mathrm{b}}$ (N m s rad$^{-1}$): (a) 0.8, (b) 15, (c) 65, (d) 150.

Otra estrategia para la atenuación de oscilaciones torsionales consiste en incrementar el amortiguamiento al nivel de la broca. Esto puede hacerse en la práctica mediante la manipulación de las características del lodo de perforación.

La Figura 13 muestra las trayectorias de la velocidad angular en el extremo inferior del sistema (55) acoplado al modelo del torque (58-59) para diversos

valores del coeficiente de amortiguamiento $c_{\mathrm{b}}$, indicando que el incremento de este coeficiente reduce el fenómeno de atore-deslizamiento.

Se concluye que las estrategias empíricas reducen satisfactoriamente la amplitud de las oscilaciones de perforación, sin embargo, éstas no pueden garantizar un desempeño óptimo del proceso. El aumento de la velocidad de rotación puede causar problemas de vibración lateral, y además, una reducción sustancial del peso sobre la broca podría detener la perforación. Las directrices operacionales empíricas no son suficientes para eliminar las vibraciones de perforación, por lo que se requiere la introducción de acciones de control. Los siguientes dos capítulos abordan el diseño de controladores para la eliminación de vibraciones no deseadas en la columna de perforación.

# Capítulo 4

En este capítulo, se aborda el problema de análisis de la estabilidad y la reducción de las vibraciones de perforación en el marco de los sistemas de parámetros distribuidos.

Una función de energía permite analizar la disipatividad del sistema y conduce al diseño de una ley de control que garantiza la supresión del fenómeno atore-deslizamiento. Este enfoque se basa en la ecuación de onda que describe el comportamiento torsional de la columna de perforación.

En este capítulo también se aborda el problema de vibraciones acopladas. Desarrollamos un enfoque de desigualdades matriciales para una clase de sistemas en el que la ecuación de onda está acoplada a la ecuación diferencial ordinaria. Este enfoque permite la síntesis de controladores estabilizantes que garantizan la eliminación simultánea de los fenómenos de atore-deslizamiento y rebote de la broca.

## Análisis de disipación de energía

La siguiente ecuación corresponde al modelo normalizado del sistema de perforación

$$z_{tt}(\sigma,t) = a z_{\sigma\sigma}(\sigma,t) - d z_t(\sigma,t), \quad t>0, \quad 0<\sigma<1, \tag{64}$$

donde $a=\frac{GJ}{IL^2}$ y $d=\frac{\beta}{I}$, con condiciones de frontera mixtas

$$\begin{aligned} z_\sigma(0,t) &= g\left(z_t(0,t)-u_1(t)\right), \quad \sigma\in(0,1), \quad t>0, \\ z_\sigma(1,t) &= -k z_t(1,t) - q\mu_{\mathrm{b}}(z_t(1,t))\mathrm{sign}(z_t(1,t)) - h z_{tt}(1,t), \end{aligned} \tag{65}$$

$u_1(t)$ es la velocidad angular provista por la mesa giratoria y $g=\frac{c_a L}{GJ}$, $k=\frac{c_b L}{GJ}$, $q=\frac{W_{ob}R_b L}{GJ}$, $h=\frac{I_B L}{GJ}$.

Considere la siguiente función de energía

$$E(t) = \int_0^1 a z_\sigma^2(\sigma,t)d\sigma + \int_0^1 z_t^2(\sigma,t)d\sigma + ahz_t^2(1,t). \tag{66}$$

Su derivada con respecto al tiempo, a lo largo de las trayectorias de (64-65) es:

$$\begin{aligned}\frac{d}{dt}E(t) &= 2a\int_0^1 z_\sigma(\sigma,t)z_{t\sigma}(\sigma,t)d\sigma + 2az_t(1,t)(-kz_t(1,t)\\ &\quad -q\mu_{\mathrm{b}}(z_t(1,t))\mathrm{sign}(z_t(1,t)) - hz_{tt}(1,t))\\ &\quad -2agz_t(0,t)\left(z_t(0,t)-u_1(t)\right)\\ &\quad -2a\int_0^1 z_\sigma(\sigma,t)z_{t\sigma}(\sigma,t)d\sigma - 2d\int_0^1 z_t(\sigma,t)z_t(\sigma,t)d\sigma\\ &\quad +2ahz_t(1,t)z_{tt}(1,t),\end{aligned}$$

puesto que

$$\mu_{\mathrm{b}}(z_t(1,t))\mathrm{sign}(z_t(1,t))z_t(1,t) = \mu_{\mathrm{b}}(z_t(1,t))\left|z_t(1,t)\right|,$$

se obtiene,

$$\begin{aligned}\tfrac{d}{dt}E(t) = &-2aq\mu_{\mathrm{b}}(z_t(1,t))\left|z_t(1,t)\right| - 2d\textstyle\int_0^1 z_t^2(\sigma,t)d\sigma\\ &-2agz_t(0,t)\left(z_t(0,t)-u_1(t)\right) - 2akz_t^2(1,t).\end{aligned} \tag{67}$$

Para asegurar la disipación de energía, la ley de control $u_1(t)$ debe garantizar la negatividad de (67).

Escogiendo la estructura siguiente para $u_1(t)$,

$$u_1(t) = (1-c_1)z_t(0,t) + 2c_1z_t(1,t) - c_1\frac{\left(z_t(1,t)\right)^2}{z_t(0,t)}, \tag{68}$$

con $c_1 > 0$, se obtiene

$$\begin{aligned}\tfrac{d}{dt}E(t) = &-2aq\mu_b(z_t(1,t))\left|z_t(1,t)\right| - 2d\textstyle\int_0^1 z_t^2(\zeta,t)d\zeta\\ &-2agc_1\left(z_t(1,t)-z_t(0,t)\right)^2\\ &-2akz_t^2(1,t).\end{aligned}$$

Tomando en cuenta que $\mu_b(z_t(1,t)) > 0$ y $a$, $q$, $k$, $d$, $g$ son constantes positivas, entonces, $\frac{d}{dt}E(t) \leq 0$, y la disipación de energía en el sistema está garantizada. Intuitivamente, la disipación de energía podría corresponder a la atenuación de oscilaciones torsionales, lo que sería confirmado mediante una simulación del sistema en lazo cerrado con la ley de control (68).

La Figura 14 muestra el resultado de la simulación del modelo (55), (58-59) en lazo cerrado con el controlador (68). Claramente, la ley de control propuesta conduce a la reducción de las vibraciones de atore-deslizamiento.

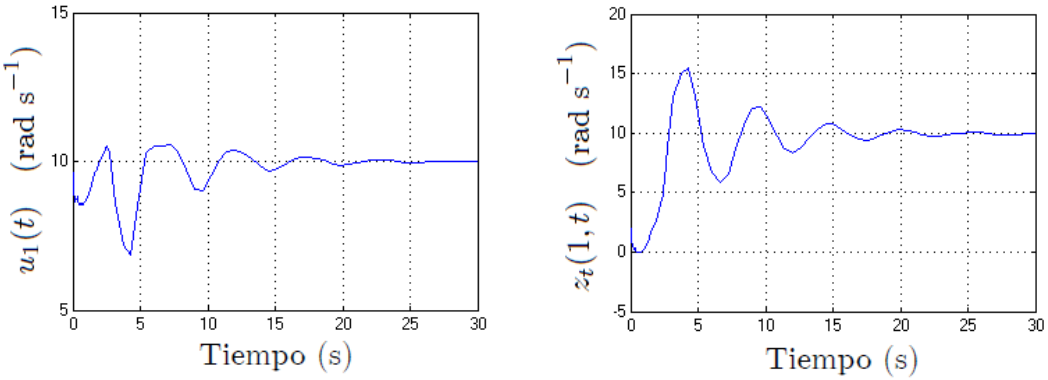


Figura 14: Eliminación del fenómeno atore-deslizamiento mediante la aplicación de la ley de control (68) con $c_1 = 0.3$.

La Figura 15 muestra la trayectoria de la variable longitudinal $y(t)$ tras la aplicación del controlador propuesto (68). Como puede observarse, la eliminación del fenómeno atore-deslizamiento induce la reducción de vibraciones axiales.

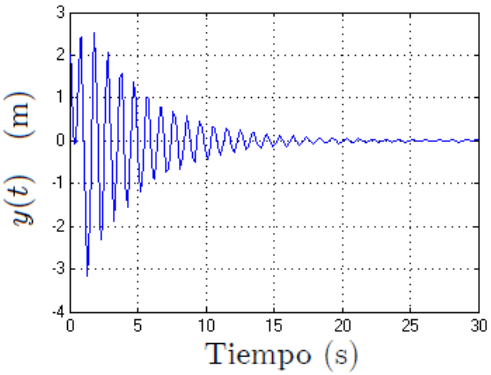


Figura 15: Reducción de oscilaciones axiales mediante la aplicación de la ley de control (68) con $c_1 = 0.3$.

## Control para la eliminación de vibraciones acopladas

El siguiente sistema corresponde al modelo de torsión normalizado (51) con condiciones de frontera (52-53) sujeto a la función del torque sobre la broca

(58-59) acoplado al modelo axial (61). Este sistema describe el acoplamiento de las dinámicas torsionales descritas por la ecuación de onda con las dinámicas longitudinales de la sarta de perforación representadas por una ecuación diferencial ordinaria.

$$
\begin{aligned}
z_{tt}(\zeta,t) &= a z_{\zeta\zeta}(\zeta,t) - d z_t(\zeta,t), \quad \zeta \in (0,1), \quad t>0, && (69)\\
z_\zeta(0,t) &= g\left(z_t(0,t) - u_1(t)\right), && (70)\\
z_\zeta(1,t) &= -h z_{tt}(1,t) - k z_t(1,t) - q T_{\mathrm{nl}}(z_t(1,t)) + \omega, && (71)
\end{aligned}
$$

$$
\dot{x}(t) = Ax(t) + Bu_2(t) + E_1 z_t(1,t) + E_2 T_{\mathrm{nl}}(z_t(1,t)). \qquad (72)
$$

Las entradas de control $u_1$, $u_2$ corresponden a la velocidad angular $\Omega$ provista por la mesa giratoria y a la tasa de perforación ROP respectivamente. El vector $x(t)$ y los parámetros del modelo, están definidos a continuación:

$$
x(t) = [y(t)\ \dot{y}(t)]^T, \quad a = \frac{GJ}{IL^2}, \quad d = \frac{\beta}{I}, \quad g = \frac{c_a L}{GJ},
$$
$$
h = \frac{I_B L}{GJ}, \quad k = \frac{c_b L}{GJ}, \quad q = \frac{W_{\mathrm{ob}} R_{\mathrm{b}} L}{GJ}.
$$

Las matrices constantes están dadas por:

$$
A = \begin{bmatrix} 0 & 1 \\ -\frac{k_0}{m_0} & -\frac{c_0}{m_0} \end{bmatrix},\ B = \begin{bmatrix} 0 \\ -\frac{c_0}{m_0} \end{bmatrix},\ E_1 = \begin{bmatrix} 0 \\ -\frac{\mu_1 c_{\mathrm{b}}}{m_0} \end{bmatrix},\ E_2 = \begin{bmatrix} 0 \\ -\frac{\mu_1 W_{\mathrm{ob}} R_{\mathrm{b}}}{m_0} \end{bmatrix}.
$$

El término no lineal $T_{\mathrm{nl}}$ está definido por:

$$
T_{\mathrm{nl}}(z_t(1,t)) = \left(\mu_{\mathrm{cb}} + (\mu_{\mathrm{sb}} - \mu_{\mathrm{cb}})\mathrm{e}^{-\frac{\gamma_{\mathrm{b}}}{v_{\mathrm{f}}}|z_t(1,t)|}\right) \mathrm{sign}\left(z_t(1,t)\right).
$$

La variable acotada $\omega$ representa la presencia de incertidumbres, perturbaciones y/o errores de modelado; se asume que ésta satisface:

$$
\omega^2 \leq \varepsilon. \qquad (73)
$$

**Lema 1** *Considere la una functional* $V(z_\zeta(\cdot,t), z_t(\cdot,t),\ x_t)$ *que satisface*

$$
\int_0^1 \tilde{z}^T(\zeta,t) P \tilde{z}(\zeta,t) d\zeta \leq V(z_\zeta(\cdot,t), z_t(\cdot,t),\ x_t) \leq \bar{V}(z_\zeta(\cdot,t), z_t(\cdot,t),\ x_t) \qquad (74)
$$

$$
\frac{d}{dt} V(z_\zeta(\cdot,t), z_t(\cdot,t),\ x_t) + \sigma V(z_\zeta(\cdot,t), z_t(\cdot,t),\ x_t) \leq \beta\varepsilon \quad \forall t \geq 0,\ \sigma > 0,\ \beta > 0, \qquad (75)
$$

*donde* $\tilde{z}(\zeta,t) = [z_\zeta(\zeta,t) \quad z_t(\zeta,t) \quad x_t]^T$ *y* $P$ *es una matriz simétrica positiva definida. Entonces, para cualquier función inicial* $\tilde{\phi}(\zeta,t) =$

$[\phi_\zeta(\zeta) \quad \phi_1(\zeta) \quad x_0]^T$, *el problema de valores en la frontera (69-72) satisface la cota siguiente*

$$\int_0^1 \tilde{z}^T(\zeta,t)P\tilde{z}(\zeta,t)d\zeta \leq e^{-\sigma t}\bar{V}(\phi_\zeta(\zeta),\ \phi_1(\zeta),\ x_0) + \frac{\beta\varepsilon}{\sigma}, \tag{76}$$

*para* $t \geq T_a(\phi,\varsigma) > 0$ *donde*

$$T_a(\tilde{\phi},\varsigma) = \frac{1}{\sigma}\ln\left(\frac{1}{\varsigma}\bar{V}(\phi_\zeta(\zeta),\ \phi_1(\zeta),\ x_0)\right).$$

En vista del resultado anterior, buscamos una funcional que satisfaga las condiciones del Lema 1. Considere la funcional de Lyapunov-Krasovskii siguiente

$$\begin{aligned} V(z_\zeta(\cdot,t),z_t(\cdot,t),\ x_t) &= V_1(z_\zeta(\zeta,t)) + V_2(z_t(\zeta,t)) \\ &\quad + V_3(z_\zeta(\zeta,t),z_t(\zeta,t)) + V_4(x_t), \end{aligned}$$

donde

$$\begin{aligned} V_1(z_\zeta(\zeta,t)) &= pa\int_0^1 z_\zeta^2(\zeta,t)d\zeta, \\ V_2(z_t(\zeta,t)) &= p\int_0^1 z_t^2(\zeta,t)d\zeta, \\ V_3(z_\zeta(\zeta,t),z_t(\zeta,t)) &= 2\chi\int_0^1 (\zeta+1)\, z_\zeta(\zeta,t)z_t(\zeta,t)d\zeta, \\ V_4(x_t) &= x^T(t)Rx(t). \end{aligned}$$

La funcional propuesta puede escribirse como

$$V(z_\zeta(\cdot,t),z_t(\cdot,t),\ x_t) = \int_0^1 \tilde{z}^T(\zeta,t)P\tilde{z}(\zeta,t)d\zeta, \quad \tilde{z}(\zeta,t) = [z_\zeta(\zeta,t)\ z_t(\zeta,t)\ x(t)]^T,$$

$$P = \begin{bmatrix} ap & \chi(\zeta+1) & 0 \\ \chi(\zeta+1) & p & 0 \\ 0 & 0 & R \end{bmatrix} > 0,\ p > 0,\ a > 0,\ R > 0.$$

Tomando la derivada con respecto al tiempo de $V(z_\zeta(\cdot,t),z_t(\cdot,t),\ x_t)$ a lo largo de las trayectorias del sistema (69-72) en lazo cerrado con las leyes de control de la forma

$$u_1(t) = c_{11}z_{tt}(1,t) + c_{12}z_t(1,t) + c_{13}T_{\text{nl}}(z_t(1,t)) + c_{14}z_t(0,t), \tag{77}$$

$$u_2(t) = c_2x(t), \tag{78}$$

y considerando el término positivo $-\beta(\omega^2 - \varepsilon)$ derivado de la condición (73), la desigualdad siguiente se satisface

$$\frac{d}{dt}V(\cdot) + \sigma V(\cdot) - \beta\varepsilon \leq \int_0^1 \eta_1^T \Psi \eta_1 d\zeta + \eta_2^T \Phi \eta_2,$$

donde

$$\begin{aligned} \eta_1 &= \left( \, z_t(\zeta,t) \; z_\zeta(\zeta,t) \, \right)^T, \\ \eta_2 &= \left( \, z_{tt}(1,t) \; z_t(1,t) \; T_{\text{nl}}(z_t(1,t)) \; z_t(0,t) \; x(t) \; \omega \, \right)^T, \end{aligned}$$

y

$$\Psi = \begin{bmatrix} -2pd - \chi + \sigma p & -d\chi\,(\zeta+1) + \sigma\chi\,(\zeta+1) \\ * & -a\chi + \sigma pa \end{bmatrix}, \tag{79}$$

$$\Phi = \begin{bmatrix} 2a\chi h^2 - a\chi g^2 c_{11}^2 & \Phi_{12} & \Phi_{13} & \Phi_{14} & 0 & -2a\chi h \\ * & \Phi_{22} & \Phi_{23} & \Phi_{24} & {E_1}^T R & -2a\chi k + pa \\ * & * & \Phi_{33} & \Phi_{34} & E_2^T R & -2a\chi q \\ * & * & * & \Phi_{44} & 0 & 0 \\ * & * & * & * & \Upsilon_1 + \sigma R & 0 \\ * & * & * & * & * & 2a\chi - \beta \end{bmatrix}, \tag{80}$$

donde

$$\begin{aligned} \Phi_{12} &= 2a\chi hk - pah - a\chi g^2 c_{11} c_{12} \\ \Phi_{13} &= 2a\chi hq - a\chi g^2 c_{11} c_{13} \\ \Phi_{14} &= a\chi g^2 c_{11}\,(1 - c_{14}) + pagc_{11} \\ \Phi_{22} &= 2a\chi k^2 + 2\chi - 2pak - a\chi g^2 c_{12}^2 \\ \Phi_{23} &= 2a\chi kq - paq - a\chi g^2 c_{12} c_{13} \\ \Upsilon_1 &= A^T R + RA + c_2^T B^T R + RBc_2. \end{aligned}$$

$$\begin{aligned} \Phi_{24} &= a\chi g^2 c_{12}\,(1 - c_{14}) + pagc_{12} \\ \Phi_{33} &= 2a\chi q^2 - a\chi g^2 c_{13}^2 \\ \Phi_{34} &= a\chi g^2 c_{13}\,(1 - c_{14}) + pagc_{13} \\ \Phi_{44} &= -a\chi g^2\,(1 - c_{14})^2 - \chi \\ &\quad - 2pag + pagc_{14} \end{aligned}$$

El resultado de estabilización del sistema acoplado (69-72) se establece en el siguiente teorema.

**Teorema 1** *Las trayectorias del sistema de perforación descrito por el modelo acoplado (69-72) en lazo cerrado con los controladores (77) y (78) admiten la cota (76) si las desigualdades matriciales $P > 0$, $\Psi < 0$ y $\Phi < 0$ se satisfacen para $p > 0$, $\chi > 0$, $\beta > 0$, $R > 0$ y cualesquiera $c_{11}$, $c_{12}$, $c_{13}$, $c_{14}$, $c_2$.*

Los parámetros usados en las siguientes simulaciones están indicados en (62). La máxima tasa de decaimiento exponencial para la cual las condiciones del Teorema 1 se satisfacen es $\sigma = 0.8$. Un resultado de la desigualdad matricial lineal $\Psi < 0$ con $\Psi$ definida en (79) es

$$p = 0.7406, \qquad \chi = 0.9559.$$

Con base en los valores anteriores, se encuentra, para la desigualdad matricial bilineal $\Phi < 0$ con $\Phi$ definido en (80), la solución siguiente:

$$\begin{array}{lll} c_{11} = -0.0067, & c_{12} = -0.04699, & c_{13} = -0.0548, \\ c_{14} = 0.6642, & c_2 = [0 \quad 2.0234], & \beta = 16.8149, \end{array} \tag{81}$$

$$R = \begin{bmatrix} 551.7373 & 11.7383 \\ 11.7383 & 13.4465 \end{bmatrix}.$$

Un simulación del modelo (55) acoplado a la función del torque sobre la broca (58-59) en lazo cerrado con la ley de control (77) y del modelo (61) en lazo cerrado con el controlador (78) ilustra el desempeño de la estrategia propuesta. La Figura 16 muestra la eliminación de los fenómenos de atore-deslizamiento y de rebote de la broca.

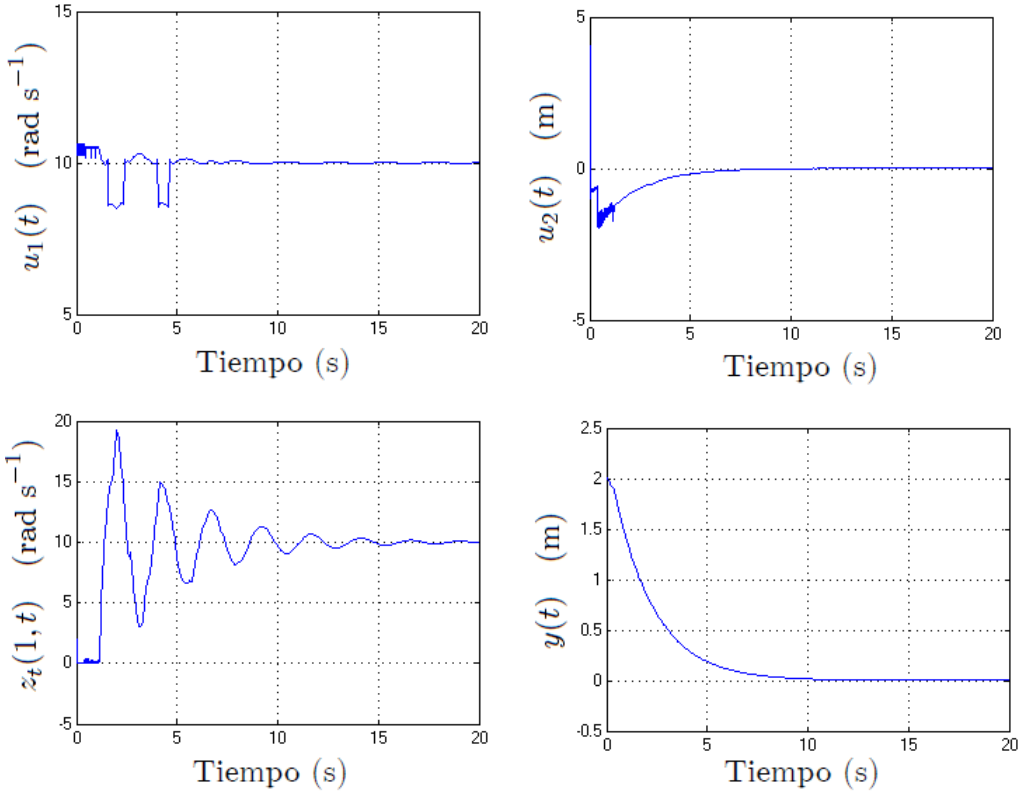


Figura 16: Trayectorias torsionales y axiales del sistema de perforación en lazo cerrado con los controladores $u_1$ y $u_2$ dados en (77) y (78).

Podemos concluir que la metodología de control basada en el análisis de disipación de energía se lleva a cabo de una manera más simple y directa

en comparación con el enfoque de desigualdades matriciales, sin embargo este último provee una eliminación integral de las vibraciones acopladas en la barra de perforación. Con respecto al tamaño del controlador, puede observarse que la trayectoria del controlador (77) es más cercana a la trayectoria referencia, lo cual resulta bastante conveniente considerando la presencia de restricciones de saturación en las entradas de control. Este problema particular será abordado en el siguiente capítulo. Es bien sabido que los modelos de parámetros distribuidos constituyen una descripción cercana a la realidad, sin embargo, la falta de herramientas numéricas para la simulación de sistemas infinito-dimensionales sujetos a no linealidades e incertidumbres conduce a la idea de abordar el problema desde una perspectiva diferente. El siguiente capítulo ataca el problema de control de vibraciones con base en el modelo con retardos de tipo neutral que describe el comportamiento del sistema de perforación vertical considerado.

# Capítulo 5

En este capítulo se aborda el problema de análisis de estabilidad y control de vibraciones en la sarta de perforación en el marco de sistemas con retardos.

Como se explicó antes, el comportamiento torsional de la barra de perforación puede modelarse mediante una ecuación no-lineal con retardos de tipo neutral que representa la relación entrada-salida del sistema. En este capítulo, este modelo es transformado en un conjunto de modelos lineales, no-linealmente ponderados, lo que permite aprovechar las herramientas de análisis y control para sistemas lineales. Mediante un análisis de estabilidad de Lyapunov, se obtienen condiciones de estabilidad y estabilización en términos de desigualdades matriciales lineales. La ley de control propuesta garantiza la estabilidad en lazo cerrado del sistema y elimina eficazmente las oscilaciones torsionales. Posteriormente, se aborda el problema de vibraciones acopladas de tipo axial y torsional. Mediante el método del elipsoide atractivo se obtiene la síntesis de controladores estabilizantes que garantizan una eliminación integral de las vibraciones de perforación. Este enfoque plantea un problema de optimización sujeto a condiciones de estabilización práctica en términos de desigualdades matriciales bilineales.

## Control de vibraciones torsionales: enfoque de aproximación multimodelo

En esta sección se investiga la estabilización de los sistemas no lineales con retardos de tipo neutral que pueden transformarse en un sistema multi-

modelo, esto es, un conjunto de modelos lineales no-linealmente ponderados representados por:

$$\dot{x}(t) - D\dot{x}(t-\tau_1) = \sum_{i\in I^r} h_i(x_t)\left\{A_i x(t) + A_{i\tau_1} x(t-\tau_1) + Bu(t)\right\}, \qquad (82)$$

donde $\tau_1 > 0$ es el retardo de tiempo constante, $I^r$ es el conjunto de números enteros $\{1, ..., r\}$, y $r$ es el número de subsistemas que se requieren para describir el sistema multimodelo. Los $h_i(\cdot)$ son funciones escalares de ponderación que satisfacen las condiciones de convexidad siguientes:

$$\sum_{i\in I^r} h_i(x_t) = 1 \quad \forall i = 1, ..., r, \quad h_i(x_t) \geq 0. \qquad (83)$$

Para garantizar la estabilidad del operador en diferencias se considera que $|D| < 1$.

El teorema siguiente presenta un algoritmo que permite la síntesis de una ganancia $K$ tal que la ley de control $u(t) = Kx(t-\tau_1)$ estabiliza exponencialmente el sistema en lazo cerrado

$$\dot{x}(t) - D\dot{x}(t-\tau_1) = \sum_{i\in I^r} h_i(x_t)\left\{A_i x(t) + (A_{i\tau_1} + BK)\, x(t-\tau_1)\right\}, \qquad (84)$$

con una tasa de decaimiento garantizada $\alpha$.

**Teorema 2** *El sistema en lazo cerrado (84) es $\alpha$-estable si existe un número real $\varepsilon > 0$ y matrices $\bar{P}_1 > 0$, $\bar{P}$, $\bar{Q} = \bar{Q}^T$, $\bar{R} = \bar{R}^T$, y $Y$ de dimensión $n \times n$, tales que para todo $i \in I^r$ la siguiente desigualdad matricial lineal se satisface*

$$\begin{pmatrix} \Phi_i & \begin{pmatrix} e^{\alpha\tau_1}\vartheta \\ \varepsilon e^{\alpha\tau_1}\vartheta \end{pmatrix} & \begin{pmatrix} e^{\alpha\tau_1} D\bar{P} \\ \varepsilon e^{\alpha\tau_1} D\bar{P} \end{pmatrix} \\ * & -\bar{R}/\tau_1 & 0 \\ * & * & -\bar{Q} \end{pmatrix} < 0, \qquad \Phi_i = \begin{pmatrix} \Phi_{11} & \Phi_{12} \\ * & \Phi_{22} \end{pmatrix},$$

$$\begin{aligned} \vartheta &= (A_{i\tau_1} - \alpha D)\,\bar{P} + BY, \\ \Phi_{11} &= (A_i + \alpha I_n + e^{\alpha\tau_1}(A_{i\tau_1} - \alpha D))\,\bar{P} \\ &\quad + \bar{P}^T (A_i + \alpha I_n + e^{\alpha\tau_1}(A_{i\tau_1} - \alpha D))^T + BY + Y^T B^T, \\ \Phi_{12} &= \bar{P}_1^T - \bar{P} + \varepsilon \bar{P}^T (A_i + \alpha I_n + e^{\alpha\tau_1}(A_{i\tau_1} - \alpha D))^T + \varepsilon Y^T B^T, \\ \Phi_{22} &= -\varepsilon\left(\bar{P} + \bar{P}^T\right) + \tau_1 \bar{R} + \bar{Q}. \end{aligned}$$

*Además, la ganancia de retroalimentación está dada por $K = Y\bar{P}^{-1}$.*

Para aplicar el resultado anterior al sistema de perforación, debe obtenerse una representación politópica del modelo no lineal (55), (58-59).

Considerando $\mu_{\rm cb} = 0$, y el cambio de variable siguiente

$$x_1(t) = z(t) - \Omega_0, \tag{85}$$

se obtiene la siguiente expresión no lineal que describe el comportamiento del sistema en el extremo inferior:

$$\begin{aligned} \dot{x}_1(t) + d\dot{x}_1(t-2\Gamma) \;=\; & a_0 x_1(t) + a_1 x_1(t-2\Gamma) + bu(t-\Gamma) \\ & -c_2 \mathrm{e}^{-\frac{\gamma_{\rm b}}{v_{\rm f}}(x_1(t)+\Omega_0)} \mathrm{sign}\left(x_1(t)+\Omega_0\right) \\ & +c_2 \Upsilon \mathrm{e}^{-\frac{\gamma_{\rm b}}{v_{\rm f}}(x_1(t-2\Gamma)+\Omega_0)} \mathrm{sign}\left(x_1(t-2\Gamma)+\Omega_0\right), \end{aligned} \tag{86}$$

donde $a_0 = -\Psi - \frac{c_{\rm b}}{I_{\rm B}}$, $a_1 = \frac{\Upsilon c_{\rm b}}{I_{\rm B}} - \Upsilon\Psi$, $d = -\Upsilon$, $b = \Pi$ et $c_2 = \frac{W_{\rm ob} R_{\rm b} \mu_{\rm sb}}{I_{\rm B}}$. Proponemos el cambio de variables siguiente:

$$\begin{cases} \varkappa_1(t) = x_1(t), \\ \varkappa_2(t) = \mathrm{e}^{-\frac{\gamma_{\rm b}}{v_{\rm f}}\varkappa_1(t)+\Omega_0}, \end{cases} \quad \text{entonces se tiene} \quad \begin{cases} \dot{\varkappa}_1(t) = \dot{x}_1(t), \\ \dot{\varkappa}_2(t) = -\frac{\gamma_{\rm b}}{v_{\rm f}} \dot{\varkappa}_1(t) \varkappa_2(t). \end{cases}$$

El sistema (86) puede escribirse como

$$\dot{x}(t) - D\dot{x}(t-2\Gamma) = A(x)x(t) + A_{2\Gamma}(x)x(t-2\Gamma) + B_\Gamma u(t-\Gamma), \tag{87}$$

donde la entrada de control $u(t)$ corresponde a la velocidad angular provista por la mesa giratoria, y donde:

$$x(t) = \left[\varkappa_1(t) \;\; \varkappa_2(t)\right]^T, \quad D = \begin{pmatrix} \Upsilon & 0 \\ 0 & 0 \end{pmatrix}, \quad B_\Gamma = \begin{pmatrix} \Pi \\ 0 \end{pmatrix},$$

$$A_{2\Gamma}(x) = \begin{pmatrix} \Upsilon\left(\frac{c_{\rm b}}{I_{\rm B}} - \Psi\right) & c_2\Upsilon \mathrm{sign}(\varkappa_1(t-2\Gamma)+\Omega_0) \\ 0 & 0 \end{pmatrix},$$

$$A(x) = \begin{pmatrix} -\left(\Psi + \frac{c_{\rm b}}{I_{\rm B}}\right) & -c_2 \mathrm{sign}(\varkappa_1(t)+\Omega_0) \\ 0 & -\frac{\gamma_{\rm b}}{v_{\rm f}} \dot{\varkappa}_1(t) \end{pmatrix}.$$

Observe que los elementos de las matrices $D$ y $B_\Gamma$ son constantes, y que el término $c_2\Upsilon \mathrm{sign}(\varkappa_1(t-2\Gamma)+\Omega_0)$ de la matriz $A_{2\Gamma}(x)$ está acotado. Puesto que $\dot{\varkappa}_1(t)$ es una variable acotada, entonces la matriz $A(x)$ también lo es.

Se obtiene la siguiente representación politópica,

$$A(x)x(t) + A_{2\Gamma}(x)x(t-2\Gamma) = \sum_{i \in I^r} h_i(x_t) \left(A_i x(t) + A_{i2\Gamma} x(t-2\Gamma)\right), \tag{88}$$

donde las matrices $A_i$ y $A_{i2\Gamma}$ tienen solamente coeficientes constantes [108].

Utilizando los parámetros dados en (62), las matrices $A(x)$, $A_{2\Gamma}(x)$, $B_\Gamma$ y $D$ del sistema (87) toman los siguientes valores:

$$\begin{aligned} D &= \begin{pmatrix} 0.7396 & 0 \\ 0 & 0 \end{pmatrix}, \; B_\Gamma = \begin{pmatrix} 5.8523 \\ 0 \end{pmatrix}, \\ A(x) &= \begin{pmatrix} -3.3645 & -136.1327\text{sign}(\varkappa_1(t)+\Omega_0) \\ 0 & -0.9\dot{\varkappa}_1(t) \end{pmatrix}, \\ A_{2\Gamma}(x) &= \begin{pmatrix} -2.4878 & 100.6802\text{sign}(\varkappa_1(t-2\Gamma)+\Omega_0) \\ 0 & 0 \end{pmatrix}. \end{aligned}$$

Para obtener una representación politópica del sistema, las matrices $A(x)$ y $A_{2\Gamma}(x)$ deben ser acotadas. Éstas dependen de tres funciones independientes: $\dot{\varkappa}_1(t)$, $\text{sign}(\varkappa_1(t)+\Omega_0)$ y $\text{sign}(\varkappa_1(t-2\Gamma)+\Omega_0)$.

Para la matriz $A$ se tiene:

$$A_i(x) = \begin{pmatrix} -3.3645 & a^i_{23}(x) \\ 0 & a^i_{33}(x) \end{pmatrix},$$

$$\begin{aligned} -136.1327 &= a^1_{23} \leq a^i_{23}(x) \leq a^2_{23} = 0, \\ -0.9Acc_{\text{máx}} &= a^1_{33} \leq a^i_{33}(x) \leq a^2_{33} = -0.9Dec_{\text{máx}}, \end{aligned}$$

$Acc_{\text{máx}}$ y $Dec_{\text{máx}}$ corresponden a la aceleración y desaceleración máximas respectivamente. Para la matriz $A_{2\Gamma}(x)$ se tiene:

$$A_{i2\Gamma}(x) = \begin{pmatrix} -2.4878 & a^i_{2\Gamma 23}(x) \\ 0 & 0 \end{pmatrix},$$

$$0 = a^1_{2\Gamma 23}(x) \leq a^i_{2\Gamma 23}(x) \leq a^2_{2\Gamma 23}(x) = 100.6802.$$

Aplicando el resultado del Teorema 2 al sistema de perforación en lazo cerrado con la ley de control $u(t) = Kx(t-\Gamma)$, se obtiene la solución siguiente:

$$K = Y\bar{P}^{-1} = \begin{pmatrix} 0.44 & -4.25 \end{pmatrix}.$$

Considerando el cambio de variable (35), la ley de control estabilizante para el sistema (86) está dada por

$$u(t) = 0.44z(t-\Gamma) - 4.25\text{e}^{-\frac{\gamma_\text{b}}{v_\text{f}}z(t-\Gamma)} - 0.44\Omega_0. \tag{89}$$

La Figura 17 muestra la eliminación eficaz del fenómeno de atore-deslizamiento mediante la aplicación de la ley de control (89).

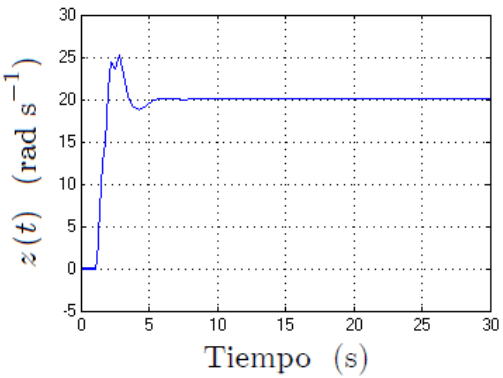


Figura 17: Trayectoria $z(t)$ del modelo torsional del sistema de perforación en lazo cerrado con la ley de control (89) con $\Omega_0 = 20\text{rad s}^{-1}$.

## Control de vibraciones acopladas: método del elipsoide atractivo

Esta sección aborda el problema de control de vibraciones acopladas en el sistema de perforación. Se propone una metodología para la síntesis de controladores estabilizantes para el sistema de perforación basada en una combinación del método de Lyapunov y el principio de conjuntos atractivos que plantea un problema de optimización sujeto a restricciones matriciales bilineales. La estrategia propuesta garantiza la eliminación de las oscilaciones axiales y torsionales acopladas y permite determinar el elipsoide mínimo atractivo para las trayectorias del sistema en lazo cerrado.

**Definición 1** *[66] Un elipsoide con centro en el origen se define como un conjunto en* $\mathcal{R}^n$ *tal que* $\mathcal{E}_M = \left\{x \in \mathcal{R}^n : x^T M x \leq 1\right\}$*, donde* $M$ *es una matriz simétrica definida positiva.*

**Definición 2 (Elipsoide atractivo)** *[86] Un elipsoide* $\mathcal{E}$ *es un dominio atractivo para el sistema (92) si*
*1)* $\phi(\theta) \in \mathcal{E}$*,* $\theta \in [-h, 0]$ *implica que* $x(t, \phi) \in \mathcal{E}$*,* $t \geq 0$*,*
*2)*$\phi(\theta) \in \mathcal{R}^n \backslash \mathcal{E}$*, para* $\theta \in [-h, 0]$ *implica que existe* $T_a$*,* $0 \leq T_a < \infty$*, tal que* $x(t, \phi) \in \mathcal{E}$*,* $t \geq 0$*.*

**Lema 2** *Sea la funcional* $V(x_t)$ *que satisface*

$$x^T(t) P x(t) \leq V(x_t) \leq \alpha \left\|x_t\right\|_h^2, \tag{90}$$

*donde* $P$ *es una matriz simétrica definida positiva y*

$$\frac{\mathsf{d}}{\mathsf{d}t} V(x_t) + \sigma V(x_t) \leq \beta, \quad \forall t \geq 0, \quad \sigma > 0, \quad \beta > 0. \tag{91}$$

*Entonces, para cualquier función inicial* $\phi \in \mathcal{PC}([-h,0],\mathcal{R}^n)$, *la solución* $x(t,\phi)$ *está contenida en el elipsoide* $\mathcal{E}_{\tilde{P}} = \left\{x \in \mathcal{R}^n : x^T\tilde{P}x \leq 1\right\}$, $\tilde{P} = \left(\frac{\sigma}{\beta}+\varsigma\right)P$, $\varsigma > 0$ *para* $t \geq T_a(\phi,\varsigma) > 0$ *donde*

$$T_a(\phi,\varsigma) = \frac{1}{\sigma}\ln\left(\frac{\alpha\left\|\phi\right\|_h^2}{\varsigma} - \frac{\beta}{\varsigma\sigma}\right).$$

Considere un sistema con retardos de tipo neutral de la forma:

$$\begin{aligned}\dot{x}(t) + D\dot{x}(t-2\tau) &= A_0x(t) + A_1x(t-2\tau) + B_1u_1(t-\tau) \\ &\quad + B_2u_2(t) + C_0f(x(t)) + C_1f(x(t-2\tau)) + \omega,\end{aligned} \tag{92}$$

donde $\omega$ satisface

$$\left\|\omega\right\|_{K_\omega} = \omega^TK_\omega\omega \leq 1, \qquad t \geq 0. \tag{93}$$

De acuerdo con la aplicación que se considera, se proponen las siguientes estructuras para $u_1$ y $u_2$

$$u_1(t-\tau) = K_0\dot{x}(t-2\tau) + K_1x(t-2\tau), \tag{94}$$

$$u_2(t) = K_2x(t). \tag{95}$$

Se asume que la ley de control $u_2$ está sujeta a la restricción:

$$|u_2(t)| \leq \bar{u}_2, \tag{96}$$

donde $\bar{u}_2$ es el nivel de saturación, esto es, el vector $u_2(t) = \text{col}\left\{u_2^1(t),...,u_2^m(t)\right\}$ está sujeto a las restricciones de amplitud siguientes:

$$\left|u_2^j(t)\right| \leq \bar{u}_2^j, \quad 0 < \bar{u}_2^j, \quad j = 1,...,m.$$

El objetivo es encontrar las condiciones que garanticen que el elipsoide definido por $\mathcal{E}_{\tilde{P}} = \left\{x \in \mathcal{R}^n : x^T\tilde{P}x \leq 1\right\}$, sea un conjunto atractivo para las trayectorias del sistema (92) en lazo cerrado con (94-95), esto es, $\overline{\lim}_{t\to\infty}x^T(t)\tilde{P}x(t) \leq 1$. Además, las matrices $K_0$, $K_1$, $K_2 \in \mathcal{R}^{m\times n}$ y $\tilde{P}$ deben garantizar la minimización del elipsoide $\mathcal{E}_{\tilde{P}}$. Dado que la traza de la matriz $\tilde{P}$ está inversamente relacionada con los ejes del elipsoide, se plantea el siguiente problema de optimización:

$$\begin{aligned}&\min \operatorname{tr}(\tilde{P}^{-1}) \\ &\text{sujeto a } \tilde{P} \in \Sigma_1, \quad K_0,K_1,K_2 \in \Sigma_2,\end{aligned} \tag{97}$$

donde $\Sigma_1$, $\Sigma_2$, definen el conjunto de matrices admisibles de dimensiones $n\times n$ y $m\times n$ respectivamente que garantizan la propiedad de invarianza del elipsoide $\mathcal{E}_{\tilde{P}}$.

Considere la funcional

$$\begin{aligned} V(x_t) &= x^T(t)Px(t) + \int_{t-2\tau}^{t} \mathrm{e}^{\sigma(s-t)} x^T(s) S x(s) \mathrm{d}s \\ &\quad + 2\tau \int_{-2\tau}^{0} \int_{t+\theta}^{t} \mathrm{e}^{\sigma(s-t)} \dot{x}^T(s) R \dot{x}(s) \mathrm{d}s \mathrm{d}\theta. \end{aligned} \tag{98}$$

Tomando la derivada de $V(x_t)$ con respecto al tiempo y siguiendo el enfoque descriptor, se obtiene:

$$\frac{\mathrm{d}V(x_t)}{\mathrm{d}t} + \sigma V(x_t) - \beta \leq \eta^T \Phi \eta,$$

donde el vector $\eta$ está definido como

$$\eta = (x(t)\ x(t-2\tau)\ \dot{x}(t)\ \dot{x}(t-2\tau)\ u_1(t-\tau)\ u_2(t)\ f(x(t))\ f(x(t-2\tau))\ \omega)^T,$$

y $\Phi$ es una matriz simétrica con elementos $\Phi_{ij}$, $i = 1, .., 9$, $j = 1, ..., 9$ definida como:

$$\begin{bmatrix} \Phi_{11} & \Phi_{12} & \Phi_{13} & \Phi_{14} & \Phi_{15} & \Phi_{16} & \Phi_{17} & P_2^T C_1 + A_0^T P_8 & P_2^T + A_0^T P_9 \\ * & \Phi_{22} & A_1^T P_3 & \Phi_{24} & \Phi_{25} & A_1^T P_6 & A_1^T P_7 & A_1^T P_8 & A_1^T P_9 \\ * & * & \Phi_{33} & \Phi_{34} & \Phi_{35} & \Phi_{36} & \Phi_{37} & P_3^T C_1 - P_8 & P_3^T - P_9 \\ * & * & * & \Phi_{44} & \Phi_{45} & \Phi_{46} & \Phi_{47} & P_4^T C_1 - D^T P_8 & P_4^T - D^T P_9 \\ * & * & * & * & \Phi_{55} & \Phi_{56} & \Phi_{57} & P_5^T C_1 + B_1^T P_8 & P_5^T + B_1^T P_9 \\ * & * & * & * & * & \Phi_{66} & \Phi_{67} & P_6^T C_1 + B_2^T P_8 & P_6^T + B_2^T P_9 \\ * & * & * & * & * & * & \Phi_{77} & P_7^T C_1 + C_0^T P_8 & P_7^T + C_0^T P_9 \\ * & * & * & * & * & * & * & P_8^T C_1 + C_1^T P_8 & P_8^T + C_1^T P_9 \\ * & * & * & * & * & * & * & * & \Phi_{99} \end{bmatrix},$$

donde:

$$\begin{aligned} \Phi_{11} &= A_0^T P_2 + P_2^T A_0 \\ &\quad + S + \sigma P - \mathrm{e}^{-\sigma 2\tau} R \\ &\quad + P_{14} K_2 + K_2^T P_{14} \\ \Phi_{12} &= \mathrm{e}^{-\sigma 2\tau} R + P_2^T A_1 \\ \Phi_{13} &= P - P_2^T + A_0^T P_3 \\ \Phi_{14} &= -P_2^T D + A_0^T P_4 \\ \Phi_{15} &= P_2^T B_1 + A_0^T P_5 \\ \Phi_{16} &= P_2^T B_2 + A_0^T P_6 \\ &\quad + K_2^T P_{13} - P_{14}^T \\ \Phi_{17} &= P_2^T C_0 + A_0^T P_7 \\ \Phi_{22} &= -\mathrm{e}^{-\sigma 2\tau}(S + R) \\ &\quad + P_{12}^T K_1 + K_1^T P_{12} \\ \Phi_{23} &= A_1^T P_3 \\ \Phi_{24} &= A_1^T P_4 + K_1^T P_{11} \\ &\quad + P_{12}^T K_0 \\ \Phi_{25} &= A_1^T P_5 + K_1^T P_{10} \\ &\quad - P_{12}^T \\ \Phi_{33} &= 4\tau^2 R - P_3 - P_3^T \\ \Phi_{34} &= -P_3^T D - P_4 \\ \Phi_{35} &= P_3^T B_1 - P_5 \\ \Phi_{36} &= P_3^T B_2 - P_6 \\ \Phi_{37} &= P_3^T C_0 - P_7 \\ \Phi_{44} &= -P_4^T D - D^T P_4 \\ &\quad + P_{11}^T K_0 + K_0^T P_{11} \\ \Phi_{45} &= P_4^T B - D^T P_5 \\ &\quad + K_0^T P_{10} - P_{11}^T \\ \Phi_{46} &= P_4^T B_2 - D^T P_6 \\ \Phi_{47} &= P_4^T C_0 - D^T P_7 \\ \Phi_{55} &= P_5^T B_1 + B_1^T P_5 \\ &\quad - P_{10}^T - P_{10} \\ \Phi_{56} &= P_5^T B_2 + B_1^T P_6 \\ \Phi_{57} &= P_5^T C_0 + B_1^T P_7 \\ \Phi_{66} &= P_6^T B_2 + B_2^T P_6 \\ &\quad - P_{13}^T - P_{13} \\ \Phi_{67} &= P_6^T C_0 + B_2^T P_7 \\ \Phi_{77} &= P_7^T C_0 + C_0^T P_7 \\ \Phi_{99} &= P_9^T + P_9 - \beta K_\omega. \end{aligned}$$

Claramente, si $\Phi < 0$, la condición (91) del Lema 2 se satisface.

La introducción de la desigualdad adicional:

$$\mathcal{H} := \begin{bmatrix} H & I_n \\ I_n & P \end{bmatrix} > 0, \ H \geq P^{-1}$$

permite reducir el problema de optimización no lineal (97) al problema lineal mín $\text{tr}(H)$. Usando la propiedad del complemento de Schur, se puede demostrar que la minimización de la traza de $H$ implica la minimización de la traza de $P^{-1}$ [48].

Para tomar en cuenta las restricciones físicas en las entradas de control, se considera la desigualdad siguiente:

$$\mathcal{I}_j := \begin{pmatrix} \left(\frac{\sigma}{\beta} + \varsigma\right) \bar{u}_2^j P & k_2^{jT} \\ * & \bar{u}_2^j \end{pmatrix} \geq 0 \quad j = 1, ..., m,$$

donde $k_2^j$ es la fila $j$ de la matriz $K_2$.

El resultado sobre el elipsoide mínimo atractivo para el sistema (92) se enuncia en el siguiente teorema.

**Teorema 3** *Considere el problema de optimización siguiente*

$$\text{mín} \ \ tr(H)$$

*sujeto a*

$$\begin{cases} \Lambda := \{H, P, S, R, K_0, K_1, K_2, P_k, \beta\}, \quad k = 1, ..., 14, \\ \Phi < 0, \\ \mathcal{H} > 0, \\ \mathcal{I}_j \geq 0 \quad j = 1, ..., m, \\ P > 0, \ S > 0, \ R > 0, \ \beta > 0, \ \sigma > 0, \ \varsigma > 0, \end{cases}$$

*con solución óptima* $\hat{\Lambda} := \left\{\hat{H}, \hat{P}, \hat{S}, \hat{R}, \hat{K}_0, \hat{K}_1, \hat{K}_2, \hat{P}_k, \hat{\beta}\right\}$, $k = 1, ..., 14$. *El elipsoide* $\mathcal{E}(0, \tilde{P})$ *determinado por la matriz* $\left(\frac{\sigma}{\hat{\beta}} + \varsigma\right)\hat{P}$, *es un conjunto mínimo atractivo para las trayectorias del sistema (92) en lazo cerrado con los controladores (94-96) para* $t \geq T_a(\phi, \varsigma) = \frac{1}{\sigma} \ln\left(\frac{\alpha \|\phi\|_h^2}{\varsigma} - \frac{\beta}{\varsigma\sigma}\right)$.

Las dinámicas axiales y torsionales acopladas de la sarta de perforación se describen mediante la siguiente ecuación:

$$\begin{aligned} \dot{x}(t) + D\dot{x}(t - 2\Gamma) = A_0 x(t) + A_1 x(t - 2\Gamma) + B_1 u_1(t - \Gamma) + B_2 u_2(t) \\ + C_0 f(x_1(t) + \Omega_0) + C_1 f(x_1(t - 2\Gamma) + \Omega_0) + \omega, \end{aligned} \tag{99}$$

donde $x(t) = \left[\begin{array}{ccc} x_1(t) & x_2(t) & x_3(t) \end{array}\right]^T$,

$$x_1(t) = z(t) - \Omega_0, \qquad x_2(t) = y(t) = Y(t) - \mathrm{ROP}t, \qquad x_3(t) = \dot{y}(t),$$

$$A_0 = \left[\begin{array}{ccc} -\Psi - \frac{c_\mathrm{b}}{I_\mathrm{B}} & 0 & 0 \\ 0 & 0 & 1 \\ -\frac{\mu_1 c_\mathrm{b}}{m_0} & -\frac{k_0}{m_0} & -\frac{c_0}{m_0} \end{array}\right], \; A_1 = \left[\begin{array}{ccc} \frac{\Upsilon c_\mathrm{b}}{I_\mathrm{B}} - \Upsilon\Psi & 0 & 0 \\ 0 & 0 & 0 \\ \frac{\mu_1 c_\mathrm{b}}{m_0} & 0 & 0 \end{array}\right], \; B_1 = \left[\begin{array}{c} \Pi \\ 0 \\ 0 \end{array}\right]$$

$$B_2 = \left[\begin{array}{c} 0 \\ 0 \\ -\frac{c_0}{m_0} \end{array}\right], \; C_0 = \left[\begin{array}{c} -\frac{1}{I_\mathrm{B}} \\ 0 \\ -\frac{\mu_1}{m_0} \end{array}\right], \; C_1 = \left[\begin{array}{c} \frac{\Upsilon}{I_\mathrm{B}} \\ 0 \\ 0 \end{array}\right], \; D = \left[\begin{array}{ccc} -\Upsilon & 0 & 0 \\ 0 & 0 & 0 \\ 0 & 0 & 0 \end{array}\right],$$

el retardo está dado por $\Gamma = \sqrt{\frac{I}{GJ}}L$, las entradas de control $u_1$ y $u_2$ corresponden a la velocidad angular $\Omega(t)$ provista por el motor y a la tasa de perforación ROP respectivamente, $f(\cdot)$ corresponde al término no lineal del modelo del torque sobre la broca:

$$T_\mathrm{nl}\left(z(t)\right) = W_\mathrm{ob} R_\mathrm{b} \left(\mu_\mathrm{cb} + (\mu_\mathrm{sb} - \mu_\mathrm{cb}) \mathrm{e}^{-\frac{\gamma_\mathrm{b}}{v_\mathrm{f}}|z(t)|}\right) \mathrm{sign}\left(z(t)\right). \tag{100}$$

Los parámetros usados en las simulaciones siguientes están dados en (62). Consideramos que debido a las condiciones físicas del sistema, la entrada de control $u_2(t)$ está sujeta a la restricción $|u_2(t)| \leq \bar{u}_2$ donde $\bar{u}_2 = 100$, y que la condición inicial $\phi$ satisface $\|\phi\|_h = 2$. Para obtener la síntesis de los controladores (94-95) usando el Teorema 3 se requiere una herramienta computacional apropiada para resolver problemas que involucren restricciones bilineales, tal como el paquete "PENBMI"de MATLAB.

La máxima tasa de decaimiento exponencial para la cual las condiciones del Teorema 3 se satisfacen es $\sigma = 1.5$. La solución al problema de optimización está dada por:

$$P = \left[\begin{array}{ccc} 6.1522 & 2.5914 & 0.2713 \\ 2.5914 & 13.0989 & 3.4865 \\ 0.2713 & 3.4865 & 1.4203 \end{array}\right], \quad \mathrm{eig}(P) = \left\{\begin{array}{c} 0.4238 \\ 5.4240 \\ 14.8236 \end{array}\right.,$$

$$\lambda_\mathrm{máx}(S) = 318.9226, \; \lambda_\mathrm{máx}(R) = 3.9407, \; \beta = 1.3620, \; \alpha = 254.1923,$$

$$K_0 = \left[\begin{array}{ccc} -0.1272 & 0 & 0 \end{array}\right], \quad K_1 = \left[\begin{array}{ccc} 0.4429 & 0.0196 & 0.0088 \end{array}\right],$$

$$K_2 = \left[\begin{array}{ccc} 24.3378 & 305.7411 & 120.3589 \end{array}\right].$$

Escogiendo $\varsigma = 0.1$ se observa que las trayectorias del sistema de perforación están contenidas en el elipsoide $\mathcal{E}_{\tilde{P}} = \left\{x \in \mathcal{R}^n : x^T \tilde{P} x \leq 1\right\}$, para $t \geq T_a(\phi, \varsigma) = 0.6667 \ln\left(2541.9 \left\|\phi\right\|_h^2 - 9.0800\right) = 6.1510$s. La Figura 18 muestra el elipsoide mínimo atractivo para las trayectorias del sistema (99).

Los resultados de simulación muestran un desempeño satisfactorio de los controladores propuestos, sin embargo, en vista de la respuesta oscilatoria de las trayectorias en lazo cerrado, el tiempo en el que las vibraciones torsionales se eliminan y la complejidad de la solución de las desigualdades matriciales, podemos concluir que el controlador no-lineal (89) derivado del enfoque de aproximación multimodelo es la mejor solución para eliminar el fenómeno atore-deslizamiento. Sin embargo, el método del elipsoide atractivo, aunque involucra cierto conservatismo derivado de la introducción de las variables de ponderación libre del enfoque descriptor, provee una solución integral al problema de las vibraciones acopladas. Esta estrategia permite obtener la síntesis de controladores estabilizantes que garantizan la eliminación de las vibraciones axiales y torsionales incluso en presencia de restricciones de saturación en la entrada de control.

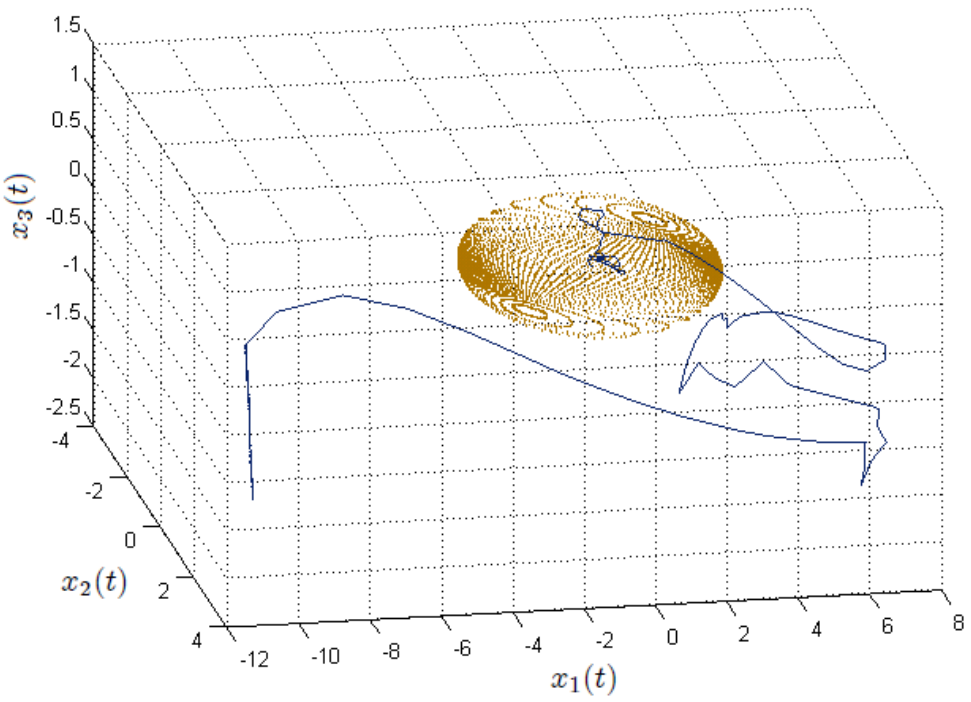


Figura 18: $x_1(t)$ vs. $x_2(t)$ vs. $x_3(t)$ convergiendo al elipsoide $\mathcal{E}(0, \tilde{P})$.

# Conclusiones generales y perspectivas

En este trabajo se resumen las principales contribuciones derivadas de una exhaustiva investigación sobre el modelado, el análisis y el control de vibraciones que se producen en el proceso de perforación.

El fenómeno de atore-deslizamiento, que constituye la fuente principal de fallos en las operaciones de perforación, es el tema central de este proyecto de tesis, sin embargo, puesto que la ocurrencia de vibraciones torsionales contribuye a la excitación de oscilaciones axiales, también se ha analizado el acoplamiento de vibraciones.

Con base en las diferentes estrategias de modelado propuestas para describir las dinámicas de la sarta de perforación, se realizaron diversos análisis de estabilidad y estabilización. Ciertamente, la ecuación de onda provee una descripción cercana a la realidad, puesto que reproduce el comportamiento distribuido del sistema, sin embargo, la complejidad que implican las simulaciones, conduce a derivar un modelo simplificado que representa razonablemente el comportamiento del sistema y permite aprovechar las técnicas de la teoría de control para sistemas con retardos.

El enfoque de desigualdades matriciales derivado de la teoría de Lyapunov es una herramienta eficaz para el análisis de estabilidad y control de sistemas dinámicos. Utilizando esta metodología, el sistema de perforación fue analizado con base en las diferentes estrategias de modelado propuestas.

Hemos diseñado controladores estabilizantes, lineales y no lineales, para la eliminación de vibraciones acopladas que involucran la medición de ciertas variables en el extremo inferior de la barra.

Podemos concluir que el modelo con retardos de tipo neutral constituye una representación simple y fiable de la dinámica torsional del sistema de perforación. Además, las técnicas de control propuestas para eliminar las oscilaciones de perforación son novedosas, simples y eficaces en comparación con las estrategias existentes. La implementación de las leyes de control que hemos propuesto permite perforar a bajas velocidades, lo que de otro modo resulta imposible. Las estrategias presentadas tienen un amplio dominio de aplicación puesto que se pueden generalizar para tratar muchos otros problemas ingenieriles, físicos, biológicos, etc.

## Perspectivas

Para describir completamente el comportamiento de la sarta durante el proceso de perforación, los trabajos futuros deberán incluir un modelo apropiado para las dinámicas laterales. Además, los parámetros desconocidos y variantes en el tiempo, podrían tomarse en consideración.

También sería interesante analizar el comportamiento de la columna de perforación en distintos entornos operacionales, por ejemplo, la perforación offshore, en la que la plataforma está situada en el mar.

Una amplia gama de líneas de investigación pueden surgir de este proyecto de tesis, dado que los fenómenos vibratorios que se producen en los diferentes tipos de dispositivos y maquinarias representan una fuente importante de fallos, bajo rendimiento y problemas de seguridad.

# Chapter 1

# General Introduction

## 1.1. General context. Drilling vibration

The presence of drillstring vibrations is the main cause of loss of performance in the perforation process for oil and gas. It provokes premature wear and tear of drilling equipment resulting in fatigue and induced failures such as pipe wash-out and twist-off [79]. It also cause significant wastage of drilling energy [78] and may induce wellbore instabilities reducing the directional control and its overall shape [37]. In the oil industry, the improvement of drilling performance is a matter of crucial economical interest.

Many studies have been conducted to identify and recognize the different types of vibrations during drilling operation. These have led to the identification and classification of vibrations into three separate and distinctive categories namely torsional (stick-slip oscillations), axial (bit bouncing phenomenon) and lateral (whirl motion due to the out-of-balance of the drillstring). Below is a brief description of each one of them.

**- Torsional vibration.** Downhole measurements show that applying a constant rotary speed at the surface does not necessarily translate into a steady rotational motion of the bit. In fact, the downhole torsional speed typically exhibits large amplitude fluctuations during a significant fraction of the drilling time. This self-excited rotational motion, also known as stick-slip, is induced by the nonlinear relationship between the torque and the angular velocity at the bit [55]. The torsional flexibility of the drilling assembly exacerbates a non-uniform oscillatory behavior causing rotational speeds as high as ten times the nominal rotary table speed or a total standstill of the bit [105]. Torsional vibrations provoke fatigue to drill collar connections, damages the drill bit and slow down the drilling operation thereby prolonging the overall

drilling process. They are detectable at the drillfloor by fluctuations in the power needed to maintain a constant rate of surface rotation

**- Axial vibration**. This vibration mode consist of irregular movements of the drilling components along its longitudinal axis causing bit bounce and rough drilling behavior that destroys the drill bit, damages the Bottom Hole Assembly (BHA) and increases total drilling time. Although, due to downhole coupling mechanisms, it also excites lateral displacements of the string [104]. The bit bounce pattern may be detected at the surface, it is likely to develop when drilling with a bit of roller-cone type, also called tricone or rock bit, consisting of multiple lobes which leads an erratic interaction of the bit with the bottom of the well making the bit to loose contact with the rock formation.

**- Lateral vibration.** One of the most destructive drillstring oscillations is the whirling phenomenon, it may be unleashed with no indication at the surface. Deep in the hole, the rotating BHA interacts with the borehole wall generating shocks from lateral vibrations. The collisions with the borehole wall will produce eccentric hole and the shocks can damage components of the BHA [83]. The lateral oscillations of the drillstring cause severe damage to the borehole wall and affect the overall drilling direction [54]. Drill collars whirling are simply the centrifugally induced bowing of the drill collar resulting from rotation. If the center of gravity of the drill collar is not initially located precisely on the centerline of the hole, then as the collar rotates, a centrifugal force acts at the center of gravity causing the collar to bend [116]. Forward and backward whirling behaviors can further intensify due to the combined effect of fluid damping, stabilizer clearance, and friction of the drilling assembly against the borehole wall [115].

Currently, drilling of deepwater wells for oil and gas production have opened new horizon for petroleum engineers and experts to try to mitigate the influence of vibration during drilling operation. Even though new technology has been deployed, such phenomena still occurs affecting considerably on drilling costs and daily operations. Before 1960s, studies were focused on material strength of the drillstring components but the trends have since changed to emphasize on its dynamic behavior [54].

## 1.2. Literature review

The great practical significance of oilwell drillstrings has attracted the attention of many researchers. In order to reduce the costs of failures, extensive

research effort has been conducted in the last five decades to suppress the drillstring vibrations, several methodologies have been proposed, both from practical and theoretical viewpoints, see for example the references cited in the survey [68]. Next, we present a brief chronological compilation of the main contributions on the subject.

The first analytical and experimental study of drillstring vibration was conducted initially in the sixties [6], [39]. Bailey and Finnie of Shell Development Company introduced the very first model of drillstring vibrations. They gave an analytical treatment of longitudinal and torsional vibrations starting from the wave equation. A surface measurement package was developed and placed beneath the rotary table to measure torque, axial force, rotation and axial displacement while drilling.

In 1968, researches from Esso Research Company reported on using a downhole recording tool to measure downhole forces and motions [34]. The tool could measure axial, torsional and bending forces and moments; axial, lateral and angular accelerations; internal and external pressure. Large Weight On Bit (WOB) fluctuations were measured. The WOB even dropped to zero in some cases, which implied that the bit had lifted off the bottom; they termed this bit-bounce. In the same year, Miller and Rollins showed raw relationships between Torque On Bit (TOB) and surface rotation speed for different formations [81]. The surface torque seemed to be independent on the surface rotation speed.

In 1982, Belokobyl'skii and Prokopov of the Leningrad Polytechnic Institute presented one of the first analytical treatments of stick-slip vibrations in drillstrings [12]. A large part of this treatment was based on earlier analytical results found by research on stick-slip in general. The authors introduced the subject of friction which induces torsional drillstring vibrations.

Besaisow et al. described the Advanced Drillstring Analysis and Measurement System (ADAMS) which only measures surface data [15], [16], [17]. The surface measurements had a large spectral content, and the authors provided a variety of explanations for the peaks that were observed.

In 1986, the French oil company "Elf Aquitaine" started the DYNAFOR research project with the purpose of improving drilling performance through a better knowledge of dynamic phenomena. A surface measurement device called the "Dynamètre" was developed enabling measurement of tension, torque and accelerations in three directions at the top of the drillstring.

In 1987, Peltier et al. proposed a linear relationship between TOB and WOB [90]. The authors verified that the torque can be related to bearing wear of the bit. In the same year, Dawson, Lin and Spanos investigated torsional stick-slip oscillations in drillstrings semianalytically [33]. They assumed a piecewise linear friction curve in the slip phase and applied this to a one Degree Of Freedom (DOF) model. The model predicted a critical rotary speed above which stick-slip oscillations would not occur. This was also observed in the field. They suggested that the oscillations could be reduced by lowering the static friction coefficient.

In 1988, Aarrestad and Kyllingstad of Rogaland Research Institute analyzed the coupling between bit torque and axial load at the bit for tricone bits drilling a bottomhole with a three lobbed pattern [1]. The authors studied downhole data obtained with a hardwire Measure While Drilling (MWD) tool. In the same year, Kyllingstad and Halsey treated the drillstring as a simple torsional pendulum and assumed a signum friction model with static point [51], [67]. This simple one DOF model made it possible to give analytical expressions for stick and slip time. Torque control via feedback at the surface was identified as a possible way to eliminate stick-slip. The idea behind the torque feedback concept is to allow the rotary table speed to respond to dynamic torque oscillations in such a way that the rotary table absorbs or dampens the vibrations. The system incorporated a torque and a velocity sensor mounted on the drillstring. The signals were processed in a computer-based feedback system and used to control the drive's speed. This system was the first controller to avoid stick-slip oscillations in drillstrings. However, the sensor package proved to be vulnerable and expensive.

In 1989, Cook et al. presented the first real-time downhole Root Mean Square (RMS) measurements of forces, accelerations and fluid pressures [31]. The quantities as RMS values were transmitted to surface using mudpulse telemetry.

In the late 1980s the Institute Français du Pétrole designed the TRAFOR system, a research tool to improve knowledge about drilling and how to model it. The TRAFOR system consists of a downhole measurement sub, called the Télévigile, and a surface measurement device known as the Survigile. The signals of the Télévigile and Survigile are gathered by a computer and synchronized. The Télévigile is connected to the surface equipment through an electric wire. Downhole WOB, TOB, accelerations in three directions and bending moments in two directions are measured. Torque, tension and rotary speed are measured at surface. The great merit of the TRAFOR system is the ability to measure both downhole and surface data at real-time.

In 1990, Lin and Wang investigated stick-slip oscillations in drillstrings numerically and came to conclusions already drawn in papers about stick-slip in general [72], [73].

In 1991, Dufeyte and Henneuse of Elf Aquitaine investigated the data of the DYNAFOR project between 1988 and 1990. Stick-slip oscillations were present during 50% of the time and were found to be highly detrimental to bits, drilling tools and drillpipe [36]. The authors verified the possible elimination of stick-slip oscillations using torque feedback. Lubricant tests were successful in eliminating stick-slip. As the lubricant passed the BHA the friction characteristic was changed which eliminated stick-slip vibrations. Stick-slip was prevalent with downhole mudmotors due to the practice of slowly rotating drillstring during these operations. This observation was confirmed numerically in [69].

In 1992, Brett studied torsional stick-slip oscillations with Polycrystalline Diamond Compact (PDC) bits on a laboratory test drilling machine, on a full scale test rig and theoretically [24]. Friction curves relating TOB versus angular velocity of the bit were obtained experimentally in the laboratory with a sharp and a dull PDC bit. The obtained friction curves showed a smoothly decreasing torque with increasing speed but the number of data points used was too small especially at low speeds thus no information about the static friction torque was obtained. The author noted that in the field, the stick-slip is reduced by decreasing WOB and/or increasing rotary speed, but suggested that increased speed can excite other forms of vibration.

Dubinsky, Henneuse and Kirkman, in 1992, gave a historical overview of Russian, European and American research in surface monitoring of downhole vibrations [35]. The Russians aimed their attention in the 1970s on optimizing the performance of turbines. A method was developed to detect stick-slip vibrations while using a turbine by inspecting the auto-spectral density of the surface axial accelerations. In the United States the goal was to reduce drillstring failures. The authors suggested that downhole dysfunctions are always observable at surface.

In 1994, Pavone and Desplans gave a description of the TRAFOR system and some experimental results [89]. The most remarkable result of this contribution is the relation found between the TOB and the bit rotary speed. The characteristic is clearly showing a stick phase and lower torques for higher speeds (a negative slope). The authors proposed a Proportional–Integral–Differential (PID) control and the use of an anti stick-slip tool to prevent stick-slip.

Shell Research in Rijswijk, The Netherlands, focused their research since 1990 on the improvement of the torque feedback system developed by Halsey et al. at Rogalandforskning Institute. The Soft Torque Rotary System (STRS), which obtains the information of speed and torque directly from the voltage and current measured at the motor terminals, was developed. Much attention was paid to the proper tuning of the STRS [54], [55].

In 1997, Van den Steen conducted a comprehensive study on the STRS [114]. The author gave a detailed model of the drive system and presented a model of the drillstring in the form of transmission matrices. A constant TOB was assumed in the slip phase. The resulting nonlinear model was thus linear in both stick and slip phase. This allowed fast numerical computation of stick-slip cycles by making use of fundamental solution matrices. The author studied different optimal control criteria for the STRS: maximized minimum damping, minimum power of the BHA velocity spectrum and maximum suppression of stick-slip oscillations.

In 1998, Serrarens developed an $\mathcal{H}_\infty$ controller as an alternative for the STRS [107]. The author concludes that the $\mathcal{H}_\infty$ controller performs better than the STRS, however, the system has a few drawbacks compared to the STRS: the controller does not satisfy hyperstability, no closed analytical solution has been found for the optimal weighting functions (tuning parameters) and the physical mechanism of the STRS is well understood while that of the $\mathcal{H}_\infty$ controller is difficult to interpret.

In 1999, Tucker and Wang analyzed a control mechanism designed to significantly ameliorate the sustained excitation of torsional oscillations due to frictional torques generated by an active bit during drilling operations [111]. The proposed mechanism of torsional rectification is compared with existing STRS in a series of mathematical models.

In 2003, Christoforou and Yigit presented a fully coupled model for axial, lateral, and torsional vibrations of actively controlled drillstrings [29]. They proposed an active control strategy based on optimal state feedback designed to control the drillstring rotational motion. Torsional vibrations are directly controlled, meanwhile, due to the oscillations coupling, axial and lateral vibrations are indirectly reduced to acceptable levels.

In 2004, Navarro-López and Suárez presented a dynamic drillstring model reproducing stick-slip vibrations under different operating conditions [84]. They took up the idea of introducing a PID controller structure at the surface in order to control the rotary speed. In the same year, Abdulgalil and

Siguerdidjane addressed the problem of stick-slip suppression by introducing a nonlinear controller based on an input-state feedback linearization of the nonlinear friction torque [2].

In 2005, Canudas-de-Wit et al. presented a new mechanism, named the oscillation killer (OSKIL) intended for extinguish limit cycles [26]. The method named D-OSKIL is applied to eliminate the stick-slip limit cycle in a drilling system with dry friction, it uses the WOB force as an additional control variable [27]. This paper reports experimental implementation of such a mechanism, in a laboratory testbed. The D-OSKIL mechanism conduces to some other contributions on the subject [77], [9].

In 2007, Zamanian, Khadem and Ghazavi studied self-excited stick-slip oscillations of a rotary drillstring with a drag bit [122]. This research shows that by increasing the damping of drilling mud, and by an appropriate selection of active damping ratios, the stick-slip oscillations can be avoided and the rotary table vibrations may be damped. In the same year, a dynamic sliding-mode control is used to avoid different bit sticking problems present in a conventional vertical oilwell drillstring [85].

In 2008, Puebla and Alvarez-Ramírez addressed the robust suppression of stick-slip oscillations in oil drillstrings [93]. The control approach is based on modeling error compensation techniques to provide robustness against uncertain parameters and friction terms.

In 2011, Bi et al. studied coupled axial torsional drilling oscillations by using the finite element method [18]. They explained that in the resonance state, the drilling string collides with the wall causing serious damage on the drilling string in a short time. The distributional regularities of the coupled resonant frequency were obtained through computer analysis. They conclude that the resonance state can be avoided by changing the rotary speed.

In 2012, Kreuzer and Steidl presented a method for controlling drilling vibrations by decomposing the drill string dynamics into two waves traveling in the direction of the top drive and in the direction of the drill bit [63]. The decomposition is derived from the wave equation governing the string vibrations. The velocity of the top drive is controlled in order to absorb the wave traveling in the direction of the top drive, thus achieving a reflection coefficient of zero for the frequency range of the undesired torsional vibrations. In the same year, Boussaada et al. studied the control of axial and torsional vibrations [21], [22]. Their analysis is based on the center manifold theorem and normal forms theory, they design two control laws allowing to suppress the undesired vibrations guaranteeing a regular drilling process.

Our contributions on stability analysis of the drilling system and vibration control are based on different modeling strategies. In [46] we presented a wave equation model describing torsional oscillations in a vertical oilwell drilling system, ultimate bounds on the solutions were obtained. In [99], based on the distributed parameter model, the proposal of an energy function allows a dissipativity analysis leading to the design of a stabilizing controller to suppress the stick-slip phenomenon. Furthermore, we presented a neutral-type time-delay model obtained through the D'Alembert transformation of the wave equation which simplifies analysis and simulations of the system. In order to validate the obtained model we tested the main practical strategies used in the field to eliminate the stick-slip. The nonlinear TOB model subject to a sign function allows to interpret the model as a switching system. Exponential stability analysis based on the switched systems theory was developed in [100]. A polytopic representation of the nonlinear time-delay model was presented in [101]. Based on this approach, we have designed a stabilizing controller to suppress torsional vibrations. A coupled model for axial and torsional oscillations was presented in [102]. Via attractive ellipsoid method we have designed stabilizing controllers able to eliminate bit-bounce and stick-slip.

## 1.3. Motivation and objectives

Oscillations in drillstrings are a well studied topic, a great number of methods have been suggested through the years to eliminate the problem. As the technology in the oil industry has evolved, the complexity in drilling oil wells has expanded. New technology has made it possible to drill deeper and deeper wells which demand high performance techniques guaranteeing an integral suppression of undesirable oscillations. Authors generally have studied every vibration mode individually, then, there are mostly particular solutions for each of the vibration problems. Furthermore just a few works have provided a proper stability analysis of their proposed control strategies.

This research project aims at analyzing the most frequently occurring vibration phenomena arising in drilling systems.

The first objective is to obtain a mathematical description of the string behavior during the drilling operation, able to efficiently reproduce the vibration coupling observed in real wells.

The second objective of our research concerns the drilling system stability analysis and control of drilling vibrations. We intend to design feedback

controllers to suppress, or at least reduce to acceptable levels the oscillatory behavior. The control solution proposals should guarantee the closed-loop system stability and the simultaneously suppression of the stick-slip and bit-bounce.

## 1.4. Thesis plan

The remaining chapters of this thesis are organized as follows:

In **Chapter 2** the drilling system modeling is presented. A distributed parameter model described by a hyperbolic Partial Differential Equation (PDE) with mixed boundary conditions describes the behavior of the drilling system along the rod. Using some mathematical procedures as the D'Alembert transformation and frequency domain techniques it is possible to derive a simpler model for the drilling system which involves only the variables of our interest. Such transformation leads to a neutral-type time-delay model describing the torsional behavior of the system, the time-delay is directly dependent on the length of the drillstring. Axial dynamics are reproduced by means of the damped harmonic oscillator model.

**Chapter 3** studies the main kinds of oscillations occurring during drilling operations: the torsional vibrations also known as stick-slip phenomenon and the axial vibrations commonly referred to as bit-bouncing phenomenon. Based on the torsional model of the drilling system described by a neutral-type time-delay equation, the main practical strategies to reduce the stick-slip vibrations are tested. The proposed model is validated through simulations.

**Chapter 4** concerns the stability analysis and control of drilling vibrations based on the wave equation model. The proposal of a Lyapunov functional for the distributed torsional model allows to provide an ultimate bound for a measure of the distributed variables describing the system in terms of Linear Matrix Inequality (LMI) type conditions. Based on the coupled wave-Ordinary Diffetential Equation (ODE) model, a control strategy allowing the suppression of axial-torsional coupled vibrations is developed.

In **Chapter 5** we address the problem of drilling vibrations suppression within the framework of time delay systems, torsional dynamics of the drill-string are modeled by a neutral-type time-delay equation subject to a non-linear expression approximating the rock-bit contact which involves the sign

function, the TOB model leads the analysis of the drilling model using different techniques of the control theory. Using switching systems theory, exponential stability conditions are obtained. A control strategy to suppress torsional vibrations is developed through a multimodel approximation of the nonlinear system. The attractive ellipsoid method allows us develop an efficient methodology to the control synthesis guaranteeing the simultaneous elimination of stick-slip and bit-bounce.

General conclusions are given in **Chapter 6**.

## 1.5. List of publications related to the Ph.D.

A list of publication submitted/accepted to various conferences and journals is provided here.

**Published journal papers**

- B. Saldivar, S. Mondié, J.J. Loiseau, V. Rasvan - *Suppressing axial-torsional coupled vibrations in oilwell drillstrings.* Journal of Control Engineering and Applied Informatics (2013) 15(1), 3-10.
- B. Saldivar, S. Mondié - *Drilling vibration reduction via attractive ellipsoid method.* Journal of the Franklin Institute - Elsevier (2013) 350(3): 485-502.
- E. Fridman, S. Mondié, B. Saldivar - *Bounds on the response of a drilling pipe model.* Special issue on Time-delay Systems in IMA Journal of Mathematical Control & Information (2010) 27(4): 513-526.

**Submitted journal papers**

- R. Villafuerte, B. Saldivar, S. Mondié - *Practical stability and stabilization of a class of nonlinear neutral type time delay systems with multiple delays: BMI's approaches.* Submitted to: International Journal of Control, Automation and Systems. February, 2013.

### Published international conference papers

- B. Saldivar, S. Mondié, J.J. Loiseau, V. Rasvan - *Stick-slip oscillations in oillwell drillstrings: distributed parameter and neutral type retarded model approaches.* 18th IFAC World Congress, Volume 8, Part 1, Milano, Italy, August 28 - September 2, 2011.

- B. Saldivar, A. Seuret, S. Mondié - *Exponential stabilization of a class of nonlinear neutral type time-delay systems, an oilwell drilling model example.* 8th International Conference on Electrical Engineering, Computer Science and Automatic Control, Mérida, Yucatan, Mexico, October 26-28, 2011.

- B. Saldivar, S. Mondié, J.J. Loiseau, V. Rasvan - *Exponential stability analysis of the drilling system described by a switched neutral type delay equation with nonlinear perturbations.* 50th IEEE Conference on Decision and Control and European Control Conference (CDC-ECC), Orlando, FL, USA, December 12-15, 2011.

- B. Saldivar, S. Mondié, E. Fridman - *Ultimate boundedness of the response of a drilling pipe model.* IFAC Workshop on Time Delay Systems (TDS 2009), Sinaia, Rumania, September 1-3, 2009.

- B. Saldivar, J.J. Loiseau, S. Mondié - *Reducing stick-slip oscillations in oilwell drillstrings.* International Conference on Electrical Engineering, Computing Science and Automatic Control (CCE-2009), Toluca, Mexico, November 10-13, 2009.

### Book chapter

- B. Saldivar, S. Mondié, A. Seuret - *Suppressing stick-slip oscillations in oilwell drillstrings.* Edited book volume for the new Springer series: Advances in Delays and Dynamics. Low Complexity Controllers for Time Delay Systems, 2013.

# Chapter 2

# Drilling system modeling

## 2.1. Introduction

A sketch of a simplified drillstring system is shown in Figure 2.1.

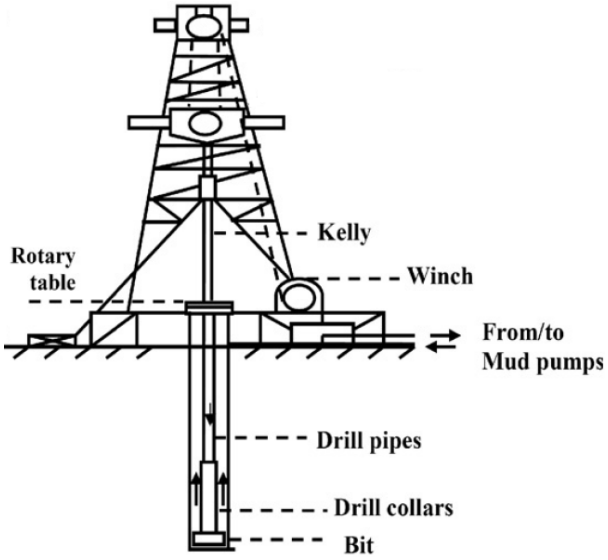


Figure 2.1: Basic scheme of a vertical drilling system.

The main process during well drilling for oil is the creation of borehole by a rock-cutting tool called a bit. The drillstring consists of the BHA and drillpipes screwed end to end to each other to form a long pipe. The BHA comprises the cutting device (bit), stabilizers (at least two spaced apart) which prevent the drillstring from unbalancing, and a series of pipe sections which are relatively heavy known as drill collars. While the length of the BHA remains constant, the total length of the drill pipes increases as the borehole

depth does. An important element of the process is the drilling mud or fluid which among others, has the function of cleaning, cooling and lubricating the bit. The drillstring is rotated from the surface by an electrical motor located at the rotary table.

Drilling system complexity brings out a modelling and a control problem. The model must accurately describe the most important phenomena arising in real wells and it has to be simple enough for analysis and control purposes.

In general, the models that have been used in literature to describe drillstring systems can be classified into two main categories: distributed parameter models and lumped parameter models.

To keep a more simple analysis, many contributions consider the drillstring as a torsional pendulum described by a lumped parameter model with one or multiple DOF. In [51] and [73] they consider a one DOF model, in [24], [27], [55], [84] and [107], they propose a two DOF mode, in [85], a discontinuous model of four DOF is introduced.

Lumped parameters models have been shown to be easy enough for the analysis, but in some cases, the distributed nature of the system can not be neglected. It is natural to think that a distributed parameter model of the system is more suitable to properly describe the oscillation phenomena.

The wave equation is widely used to reproduce the oscillatory behavior of physical systems. In the 1960s, some analyses have been carried out using the classical wave equation to describe the torsional behavior of drillstring assemblies [6], [39]. This modeling strategy was also adopted in [28], [111], [112] and [113].

Normally, when a distributed parameter model is subject to nonlinearities and uncertainties, analysis and simulations are not easy tasks. In this case, it is desirable to derive a simpler model involving only the variables of main interest. By means of a direct transformation, an input-output model described by a neutral-type time-delay equation which clearly simplifies the analysis and simulations, can be obtained. The procedure allowing to transform the PDE model to a delay system of neutral type was presented for the first time in [3], see also [5], [10], [19], [21], [22], [30], [40], [49] and [99].

In this chapter, we introduce an unidimensional wave equation to describe the drillstring torsional behavior. The distributed parameter model is subject to mixed boundary conditions chosen accordingly to the observed dynamics at both extremities of the string. Neutral-type time-delay equations relating

variables at both ends of the rod are obtained. We explain in detail the transformation techniques (D'Alembert and Laplace methods) allowing the simplified model derivation. Formal stability analysis of the neutral-type time-delay model is provided.

## 2.2. Distributed parameter model

The purely torsional excitations of a drillstring of length $L$, described by the rotary angle $\theta(\xi,t)$ can be modeled by the wave equation [21], [22], [28], [46], [111], [112], [113]:

$$GJ\frac{\partial^2\theta}{\partial\xi^2}(\xi,t) - I\frac{\partial^2\theta}{\partial t^2}(\xi,t) - \beta\frac{\partial\theta}{\partial t}(\xi,t) = 0, \qquad \xi\in(0,L), \qquad t>0, \tag{2.1}$$

with the twist angle $\theta$ depending on the length coordinate $\xi$ and time $t$. The parameters $I$, $G$ and $J$ are the inertia, the shear modulus and the geometrical moment of inertia respectively. A damping $\beta \geq 0$ which includes the viscous and structural damping, is assumed along the structure.

The boundary conditions are chosen according to the dynamics taking place at the upper and lower ends of the drill string. In [28] the following boundary conditions are considered:

$$\theta(0,t) = \Omega t, \tag{2.2}$$

$$GJ\frac{\partial\theta}{\partial\xi}(L,t) + I_B\frac{\partial^2\theta}{\partial t^2}(L,t) = -T\left(\frac{\partial\theta}{\partial t}(L,t)\right). \tag{2.3}$$

A lumped inertia $I_B$ is chosen to represent the assembly at the bottom hole. It is assumed that the speed of the surface ($\xi = 0$) is restricted to a constant value $\Omega$, the other extremity ($\xi = L$), which symbolizes the bit, is subject to a torque $T$, which is a function of the bit speed.

The following nonlinear equation, introduced in [85], allows to approximate the physical phenomenon at the bottom hole

$$T\left(\frac{\partial\theta}{\partial t}(L,t)\right) = c_{\mathrm{b}}\frac{\partial\theta}{\partial t}(L,t) + W_{\mathrm{ob}}R_{\mathrm{b}}\mu_{\mathrm{b}}\left(\frac{\partial\theta}{\partial t}(L,t)\right)\operatorname{sign}\left(\frac{\partial\theta}{\partial t}(L,t)\right), \tag{2.4}$$

the term $c_{\mathrm{b}}\frac{\partial\theta}{\partial t}(L,t)$ is a viscous damping torque at the bit which approximates the influence of the mud drilling and the term $W_{\mathrm{ob}}R_{\mathrm{b}}\mu_{\mathrm{b}}\left(\frac{\partial\theta}{\partial t}(L,t)\right)\operatorname{sign}\left(\frac{\partial\theta}{\partial t}(L,t)\right)$ is a dry friction torque modelling the

bit-rock contact. $R_{\mathrm{b}} > 0$ is the bit radius and $W_{\mathrm{ob}} > 0$ the WOB. The bit dry friction coefficient $\mu_{\mathrm{b}}(\frac{\partial\theta}{\partial t}(L,t))$ is modeled as

$$\mu_{\mathrm{b}}\left(\frac{\partial\theta}{\partial t}(L,t)\right) = \mu_{\mathrm{cb}} + (\mu_{\mathrm{sb}} - \mu_{\mathrm{cb}})\mathrm{e}^{-\frac{\gamma_{\mathrm{b}}}{v_{\mathrm{f}}}\left|\frac{\partial\theta}{\partial t}(L,t)\right|}, \tag{2.5}$$

where $\mu_{\mathrm{sb}}, \mu_{\mathrm{cb}} \in (0,1)$ are the static and Coulomb friction coefficients and $0 < \gamma_{\mathrm{b}} < 1$ is a constant defining the velocity decrease rate. The constant velocity $v_{\mathrm{f}} > 0$ is introduced in order to have appropriate units.

The boundary condition (2.3) coupled to the torque on the bit model (2.4-2.5) satisfactorily reproduces the behavior at the ground level, however (2.2) does not reflect an important dynamic occurring at the top extremity. The angular velocity coming from the rotor $\Omega$ does not match the rotational speed of the load $\frac{\partial\theta}{\partial t}(0,t)$, this sliding speed results in the local torsion of the drillstring. In order to take into account this phenomenon, we introduce the following boundary condition which is validated in [99]:

$$GJ\frac{\partial\theta}{\partial\xi}(0,t) = c_{\mathrm{a}}\left(\frac{\partial\theta}{\partial t}(0,t) - \Omega(t)\right). \tag{2.6}$$

Alternative boundary conditions to represent the drilling behavior at the upper extremity are derived from the classical Newton equation such as the following one introduced in [32]:

$$J_T\frac{\partial^2\theta}{\partial t^2}(0,t) + \Theta(t) = -T_{top}\left(\frac{\partial\theta}{\partial t}(0,t), \frac{\partial\theta}{\partial t}(L,t)\right) \tag{2.7}$$

where $J_T$ is the effective moment of inertia of the top-drive The forcing function $\Theta(t)$ denotes the external torque delivered by the top-drive, taken as control input with the following structure

$$\Theta(t) = \kappa_p\left(\frac{\partial\theta}{\partial t}(0,t) - \Omega_0\right) + \kappa_i\left(\theta(0,t) - \Omega_0 t\right)$$

where $\kappa_p$ and $\kappa_i$ are the rotary speed control parameters and $\Omega_0$ is the target angular speed. The function $T_{top}$, depending on the angular velocities at the top and bottom extremities, describes the transmitted torque and damping due to viscous effects.

Throughout this work we assume the existence of the solutions to the considered boundary value problems with appropriate initial conditions.

## 2.3. Neutral-type time-delay model

Integration along characteristics of the hyperbolic PDE allows the association of certain system of functional differential equations to the mixed problem, more precisely, a one-to-one correspondence may be established and proved between the solutions of the mixed problem for hyperbolic PDE and the initial value problem for the associated system of functional equations [94], [95].

By reducing the boundary value problem introduced in the above section to a neutral-type time-delay equation we are able to exploit techniques from dynamic systems theory to gain insight into the complexity involved in the analysis and simulation of infinite dimensional systems.

Since most of the energy dissipation in drilling systems is taking place at the bit-rock interface, we consider that the damping along the structure $\beta$ is null. The distributed parameter model (2.1) reduces to the unidimensional wave equation:

$$\frac{\partial^2\theta}{\partial\xi^2}(\xi,t) = p^2\frac{\partial^2\theta}{\partial t^2}(\xi,t), \qquad \xi\in(0,L), \tag{2.8}$$

where $p=\sqrt{\frac{I}{GJ}}$.

A direct transformation of the wave equation model (2.8) with boundary conditions (2.3-2.6) allows to obtain the following neutral-type time-delay model describing the drilling behavior [99]:

$$\begin{aligned}\dot z(t)-\Upsilon\dot z(t-2\Gamma) &= -\Psi z(t)-\Upsilon\Psi z(t-2\Gamma) \\ &\quad -\frac{1}{I_{\mathrm{B}}}T\left(z(t)\right)+\frac{1}{I_{\mathrm{B}}}\Upsilon T\left(z(t-2\Gamma)\right)+\Pi\Omega(t-\Gamma),\end{aligned} \tag{2.9}$$

where $z(t)$ is the angular velocity at the bottom extremity, and

$$\Pi=\frac{2\Psi c_{\mathrm{a}}}{c_{\mathrm{a}}+\sqrt{IGJ}},\ \Upsilon=\frac{c_{\mathrm{a}}-\sqrt{IGJ}}{c_{\mathrm{a}}+\sqrt{IGJ}},\ \Psi=\frac{\sqrt{IGJ}}{I_{\mathrm{B}}},\ \Gamma=\sqrt{\frac{I}{GJ}}L. \tag{2.10}$$

Similarly, we obtain a neutral type retarded expression for the behavior at the upper extremity of the drillstring:

$$\dot v(t)+\Upsilon\dot v(t-2\Gamma)=(c_a/\Lambda)\left[\Omega(t)+\Omega(t-2\Gamma)\right]-(2/\Lambda)\left[I_B\dot z(t-\Gamma)+T\left(z(t-\Gamma)\right)\right] \tag{2.11}$$

where $v(t)$ is the displacement from the unexcited position at the top extremity and $\Lambda=c_a+\sqrt{IGJ}$.

The input-output model obtained from (2.8) with the boundary conditions (2.2-2.3) considered in [28] is:

$$\dot{z}_1(t) - \dot{z}_1(t-2\Gamma) + \frac{\sqrt{IGJ}}{I_B} z_1(t) + \frac{\sqrt{IGJ}}{I_B} z_1(t-2\Gamma) = -\frac{1}{I_B} T(t) \qquad (2.12)$$
$$+\frac{1}{I_B} T(t-2\Gamma) + \frac{2\sqrt{IGJ}}{I_B} \Omega(t-\Gamma),$$

where $z_1(t)$ corresponds to the angular velocity at the bit level [98].

The following neutral-type model is derived from (2.8) coupled to the boundary conditions (2.3-2.7),

$$\ddot{z}_2(t) - \ddot{z}_2(t-2\Gamma) + \frac{\sqrt{IGJ}}{I_{\mathrm{B}}} \dot{z}_2(t) + \frac{\sqrt{IGJ}}{I_{\mathrm{B}}} \dot{z}_2(t-2\Gamma) = -\frac{1}{I_{\mathrm{B}}} \frac{d}{dt} T(t) \qquad (2.13)$$
$$+ \frac{1}{I_{\mathrm{B}}} \frac{d}{dt} T(t-2\Gamma) - \frac{2\sqrt{IGJ}}{I_{\mathrm{B}} J_T} \Omega(t-\Gamma) - \frac{2\sqrt{IGJ}}{I_{\mathrm{B}} J_T} T_{top}(t-\Gamma).$$

where $z_2(t)$ stands for the angular speed at the bottom end. Setting $\bar{Z}_1(t) = z_2(t)$, $\bar{Z}_2(t) = \dot{z}_2(t)$, $Z(t) = \begin{bmatrix} \bar{Z}_1(t) & \bar{Z}_2(t) \end{bmatrix}^T$, we can rewrite (2.13) in matrix form as follows:

$$\begin{aligned} \dot{Z}(t) + \tilde{D}\dot{Z}(t-2\Gamma) &= \tilde{A}_0 Z(t) + \tilde{A}_1 Z(t-2\Gamma) + \tilde{C}_0 \frac{d}{dt} T(t) \\ &\quad + \tilde{C}_1 \frac{d}{dt} T(t-2\Gamma) + \tilde{C}_2 T_{top}(t-\Gamma) + \tilde{B}\Omega(t-\Gamma), \end{aligned}$$

where

$$\tilde{D} = \begin{bmatrix} 0 & 0 \\ 0 & -1 \end{bmatrix}, \quad \tilde{A}_0 = \begin{bmatrix} 0 & 1 \\ 0 & -\frac{\sqrt{IGJ}}{I_{\mathrm{B}}} \end{bmatrix}, \quad \tilde{A}_1 = \begin{bmatrix} 0 & 0 \\ 0 & -\frac{\sqrt{IGJ}}{I_{\mathrm{B}}} \end{bmatrix},$$

$$\tilde{C}_0 = \begin{bmatrix} 0 \\ -\frac{1}{I_{\mathrm{B}}} \end{bmatrix}, \quad \tilde{C}_1 = \begin{bmatrix} 0 \\ \frac{1}{I_{\mathrm{B}}} \end{bmatrix}, \quad \tilde{C}_2 = \tilde{B} = \begin{bmatrix} 0 \\ -\frac{2\sqrt{IGJ}}{I_{\mathrm{B}} J_T} \end{bmatrix}.$$

This model is not a suitable representation of torsional vibrations since the function $T$ used to approximate the rock-bit contact is generally assumed non-differentiable.

A similar reduction of analogous PDE boundary value problems to time-delay equations, and the techniques exploited here, have relevance to a broad range of other engineering, physical and biological problems. These include power transmission line networks [23], laser optical fibres, sonar/radar ranging technologies [11], cardiovascular system dynamics and many other applications [53], [52], [88], [106].

Next, we present two different ways to develop this transformation [98], [99]. It should be pointed out that this is an exact transformation, i.e., the model (2.9) is not an approximation of the wave equation model (2.8).

### 2.3.1. D'Alembert transformation

The d'Alembert method provides a solution to the one-dimensional wave equation (2.8) that describes the torsional vibrations of a drillstring. The general solution is obtained by introducing new variables $\gamma = t + p\xi$, and $\eta = t - p\xi$, which result from the application of the method of characteristics to (2.8).

Applying the chain rule yields:

$$\begin{aligned} \frac{\partial}{\partial \xi} &= \frac{\partial \gamma}{\partial \xi}\frac{\partial}{\partial \gamma} + \frac{\partial \eta}{\partial \xi}\frac{\partial}{\partial \eta} \\ &= p\frac{\partial}{\partial \gamma} - p\frac{\partial}{\partial \eta}, \end{aligned} \tag{2.14}$$

$$\begin{aligned} \frac{\partial}{\partial t} &= \frac{\partial \gamma}{\partial t}\frac{\partial}{\partial \gamma} + \frac{\partial \eta}{\partial t}\frac{\partial}{\partial \eta} \\ &= \frac{\partial}{\partial \gamma} + \frac{\partial}{\partial \eta}. \end{aligned} \tag{2.15}$$

Using (2.14) and (2.15) to compute the left and right sides of (2.8) gives

$$\begin{aligned} \frac{\partial^2 \theta}{\partial \xi^2} &= \left(p\frac{\partial \theta}{\partial \gamma} - p\frac{\partial \theta}{\partial \eta}\right)\left(p\frac{\partial \theta}{\partial \gamma} - p\frac{\partial \theta}{\partial \eta}\right) \\ &= p^2\frac{\partial^2 \theta}{\partial \gamma^2} - 2p^2\frac{\partial^2 \theta}{\partial \gamma \partial \eta} + p^2\frac{\partial^2 \theta}{\partial \eta^2}, \end{aligned} \tag{2.16}$$

$$\begin{aligned} \frac{\partial^2 \theta}{\partial t^2} &= \left(\frac{\partial \theta}{\partial \gamma} + \frac{\partial \theta}{\partial \eta}\right)\left(\frac{\partial \theta}{\partial \gamma} + \frac{\partial \theta}{\partial \eta}\right) \\ &= \frac{\partial^2 \theta}{\partial \gamma^2} + 2\frac{\partial^2 \theta}{\partial \gamma \partial \eta} + \frac{\partial^2 \theta}{\partial \eta^2}. \end{aligned} \tag{2.17}$$

Now, substituting (2.16) and (2.17) into (2.8) yields

$$\frac{\partial^2 \theta}{\partial \gamma \partial \eta} = 0.$$

This PDE has the general solution

$$\begin{aligned}\theta(\xi,t) &= \phi(\gamma)+\psi(\eta) \\ &= \phi(t+p\xi)+\psi(t-p\xi),\end{aligned} \tag{2.18}$$

where $\phi$ and $\psi$ are arbitrary continuously differentiable real-valued functions, with $\phi$ representing a left-traveling wave and $\psi$ a right-traveling wave.

According to (2.14) and (2.15), we have:

$$\begin{aligned}\frac{\partial\theta}{\partial t} &= \frac{\partial\theta}{\partial\gamma}+\frac{\partial\theta}{\partial\eta} \\ \frac{\partial\theta}{\partial\xi} &= p\frac{\partial\theta}{\partial\gamma}-p\frac{\partial\theta}{\partial\eta}.\end{aligned}$$

The boundary conditions (2.3-2.6) can be rewritten as

$$p\frac{\partial\phi}{\partial\gamma}(t)-p\frac{\partial\psi}{\partial\eta}(t)=\frac{c_{\mathrm{a}}}{GJ}\left(\frac{\partial\phi}{\partial\gamma}(t)+\frac{\partial\psi}{\partial\eta}(t)-\Omega(t)\right), \tag{2.19}$$

$$\begin{aligned}p\frac{\partial\phi}{\partial\gamma}(t+\Gamma)-p\frac{\partial\psi}{\partial\eta}(t-\Gamma) &= -\frac{I_{\mathrm{B}}}{GJ}\left(\frac{\partial^2\phi}{\partial\gamma^2}(t+\Gamma)+\frac{\partial^2\psi}{\partial\eta^2}(t-\Gamma)\right) \\ &\quad -\frac{1}{GJ}T\left(\frac{\partial\phi}{\partial\gamma}(t+\Gamma)+\frac{\partial\psi}{\partial\eta}(t-\Gamma)\right),\end{aligned} \tag{2.20}$$

where $\Gamma = pL$.

By considering $\phi$ and $\psi$ as functions of the time $t$, and denoting by $z(t)$ the angular velocity at the bottom extremity we obtain

$$z(t)=\frac{\partial\theta}{\partial t}(L,t)=\dot{\phi}(t+\Gamma)+\dot{\psi}(t-\Gamma), \tag{2.21}$$

and we can rewrite (2.19) and (2.20) as:

$$p\dot{\phi}(t)-p\dot{\psi}(t) = \frac{c_{\mathrm{a}}}{GJ}\left(\dot{\phi}(t)+\dot{\psi}(t)-\Omega(t)\right), \tag{2.22}$$

$$p\dot{\phi}(t+\Gamma)-p\dot{\psi}(t-\Gamma) = -\frac{I_{\mathrm{B}}}{GJ}\dot{z}(t)-\frac{1}{GJ}T\left(z(t)\right). \tag{2.23}$$

Equation (2.21) implies that

$$\dot{\phi}(t)=-\dot{\psi}(t-2\Gamma)+z(t-\Gamma), \tag{2.24}$$

substituting (2.24) into (2.23) yields

$$-2p\dot{\psi}(t-\Gamma)+pz(t)=-\frac{I_{\mathrm{B}}}{GJ}\dot{z}(t)-\frac{1}{GJ}T\left(z(t)\right),$$

then, we can write $\dot{\psi}$ as:

$$\dot{\psi}(t-\Gamma) = \frac{1}{2}z(t) + \frac{I_{\mathrm{B}}}{2pGJ}\dot{z}(t) + \frac{1}{2pGJ}T\left(z(t)\right). \tag{2.25}$$

Substituting (2.25) into (2.24) gives

$$\dot{\phi}(t) = \frac{1}{2}z(t-\Gamma) - \frac{I_{\mathrm{B}}}{2pGJ}\dot{z}(t-\Gamma) - \frac{1}{2pGJ}T\left(z(t-\Gamma)\right). \tag{2.26}$$

We can write (2.22) as

$$\left(p - \frac{c_{\mathrm{a}}}{GJ}\right)\dot{\phi}(t) - \left(p + \frac{c_{\mathrm{a}}}{GJ}\right)\dot{\psi}(t) = -\frac{c_{\mathrm{a}}}{GJ}\Omega(t). \tag{2.27}$$

Substituting the expressions for $\dot{\psi}$ and $\dot{\phi}$ given in (2.25) and (2.26) into (2.27) yields:

$$\left(p - \frac{c_{\mathrm{a}}}{GJ}\right)\left(\frac{1}{2}z(t-\Gamma) - \frac{I_{\mathrm{B}}}{2pGJ}\dot{z}(t-\Gamma) - \frac{1}{2pGJ}T\left(z(t-\Gamma)\right)\right)$$
$$-\left(p + \frac{c_{\mathrm{a}}}{GJ}\right)\left(\frac{1}{2}z(t+\Gamma) + \frac{I_{\mathrm{B}}}{2pGJ}\dot{z}(t+\Gamma) + \frac{1}{2pGJ}T\left(z(t+\Gamma)\right)\right) = -\frac{c_{\mathrm{a}}}{GJ}\Omega(t),$$

or

$$\left(p - \frac{c_{\mathrm{a}}}{GJ}\right)\left(\frac{1}{2}z(t-2\Gamma) - \frac{I_{\mathrm{B}}}{2pGJ}\dot{z}(t-2\Gamma) - \frac{1}{2pGJ}T\left(z(t-2\Gamma)\right)\right)$$
$$-\left(p + \frac{c_{\mathrm{a}}}{GJ}\right)\left(\frac{1}{2}z(t) + \frac{I_{\mathrm{B}}}{2pGJ}\dot{z}(t) + \frac{1}{2pGJ}T\left(z(t)\right)\right) = -\frac{c_{\mathrm{a}}}{GJ}\Omega(t-\Gamma).$$

Simplifying, we get

$$\dot{z}(t) - \frac{\left(c_{\mathrm{a}} - \sqrt{IGJ}\right)}{\left(c_{\mathrm{a}} + \sqrt{IGJ}\right)}\dot{z}(t-2\Gamma) + \frac{\sqrt{IGJ}}{I_B}z(t) + \frac{\left(c_{\mathrm{a}} - \sqrt{IGJ}\right)\sqrt{IGJ}}{\left(c_{\mathrm{a}} + \sqrt{IGJ}\right)I_B}z(t-2\Gamma) =$$
$$\frac{2\sqrt{IGJ}c_{\mathrm{a}}}{\left(c_{\mathrm{a}} + \sqrt{IGJ}\right)I_B}\Omega(t-\Gamma) - \frac{1}{I_B}T(z(t)) + \frac{c_{\mathrm{a}} - \sqrt{IGJ}}{\left(c_{\mathrm{a}} + \sqrt{IGJ}\right)I_B}T(z(t-2\Gamma)),$$

which corresponds to (2.9), where $z(t)$ stands for the angular velocity at the bottom end.

Similarly, to obtain the neutral-type equation (2.13) we define $z_2(t)$ as the angular velocity at the bottom end: $z_2(t) = \frac{\partial\theta}{\partial t}(L,t) = \dot{\phi}(t+\Gamma) + \dot{\psi}(t-\Gamma)$. For the sake of simplicity, we consider that $T$ and $T_{top}$ are arbitrary time

dependent functions. The boundary condition (2.7) can be rewritten in terms of the D'Alembert solution as

$$J_T \frac{\partial^2 \phi}{\partial \gamma^2}(t) + J_T \frac{\partial^2 \psi}{\partial \eta^2}(t) + \Omega(t) = -T_{top}(t), \tag{2.28}$$

equivalently

$$J_T \ddot{\phi}(t) + J_T \ddot{\psi}(t) + \Omega(t) = -T_{top}(t). \tag{2.29}$$

Following the steps presented before, we obtain:

$$\ddot{\psi}(t-\Gamma) = \frac{1}{2}\dot{z}_2(t) + \frac{I_B}{2pGJ}\ddot{z}_2(t) + \frac{1}{2pGJ}\frac{d}{dt}T(t),$$

$$\ddot{\phi}(t) = \frac{1}{2}\dot{z}_2(t-\Gamma) - \frac{I_B}{2pGJ}\ddot{z}_2(t-\Gamma) - \frac{1}{2pGJ}\frac{d}{dt}T(t-\Gamma).$$

By substituting the above expressions into (2.29), we rewrite (2.29) as:

$$J_T\left(\frac{1}{2}\dot{z}_2(t-\Gamma) - \frac{I_B}{2pGJ}\ddot{z}_2(t-\Gamma) - \frac{1}{2pGJ}\frac{d}{dt}T(t-\Gamma)\right)$$
$$+J_T\left(\frac{1}{2}\dot{z}_2(t+\Gamma) + \frac{I_B}{2pGJ}\ddot{z}_2(t+\Gamma) + \frac{1}{2pGJ}\frac{d}{dt}T(t+\Gamma)\right) + \Omega(t) = -T_{top}(t),$$

equivalently,

$$\ddot{z}_2(t) - \ddot{z}_2(t-2\Gamma) + \frac{pGJ}{I_B}\dot{z}_2(t-2\Gamma) + \frac{pGJ}{I_B}\dot{z}_2(t) = \frac{1}{I_B}\frac{d}{dt}T(t-2\Gamma)$$
$$-\frac{1}{I_B}\frac{d}{dt}T(t) - \frac{2pGJ}{I_B J_T}\Omega(t-\Gamma) - \frac{2pGJ}{I_B J_T}T_{top}(t-\Gamma).$$

The expression (2.11) is similarly obtained by defining $v(t)$ as the displacement from the unexcited position at the top extremity:

$$v(t) = \theta(0,t) = \phi(t) + \psi(t).$$

Equation (2.12) is analogously derived using the boundary conditions (2.2-2.3).

### 2.3.2. Frequency domain analysis

The frequency domain analysis of the drilling model (2.8) with boundary conditions (2.3-2.6) using the Laplace transform is an alternative way to obtain the neutral type model (2.9).

**Definition 1** *The unilateral Laplace transform of* $\theta(\xi,t)$ *is defined by*

$$\pounds(\theta(\xi,t)) = \int_0^\infty e^{-st}\theta(\xi,t)dt = \hat{\theta}(\xi,s),$$

*where* $\theta(\xi,t)$ *is defined for* $t \geq 0$. *The inverse Laplace transform is given by the following complex integral*

$$\pounds^{-1}(\hat{\theta}(\xi,s)) = \frac{1}{2\pi i}\int_{c-i\infty}^{c+i\infty} \hat{\theta}(\xi,s)\, e^{st}ds = \theta(\xi,t).$$

**Lemma 1** *Let* $\theta : [0,+\infty) \to \mathcal{R}$ *be a piecewise continuous function on every finite interval* $[a,b]$ *in* $[0,+\infty)$. *If there exist nonnegative constants* $M$, $c$, $t_0 > 0$ *and* $s_0 \in \mathcal{R}$, *such that*

$$|\theta(t)| \leq M e^{ct} \quad \text{for all } t > t_0,$$

*then, the Laplace transform of* $\theta(t)$ *exists, i.e., there is a number* $s_0$ *such that* $\pounds(\theta(t))$ *exists for* $s > s_0$.

According to the Definition 1, the Laplace transform of $\frac{\partial\theta}{\partial t}$ is:

$$\pounds\left(\frac{\partial\theta}{\partial t}\right) = \int_0^\infty \mathrm{e}^{-st}\frac{\partial\theta}{\partial t}dt,$$

integration by parts gives

$$\pounds\left(\frac{\partial\theta}{\partial t}\right) = s\int_0^\infty \mathrm{e}^{-st}\theta dt - \theta(\xi,0) = s\hat{\theta}(\xi,s) - \theta(\xi,0),$$

where $\hat{\theta}$ is the Laplace transform of $\theta$.

Similarly, for $\frac{\partial^2\theta}{\partial t^2}$ we have:

$$\begin{aligned}\pounds\left(\frac{\partial^2\theta}{\partial t^2}\right) &= s\pounds\left(\frac{\partial\theta}{\partial t}\right) - \frac{\partial\theta(\xi,0)}{\partial t} \\ &= s^2\hat{\theta}(\xi,s) - s\theta(\xi,0) - \frac{\partial\theta(\xi,0)}{\partial t}.\end{aligned}$$

Now, for $\frac{\partial\theta}{\partial\xi}$, we have:

$$\pounds\left(\frac{\partial\theta}{\partial\xi}\right) = \int_0^\infty \mathrm{e}^{-st}\frac{\partial\theta}{\partial\xi}dt,$$

applying the Leibnitz rule yields

$$\int_0^\infty \mathrm{e}^{-st}\frac{\partial\theta}{\partial\xi}dt = \frac{\partial}{\partial\xi}\int_0^\infty \mathrm{e}^{-st}\theta dt,$$

then,

$$\pounds\left(\frac{\partial\theta}{\partial\xi}\right) = \frac{\partial}{\partial\xi}\pounds\left(\theta\right) = \frac{\partial\hat{\theta}(\xi,s)}{\partial\xi}.$$

Similarly,

$$\pounds\left(\frac{\partial^2\theta(\xi,t)}{\partial\xi^2}\right) = \int_0^\infty \mathrm{e}^{-st}\frac{\partial^2\theta(\xi,t)}{\partial\xi^2}dt = \frac{\partial^2}{\partial\xi^2}\int_0^\infty \mathrm{e}^{-st}\theta dt = \frac{\partial^2\hat{\theta}(\xi,s)}{\partial\xi^2}.$$

Summarizing,

$$\begin{aligned}
\pounds\left(\frac{\partial^2\theta(\xi,t)}{\partial t^2}\right) &= s^2\hat{\theta}(\xi,s) - s\theta(\xi,0) - \theta_t(\xi,0),\\
\pounds\left(\frac{\partial\theta(\xi,t)}{\partial t}\right) &= s\hat{\theta}(\xi,s) - \theta(\xi,0),\\
\pounds\left(\frac{\partial^2\theta(\xi,t)}{\partial\xi^2}\right) &= \frac{\partial^2\hat{\theta}(\xi,s)}{\partial\xi^2},\\
\pounds\left(\frac{\partial\theta(\xi,t)}{\partial\xi}\right) &= \frac{\partial\hat{\theta}(\xi,s)}{\partial\xi}.
\end{aligned}$$

For zero initial conditions, in terms of Laplace transform, (2.8) can be rewriten as

$$GJ\frac{\partial^2\hat{\theta}(\xi,s)}{\partial\xi^2} = Is^2\hat{\theta}(\xi,s). \tag{2.30}$$

The general solution of (2.30) is:

$$\hat{\theta}(\xi,s) = \theta_1(s)\mathrm{e}^{\sqrt{\frac{I}{GJ}}s\xi} + \theta_2(s)\mathrm{e}^{-\sqrt{\frac{I}{GJ}}s\xi}, \tag{2.31}$$

where $\theta_1(s)$ and $\theta_2(s)$ are particular solutions to be determined. The derivative of (2.31) is

$$\frac{d\hat{\theta}(\xi,s)}{d\xi} = \theta_1(s)\sqrt{\frac{I}{GJ}}s\mathrm{e}^{\sqrt{\frac{I}{GJ}}s\xi} - \theta_2(s)\sqrt{\frac{I}{GJ}}s\mathrm{e}^{-\sqrt{\frac{I}{GJ}}s\xi}. \tag{2.32}$$

For the sake of simplicity, consider that the torque $T$ is an arbitrary time dependent function. From the boundary conditions (2.3-2.6) we have:

$$GJ\frac{\partial\hat{\theta}(0,s)}{\partial\xi} = c_{\mathrm{a}}\left(s\hat{\theta}(0,s)-\Omega(s)\right), \tag{2.33}$$

$$GJ\frac{\partial\hat{\theta}(L,s)}{\partial\xi}+I_{\mathrm{B}}s^2\hat{\theta}(L,s) = -T(s). \tag{2.34}$$

Using (2.31), (2.32), we get:

$$GJ\left(\theta_1(s)\sqrt{\frac{I}{GJ}}s-\theta_2(s)\sqrt{\frac{I}{GJ}}s\right)=c_{\mathrm{a}}\left(s\left(\theta_1(s)+\theta_2(s)\right)-\Omega(s)\right),$$

$$GJ\left(\theta_1(s)\sqrt{\frac{I}{GJ}}s\mathrm{e}^{\sqrt{\frac{I}{GJ}}sL}-\theta_2(s)\sqrt{\frac{I}{GJ}}s\mathrm{e}^{-\sqrt{\frac{I}{GJ}}sL}\right)$$

$$+I_{\mathrm{B}}s^2\left(\theta_1(s)\mathrm{e}^{\sqrt{\frac{I}{GJ}}sL}+\theta_2(s)\mathrm{e}^{-\sqrt{\frac{I}{GJ}}sL}\right)=-T(s).$$

In matrix form,

$$\begin{pmatrix} \sqrt{IGJ}s-c_{\mathrm{a}}s & -\sqrt{IGJ}s-c_{\mathrm{a}}s \\ \mathrm{e}^{\Gamma s}(\sqrt{IGJ}s+I_Bs^2) & e^{-\Gamma s}\left(-\sqrt{IGJ}s+I_Bs^2\right)\end{pmatrix}\begin{pmatrix}\theta_1(s)\\ \theta_2(s)\end{pmatrix}=\begin{pmatrix}-c_{\mathrm{a}}\Omega(s)\\ -T(s)\end{pmatrix},$$

where $\Gamma=\sqrt{\frac{I}{GJ}}L$. Then, the particular solutions $\theta_1(s)$ and $\theta_2(s)$ are:

$$\begin{pmatrix}\theta_1(s)\\ \theta_2(s)\end{pmatrix}=\frac{1}{D(s)}\begin{pmatrix} \mathrm{e}^{-\Gamma s}\left(-\sqrt{IGJ}s+I_Bs^2\right) & \sqrt{IGJ}s+c_{\mathrm{a}}s \\ -\mathrm{e}^{\Gamma s}(\sqrt{IGJ}s+I_Bs^2) & \sqrt{IGJ}s-c_{\mathrm{a}}s\end{pmatrix}\begin{pmatrix}-c_{\mathrm{a}}\Omega(s)\\ -T(s)\end{pmatrix},$$

where

$$D(s)=s\left[\mathrm{e}^{-\Gamma s}(-\sqrt{IGJ}s+I_Bs^2)(\sqrt{IGJ}-c_{\mathrm{a}})+\mathrm{e}^{\Gamma s}(\sqrt{IGJ}s+I_Bs^2)(\sqrt{IGJ}+c_{\mathrm{a}})\right].$$

Then,

$$\begin{aligned}\theta_1(s) &= \frac{-\mathrm{e}^{-\Gamma s}(-\sqrt{IGJ}s+I_Bs^2)c_{\mathrm{a}}\Omega(s)-(\sqrt{IGJ}s+c_{\mathrm{a}}s)T(s)}{s[\mathrm{e}^{-\Gamma s}(-\sqrt{IGJ}s+I_Bs^2)(\sqrt{IGJ}-c_{\mathrm{a}})+\mathrm{e}^{\Gamma s}(\sqrt{IGJ}s+I_Bs^2)(\sqrt{IGJ}+c_{\mathrm{a}})]}\\ &= \frac{-\mathrm{e}^{-2\Gamma s}(-\sqrt{IGJ}s+I_Bs^2)c_{\mathrm{a}}\Omega(s)-\mathrm{e}^{-\Gamma s}(\sqrt{IGJ}s+c_{\mathrm{a}}s)T(s)}{s[\mathrm{e}^{-2\Gamma s}(-\sqrt{IGJ}s+I_Bs^2)(\sqrt{IGJ}-c_{\mathrm{a}})+(\sqrt{IGJ}s+I_Bs^2)(\sqrt{IGJ}+c_{\mathrm{a}})]}\\ &= \frac{-\mathrm{e}^{-2\Gamma s}(-\sqrt{IGJ}+I_Bs)c_{\mathrm{a}}\Omega(s)-\mathrm{e}^{-\Gamma s}(\sqrt{IGJ}+c_{\mathrm{a}})T(s)}{\mathrm{e}^{-2\Gamma s}(-\sqrt{IGJ}s+I_Bs^2)(\sqrt{IGJ}-c_{\mathrm{a}})+(\sqrt{IGJ}s+I_Bs^2)(\sqrt{IGJ}+c_{\mathrm{a}})},\end{aligned}$$

and

$$\begin{aligned}\theta_2(s) &= \frac{\mathrm{e}^{\Gamma s}(\sqrt{IGJ}s + I_B s^2)c_\mathrm{a}\Omega(s) - (\sqrt{IGJ}s - c_\mathrm{a}s)T(s)}{s[\mathrm{e}^{-\Gamma s}(-\sqrt{IGJ}s + I_B s^2)(\sqrt{IGJ} - c_\mathrm{a}) + \mathrm{e}^{\Gamma s}(\sqrt{IGJ}s + I_B s^2)(\sqrt{IGJ} + c_\mathrm{a})]} \\ &= \frac{(\sqrt{IGJ}s + I_B s^2)c_\mathrm{a}\Omega(s) - \mathrm{e}^{-\Gamma s}(\sqrt{IGJ}s - c_\mathrm{a}s)T(s)}{s[\mathrm{e}^{-2\Gamma s}(-\sqrt{IGJ}s + I_B s^2)(\sqrt{IGJ} - c_\mathrm{a}) + (\sqrt{IGJ}s + I_B s^2)(\sqrt{IGJ} + c_\mathrm{a})]} \\ &= \frac{(\sqrt{IGJ} + I_B s)c_\mathrm{a}\Omega(s) - \mathrm{e}^{-\Gamma s}(\sqrt{IGJ} - c_\mathrm{a})T(s)}{\mathrm{e}^{-2\Gamma s}(-\sqrt{IGJ}s + I_B s^2)(\sqrt{IGJ} - c_\mathrm{a}) + (\sqrt{IGJ}s + I_B s^2)(\sqrt{IGJ} + c_\mathrm{a})}.\end{aligned}$$

Let $z(s)$ be the angular velocity at the bottom extremity:

$$z(s) = s\hat{\theta}(L,s) = s\left(\theta_1(s)\mathrm{e}^{\Gamma s} + \theta_2(s)\mathrm{e}^{-\Gamma s}\right),$$

substituting the particular solutions $\theta_1$ and $\theta_2$ yields

$$\begin{aligned}z(s) &= \frac{s[-\mathrm{e}^{-\Gamma s}(-\sqrt{IGJ} + I_B s)c_\mathrm{a}\Omega(s) - (\sqrt{IGJ} + c_\mathrm{a})T(s)]}{\mathrm{e}^{-2\Gamma s}(-\sqrt{IGJ}s + I_B s^2)(\sqrt{IGJ} - c_\mathrm{a}) + (\sqrt{IGJ}s + I_B s^2)(\sqrt{IGJ} + c_\mathrm{a})} \\ &\quad + \frac{s[\mathrm{e}^{-\Gamma s}(\sqrt{IGJ} + I_B s)c_\mathrm{a}\Omega(s) - \mathrm{e}^{-2\Gamma s}(\sqrt{IGJ} - c_\mathrm{a})T(s)]}{\mathrm{e}^{-2\Gamma s}(-\sqrt{IGJ}s + I_B s^2)(\sqrt{IGJ} - c_\mathrm{a}) + (\sqrt{IGJ}s + I_B s^2)(\sqrt{IGJ} + c_\mathrm{a})},\end{aligned}$$

simplifying

$$\begin{aligned}z(s) &= \frac{-\mathrm{e}^{-\Gamma s}(-\sqrt{IGJ} + I_B s)c_\mathrm{a}\Omega(s) - (\sqrt{IGJ} + c_\mathrm{a})T(s)}{\mathrm{e}^{-2\Gamma s}(-\sqrt{IGJ} + I_B s)(\sqrt{IGJ} - c_\mathrm{a}) + (\sqrt{IGJ} + I_B s)(\sqrt{IGJ} + c_\mathrm{a})} \\ &\quad + \frac{\mathrm{e}^{-\Gamma s}(\sqrt{IGJ} + I_B s)c_\mathrm{a}\Omega(s) - \mathrm{e}^{-2\Gamma s}(\sqrt{IGJ} - c_\mathrm{a})T(s)}{\mathrm{e}^{-2\Gamma s}(-\sqrt{IGJ} + I_B s)(\sqrt{IGJ} - c_\mathrm{a}) + (\sqrt{IGJ} + I_B s)(\sqrt{IGJ} + c_\mathrm{a})},\end{aligned}$$

equivalently,

$$\begin{aligned}z(s)[\mathrm{e}^{-2\Gamma s}(-\sqrt{IGJ} + I_B s)(\sqrt{IGJ} - c_\mathrm{a}) + (\sqrt{IGJ} + I_B s)(\sqrt{IGJ} + c_\mathrm{a})] = \\ - \mathrm{e}^{-\Gamma s}(-\sqrt{IGJ} + I_B s)c_\mathrm{a}\Omega(s) - (\sqrt{IGJ} + c_\mathrm{a})T(s) \\ + \mathrm{e}^{-\Gamma s}(\sqrt{IGJ} + I_B s)c_\mathrm{a}\Omega(s) - \mathrm{e}^{-2\Gamma s}(\sqrt{IGJ} - c_\mathrm{a})T(s),\end{aligned}$$

or,

$$\begin{aligned}&-\sqrt{IGJ}(\sqrt{IGJ} - c_\mathrm{a})\mathrm{e}^{-2\Gamma s}z(s) + I_\mathrm{B}(\sqrt{IGJ} - c_\mathrm{a})s\mathrm{e}^{-2\Gamma s}z(s) \\ &+\sqrt{IGJ}(\sqrt{IGJ} + c_\mathrm{a})z(s) + I_\mathrm{B}(\sqrt{IGJ} + c_\mathrm{a})sz(s) = \\ &\qquad + \sqrt{IGJ}c_\mathrm{a}\mathrm{e}^{-\Gamma s}\Omega(s) - I_B c_\mathrm{a} s\mathrm{e}^{-\Gamma s}\Omega(s) - (\sqrt{IGJ} + c_\mathrm{a})T(s) \\ &\qquad + \sqrt{IGJ}c_\mathrm{a}\mathrm{e}^{-\Gamma s}\Omega(s) + I_B c_\mathrm{a} s\mathrm{e}^{-\Gamma s}\Omega(s) - (\sqrt{IGJ} - c_\mathrm{a})\mathrm{e}^{-2\Gamma s}T(s).\end{aligned}$$

Rearranging terms we get

$$I_{\mathrm{B}}(\sqrt{IGJ}+c_{\mathrm{a}})sz(s)+I_{\mathrm{B}}(\sqrt{IGJ}-c_{\mathrm{a}})s\mathrm{e}^{-2\Gamma s}z(s)$$
$$+\sqrt{IGJ}(\sqrt{IGJ}+c_{\mathrm{a}})z(s)-\sqrt{IGJ}(\sqrt{IGJ}-c_{\mathrm{a}})\mathrm{e}^{-2\Gamma s}z(s)=$$
$$+2\sqrt{IGJ}c_{\mathrm{a}}\mathrm{e}^{-\Gamma s}\Omega(s)-(\sqrt{IGJ}+c_{\mathrm{a}})T(s)-(\sqrt{IGJ}-c_{\mathrm{a}})\mathrm{e}^{-2\Gamma s}T(s),$$

multiplying the above expression by $1/[I_{\mathrm{B}}(\sqrt{IGJ}+c_{\mathrm{a}})]$ yields

$$sz(s)+\frac{\sqrt{IGJ}-c_{\mathrm{a}}}{\sqrt{IGJ}+c_{\mathrm{a}}}s\mathrm{e}^{-2\Gamma s}z(s)+\frac{\sqrt{IGJ}}{I_{\mathrm{B}}}z(s)-\frac{\sqrt{IGJ}(\sqrt{IGJ}-c_{\mathrm{a}})}{I_{\mathrm{B}}(\sqrt{IGJ}+c_{\mathrm{a}})}\mathrm{e}^{-2\Gamma s}z(s)=$$
$$+\frac{2\sqrt{IGJ}c_{\mathrm{a}}}{I_{\mathrm{B}}(\sqrt{IGJ}+c_{\mathrm{a}})}\mathrm{e}^{-\Gamma s}\Omega(s)-\frac{1}{I_{\mathrm{B}}}T(s)-\frac{(\sqrt{IGJ}-c_{\mathrm{a}})}{I_{\mathrm{B}}(\sqrt{IGJ}+c_{\mathrm{a}})}\mathrm{e}^{-2\Gamma s}T(s),$$

equivalently,

$$sz(s)-\frac{c_{\mathrm{a}}-\sqrt{IGJ}}{c_{\mathrm{a}}+\sqrt{IGJ}}s\mathrm{e}^{-2\Gamma s}z(s)+\frac{\sqrt{IGJ}}{I_{\mathrm{B}}}z(s)+\frac{(c_{\mathrm{a}}-\sqrt{IGJ})\sqrt{IGJ}}{(c_{\mathrm{a}}+\sqrt{IGJ})I_{\mathrm{B}}}\mathrm{e}^{-2\Gamma s}z(s)=$$
$$+\frac{2\sqrt{IGJ}c_{\mathrm{a}}}{(c_{\mathrm{a}}+\sqrt{IGJ})I_{\mathrm{B}}}\mathrm{e}^{-\Gamma s}\Omega(s)-\frac{1}{I_{\mathrm{B}}}T(s)+\frac{c_{\mathrm{a}}-\sqrt{IGJ}}{(c_{\mathrm{a}}+\sqrt{IGJ})I_{\mathrm{B}}}\mathrm{e}^{-2\Gamma s}T(s).$$

Finally, taking the inverse Laplace transform of the above expression we obtain the neutral-type time-delay equation describing the drilling system behavior given by (2.9).

### 2.3.3. Formal stability analysis

The term formal stability was introduced in [25]. According to [91], it means that a neutral type delay system has only a finite number of zeros in the right half complex plane. The formal stability property corresponds to the stability of the difference operator associated with the neutral system. Its well known that the formal stability is a necessary condition to the stability and stabilization of such systems [76].

**Definition 2** *[76] Consider a system of the form*

$$\begin{aligned}\dot{x}(t)=&\sum_{k=1}^{q}E_k\dot{x}(t-k\Gamma)+\sum_{k=0}^{q}A_kx(t-k\Gamma)\\&+\sum_{k=0}^{q}B_ku(t-k\Gamma)+\sum_{k=o}^{q}C_kf(x(t-k\Gamma)),\end{aligned}\tag{2.35}$$

*where $x(t)\in\mathcal{R}^n$ is the state, $u(t)\in\mathcal{R}^m$ is the control input and $f(\cdot)$ is a nonlinear bounded function depending on the state. Such system is said to be formally stable if*

$$Rank(I_n-\hat{E}(s))=n,\qquad \forall s\ \ such\ that\ \ Re(s)\geq 0,$$

*where*

$$\hat{E}(s) = \sum_{k=1}^{q} E_k e^{-ks\theta} \tag{2.36}$$

*and* $Re(s)$ *denotes the real part of the complex number* $s$.

The drilling model (2.9) is a scalar neutral-type equation with

$$\hat{E}(s) = \frac{c_a - \sqrt{IGJ}}{c_a + \sqrt{IGJ}} e^{-2\Gamma s}.$$

This model is formally stable if

$$1 - \frac{c_a - \sqrt{IGJ}}{c_a + \sqrt{IGJ}} e^{-2\Gamma s} \neq 0 \quad \forall s \text{ such that } \mathrm{Re}(s) \geq 0.$$

Since

$$e^{-2\Gamma s} \leq 1, \quad \forall s \text{ such that } \mathrm{Re}(s) \geq 0,$$

and

$$\left| \frac{c_a - \sqrt{IGJ}}{c_a + \sqrt{IGJ}} \right| < 1, \quad \text{for } c_a > 0,$$

we can conclude that the neutral type model (2.9) is formally stable.

Notice that, the model (2.12) is not formally stable since $\hat{E}(s) = e^{-2\Gamma s}$ and the equality $1 - \hat{E}(s) = 0$ is satisfied for $s = 0$.

## 2.4. Conclusion

A distributed parameter model of the drillstring behavior described by a hyperbolic PDE was presented. This model corresponds to the unidimensional wave equation, widely used to represent the oscillatory behavior of physical systems. Coupled to this equation, mixed boundary conditions are chosen according to the dynamics observed at both ends of the string. The boundary condition at the bottom end is subject to a TOB model which constitutes a crucial aspect of the model since it allows to reproduce the stick-slip phenomena; an explicit nonlinear TOB model will be given in the next chapter. For the boundary condition at the upper extremity, we have presented two options, one of them, equation (2.2), considers a constant rotary speed at the top end, the other one, equation (2.6), assumes a sliding velocity at the upper part resulting from the non-matching velocities, of the load and of the rotary table.

By means of a direct transformation, input-output models have been derived from the undamped wave equation model. Two different procedures allowing the model transformation have been presented: the D'Alembert method and Laplace techniques. The model transformation leads to neutral-type time-delay equations describing the behavior at each extremity of the string; equation (2.9) was derived using the boundary condition (2.6) and equation (2.12) using (2.2).

The formal stability property is a necessary condition to the stability and stabilization of neutral-type time-delay systems, we have shown that model (2.9) is formally stable meanwhile model (2.12) is not. Subsequent discussions on stability analysis and control design will be based on the formally stable model.

# Chapter 3

# Undesirable vibrations in oilwell drilling systems

## 3.1. Introduction

The drillstring interaction with the borehole gives rise to a wide variety of non-desired oscillations which are classified depending on the direction they appear.

Three main types of vibrations (illustrated in Figure 3.1) can be distinguished: torsional (stick-slip oscillations), axial (bit bouncing phenomenon) and lateral (whirl motion due to the out-of-balance of the drillstring).

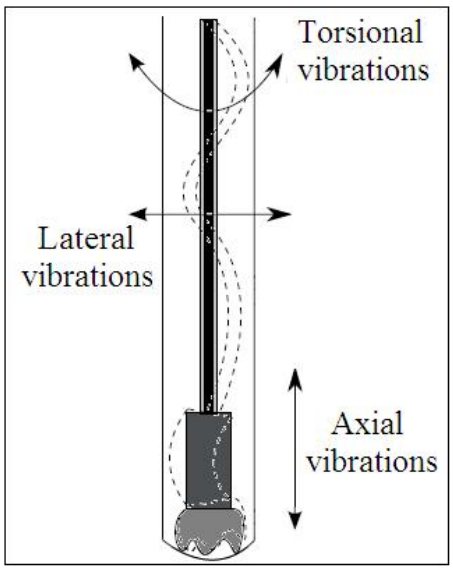


Figure 3.1: Vibrations in oilwell drillstrings.

Throughout this work, we will focus on the most frequently occurring vibration mode: the stick-slip phenomenon. Since the presence of torsional vibration usually excites axial vibration, some analysis on the bit-bounce will also be presented.

This chapter addresses the problem of modeling the stick-slip and bit-bounce behaviors. In order to properly represent the stick-slip phenomenon, it is important to have a suitable model describing the rock-bit interaction.

In the next section, we present a mathematical description for the bit-rock contact; the model consists of a dry friction combined with an exponential decaying law which introduces the discontinuity in the open-loop system. The bit-bounce is approximated by means of the damped harmonic oscillator model describing the axial dynamics. Axial and torsional models that adequately capture the drilling dynamics are coupled via the TOB function describing the rock-bit contact; they will be used to simulate the effects of varying operating conditions on stick-slip and bit-bounce interactions.

This chapter also refers to practical approaches that reduce the stick-slip behavior. The practical strategies that qualitatively capture the driller's expertise consist of the alignment of different drilling parameters: rotary speed, WOB and drilling fluid.

## 3.2. Torsional dynamics

Torsional drillstring vibrations appear due to downhole conditions, such as significant drag, tight hole, and formation characteristics. It can cause the bit to stall in the formation while the rotary table continues to rotate. When the trapped torsional energy (similar to a wound-up spring) reaches a level that the bit can no longer resist, the bit suddenly comes loose, rotating and whipping at very high speeds. This stick-slip behavior can generate a torsional wave that travels up the drillstring to the rotary top system. Because of the high inertia of the rotary table, it acts like a fixed end to the drillstring and reflects the torsional wave back down the drillstring to the bit. The bit may stall again, and the torsional wave cycle repeats [84].

The whipping and high speed rotations of the bit in the slip phase can generate both severe axial and lateral vibrations at the BHA. The vibrations can originate problems such as drill pipe fatigue problems, drillstring components failures and wellbore instability [64].

Torsional vibrations are characterized by stick phases, during which the rotation stops completely, and slip phases, during which the angular velocity of the tool increases up to two times the nominal angular velocity. This phenomenon occurs when a section of the rotating drillstring is momentarily caught by friction against the borehole, then releases. The bit might eventually get stuck and then, after accumulating energy in terms of torsion, be suddenly released, the collar rotation speeds up dramatically and large centrifugal accelerations occur. The stick-slip phenomenon is identified by periodic torque fluctuations.

It is usually assumed that the growth of instabilities leading eventually to stick-slip oscillations arises from the friction model, which empirically captures the bit-rock interaction. The most common friction models include velocity weakening laws as in [28], stiction plus Coulomb friction [55], [107], and the Stribeck effect characterized by a decreasing friction-velocity map localized around zero velocity [70], [84].

The friction torque model (2.4-2.5) rewritten as

$$T\left(z(t)\right) = c_{\mathrm{b}} z(t) + W_{\mathrm{ob}} R_{\mathrm{b}} \mu_{\mathrm{b}}\left(z(t)\right) \operatorname{sign}\left(z(t)\right), \tag{3.1}$$

$$\mu_{\mathrm{b}}\left(z(t)\right) = \mu_{\mathrm{cb}} + (\mu_{\mathrm{sb}} - \mu_{\mathrm{cb}}) \mathrm{e}^{-\frac{\gamma_{\mathrm{b}}}{v_{\mathrm{f}}}|z(t)|}, \tag{3.2}$$

leads to a decreasing TOB with increasing bit angular velocity for low velocities which acts as a negative damping (Stribeck effect) and is the cause of stick-slip self-excited vibrations. The exponential decaying behavior of $T\left(z(t)\right)$ coincides with experimental torque values.

The vibrations of the drillstring lead to fatigue and diminish the accuracy of the drilling process. Thus, control actions are necessary in order to induce the suppression of this undesirable behavior.

The angular velocity coming from the rotary table $\Omega(t)$ is usually taken as control input $\bar{u}(t)$. We consider here, the following structure:

$$\bar{u}(t) = u(t) + \Omega_0, \tag{3.3}$$

where $u(t)$ is a stabilizing controller which should eliminate the stick-slip phenomenon and $\Omega_0$ is the constant angular velocity desired at the bottom end. In view of the model for the TOB (3.1-3.2) and (3.3) we can rewrite (2.9) as:

$$\begin{aligned} \dot{z}(t) - \Upsilon \dot{z}(t - 2\Gamma) \;=\; & \left(-\Psi - \frac{c_{\mathrm{b}}}{I_{\mathrm{B}}}\right) z(t) + \left(\frac{\Upsilon c_{\mathrm{b}}}{I_{\mathrm{B}}} - \Upsilon\Psi\right) z(t - 2\Gamma) \\ & + \Pi u(t - \Gamma) + \Pi\Omega_0 - \frac{1}{I_{\mathrm{B}}} T_{\mathrm{nl}}\left(z(t)\right) + \frac{\Upsilon}{I_{\mathrm{B}}} T_{\mathrm{nl}}\left(z(t - 2\Gamma)\right), \end{aligned} \tag{3.4}$$

where $T_{\rm nl}$ stands for the nonlinear term of the TOB model (3.1), i.e.,

$$T_{\rm nl}\left(z(t)\right) = W_{\rm ob}R_{\rm b}\left(\mu_{\rm cb}+(\mu_{\rm sb}-\mu_{\rm cb})\mathrm{e}^{-\frac{\gamma_{\rm b}}{v_{\rm f}}|z(t)|}\right)\mathrm{sign}\left(z(t)\right). \tag{3.5}$$

In order to shift the operating point, we introduce the new variable $x_1$ defined as:

$$x_1(t) = z(t) - \Omega_0. \tag{3.6}$$

Then, we obtain the following equivalent system:

$$\begin{aligned}\dot{x}_1(t) + d\dot{x}_1(t-2\Gamma) &= a_0x_1(t) + a_1x_1(t-2\Gamma) + bu(t-\Gamma) \\ &\quad -\frac{1}{I_{\rm B}}T_{\rm nl}\left(x_1(t)+\Omega_0\right) + \frac{\Upsilon}{I_{\rm B}}T_{\rm nl}\left(x_1(t-2\Gamma)+\Omega_0\right) + \omega,\end{aligned} \tag{3.7}$$

where $|d| < 1$, and

$$\begin{array}{ll} a_0 = -\Psi - \frac{c_{\rm b}}{I_{\rm B}}, & a_1 = \frac{\Upsilon c_{\rm b}}{I_{\rm B}} - \Upsilon\Psi, \\ d = -\Upsilon, & b = \Pi. \end{array}$$

## 3.3. Axial dynamics

Axial vibrations, also known as bit-bouncing phenomenon happens when the bit loses contact with the rock, hitting the drill area with great strength.

Axial and torsional vibrations are generally quite complex in nature. They are self-excited oscillations intimately coupled together and may occur simultaneously. For example, the high bit speed level caused by stick-slip torsional motion can excite severe axial vibrations in the BHA, which may cause bit bounce, excessive bit wear and reduction in the penetration rate.

The wave equation modeling approach constitutes a reliable approximation of the drillstring axial behavior. In [21], [22] the axial excitations of a drillstring of length $L$, described by the longitudinal position $U(\xi,t)$ are modeled by the wave equation:

$$\begin{aligned}\frac{\partial^2 U}{\partial t^2}(\xi,t) &= \breve{c}^2\frac{\partial^2 U}{\partial \xi^2}(\xi,t), \\ \breve{E}\breve{\Gamma}\frac{\partial U}{\partial \xi}(0,t) &= \breve{\alpha}\frac{\partial U}{\partial t}(0,t) - \breve{H}(t), \\ \breve{M}\frac{\partial^2 U}{\partial t^2}(L,t) &= -\breve{E}\breve{\Gamma}\frac{\partial U}{\partial \xi}(L,t) + \breve{F}\left(\frac{\partial U}{\partial t}(L,t)\right)\end{aligned} \tag{3.8}$$

where $\breve{H}(t)$ is the brake motor control and $\breve{\alpha}\frac{\partial U}{\partial t}(0,t)$ represents a friction force of viscous type, $\breve{E}$ is the elasticity Young's modulus, the wave speed is expressed by $\breve{c} = \sqrt{\breve{E}/\rho}$, $\breve{\Gamma}$ is the averaged section of the drillpipe, $\rho$ and $\breve{M}$ stand for the density and mass of the string respectively and the function $\breve{F}$ approximates the nonlinear dynamics at the bottom extremity.

A simplified model described by an ordinary differential equation is presented in [28], the damped harmonic oscillator model is used to represent the axial dynamics of the drillstring:

$$m_0\ddot{Y} + c_0\dot{Y} + k_0(Y - \mathrm{ROP}t) = -\mu_1 T\left(z(t)\right), \tag{3.9}$$

where $Y$, $\dot{Y}$ and $\ddot{Y}$ stand for the axial variables: position, velocity and acceleration respectively, the Rate Of Penetration (ROP) is a constant axial speed imposed at the surface, $m_0$, $c_0$, and $k_0$ represent the mass, damping and spring constant. The constant $\mu_1$ depends on the bit geometry (bit radius, rake angle), it is easily obtained for a flat bit [28].

This modeling strategy is inspired by the fact that any mass subject to a force in stable equilibrium acts as a harmonic oscillator for small vibrations.

In this work we analyze the drilling vibration coupling based on the simplified axial model. The coupling between the torsional model (2.9) and the axial model (3.9) is due to the TOB affecting both dynamics. Simulation results presented in the following section confirm that these vibration phenomena affect each other.

The change of variable

$$y = Y - \mathrm{ROP}t$$

yields the following equivalent model:

$$m_0\ddot{y} + c_0\left(\dot{y} + \mathrm{ROP}\right) + k_0 y = -\mu_1 T\left(z(t)\right). \tag{3.10}$$

## 3.4. Simulation results

The model parameters used in the following simulations are shown below, they represent a typical case in oilwell drilling operations [28], [84].

$$
\begin{array}{lll}
G = 79.3x10^{9}\text{N m}^{-2}, & I = 0.095\text{Kg m}, & L = 1172\text{m}, \\
J = 1.19x10^{-5}\text{m}^{4}, & R_{\text{b}} = 0.155575\text{m}, & v_{\text{f}} = 1, \\
W_{\text{ob}} = 97347\text{N}, & I_{\text{B}} = 89\text{Kg m}^{2}, & c_{\text{a}} = 2000\text{N m s}, \\
\mu_{\text{cb}} = 0.5, & \mu_{\text{sb}} = 0.8, & \gamma_{\text{b}} = 0.9, \\
c_{\text{b}} = 0.03\text{N m s rad}^{-1}, & m_0 = 37278\text{Kg}, & c_0 = 16100\text{kg s}^{-1}, \\
k_0 = 1.55 \times 10^{6}\text{Kg s}^{-2}, & \text{ROP} = 0.01\text{m s}^{-1}, & \mu_1 = 257\text{m}^{-1}.
\end{array}
\tag{3.11}
$$

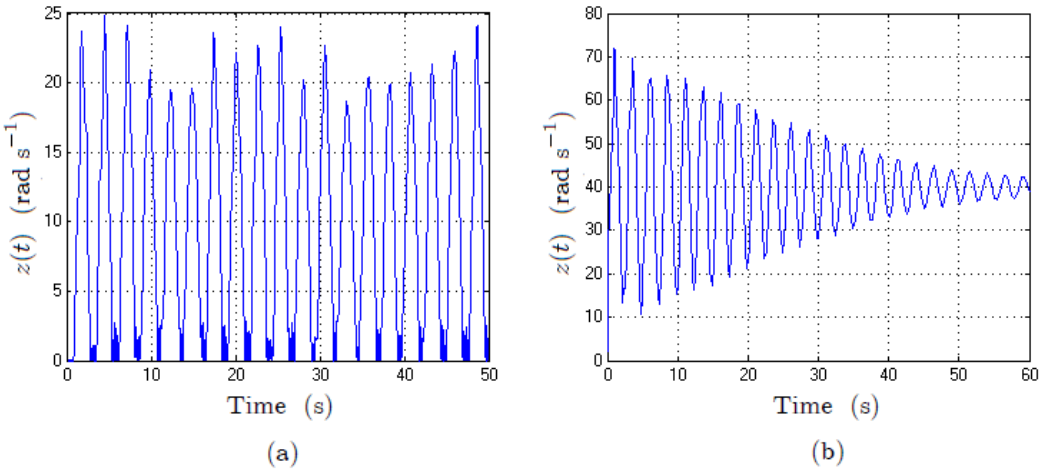


Figure 3.2: Angular velocity at the bottom extremity $z(t)$ for: (a) $\Omega_0 = 10$rad s$^{-1}$ (stick-slip), (b) $\Omega_0 = 40$rad s$^{-1}$.

The simulations are developed using the variable step Matlab-Simulink solver ode45 (Dormand Prince Method). Figures 3.2-3.5 show the response when there is no feedback control.

Equations (2.9), (3.1-3.2) describe the drillstring behavior and the occurrence of stick-slip oscillations. A simulation of the system (2.9), (3.1-3.2) is shown in Figure 3.2. Notice that when the phenomenon occurs, as reported in real wells, important torque fluctuations appear [64].

It is assumed that the rotary table and the bit are rotating at the desired speed when the bit is off bottom. When the bit starts to interact with the formation the system will inevitably be disturbed with the possibility of axial and torsional vibrations, occurring simultaneously.

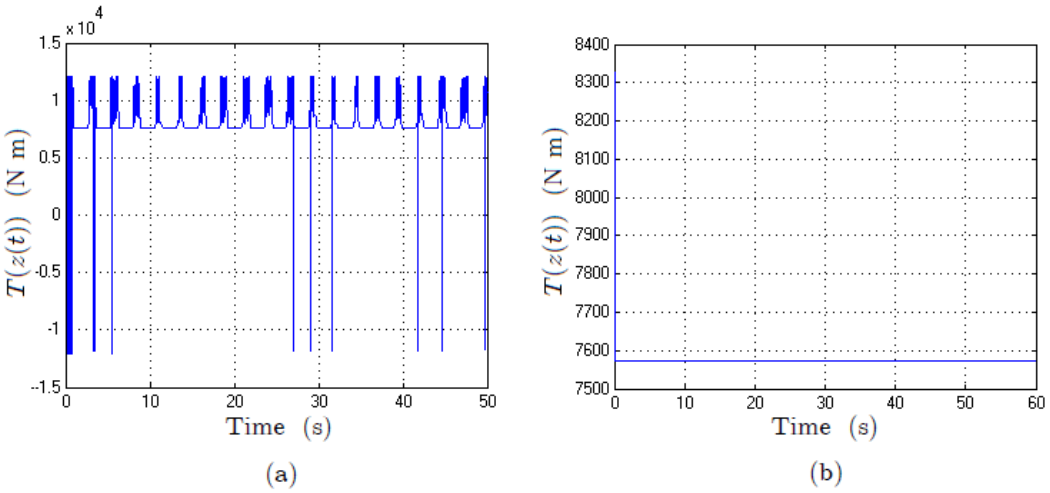


Figure 3.3: Torque on the bit $T(z(t))$ for: (a) $\Omega_0 = 10\text{rad s}^{-1}$, (b) $\Omega_0 = 40\text{rad s}^{-1}$.

Though the rotary table speed does not change, significant stick-slip behavior is seen at the bit as shown in Figure 3.2. Notice that increasing the angular velocity $\Omega(t)$ leads to the reduction of the stick-slip. The qualitative agreement between this result and the field data observed in [51] is remarkable.

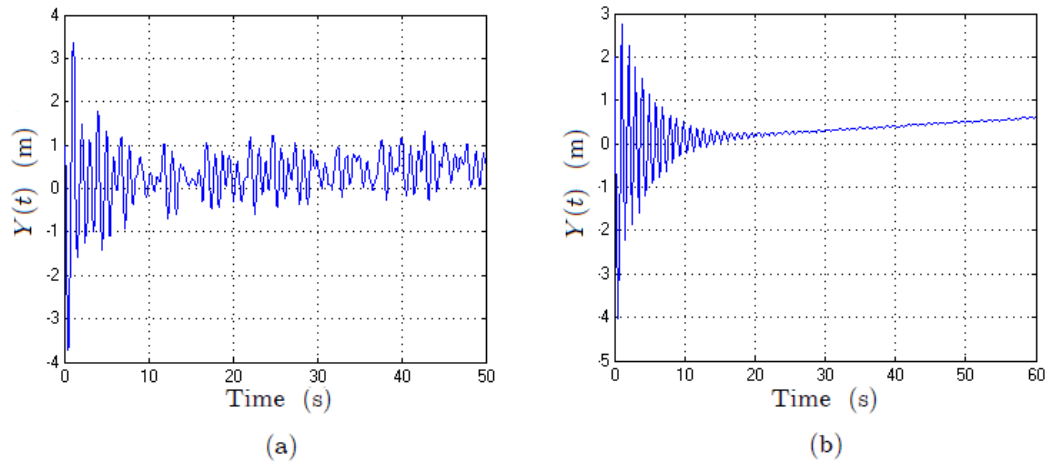


Figure 3.4: Axial displacement of the drillstring $Y(t)$ for: (a) $\Omega_0 = 10\text{rad s}^{-1}$ (bit-bouncing), (b) $\Omega_0 = 40\text{rad s}^{-1}$.

The bit momentarily stops causing the TOB to reach very high values

(Figure 3.3). When the bit starts slipping, the energy stored in the drillstring is released causing very large torsional vibrations. During this time the bit remains in contact with the formation. It appears that some of the energy stored during stick phase is transferred into axial vibrations.

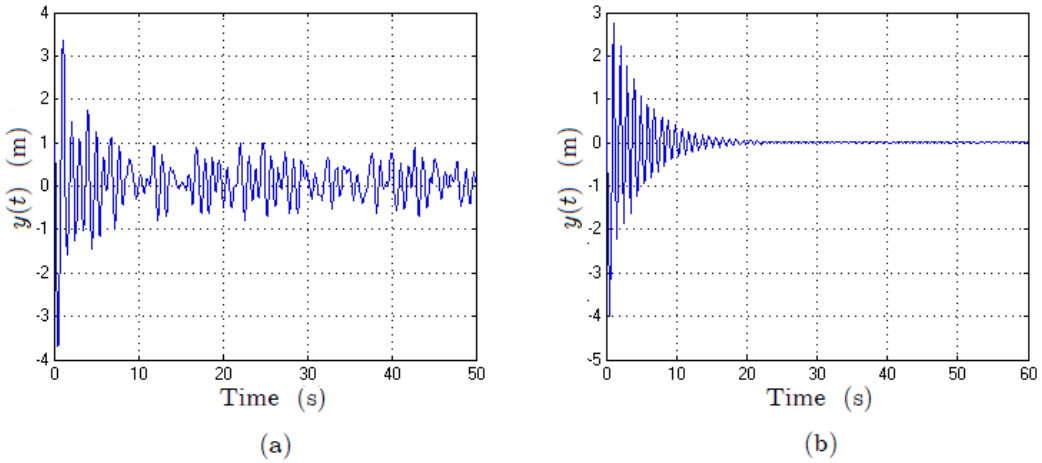


Figure 3.5: Variable $y = Y - \mathrm{ROP}t$ for: (a) $\Omega_0 = 10\mathrm{rad\ s}^{-1}$ (bit-bouncing), (b) $\Omega_0 = 40\mathrm{rad\ s}^{-1}$.

The simulation result shown in Figure 3.4 confirm that the fluctuations of angular velocity at the bit level excites axial vibrations.

The axial resonance causes the bit to lose contact with formation (bit bounce). Once the bit is off-bottom, the TOB is zero, and consequently, the critical frequencies for lateral and axial vibrations change [29]. Since there is no feedback, these large amplitude vibrations remain with continuous energy exchange between various modes of vibration. Clearly, this type of behavior will eventually lead to failure due to very large and often cyclic stresses present at different sections of the drillstring.

It is clear that most of the downhole vibrations are driven by bit motion. Therefore, for an effective control of vibrations, the measurement and feedback of certain variables at the bit level are required.

## 3.5. Practical strategies to reduce the stick-slip phenomenon

In practice, the driller operator typically has access to the surface-controlled drilling parameters, such as the WOB, drilling fluid flow through the drill pipe, the drillstring rotational speed and the density and viscosity of the drilling fluid to optimize the drilling operations.

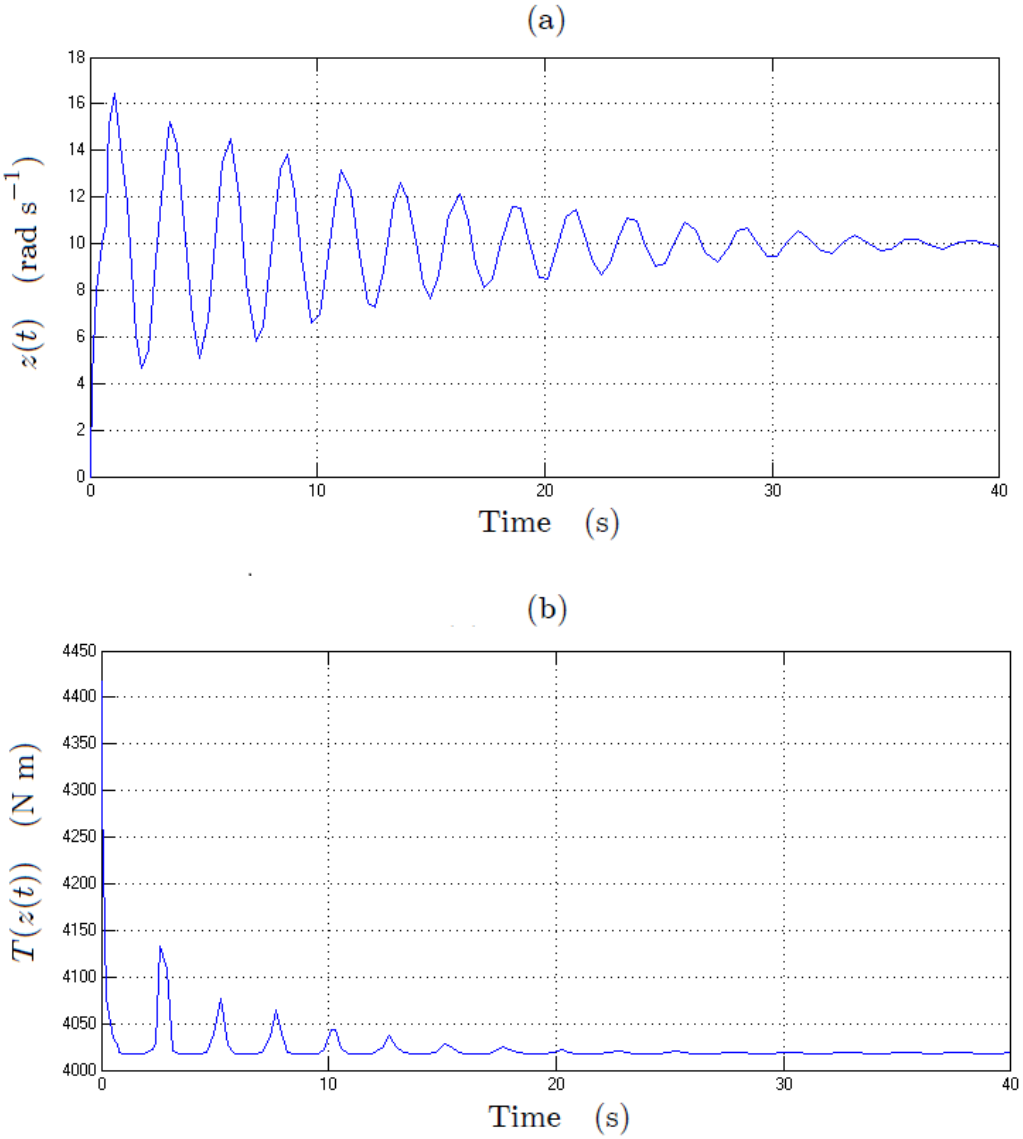


Figure 3.6: Reduction of stick-slip phenomenon by decreasing the WOB.

Next, we present some of the main strategies based on drillers' experience used in practice to reduce the stick-slip phenomenon.

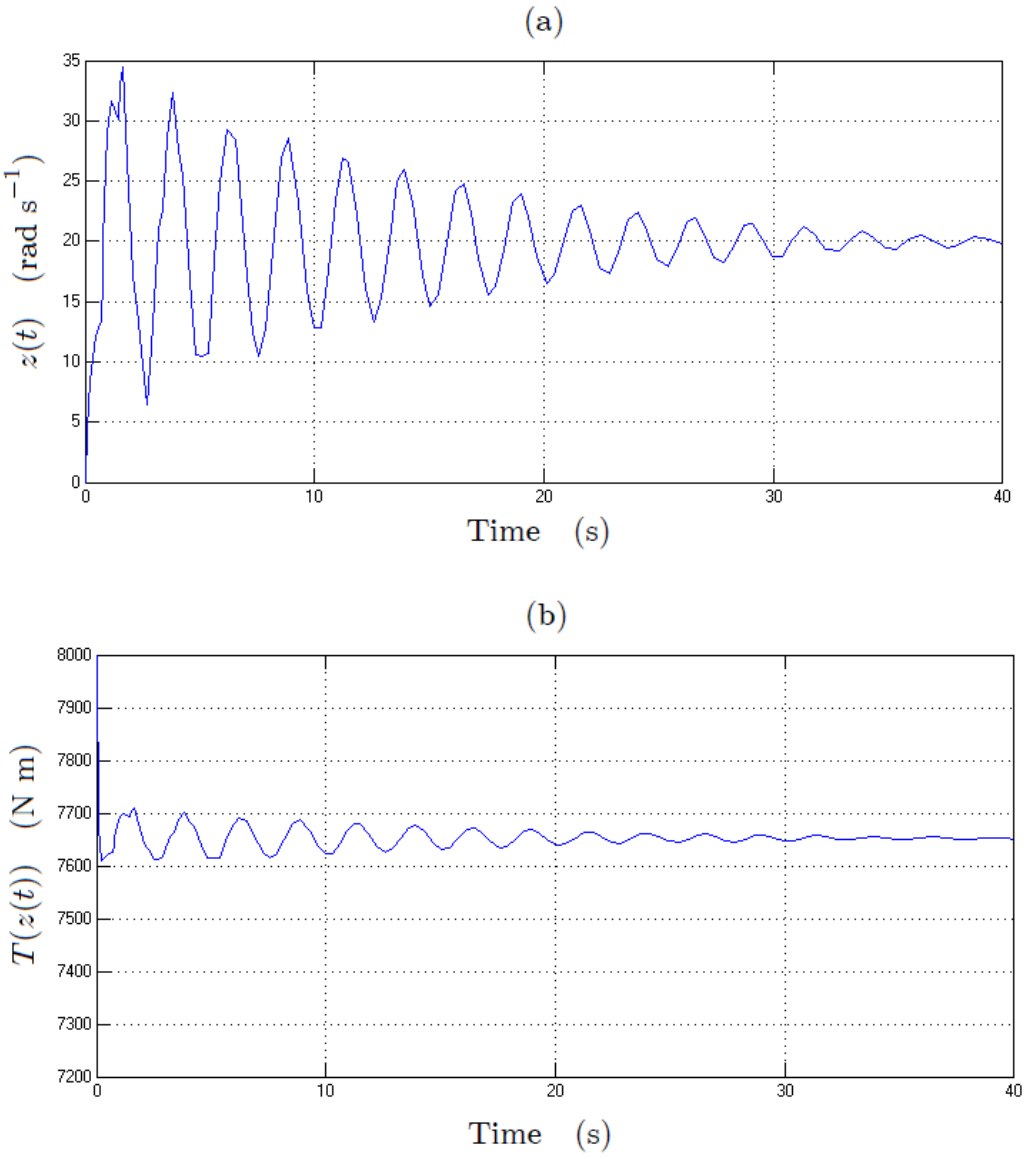


Figure 3.7: Reduction of stick-slip phenomenon by increasing $\Omega$.

### 3.5.1. Decreasing the weight on the bit

According to drillers'experience, for a fixed angular velocity at the surface $\Omega$, reducing the WOB makes the stick-slip phenomenon disappear, and when the WOB is very large the bit is stopped [103]. A simulation of the system

(2.9-3.1) with $\Omega = 10\text{rad s}^{-1}$ and the WOB decreased from 97347N to 31649N shows an important reduction of the stick-slip oscillations (Figure 3.6).

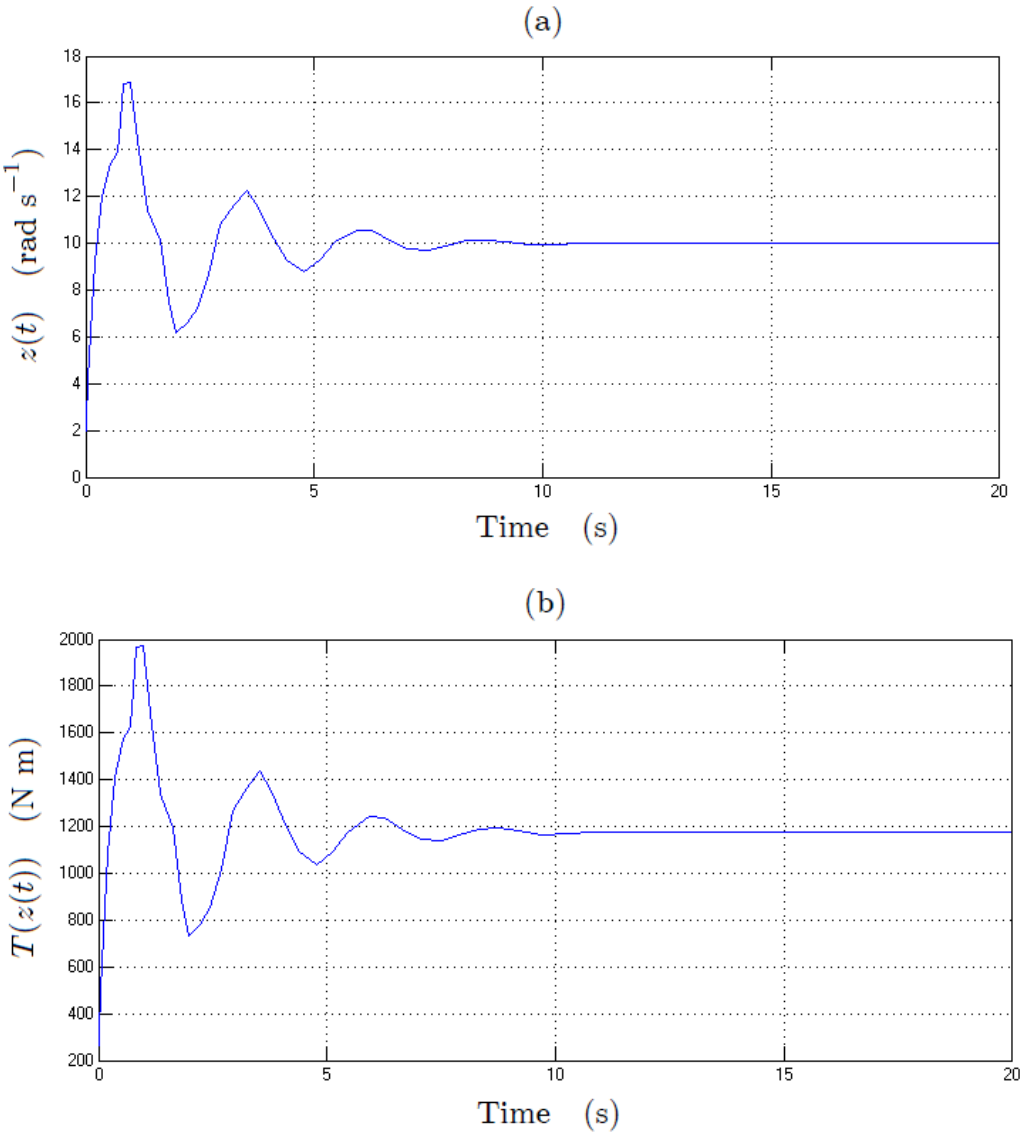


Figure 3.8: Reduction of stick-slip oscillations by using the variation law (3.12).

To ensure an optimal perforation rate it is necesary to maintain a certain amount of weight on the cutting device. A shortcoming of the proposed empirical method is that, to reduce torsional oscilations, it may require a substantial reduction of the WOB implying an inefficient drilling speed or even

stopping the perforation process.

### 3.5.2. Increasing the angular velocity at the upper part

Experimental results indicate that the stick-slip phenomenon is avoided by increasing the velocity $\Omega$ provided by the rotary table. The simulation results of Figure 3.7 show that the stick-slip vibrations are reduced by means of increasing the velocity at the top extremity from $\Omega = 10\text{rad s}^{-1}$ to $\Omega = 20\text{rad s}^{-1}$ while the WOB remains constant ($W_{\text{ob}} = 97347\text{N}$).

The disadvantage of the strategy lies in the fact that a substantial increment of the angular speed induce lateral problems like irregular rotation causing repeated collisions between the rod and the borehole walls producing an eccentric hole. The shocks may damage the drilling system components and deteriorate the borehole wall affecting the overall drilling direction.

### 3.5.3. Introducing a variation law of the weight on the bit

From field data experience and from simulations of the model studied, it is concluded that the manipulation of the WOB can be a solution for stick-slip oscillations even for low velocities at the surface $\Omega$. Increasing velocities at the rotary top driving system may lead to lateral vibrations, that is why the manipulation of the WOB can be an alternative solution in order to attenuate stick-slip oscillations.

The variation of the WOB is proposed in [84] as follows:

$$W_{\text{ob}}(z(t)) = K_{\text{w}} \left| z(t) \right| + W_{\text{ob0}}, \tag{3.12}$$

with $W_{\text{ob0}} > 0$ and $W_{\text{ob}} > W_{\text{ob0}}$. The variation law (3.12) implies a WOB reduction for a decreasing $z(t)$. Furthermore, considering that low values of WOB would make drilling stop, the constant value $W_{\text{ob0}}$ guarantees a desirable ROP.

The simulation results of Figure 3.8 show the successful stick-slip elimination by means of the introduction of the variation law (3.12). We have considered a drilling parameters combination for which torsional oscillations occur, i.e., $\Omega = 10\text{rad s}^{-1}$ and $W_{\text{ob0}} = 97347\text{N}$.

The variation of the weight on the bit seems to be a good strategy to counteract torsional oscillations, in fact, nowadays many control strategies are based on the manipulation of this variable. However, due to the occurence of

the stick-slip phenomenon, the formulation (3.12) may demand abrupt fluctuations of the weight on the bit, which under certain circumstances, may be impossible to implement, i.e., since the drill collars provide the WOB, the implementation of this methodology would require the sudden addition and removal of drill collar sections.

### 3.5.4. Increasing the damping at the down end

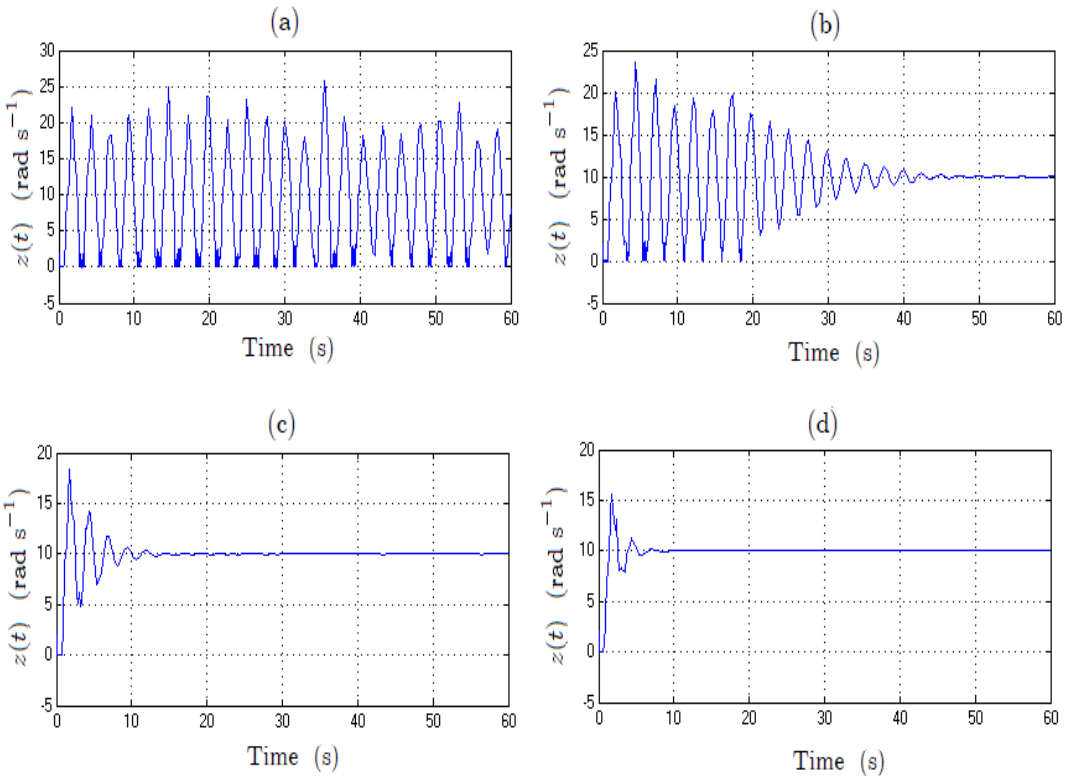


Figure 3.9: Angular velocity at the bottom extremity for diferent values of $c_b$ (N m s rad$^{-1}$): (a) 0.8, (b) 15, (c) 65, (d) 150.

An alternative strategy to reduce the stick-slip oscillations at the BHA consists in increasing the damping at the down end of the drillstring. This can mainly be done in two ways: modifying the drilling fluid characteristics (it could be approximated by means of increasing the damping coefficient $c_b$) and with the inclusion of vibration absorbers at the BHA in order to dampen torsional vibrations generated at the bit and prevent them from travelling up and back down the drillstring [84].

Angular velocity trajectories at the bit level of the system (2.9) coupled to the TOB model (3.1-3.2) for different values of $c_b$ are shown in Figure 3.9.

The strategy of modifying drilling fluid characteristics is a good option to be applied jointly with a more sophisticated methodology to avoid drillstring vibrations. In practice, the single application of this empirical method is insufficient to suppress the stick-slip.

## 3.6. Conclusion

The proposed axial-torsional model has been validated through simulations in close agreement with field observations regarding the stick-slip and bit-bounce.

We have presented the main practical strategies used in the field to reduce torsional vibrations. The most common operational instructions to avoid the stick-slip are the increase of the rotary table speed and the reduction of the WOB. Some other strategies are based on the manipulation of BHA characteristics such as the modification of the drilling fluid characteristics to increase the damping at the down end and the introduction of a variation law of the WOB of the form (3.12). Simulations obtained after applying such methodologies are in accordance with experimental field data.

Practical solutions satisfactorily reduce the amplitude of drilling oscillations, however they can not guarantee an optimal drilling operation. Increasing the rotary speed may cause lateral problems such as backward and forward whirling, impacts with the borehole wall and parametric instabilities. Furthermore a substantial reduction of the WOB would make drilling stop, thus, simple operational guidelines are not sufficient to eliminate drilling vibrations, control actions are required. The next two chapters are devoted to the control design to suppress undesirable behavior.

# Chapter 4

# Stability analysis and control of drilling vibrations: distributed parameter model approach

## 4.1. Introduction

In this chapter, we address the problem of stability analysis and drilling vibration reduction in the framework of distributed parameter systems.

In Chapter 2 the distributed parameter model of a vertical oilwell drilling system was introduced. As we have explained, the wave equation model is subject to mixed boundary conditions chosen according the observed dynamics at both extremities of the drillstring; the bottom boundary condition (2.3) is subject to a TOB function describing the rock-bit interaction, for the upper boundary condition we have presented two different options, one of them, equation (2.2), considers a constant speed at the top end, the other one, equation (2.6), considers a local torsion of the string at the upper part.

In this chapter, we deal with the wave equation model subject to the upper boundary condition (2.2). We assume that the TOB model is unknown, an additive perturbation is considered at the bottom boundary condition (2.3) to take into account unmodeled dynamics and/or external disturbances; with this consideration it is impossible to achieve exponential stability, instead, we seek ultimate bounds on the response.

Subsequent analysis involve the TOB model (3.1-3.2). A proposal of energy function allows a dissipativity analysis of the drilling system. In a first stage,

the drilling system is analyzed assuming a constant speed provided by the rotary table, without control actions. The energy dissipation concept leads to the idea of designing a controller guaranteeing a non-growth of energy during the drilling process. Thinking that the system dissipates energy when the stick-slip is not occurring, the obtained controller should be effective in suppressing torsional oscillations. To derive this analysis we consider the wave equation model subject now to the boundary conditions (2.3-2.6).

Finally, we address the problem of coupled axial-torsional vibrations, we derive matrix inequality conditions to the synthesis of stabilizing controllers to suppress the stick-slip and bit-bounce. The LMI approach to stability and control of distributed parameter systems is an interesting area just opening up for research. In [44] LMIs are shown to provide effective and simple tools for control of systems described by PDEs. Here, we extend this approach to a class of coupled wave-ODE system, stabilization conditions are derived from an appropriate functional to handle the problem of control of coupled drilling oscillations.

## 4.2. Ultimate Boundedness on the response of a drilling pipe model

In particular, although the dimensional parameters of the plant are known, a linearization of the behavior of the torque at the bottom hole boundary introduces uncertainty. Moreover, it is reasonable to consider the presence of a bounded additive noise signal $w(t)$ at the bottom in order to account for external disturbances and modeling errors. It is clear that under these circumstances, exponential or asymptotic stability cannot be achieved, we will seek instead ultimate boundedness of the solution [56].

The stationary solution of the drilling system described by (2.1) coupled to the boundary conditions (2.2-2.3) is:

$$\theta^0(\xi,t) = \Omega t - \left(\frac{T(\Omega)}{GJ} + \frac{\beta\Omega}{GJ}L\right)\xi + \frac{\beta\Omega}{2GJ}\xi^2.$$

The change of variable $z(\xi,t) = \theta(\xi,t) - \theta^0(\xi,t)$ leads to an equivalent autonomous system for which the function $z^0(\xi,t) = 0$ is a solution. Nonlinear phenomena at the bottom extremity such as stick-slip and noise due to the bit interaction are modeled with the additive bounded disturbance $w(t)$ such that $|w(t)| \leq \overline{w}$, $t \in (0,\infty)$. This additive noise is consistent with the TOB model

given in (3.1) in which an additive nonlinear dry friction term is considered to approximate the rock-bit contact.

The distributed model is rewritten as:

$$GJ\frac{\partial^2 z}{\partial \xi^2}(\xi,t) - I\frac{\partial^2 z}{\partial t^2}(\xi,t) - \beta\frac{\partial z}{\partial t}(\xi,t) = 0, \qquad \xi \in (0,L),$$

subject to the boundary conditions:

$$z(0,t) = 0,$$
$$GJ\frac{\partial z}{\partial \xi}(L,t) + I_B\frac{\partial^2 z}{\partial t^2}(L,t) = T(\Omega) - T\left(\Omega + \frac{\partial z}{\partial t}(L,t)\right) + w(t).$$

The end $\xi = 0$ is now fixed and the wave propagation has not changed. The stability of the trivial solution $z^0(\xi,t)$ is equivalent to the stability of the equilibrium $\theta^0(\xi,t)$.

We consider a linearization of the torque $T$:

$$T(\Omega) - T(\Omega + z_t(L,t)) = -T'(\Omega + \theta z_t(L,t))z_t(L,t), \qquad \theta \in (0,1).$$

For the sake of simplicity, we introduce the normalized rod length $\sigma = \xi/L$. The normalized drill pipe model is then:

$$\frac{GJ}{L^2}\frac{\partial^2 z}{\partial \sigma^2}(\sigma,t) - I\frac{\partial^2 z}{\partial t^2}(\sigma,t) - \beta\frac{\partial z}{\partial t}(\sigma,t) = 0, \qquad \sigma \in (0,1), \tag{4.1}$$

with boundary conditions:

$$z(0,t) = 0,$$
$$\frac{GJ}{L}\frac{\partial z}{\partial \sigma}(1,t) + I_B\frac{\partial^2 z}{\partial t^2}(1,t) = -T'(\Omega + \theta z_t(L,t))z_t(1,t) + w(t), \ \theta \in (0,1),$$

and initial conditions:

$$\begin{aligned} &z(\sigma,0) = \zeta(\sigma), \quad z_\sigma(\sigma,0) = \dot{\zeta}(\sigma) \in L_2(0,1),\\ &z_t(\sigma,0) = \zeta_1(\sigma) \in L_2(0,1). \end{aligned} \tag{4.2}$$

When the disturbance term $w(t)$ is not identically zero, we cannot prove exponential stability of the solution. However, it is possible to prove ultimate boundedness of the solutions for a bounded $w(t)$. We introduce the following technical lemma.

**Lemma 2** *[45]. Let $V : [0, \infty) \to \mathcal{R}^+$ be an absolutely continuous function. If there exists $\delta > 0$, $b > 0$ such that the derivative of $V$ satisfies almost everywhere the inequality*

$$\frac{d}{dt}V(t) + 2\delta V(t) - bw^2(t) \leq 0,$$

*then it follows that for all $w(t)$ satisfying $|w(t)| \leq \bar{w}$, the inequality*

$$V(t) \leq e^{-2\delta(t-t_0)}V(t_0) + (1 - e^{-2\delta(t-t_0)})\frac{b}{2\delta}\bar{w}^2,$$

*holds.*

**Proof 1** *Multiplying by $e^{2\delta(\theta-t)}$ the inequality $\frac{d}{dt}V+2\delta V \leq bw^2$ and integrating further from $t_0$ to $t$, we have*

$$\int_{t_0}^{t} \frac{d}{d\theta}(e^{2\delta(\theta-t)}V(\theta))d\theta \leq b\int_{t_0}^{t} e^{2\delta(\theta-t)}w^2(\theta)d\theta,$$

*thus,*

$$V(t) - e^{-2\delta(t-t_0)}V(t_0) \leq \frac{b}{2\delta}(1 - e^{-2\delta(t-t_0)})\overline{w}^2,$$

*and the result follows.*

For later use, we recall the following result.

**Lemma 3** *[118]. Let $z \in W^{1,2}([a, b], \mathcal{R})$ be a scalar function with $z(a) = 0$. Then*

$$max_{\sigma\in[a,b]}z^2(\sigma) \leq (b - a)\int_a^b (z'(\sigma))^2 d\sigma. \tag{4.3}$$

The lumped inertia $I_B$ is considered to be negligible, we assume that $T'$ is bounded: $0 < T_0 \leq T' \leq T_1$. Then we have:

$$z_{tt}(\sigma, t) = az_{\sigma\sigma}(\sigma, t) + dz_t(\sigma, t), \quad t > t_0, \quad 0 < \sigma < 1, \tag{4.4}$$

with the boundary conditions:

$$\begin{aligned} &z(0, t) = 0, \\ &z_\sigma(1, t) = -kz_t(1, t) + rw(t), \ t > 0, \end{aligned} \tag{4.5}$$

where $a = \frac{GJ}{IL^2}$, $d = \frac{-\beta}{I} \leq 0$, $r = \frac{L}{GJ}$ and $k = \frac{LT'}{GJ}$, satisfying $0 < k_0 \leq k \leq k_1$ with $k_i = \frac{LT_i}{GJ}$, $i = 0, 1$. The initial conditions are given by (4.2).

Now, we look for conditions such that the inequality $\frac{d}{dt}V + 2\delta V - bw^2 \leq 0$ holds. To this end, consider the Lyapunov functional

$$V(z_\sigma(\cdot,t),z_t(\cdot,t)) = p\int_0^1 az_\sigma^2(\sigma,t)d\sigma + p\int_0^1 z_t^2(\sigma,t)d\sigma + 2\chi\int_0^1 \sigma z_\sigma(\sigma,t)z_t(\sigma,t)d\sigma$$

proposed in [87] with constants $p > 0$ and small enough $\chi$. In [44] the following LMI

$$\begin{bmatrix} ap & \chi \\ \chi & p \end{bmatrix} > 0 \tag{4.6}$$

was introduced to guarantee that $V > 0$ for $\int_0^1 [z_\sigma^2(\sigma,t) + z_t^2(\sigma,t)]d\sigma > 0$.

**Theorem 1** *Given $\delta > 0$, if there exist $p > 0$ and $\chi > 0$ such that (4.6) and two LMIs*

$$\begin{bmatrix} -2ak_ip + \chi & 0 & 0 & -a\chi k_i r + apr & ak_i\chi \\ * & \psi_2 & (2\delta + d)\chi & 0 & 0 \\ * & * & \psi_3 & 0 & 0 \\ * & * & * & -b + \chi a r^2 & 0 \\ * & * & * & * & -a\chi \end{bmatrix} < 0, \ i = 0, 1, \tag{4.7}$$

*where*

$$\begin{aligned} \psi_2 &= -a\chi + 2\delta ap, \\ \psi_3 &= -\chi + 2pd + 2\delta p, \end{aligned} \tag{4.8}$$

*are feasible, then the solutions of the boundary-value problem (4.4), (4.5) with initial conditions (4.2) satisfy the inequality*

$$\begin{aligned} max_{\sigma\in[0,1]} z^2(\sigma,t) \quad \leq \quad & \int_0^1 [z_\sigma^2(\sigma,t) + z_t^2(\sigma,t)]d\sigma \leq \frac{\alpha_2}{\alpha_1} e^{-2\delta(t-t_0)} \int_0^1 [\zeta_1^2(\sigma) + \dot{\zeta}^2(\sigma)]d\sigma \\ & + \frac{b}{\alpha_1 2\delta}\bar{w}^2, \end{aligned} \tag{4.9}$$

*where*

$$\alpha_1 = \lambda_{\min}\begin{bmatrix} ap & 0 \\ 0 & p \end{bmatrix}, \quad \alpha_2 = \lambda_{\max}\begin{bmatrix} ap & \chi \\ \chi & p \end{bmatrix}. \tag{4.10}$$

**Proof 2** *As the LMI* $\begin{bmatrix} ap & \chi\sigma \\ \chi\sigma & p \end{bmatrix} > 0$ *is affine in* $\sigma \in [0,1]$*, it follows from Schur complements and Rayleigh's Theorem that*

$$\alpha_1 \int_0^1 [z_\sigma^2(\sigma,t) + z_t^2(\sigma,t)]d\sigma \leq V(z_\sigma(\cdot,t),z_t(\cdot,t)) \leq \alpha_2 \int_0^1 [z_\sigma^2(\sigma,t) + z_t^2(\sigma,t)]d\sigma, \tag{4.11}$$

*with* $\alpha_1$ *and* $\alpha_2$ *satisfying (4.10).*

*Next, we find* $\frac{d}{dt}V$*. Following [44], we derive*

$$\begin{aligned}\tfrac{d}{dt}\left(2\textstyle\int_0^1 \sigma z_t z_\sigma d\sigma\right) &= 2\textstyle\int_0^1 \sigma z_{tt} z_\sigma d\sigma + 2\int_0^1 \sigma z_t z_{\sigma t} d\sigma \\ &= 2a\textstyle\int_0^1 \sigma z_{\sigma\sigma}(\sigma,t) z_\sigma d\sigma + 2\int_0^1 \sigma z_t z_{\sigma t} d\sigma + 2d\int_0^1 \sigma z_t(\sigma,t) z_\sigma d\sigma.\end{aligned}$$

*Integration by parts gives*

$$2\int_0^1 \sigma z_t z_{\sigma t} d\sigma = -2\int_0^1 \sigma z_{\sigma t} z_t d\sigma - 2\int_0^1 z_t^2 d\sigma + 2z_t^2(1,t),$$

*and*

$$2\int_0^1 \sigma z_t z_{\sigma t} d\sigma = -\int_0^1 z_t^2 d\sigma + z_t^2(1,t).$$

*Similarly,*

$$2\int_0^1 \sigma z_{\sigma\sigma}(\sigma,t) z_\sigma d\sigma = -\int_0^1 z_\sigma^2 d\sigma + z_\sigma^2(1,t).$$

*Substitution of the boundary condition yields*

$$\begin{aligned}2\frac{d}{dt}\left(\int_0^1 \sigma z_t z_\sigma d\sigma\right) &= -\int_0^1 (z_t^2 + a z_\sigma^2) d\sigma + z_t^2(1,\,t) + a\left(-k z_t(1,t) + r w(t)\right)^2 \\ &\quad + 2d\int_0^1 \sigma z_t(\sigma,t) z_\sigma d\sigma.\end{aligned}$$

*Thus, differentiating* $V$ *along (4.4), we obtain*

$$\begin{aligned}\frac{d}{dt}V &= 2p\int_0^1 a z_\sigma(\sigma,t) z_{t\sigma}(\sigma,t) d\sigma + 2p\int_0^1 z_t(\sigma,t) z_{tt}(\sigma,t) d\xi \\ &\quad + 2\chi\frac{d}{dt}\left(\int_0^1 \sigma z_t z_\sigma d\sigma\right) \\ &= 2p\int_0^1 [a z_\sigma(\sigma,t) z_{t\sigma}(\sigma,t) + a z_t(\sigma,t) z_{\sigma\sigma}(\sigma,t)] d\sigma \\ &\quad + 2pd\int_0^1 z_t(\sigma,t) z_t(\sigma,t) d\sigma + 2\chi\frac{d}{dt}\left(\int_0^1 \sigma z_t z_\sigma d\sigma\right).\end{aligned}$$

*Then, integrating by parts and substituting the boundary condition (4.5), we obtain*

$$\begin{aligned}\int_0^1 z_t(\sigma,t)z_{\sigma\sigma}(\sigma,t)d\sigma &= z_t(\sigma,t)z_\sigma(\sigma,t)|_0^1 - \int_0^1 z_{t\sigma}(\sigma,t)z_\sigma(\sigma,t)d\sigma \\ &= z_t(1,t)(-kz_t(1,t)+rw(t)) - \int_0^1 z_{t\sigma}(\sigma,t)z_\sigma(\sigma,t)d\sigma.\end{aligned}$$

*Therefore*

$$\begin{array}{l}\frac{d}{dt}V = -2apkz_t^2(1,t) + 2apz_t(1,t)rw(t) + 2pd\int_0^1 z_t(\sigma,t)z_t(\sigma,t)d\sigma \\ +\chi\left[-\int_0^1(z_t^2+az_\sigma^2)d\sigma + z_t^2(1,\,t) + az_\sigma^2(1,\,t) + 2d\int_0^1\sigma z_t(\sigma,t)z_\sigma d\sigma\right].\end{array}$$

*It follows that*

$$\begin{array}{l}\frac{d}{dt}V + 2\delta V - bw^2 = -2apkz_t^2(1,t) + 2apz_t(1,t)rw(t) + 2pd\int_0^1 z_t(\sigma,t)z_t(\sigma,t)d\sigma \\ +\chi\Big[-\int_0^1(z_t^2+az_\sigma^2)d\sigma + z_t^2(1,t) + a(-kz_t(1,t)+rw(t))^2 + 2d\int_0^1\sigma z_t(\sigma,t)z_\sigma d\sigma\Big] \\ +\int_0^1 2\delta[apz_\sigma^2(\sigma,t) + 2\chi\sigma z_\sigma(\sigma,t)z_t(\sigma,t) + pz_t^2(\sigma,t)]d\sigma - bw^2.\end{array} \tag{4.12}$$

*By setting* $\vartheta^T(\sigma,t) = [z_t(1,t)\ z_\sigma(\sigma,t)\ z_t(\sigma,t)\ w(t)]$, *we conclude that*

$$\frac{d}{dt}V + 2\delta V - bw^2 = \int_0^1 \vartheta^T(\sigma,t)\Psi\vartheta(\sigma,t)d\sigma < 0,$$

*if*

$$\Psi = \begin{bmatrix} -2akp + (1+ak^2)\chi & 0 & 0 & -a\chi kr + apr \\ * & \psi_2 & (2\delta+d)\chi\sigma & 0 \\ * & * & \psi_3 & 0 \\ * & * & * & -b + \chi ar^2 \end{bmatrix} < 0, \tag{4.13}$$

*with notations given in (4.8). Applying Schur complements to* $ak^2\chi$ *in (4.13) and using the affinity of the resulting LMI in* $\sigma \in [0,1]$ *and* $k \in [k_0, k_1]$, *it is easy to see that (4.13) holds if (4.7) is feasible.*

*Then, if (4.7) is feasible, it follows from (4.11) and Lemma 2 that*

$$\begin{array}{l}\alpha_1\int_0^1[z_\sigma^2(\sigma,t) + z_t^2(\sigma,t)]d\sigma \le V(z_\sigma(\cdot,t),z_t(\cdot,t)) \\ \le V(z_\sigma(\cdot,t_0),z_t(\cdot,t_0))e^{-2\delta(t-t_0)} + \frac{b}{2\delta}(1-e^{-2\delta(t-t_0)})\overline{w}^2 \\ \le \alpha_2 e^{-2\delta(t-t_0)}\int_0^1[\zeta_1^2(\sigma) + \dot{\zeta}^2(\sigma]d\sigma + \frac{b}{2\delta}(1-e^{-2\delta(t-t_0)})\overline{w}^2.\end{array}$$

*In addition, it follows from (4.3) that*

$$max_{\sigma\in[0,1]}z^2(\sigma,t) \le \int_0^1 (z_\sigma(\sigma,t))^2 d\sigma \le \int_0^1 [z_\sigma^2(\sigma,t) + z_t^2(\sigma,t)]d\sigma.$$

**Remark 1** *The inequality (4.9) means that (4.4), (4.5) is input-to-state stable. The conditions for exponential stability of the disturbance free system given in Theorem 1 coincide with the ones from [44].*

### 4.2.1. Stick-slip oscillations and the non-growth of energy

In this subsection we give a new look at the problem. We leave out the bounded additive noise signal $w(t)$ taken into account for external disturbances in previous analysis and we consider the TOB model given in (3.1-3.2) to develop a dissipativity analysis of the system. Notice that $z_t(1,t)$ stands for the angular velocity at the bottom extremity, then the variable $z(t)$ of (3.1-3.2) corresponds to $z_t(1,t)$.

The boundary conditions of the drilling system described by the wave equation (4.4) are:

$$\begin{aligned} &z_t(0,t) = 0, \\ &z_\sigma(1,t) = -kz_t(1,t) - q\mu_{\mathrm{b}}(z_t(1,t))\mathrm{sign}(z_t(1,t)) - hz_{tt}(1,t),\ t>0, \end{aligned} \tag{4.14}$$

where $k = \frac{c_b L}{GJ}$, $q = \frac{W_{ob} R_b L}{GJ}$ and $h = \frac{I_B L}{GJ}$.

Consider the energy function

$$E(t) = \int_0^1 a z_\sigma^2(\sigma,t)d\sigma + \int_0^1 z_t^2(\sigma,t)d\sigma + ahz_t^2(1,t). \tag{4.15}$$

Differentiating $E(t)$ along (4.4), yields

$$\begin{aligned} \frac{d}{dt}E(t) &= 2\int_0^1 a z_\sigma(\sigma,t) z_{t\sigma}(\sigma,t)d\sigma \\ &\quad +2\int_0^1 z_t(\sigma,t) z_{tt}(\sigma,t)d\sigma + 2ahz_t(1,t)z_{tt}(1,t), \\ &= 2\int_0^1 [a z_\sigma(\sigma,t) z_{t\sigma}(\sigma,t) + a z_t(\sigma,t) z_{\sigma\sigma}(\sigma,t)]d\sigma \\ &\quad +2d\int_0^1 z_t(\sigma,t) z_t(\sigma,t)d\sigma + 2ahz_t(1,t)z_{tt}(1,t). \end{aligned}$$

Integrating by parts and substituting the boundary condition (4.14) gives

$$\begin{aligned}\int_0^1 z_t(\sigma,t)z_{\sigma\sigma}(\sigma,t)d\sigma &= z_t(\sigma,t)z_\sigma(\sigma,t)|_0^1 - \int_0^1 z_{t\sigma}(\sigma,t)z_\sigma(\sigma,t)d\sigma \\ &= z_t(1,t)(-kz_t(1,t) - q\mu_{\rm b}(z_t(1,t))\text{sign}(z_t(1,t)) \\ &\quad -hz_{tt}(1,t)) - \int_0^1 z_{t\sigma}(\sigma,t)z_\sigma(\sigma,t)d\sigma.\end{aligned}$$

Hence,

$$\begin{aligned}\tfrac{d}{dt}E(t) &= 2\textstyle\int_0^1 az_\sigma(\sigma,t)z_{t\sigma}(\sigma,t)d\sigma \\ &\quad + 2az_t(1,t)(-kz_t(1,t) - q\mu_{\rm b}(z_t(1,t))\text{sign}(z_t(1,t)) - hz_{tt}(1,t)) \\ &\quad - 2a\textstyle\int_0^1 z_{t\sigma}(\sigma,t)z_\sigma(\sigma,t)d\sigma \\ &\quad + 2d\textstyle\int_0^1 z_t(\sigma,t)z_t(\sigma,t)d\sigma + 2ahz_t(1,t)z_{tt}(1,t).\end{aligned}$$

Since $\mu_{\rm b}(z_t(1,t))\text{sign}(z_t(1,t))z_t(1,t) = \mu_{\rm b}(z_t(1,t))\,|z_t(1,t)|$, we have

$$\frac{d}{dt}E(t) = -2akz_t^2(1,t) - 2aq\mu_{\rm b}(z_t(1,t))\,|z_t(1,t)| + 2d\int_0^1 z_t^2(\sigma,t)d\sigma.$$

Taking into account that $\mu_{\rm b}(z_t(1,t)) > 0$ and that $d \leq 0$, we find that

$$\frac{d}{dt}E(t) \leq -2akz_t^2(1,t) \leq 0.$$

The non-growth of the energy of the drilling system (which reflects the oscillatory behavior of the system) is established:

**Proposition 1** *For all solutions of (4.4) under the boundary conditions (4.14), the energy given by (4.15) does not grow.*

### 4.2.2. Numerical results

The numerical results presented below are for the following parameter values:

$$\begin{aligned} G &= 79.3x10^9 N/m^2, \quad I = 0.095 Kg \cdot m, \\ T' &= 3000 N \cdot m, \quad J = 1.19x10^{-5} m^4, \\ L &= 3145m. \end{aligned}$$

The LMI conditions of Theorem 1 lead to the following pairs $(\delta, b)$.

| $Case$ | 1 | 2 | 3 | 4 | 5 |
|---|---|---|---|---|---|
| $\delta$ | 0.08 | 0.06 | 0.04 | 0.01 | 0.0001 |
| $b$ | 3.2521 | 1.0707 | 1.2145 | 1.5221 | 1.7951 |
| $\alpha_1$ | 5.0009 | 1.0934 | 1.2657 | 1.6273 | 1.9328 |
| $\alpha_2$ | 5.9854 | 1.3019 | 1.5074 | 1.9383 | 2.3023 |

For $\delta = 0.04$, $\beta = 0$ and initial conditions $z_\sigma(\sigma, t_0) = \dot{\zeta}$, $z_t(\sigma, t_0) = \zeta_1(\sigma)$, the expression (4.9) in Theorem 1 provides the following ultimate boundedness condition:

$$\int_0^1 [z_\sigma^2(\sigma,t) + z_t^2(\sigma,t)]d\sigma \leq 1.1909e^{-0.08t} \int_0^1 [\zeta_1^2(\sigma) + \dot{\zeta}^2(\sigma)]d\sigma + 11.9944\bar{w}^2.$$

For $\delta = 0.04$, $\beta = 0.1$Ns, the ultimate bound is:

$$\int_0^1 [z_\sigma^2(\sigma,t) + z_t^2(\sigma,t)]d\sigma \leq 1.1854e^{-0.08t} \int_0^1 [\zeta_1^2(\sigma) + \dot{\zeta}^2(\sigma)]d\sigma + 18.8654\bar{w}^2.$$

## 4.3. Control design: dissipativity analysis

So far, we have analyzed the drilling system assuming a constant velocity at the rotary table end, with no control actions. Based on the ideas presented in the previous section about the energy dissipation, it is possible to design a stabilizing controller ensuring the suppression of the stick-slip phenomenon. To this end, we consider the wave equation (2.1) coupled now to the boundary conditions (2.3-2.6).

Taking into account the TOB model (3.1-3.2), the normalized drilling system is:

$$z_{tt}(\sigma,t) = a z_{\sigma\sigma}(\sigma,t) - d z_t(\sigma,t), \quad t > 0, \quad 0 < \sigma < 1, \tag{4.16}$$

where $a = \frac{GJ}{IL^2}$ and $d = \frac{\beta}{I}$ coupled to the mixed boundary conditions:

$$\begin{array}{l} z_\sigma(0,t) = g\left(z_t(0,t) - u_1(t)\right), \quad \sigma \in (0,1), \quad t > 0, \\ z_\sigma(1,t) = -kz_t(1,t) - q\mu_{\rm b}(z_t(1,t))\text{sign}(z_t(1,t)) - hz_{tt}(1,t), \end{array} \tag{4.17}$$

where $u_1(t)$ is the angular velocity coming from the rotary table and $g = \frac{c_a L}{GJ}$, $k = \frac{c_b L}{GJ}$, $q = \frac{W_{ob} R_b L}{GJ}$, $h = \frac{I_B L}{GJ}$.

As in the previous section, we consider the energy function given in (4.15).

Differentiating $E(t)$ along (4.16), yields

$$\begin{array}{l} \frac{d}{dt}E(t) = 2\int_0^1 az_\sigma(\sigma,t)z_{t\sigma}(\sigma,t)d\sigma + 2\int_0^1 z_t(\sigma,t)z_{tt}(\sigma,t)d\sigma \\ \qquad\qquad + 2ahz_t(1,t)z_{tt}(1,t), \end{array}$$

$$\begin{array}{l} \frac{d}{dt}E(t) = 2a\int_0^1 \left[z_\sigma(\sigma,t)z_{t\sigma}(\sigma,t) + z_t(\sigma,t)z_{\sigma\sigma}(\sigma,t)\right]d\sigma \\ \qquad\qquad - 2d\int_0^1 z_t(\sigma,t)z_t(\sigma,t)d\sigma + 2ahz_t(1,t)z_{tt}(1,t). \end{array}$$

Integrating by parts and substituting the boundary conditions (4.17) gives

$$\begin{array}{l} \int_0^1 z_t(\sigma,t)z_{\sigma\sigma}(\sigma,t)d\sigma = z_t(\sigma,t)z_\sigma(\sigma,t)|_0^1 - \int_0^1 z_\sigma(\sigma,t)z_{t\sigma}(\sigma,t)d\sigma \\ = z_t(1,t)(-kz_t(1,t) - q\mu_{\rm b}(z_t(1,t))\text{sign}(z_t(1,t)) - hz_{tt}(1,t)) \\ \quad - gz_t(0,t)\left(z_t(0,t) - u_1(t)\right) - \int_0^1 z_\sigma(\sigma,t)z_{t\sigma}(\sigma,t)d\sigma. \end{array}$$

Hence,

$$\begin{array}{rcl} \frac{d}{dt}E(t) & = & 2a\int_0^1 z_\sigma(\sigma,t)z_{t\sigma}(\sigma,t)d\sigma + 2az_t(1,t)(-kz_t(1,t) \\ & & -q\mu_{\rm b}(z_t(1,t))\text{sign}(z_t(1,t)) - hz_{tt}(1,t)) \\ & & -2agz_t(0,t)\left(z_t(0,t) - u_1(t)\right) \\ & & -2a\int_0^1 z_\sigma(\sigma,t)z_{t\sigma}(\sigma,t)d\sigma - 2d\int_0^1 z_t(\sigma,t)z_t(\sigma,t)d\sigma \\ & & +2ahz_t(1,t)z_{tt}(1,t), \end{array}$$

since

$$\mu_{\rm b}(z_t(1,t))\text{sign}(z_t(1,t))z_t(1,t) = \mu_{\rm b}(z_t(1,t))\left|z_t(1,t)\right|,$$

we have

$$\begin{array}{l} \frac{d}{dt}E(t) = -2aq\mu_{\rm b}(z_t(1,t))\left|z_t(1,t)\right| - 2d\int_0^1 z_t^2(\sigma,t)d\sigma \\ \qquad - 2agz_t(0,t)\left(z_t(0,t) - u_1(t)\right) - 2akz_t^2(1,t). \end{array} \tag{4.18}$$

In order to ensure the dissipativity of the system, the control law $u_1(t)$ should allow the negativity of (4.18).

Choosing as a control law the following expression

$$u_1(t) = (1 - c_1)z_t(0,t) + 2c_1 z_t(1,t) - c_1 \frac{(z_t(1,t))^2}{z_t(0,t)}, \tag{4.19}$$

where $c_1 > 0$ is a free design parameter we obtain that

$$\begin{aligned} \frac{d}{dt}E(t) = & -2aq\mu_b(z_t(1,t))\,|z_t(1,t)| - 2d\int_0^1 z_t^2(\zeta,t)d\zeta \\ & - 2agc_1\left(z_t(1,t) - z_t(0,t)\right)^2 \\ & - 2akz_t^2(1,t). \end{aligned}$$

Taking into account that $\mu_b(z_t(1,t)) > 0$ and $a$, $q$, $k$, $d$ and $g$ are positive constants we find that $\frac{d}{dt}E(t) \leq 0$. The energy dissipation of the drilling system is established:

**Proposition 2** *For all solutions of (4.16) under the boundary conditions (4.17), the energy given by (4.15) does not grow if the control law (4.19) is applied.*

### 4.3.1. Simulation results

We have shown that the control law (4.19) ensures a dissipative behavior of the drilling system. This could lead to the idea that the system dissipates energy when the stick-slip phenomenon is not happening. To assert this idea, we aim to simulate the drilling system in closed loop with the proposed controller (4.19). A simple way to do this is by using the neutral-type models (2.9-2.11) subject to the TOB model (3.1-3.2) coupled to the boundary conditions (2.3-2.6). The control law (4.19) is rewritten in terms of the neutral-type model variables as:

$$u_1(t) = (1 - c_1)\dot{v}(t) + 2c_1 z(t) - c_1 \frac{z^2(t)}{\dot{v}(t)},$$

where $z(t)$ is the angular velocity at the bit level and $\dot{v}(t)$ the angular velocity at the upper part. The simulation results of Figure 4.1 show that the stick-slip vibrations are reduced by means of the application of the control law (4.19) depending on the angular velocity at the top and bottom extremities.

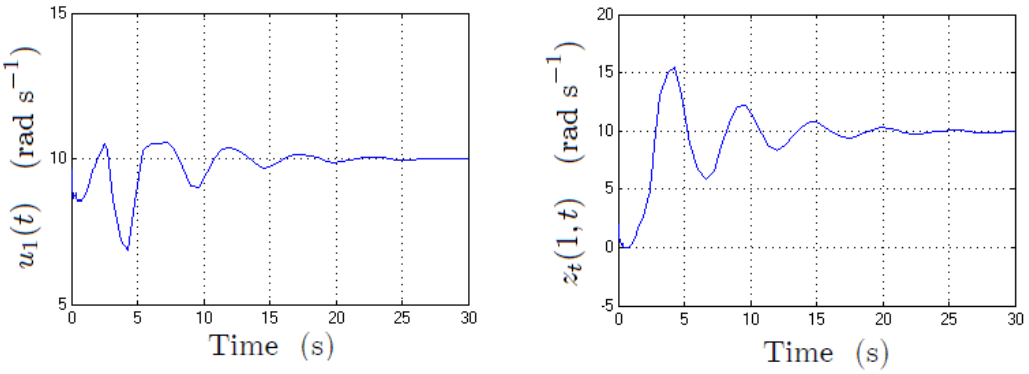


Figure 4.1: Stick-slip elimination by means of applying the control law (4.19) with $c_1 = 0.3$.

As previously explained, the occurrence of stick-slip is one of the factors leading to axial oscillation resulting in bit bounce, so it's interesting to know the effect of the proposed controller application on the bit-bounce. The trajectory of the longitudinal variable $y(t)$ of model (3.10) is shown in Figure 4.2. As can be seen, due to the coupling of the axial and torsional dynamics, the elimination of the stick-slip conduces to the reduction of the bit-bounce. Axial vibrations are reduced by means of the controller $u_1(t)$ because their primary excitation source was eliminated.

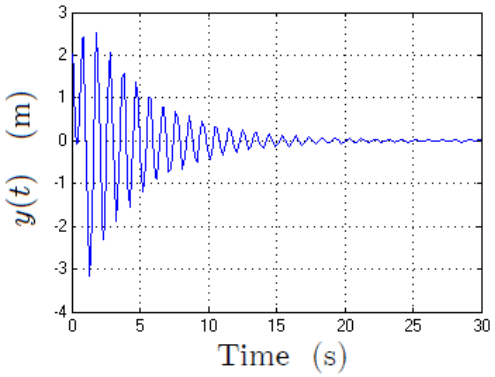


Figure 4.2: Bit-bounce reduction by means of applying the control law (4.19) with $c_1 = 0.3$.

## 4.4. Control of axial-torsional vibrations: coupled wave-ODE approach

In the previous section, based on the wave equation model describing torsional behavior, we have obtained an effective controller to eliminate the stick-slip which indirectly reduces axial vibrations. Now, we will perform a comprehensive analysis of the torsional drilling model coupled to the axial model to obtain stabilizing controllers aimed at eliminating the stick-slip and the bit-bounce. To this end, we propose a Lyapunov-Krasovskii functional suitable for the coupled PDE-ODE model which allows to obtain practical stabilization conditions in terms of matrix inequalities.

Consider the torsional drilling model (2.1) coupled to the boundary conditions (2.3-2.6) and subject to the TOB model (3.1-3.2), consider also the axial model given in (3.10). The following normalized wave-ODE model describes the torsional-axial dynamics of the drilling system:

$$z_{tt}(\zeta,t) = a z_{\zeta\zeta}(\zeta,t) - d z_t(\zeta,t), \quad \zeta \in (0,1), \quad t>0, \tag{4.20}$$
$$z_\zeta(0,t) = g\left(z_t(0,t) - u_1(t)\right), \tag{4.21}$$
$$z_\zeta(1,t) = -h z_{tt}(1,t) - k z_t(1,t) - q T_{\mathrm{nl}}(z_t(1,t)) + \omega, \tag{4.22}$$
$$\dot{x}(t) = Ax(t) + Bu_2(t) + E_1 z_t(1,t) + E_2 T_{\mathrm{nl}}(z_t(1,t)), \tag{4.23}$$

where the control inputs $u_1$, $u_2$ correspond to the angular velocity coming from the rotary table $\Omega$ and the ROP respectively, the vector $x(t)$ and the model parameters are given by:

$$x(t) = [y(t)\ \dot{y}(t)]^T,\ a = \frac{GJ}{IL^2},\ d = \frac{\beta}{I},\ g = \frac{c_a L}{GJ},$$
$$h = \frac{I_B L}{GJ},\ k = \frac{c_b L}{GJ},\ q = \frac{W_{\mathrm{ob}} R_{\mathrm{b}} L}{GJ},$$

and the constant matrices are defined as:

$$A = \begin{bmatrix} 0 & 1 \\ -\frac{k_0}{m_0} & -\frac{c_0}{m_0} \end{bmatrix},\ B = \begin{bmatrix} 0 \\ -\frac{c_0}{m_0} \end{bmatrix},\ E_1 = \begin{bmatrix} 0 \\ -\frac{\mu_1 c_{\mathrm{b}}}{m_0} \end{bmatrix},\ E_2 = \begin{bmatrix} 0 \\ -\frac{\mu_1 W_{\mathrm{ob}} R_{\mathrm{b}}}{m_0} \end{bmatrix}.$$

The nonlinear term $T_{\mathrm{nl}}$ is defined below,

$$T_{\mathrm{nl}}(z_t(1,t)) = \left(\mu_{\mathrm{cb}} + (\mu_{\mathrm{sb}} - \mu_{\mathrm{cb}})\mathrm{e}^{-\frac{\gamma_{\mathrm{b}}}{v_{\mathrm{f}}}|z_t(1,t)|}\right)\mathrm{sign}\left(z_t(1,t)\right).$$

As in Section 4.2, we consider an additive bounded variable $\omega$ which allows us to take into consideration uncertainties, disturbances and/or unmodeled dynamics in the system, we assume that $\omega$ satisfies:

$$\omega^2 \leq \varepsilon. \tag{4.24}$$

**Lemma 4** *Let the functional* $V(z_\zeta(\cdot,t),z_t(\cdot,t),\ x_t)$ *satisfying*

$$\int_0^1 \tilde{z}^T(\zeta,t)P\tilde{z}(\zeta,t)d\zeta \leq V(z_\zeta(\cdot,t),z_t(\cdot,t),\ x_t) \leq \bar{V}(z_\zeta(\cdot,t),z_t(\cdot,t),\ x_t) \quad (4.25)$$

$$\frac{d}{dt}V(z_\zeta(\cdot,t),z_t(\cdot,t),\ x_t) + \sigma V(z_\zeta(\cdot,t),z_t(\cdot,t),\ x_t) \leq \beta\varepsilon \quad \forall t \geq 0,\ \sigma > 0,\ \beta > 0, \quad (4.26)$$

*where* $\tilde{z}(\zeta,t) = [z_\zeta(\zeta,t) \quad z_t(\zeta,t) \quad x_t]^T$ *and* $P$ *is a symmetric positive definite matrix. Then for any initial function* $\tilde{\phi}(\zeta,t) = [\phi_\zeta(\zeta) \quad \phi_1(\zeta) \quad x_0]^T$, *the boundary-value problem (4.20-4.23) satisfies the ultimate bound:*

$$\int_0^1 \tilde{z}^T(\zeta,t)P\tilde{z}(\zeta,t)d\zeta \leq e^{-\sigma t}\bar{V}(\phi_\zeta(\zeta),\ \phi_1(\zeta),\ x_0) + \frac{\beta\varepsilon}{\sigma}, \quad (4.27)$$

*for* $t \geq T_a(\phi,\varsigma) > 0$ *where*

$$T_a(\tilde{\phi},\varsigma) = \frac{1}{\sigma}\ln\left(\frac{1}{\varsigma}\bar{V}(\phi_\zeta(\zeta),\ \phi_1(\zeta),\ x_0)\right).$$

**Proof 3** *Multiplying (4.26) by* $e^{\sigma\theta}$ *gives*

$$\frac{d}{d\theta}\left(e^{\sigma\theta}V(z_\zeta(\cdot,t),z_t(\cdot,t)),\ x_t\right) \leq \beta\varepsilon e^{\sigma\theta}.$$

*Integrating the above expression from* 0 *to* $t$ *yields*

$$V(z_\zeta(\cdot,t),z_t(\cdot,t),\ x_t) \leq e^{-\sigma t}V(\phi_\zeta(\zeta),\ \phi_1(\zeta),\ x_0) + \frac{\beta\varepsilon}{\sigma}\left(1 - e^{-\sigma t}\right).$$

*It follows from (4.25) that*

$$\begin{aligned}\int_0^1 \tilde{z}^T(\zeta,t)P\tilde{z}(\zeta,t)d\zeta &\leq e^{-\sigma t}\bar{V}(\phi_\zeta(\zeta),\ \phi_1(\zeta),\ x_0) + \frac{\beta\varepsilon}{\sigma}\left(1 - e^{-\sigma t}\right)\\ &\leq e^{-\sigma t}\bar{V}(\phi_\zeta(\zeta),\ \phi_1(\zeta),\ x_0) + \frac{\beta\varepsilon}{\sigma}, \end{aligned} \quad (4.28)$$

*we look for the time instant* $T_a(\tilde{\phi},\varsigma)$ *at which the solution of the boundary-value problem (4.20-4.23) satisfies (4.27). In view of (4.28),* $T_a(\tilde{\phi},\varsigma)$ *should guarantee* $\int_0^1 \tilde{z}^T(\zeta,t)P\tilde{z}(\zeta,t)d\zeta \leq \varsigma + \frac{\beta\varepsilon}{\sigma}$ *for a small enough* $\varsigma > 0$, *i.e.,*

$$\varsigma = e^{-\sigma T_a}\bar{V}(\phi_\zeta(\zeta),\ \phi_1(\zeta),\ x_0),$$

*from the above expression we have*

$$e^{\sigma T_a} = \frac{1}{\varsigma}\bar{V}(\phi_\zeta(\zeta),\ \phi_1(\zeta),\ x_0),$$

*and the result follows.*

### 4.4.1. Practical stabilization conditions

We look for conditions such that the inequality

$$\frac{d}{dt}V(z_\zeta(\cdot,t),z_t(\cdot,t),\ x_t) + \sigma V(z_\zeta(\cdot,t),z_t(\cdot,t),\ x_t) - \beta\varepsilon \leq 0$$

holds. To this end, consider the Lyapunov-Krasovskii functional

$$\begin{aligned} V(z_\zeta(\cdot,t),z_t(\cdot,t),\ x_t) &= V_1(z_\zeta(\zeta,t)) + V_2(z_t(\zeta,t)) \\ &\quad + V_3(z_\zeta(\zeta,t),z_t(\zeta,t)) + V_4(x_t), \end{aligned}$$

where

$$\begin{aligned} V_1(z_\zeta(\zeta,t)) &= pa\int_0^1 z_\zeta^2(\zeta,t)d\zeta, \\ V_2(z_t(\zeta,t)) &= p\int_0^1 z_t^2(\zeta,t)d\zeta, \\ V_3(z_\zeta(\zeta,t),z_t(\zeta,t)) &= 2\chi\int_0^1 (\zeta+1)\, z_\zeta(\zeta,t)z_t(\zeta,t)d\zeta, \\ V_4(x_t) &= x^T(t)Rx(t), \end{aligned}$$

which can be written as:

$$V(z_\zeta(\cdot,t),z_t(\cdot,t),\ x_t) = \int_0^1 \tilde{z}^T(\zeta,t)P\tilde{z}(\zeta,t)d\zeta, \quad \tilde{z}(\zeta,t) = [z_\zeta(\zeta,t)\ z_t(\zeta,t)\ x(t)]^T,$$

$$P = \begin{bmatrix} ap & \chi(\zeta+1) & 0 \\ \chi(\zeta+1) & p & 0 \\ 0 & 0 & R \end{bmatrix} > 0,\ p>0,\ a>0,\ R>0.$$

The time derivative of $V_1$ is:

$$\dot{V}_1(z_\zeta(\zeta,t),z_{\zeta t}(\zeta,t)) = 2pa\int_0^1 z_\zeta(\zeta,t)z_{\zeta t}(\zeta,t)d\zeta. \tag{4.29}$$

The time derivative of $V_2$ is:

$$\dot{V}_2(z_t(\zeta,t),z_{tt}(\zeta,t)) = 2p\int_0^1 z_t(\zeta,t)z_{tt}(\zeta,t)d\zeta,$$

substituting the wave equation (4.20) yields:

$$\dot{V}_2(z_t(\zeta,t),z_{\zeta\zeta}(\zeta,t)) = 2pa\int_0^1 z_t(\zeta,t)z_{\zeta\zeta}(\zeta,t)d\zeta - 2pd\int_0^1 z_t^2(\zeta,t)d\zeta,$$

integration by parts of $\int_0^1 z_t(\zeta,t)z_{\zeta\zeta}(\zeta,t)d\zeta$ with $u = z_t(\zeta,t)$, $dv = z_{\zeta\zeta}(\zeta,t)d\zeta$, $du = z_{t\zeta}(\zeta,t)$, $v = z_\zeta(\zeta,t)$ gives:

$$\int_0^1 z_t(\zeta,t)z_{\zeta\zeta}(\zeta,t)d\zeta = z_t(\zeta,t)z_\zeta(\zeta,t)\big|_0^1 - \int_0^1 z_{t\zeta}(\zeta,t)z_\zeta(\zeta,t)d\zeta.$$

Then we obtain:

$$\begin{aligned}\dot{V}_2(z_\zeta(\zeta,t),z_t(\zeta,t),\ z_{t\zeta}(\zeta,t)) &= 2pa\ z_t(\zeta,t)z_\zeta(\zeta,t)\big|_0^1 - 2pa\int_0^1 z_{t\zeta}(\zeta,t)z_\zeta(\zeta,t)d\zeta \\ &\quad -2pd\int_0^1 z_t^2(\zeta,t)d\zeta. \end{aligned} \tag{4.30}$$

The derivative of $V_3$ is:

$$\begin{aligned}\dot{V}_3(z_\zeta(\zeta,t),z_t(\zeta,t),\ z_{tt}(\zeta,t),\ z_{\zeta t}(\zeta,t)) &= 2\chi\int_0^1 (\zeta+1)\, z_\zeta(\zeta,t)z_{tt}(\zeta,t)d\zeta \\ &\quad +2\chi\int_0^1 (\zeta+1)\, z_{\zeta t}(\zeta,t)z_t(\zeta,t)d\zeta,\end{aligned}$$

substituting the wave equation (4.20) yields:

$$\begin{aligned}\dot{V}_3(z_\zeta(\zeta,t),z_t(\zeta,t),\ z_{\zeta\zeta}(\zeta,t),\ z_{\zeta t}(\zeta,t)) &= 2a\chi\int_0^1 (\zeta+1)\, z_\zeta(\zeta,t)z_{\zeta\zeta}(\zeta,t)d\zeta \\ &\quad -2d\chi\int_0^1 (\zeta+1)\, z_\zeta(\zeta,t)z_t(\zeta,t)d\zeta \\ &\quad +2\chi\int_0^1 (\zeta+1)\, z_{\zeta t}(\zeta,t)z_t(\zeta,t)d\zeta.\end{aligned} \tag{4.31}$$

Integration by parts of $\int_0^1 (\zeta+1)\, z_\zeta(\zeta,t)z_{\zeta\zeta}(\zeta,t)d\zeta$ with $u = (\zeta+1)\, z_\zeta(\zeta,t)$, $dv = z_{\zeta\zeta}(\zeta,t)d\zeta$, $du = (\zeta+1)\, z_{\zeta\zeta}(\zeta,t) + z_\zeta(\zeta,t)$, $v = z_\zeta(\zeta,t)$ gives:

$$\begin{aligned}\int_0^1 (\zeta+1)\, z_\zeta(\zeta,t)z_{\zeta\zeta}(\zeta,t)d\zeta &= (\zeta+1)\, z_\zeta^2(\zeta,t)\big|_0^1 - \int_0^1 (\zeta+1)\, z_{\zeta\zeta}(\zeta,t)z_\zeta(\zeta,t)d\zeta \\ &\quad -\int_0^1 z_\zeta^2(\zeta,t)d\zeta,\end{aligned}$$

then we obtain:

$$2\int_0^1 (\zeta+1)\, z_\zeta(\zeta,t)z_{\zeta\zeta}(\zeta,t)d\zeta = (\zeta+1)\, z_\zeta^2(\zeta,t)\big|_0^1 - \int_0^1 z_\zeta^2(\zeta,t)d\zeta. \tag{4.32}$$

Now, observe that

$$2z_{\zeta t}(\zeta,t)z_t(\zeta,t) = \frac{\partial}{\partial\zeta}\left(z_t^2(\zeta,t)\right),$$

then,

$$2\int_0^1 (\zeta+1)\, z_{\zeta t}(\zeta,t) z_t(\zeta,t) d\zeta = \int_0^1 (\zeta+1)\, \frac{\partial}{\partial \zeta}\left(z_t^2(\zeta,t)\right) d\zeta.$$

Integration by parts of $\int_0^1 (\zeta+1)\, \frac{\partial}{\partial \zeta}\left(z_t^2(\zeta,t)\right) d\zeta$ with $u = (\zeta+1)$, $du = 1$, $v = z_t^2(\zeta,t)$ gives

$$2\int_0^1 (\zeta+1)\, z_{\zeta t}(\zeta,t) z_t(\zeta,t) d\zeta = (\zeta+1)\, z_t^2(\zeta,t)\big|_0^1 - \int_0^1 z_t^2(\zeta,t) d\zeta. \quad (4.33)$$

Substituting (4.32) and (4.33) into (4.31) yields:

$$\begin{aligned} \dot{V}_3(z_\zeta(\zeta,t), z_t(\zeta,t)) &= a\chi\,(\zeta+1)\, z_\zeta^2(\zeta,t)\big|_0^1 - a\chi \int_0^1 z_\zeta^2(\zeta,t) d\zeta \\ &\quad -2d\chi \int_0^1 (\zeta+1)\, z_\zeta(\zeta,t) z_t(\zeta,t) d\zeta \\ &\quad +\chi\,(\zeta+1)\, z_t^2(\zeta,t)\big|_0^1 - \chi \int_0^1 z_t^2(\zeta,t) d\zeta. \quad (4.34) \end{aligned}$$

The derivative of $V_4$ along the trajectories of (4.23) is:

$$\begin{aligned} \dot{V}_4(x_t) &= \dot{x}^T(t) R x(t) + x^T(t) R \dot{x}(t) \\ &= \left(Ax(t) + Bu_2(t) + E_1 z_t(1,t) + E_2 T_{\mathrm{nl}}(z_t(1,t))\right)^T R x(t) \\ &\quad + x^T(t) R \left(Ax(t) + Bu_2(t) + E_1 z_t(1,t) + E_2 T_{\mathrm{nl}}(z_t(1,t))\right). \end{aligned}$$

Consider the following structure for the controller $u_2(t)$:

$$u_2(t) = c_2 x(t) \quad (4.35)$$

where $c_2 \in \mathcal{R}^{1\times 2}$, then we obtain:

$$\begin{aligned} \dot{V}_4(x_t) &= \dot{x}^T(t) R x(t) + x^T(t) R \dot{x}(t) \\ &= \left[Ax(t) + Bc_2 x(t) + E_1 z_t(1,t) + E_2 T_{\mathrm{nl}}(z_t(1,t))\right]^T R x(t) \\ &\quad + x^T(t) R \left[Ax(t) + Bc_2 x(t) + E_1 z_t(1,t) + E_2 T_{\mathrm{nl}}(z_t(1,t))\right], \end{aligned}$$

or

$$\dot{V}_4(x_t) = x^T(t) \Upsilon_1 x(t) + \Upsilon_2^T R x(t) + x^T(t) R \Upsilon_2, \quad (4.36)$$

where $\Upsilon_1 = A^T R + RA + c_2^T B^T R + RBc_2$, $\Upsilon_2 = E_1 z_t(1,t) + E_2 T_{\mathrm{nl}}(z_t(1,t))$.

In view of (4.29), (4.30), (4.34) and (4.36) we obtain:

$$\begin{aligned} \dot{V}(\cdot) = \; & 2pa \textstyle\int_0^1 z_\zeta(\zeta,t) z_{\zeta t}(\zeta,t) d\zeta - 2pa \int_0^1 z_{t\zeta}(\zeta,t) z_\zeta(\zeta,t) d\zeta \\ & -2pd \textstyle\int_0^1 z_t^2(\zeta,t) d\zeta - a\chi \int_0^1 z_\zeta^2(\zeta,t) d\zeta \\ & -2d\chi \textstyle\int_0^1 (\zeta+1)\, z_\zeta(\zeta,t) z_t(\zeta,t) d\zeta - \chi \int_0^1 z_t^2(\zeta,t) d\zeta \\ & +2pa\, z_t(\zeta,t) z_\zeta(\zeta,t)\big|_0^1 + a\chi\,(\zeta+1)\, z_\zeta^2(\zeta,t)\big|_0^1 \\ & +\chi\,(\zeta+1)\, z_t^2(\zeta,t)\big|_0^1 + x^T(t)\Upsilon_1 x(t) + \Upsilon_2^T R x(t) + x^T(t) R \Upsilon_2. \end{aligned}$$

Then,

$$\begin{aligned}\dot{V}(\cdot)+\sigma V(\cdot) = \; & -2pd\int_0^1 z_t^2(\zeta,t)d\zeta - a\chi\int_0^1 z_\zeta^2(\zeta,t)d\zeta \\ & -2d\chi\int_0^1(\zeta+1)\,z_\zeta(\zeta,t)z_t(\zeta,t)d\zeta - \chi\int_0^1 z_t^2(\zeta,t)d\zeta \\ & +x^T(t)\Upsilon_1 x(t)+\Upsilon_2^T Rx(t)+x^T(t)R\Upsilon_2 \\ & +\sigma pa\int_0^1 z_\zeta^2(\zeta,t)d\zeta+\sigma p\int_0^1 z_t^2(\zeta,t)d\zeta \\ & +2\sigma\chi\int_0^1(\zeta+1)\,z_\zeta(\zeta,t)z_t(\zeta,t)d\zeta+\sigma x^T(t)Rx(t)+\Pi,\end{aligned} \tag{4.37}$$

where

$$\begin{aligned}\Pi &= 2pa\,z_t(\zeta,t)z_\zeta(\zeta,t)\big|_0^1 + a\chi\,(\zeta+1)\,z_\zeta^2(\zeta,t)\big|_0^1+\chi\,(\zeta+1)\,z_t^2(\zeta,t)\big|_0^1 \\ &= 2\chi z_t^2(1,t)+2a\chi z_\zeta^2(1,t)+2paz_t(1,t)z_\zeta(1,t)-\chi z_t^2(0,t) \\ &\quad -a\chi z_\zeta^2(0,t)-2paz_t(0,t)z_\zeta(0,t).\end{aligned}$$

Introducing the boundary conditions (4.21-4.22) we get,

$$\begin{aligned}\Pi = \; & 2\chi z_t^2(1,t)+2a\chi\left(-hz_{tt}(1,t)-kz_t(1,t)-qT_{\rm nl}(z_t(1,t))+\omega\right)^2 \\ & +2paz_t(1,t)\left(-hz_{tt}(1,t)-kz_t(1,t)-qT_{\rm nl}(z_t(1,t))+\omega\right) \\ & -\chi z_t^2(0,t)-a\chi\left(g\left(z_t(0,t)-u_1(t)\right)\right)^2-2paz_t(0,t)\left(g\left(z_t(0,t)-u_1(t)\right)\right).\end{aligned}$$

Considering the following controller structure

$$u_1(t)=c_{11}z_{tt}(1,t)+c_{12}z_t(1,t)+c_{13}T_{\rm nl}(z_t(1,t))+c_{14}z_t(0,t), \tag{4.38}$$

we get

$$\begin{aligned}\Pi = \; & 2a\chi\left[h^2z_{tt}^2(1,t)+2hkz_t(1,t)z_{tt}(1,t)+2hqz_{tt}(1,t)T_{\rm nl}(z_t(1,t))\right. \\ & -2hz_{tt}(1,t)\omega+k^2z_t^2(1,t)+2kqz_t(1,t)T_{\rm nl}(z_t(1,t))-2kz_t(1,t)\omega \\ & \left.+q^2T_{\rm nl}^2(z_t(1,t))-2qT_{\rm nl}(z_t(1,t))\omega+\omega^2\right] \\ & +2\chi z_t^2(1,t)+2paz_t(1,t)\left[-hz_{tt}(1,t)-kz_t(1,t)-qT_{\rm nl}(z_t(1,t))+\omega\right] \\ & -a\chi g^2\left[c_{11}^2z_{tt}^2(1,t)+2c_{11}c_{12}z_t(1,t)z_{tt}(1,t)+2c_{11}c_{13}z_{tt}(1,t)T_{\rm nl}(z_t(1,t))\right. \\ & -2c_{11}\left(1-c_{14}\right)z_{tt}(1,t)z_t(0,t)+c_{12}^2z_t^2(1,t) \\ & +2c_{12}c_{13}z_t(1,t)T_{\rm nl}(z_t(1,t))-2c_{12}\left(1-c_{14}\right)z_t(1,t)z_t(0,t) \\ & +c_{13}^2T_{\rm nl}^2(z_t(1,t))-2c_{13}\left(1-c_{14}\right)T_{\rm nl}(z_t(1,t))z_t(0,t) \\ & \left.+\left(1-c_{14}\right)^2z_t^2(0,t)\right]-\chi z_t^2(0,t) \\ & -2pagz_t(0,t)\left[z_t(0,t)-c_{11}z_{tt}(1,t)-c_{12}z_t(1,t)\right. \\ & \left.-c_{13}T_{\rm nl}(z_t(1,t))-c_{14}z_t(0,t)\right].\end{aligned}$$

The condition (4.24) implies that $\omega^2-\varepsilon\leq 0$, then, for a $\beta>0$, we have that

$$-\beta(\omega^2-\varepsilon)\geq 0. \tag{4.39}$$

In order to take into account the perturbation restriction we can add to (4.37) the term (4.39). We obtain after symmetrization of the cross terms:

$$\frac{d}{dt}V(\cdot)+\sigma V(\cdot)-\beta\varepsilon\leq\int_0^1\eta_1^T\Psi\eta_1 d\zeta+\eta_2^T\Phi\eta_2,$$

where

$$\begin{aligned}\eta_1 &= (\ z_t(\zeta,t)\ z_\zeta(\zeta,t)\ )^T,\\ \eta_2 &= (\ z_{tt}(1,t)\ z_t(1,t)\ T_{\rm nl}(z_t(1,t))\ z_t(0,t)\ x(t)\ \omega\ )^T,\end{aligned}$$

and

$$\Psi=\begin{bmatrix}-2pd-\chi+\sigma p & -d\chi\,(\zeta+1)+\sigma\chi\,(\zeta+1)\\ * & -a\chi+\sigma pa\end{bmatrix},\tag{4.40}$$

$$\Phi=\begin{bmatrix}2a\chi h^2-a\chi g^2c_{11}^2 & \Phi_{12} & \Phi_{13} & \Phi_{14} & 0 & -2a\chi h\\ * & \Phi_{22} & \Phi_{23} & \Phi_{24} & {E_1}^TR & -2a\chi k+pa\\ * & * & \Phi_{33} & \Phi_{34} & E_2^TR & -2a\chi q\\ * & * & * & \Phi_{44} & 0 & 0\\ * & * & * & * & \Upsilon_1+\sigma R & 0\\ * & * & * & * & * & 2a\chi-\beta\end{bmatrix},\tag{4.41}$$

with

$$\begin{aligned}\Phi_{12}&=2a\chi hk-pah-a\chi g^2c_{11}c_{12}\\ \Phi_{13}&=2a\chi hq-a\chi g^2c_{11}c_{13}\\ \Phi_{14}&=a\chi g^2c_{11}\,(1-c_{14})+pagc_{11}\\ \Phi_{22}&=2a\chi k^2+2\chi-2pak-a\chi g^2c_{12}^2\\ \Phi_{23}&=2a\chi kq-paq-a\chi g^2c_{12}c_{13}\\ \Upsilon_1&=A^TR+RA+c_2^TB^TR+RBc_2\\ \Phi_{24}&=a\chi g^2c_{12}\,(1-c_{14})+pagc_{12}\\ \Phi_{33}&=2a\chi q^2-a\chi g^2c_{13}^2\\ \Phi_{34}&=a\chi g^2c_{13}\,(1-c_{14})+pagc_{13}\\ \Phi_{44}&=-a\chi g^2\,(1-c_{14})^2-\chi\\ &\quad-2pag+pagc_{14}.\end{aligned}$$

Summarizing the above ideas, the result on the practical stabilization of the wave-ODE model (4.20-4.23) can be stated as follows:

**Theorem 2** *The trajectories of the drilling system described by the coupled wave-ODE model (4.20-4.23) in closed loop with the controllers (4.38) and (4.35) admits the ultimate bound (4.27) if the matrix inequalities* $P>0$, $\Psi<0$ *and* $\Phi<0$ *are satisfied for some* $p>0$, $\chi>0$, $\beta>0$, $R>0$ *and any* $c_{11}$, $c_{12}$, $c_{13}$, $c_{14}$. $c_2$.

### 4.4.2. Numerical results

The parameters used in the following simulations are given in (3.11). The maximum exponential decay rate for which the conditions of Theorem 2 are satisfied is $\sigma = 0.8$.

A feasible result of the LMI $\Psi < 0$ with $\Psi$ given in (4.40) is:

$$p = 0.7406, \qquad \chi = 0.9559.$$

Using the above values, a feasible result of the Bilinear Matrix Inequality (BMI) $\Phi < 0$ with $\Phi$ given in (4.41) is:

$$\begin{array}{lll} c_{11} = -0.0067, & c_{12} = -0.04699, & c_{13} = -0.0548, \\ c_{14} = 0.6642, & c_2 = [0 \quad 2.0234], & \beta = 16.8149, \end{array} \tag{4.42}$$

$$R = \begin{bmatrix} 551.7373 & 11.7383 \\ 11.7383 & 13.4465 \end{bmatrix}.$$

The performance of the proposed controllers is illustrated by simulations of the drilling model describing the rotational and longitudinal dynamics of the rod. The axial dynamics are described by a simple nonlinear ODE subject to the TOB model describing the rock-bit contact, the simulation can be easily developed using Matlab. Conversely, the simulation of a nonlinear PDE subject to mixed boundary conditions is not a direct task, however, the simplified neutral-type model provides a reliable approximation of the torsional dynamics and it can be readily simulated.

The variables $z(t)$ and $v(t)$ of the neutral-type models (2.9-2.11) stand for the angular velocities at the bottom and upper extremities respectively ($z_t(1,t)$, $z_t(0,t)$). The proposed controller $u_1$ given in (4.38) can be rewritten as:

$$u_1(t) = c_{11}\dot{z}(t) + c_{12}z(t) + c_{13}T_{\text{nl}}(z(t)) + c_{14}v(t).$$

Figure 4.3 show the trajectories of the drilling system described by the model (2.9-2.11), (3.10) coupled to the TOB function (3.1-3.2) in closed loop with the controllers (4.35) and (4.38). The elimination of stick-slip and bit bounce phenomena is achieved. The controller gain values are given in (4.42).

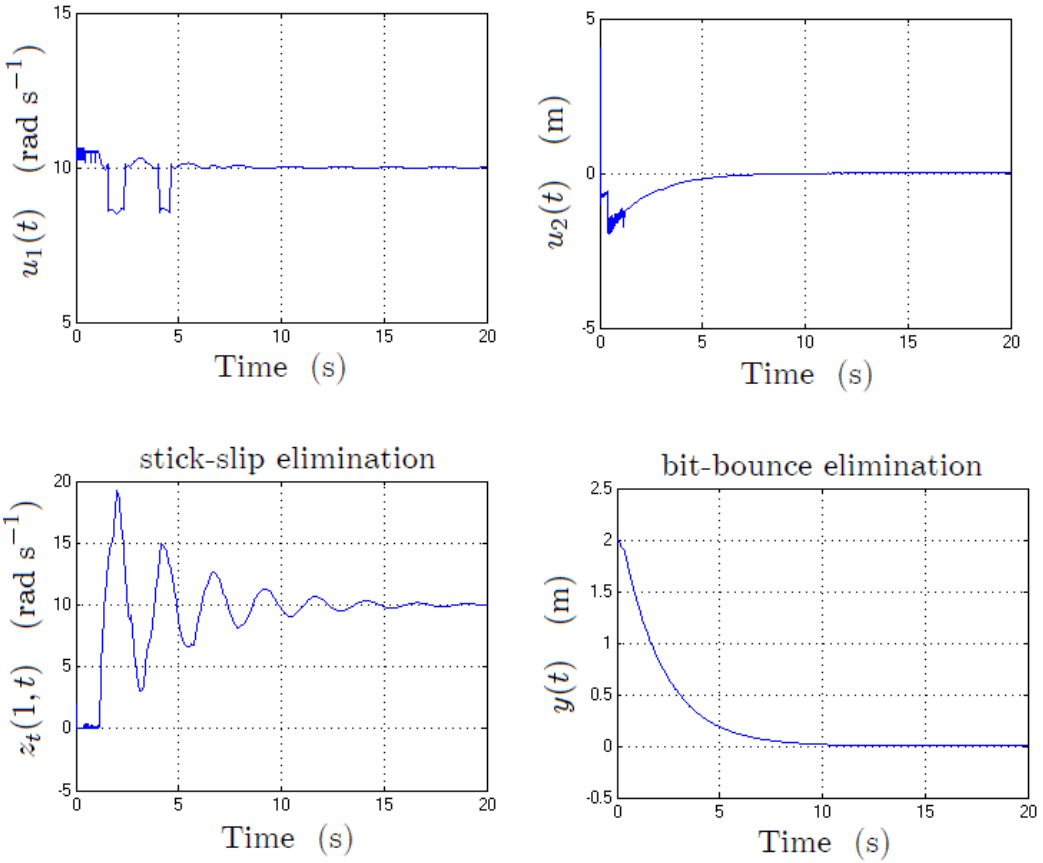


Figure 4.3: Torsional and axial trajectories of the drilling system in closed loop with the controllers $u_1$ and $u_2$ given in (4.38), (4.35).

## 4.5. Conclusion

Drilling system analyses were carried out through the wave equation model. In a first stage, it is considered that the system is subject to a constant rotary speed provided by the rotary table and it is not under control actions. Ultimate bounds on the solution were found, the non-growth of energy was established even in presence of stick-slip vibrations. However, this property is not sufficient to guarantee an optimal drilling process, in fact, the occurrence of stick-slip is the major source of failures in oil fields. Here, we have developed two different control strategies to deal with the drilling vibration problem. The first one is based on an energy dissipation analysis, the proposal of an energy function leads to the control law given in (4.19) which ensures the stick-slip suppression. The second one uses Lyapunov techniques,

two control laws have been proposed, one of them to suppress the stick-slip and the other one to eliminate the bit-bounce; they are given in (4.38) and (4.35) respectively. Stabilization conditions in terms of matrix inequalities were found.

As can be noticed, the controller based on the energy dissipation, given in (4.19), is strategically designed to ensure the negativity of the proposed energy function, it involves a free design parameter $c_1$ and the angular velocities at the upper and lower ends of the string. This controller provides a simpler structure in comparison with the controller given in (4.38) which in addition involves the angular acceleration at the bit level and requires knowledge of the nonlinear TOB function describing the rock-bit contact. Furthermore, the controller based on Lyapunov techniques involves certain conservatism derived from the matrix inequalities.

The control law obtained from the dissipativity analysis is aimed at eliminating the stick-slip phenomenon, albeit indirectly it also reduces the bit-bounce due to the oscillations coupling. The matrix inequality approach to control of axial and torsional drilling oscillations allows the design of a control strategy for each vibration type. The effectiveness of the proposed controllers is highlighted through simulations showing the elimination of the stick-slip and bit-bounce.

Summarizing, we can conclude that the first control methodology presented which is based on the dissipativity analysis of the system was carried out in a simple and straightforward way, but the obtained controller leads only to a decrease of axial vibrations. The methodology based on Lyapunov techniques require a feasible solution of a set of matrix inequalities, nevertheless it yields an integral suppression of coupled oscillations. Regarding the controller size, it can be noticed that the trajectory of the controller (4.38) is closer to the reference velocity which is quite convenient in view of control input saturation restriction, this particular issue will be addressed in the next chapter.

For a physical system, a distributed parameter model is the closest description to reality. However the lack of computational tools to perform simulations of infinite dimensional systems subject to nonlinearities and uncertainties brings out the idea of taking over the problem from a different perspective. In the next chapter, we address the problem of the stability analysis and control of drilling vibration based on the neutral-type time-delay model of the vertical oilwell drilling system under consideration.

# Chapter 5

# Stability analysis and control of drilling vibrations: neutral-type time-delay model approach

## 5.1. Introduction

In this chapter we tackle the problem of stability analysis and control of drilling vibrations within the framework of time delay systems.

Time-delay systems are also called systems with aftereffect or dead-time, hereditary systems, equations with deviating argument or differential-difference equations. They belong to the class of functional differential equations which are infinite dimensional, as opposed to ODE. There is a great number of references devoted to this field of active research see for instance the survey papers [57], [62], [75], [97] and the references therein.

A large number of motivational issues leads the continuous interest and development on time delay systems research, some of them are listed below.

- Aftereffect is an applied problem, it is well known that, together with the increasing expectations of dynamic performances, engineers need their models to behave more like the real process. Many processes include aftereffect phenomena in their inner dynamics. There are examples in biology, chemistry, economics, mechanics, viscoelasticity, physics, physiology, population dynamics, information technologies, engineering sciences, etc. The interest for functional differential equations keeps on growing in all scientific areas and, especially, in control engineering.

- Delay systems are still resistant to many "classical controllers", one could think that the simplest approach would consist in replacing them by some finite-dimensional approximations. Unfortunately, ignoring effects which are adequately represented by functional differential equations is not a general alternative. In the best situation (constant and known delays), it leads to the same degree of complexity in the control design; in worst cases (time-varying delays, for instance), it is potentially disastrous in terms of stability and oscillations [97].

- Delay properties are also surprising since several studies have shown that voluntary introduction of delays can also benefit the control, see for instance [80].

- In spite of their complexity, time-delay systems however often appear as simple infinite-dimensional models in the very complex area of PDEs. As mentioned in [61], "it is usually not difficult to show that the appearance of delay in a differential equation results of some essential simplification of the model". For instance, hyperbolic PDEs can be locally understood as neutral delay systems [50], [60] and, conversely, any time-delay can be represented by a classical transport equation [65].

As explained in Chapter 2, torsional dynamics of the drillstring can be modeled by a time-delay equation of neutral-type, derived through a direct transformation of the wave equation model, which constitutes an input-output representation of the drilling system. Based on this modeling strategy, the stability analysis and control of the system are performed using some tools of the broad control theory for time-delay systems.

First, exponential stability analysis of the system is carried out using a switching systems theory. The TOB model given in (3.1-3.2) comprises a nonlinear function involving the sign function which allows the system to be represented as a particular class of state-dependent switching system. The proposal of an energy functional allows to get LMI-type conditions guaranteeing an exponential convergence of the system trajectories.

Subsequent analysis gives stability and stabilization conditions in terms of LMIs based on a polytopic representation of the drilling system. The nonlinear neutral-type equation is transformed into a set of linear models, non-linearly weighted. This approach leads the design of a nonlinear controller ensuring the exponential stability of the closed loop system and consequently the suppression of torsional oscillations.

Assuming that the system is subject to perturbations or disturbances arising from external errors or unmodeled dynamics, as explained in the previous chapter, an exponential convergence of the system trajectories can not be guaranteed. However, they may exhibit dynamic behavior which is entirely acceptable over a specified finite time interval. This leads to the concept of practical stability or ultimate boundedness with a fixed bound which involves the notion of invariant sets and is particularly investigated in many problems of practical importance. Here, we tackle the problem of practical stabilization of the drilling system based on Lyapunov techniques and the descriptor approach introduced in [41]. We aim at designing a stabilizing controller to suppress the stick-slip phenomenon.

Finally, we analyze coupled axial-torsional vibrations. The attractive ellipsoid method allows to the design of stabilizing controllers guaranteeing an integral elimination of drilling vibrations. This approach gives stabilization conditions in terms of BMIs and poses an optimization problem to ensure the minimization of the attractive set retaining the system trajectories. Furthermore, to address the presence of saturation on the control inputs, a set of additional stability conditions in terms of LMIs will be presented.

The particular significance of this chapter lies in the fact that the presented methodologies can be easily generalized to be applied to any time-delay system meeting the stated specifications.

## 5.2. Stability analysis: switched system approach

Switched systems, as an important branch of hybrid control systems, have received great attention of researchers in recent years. A switched system is a dynamic system that consists of a finite number of subsystems and a logical rule which orchestrates switching between these subsystems. Such systems are useful for modeling various real-world systems such as chemical processes, communication networks, traffic control, manufacturing system control, among many others.

Switched systems with delay deserve attention because actuators, sensors and transmission lines may introduce time lags. In fact, many models involve not only time delay but also the derivative of the past state, due to the reduction of distributed parameter models into neutral type delay models. In recent years, some stability criteria of switched systems with time delay have been obtained (see for instance [59] and [119]). In [74], [109] and [123] the

stability of switched neutral type delay systems is investigated. The proposed approaches require that all the neutral difference operators are stable, or that there exist Hurwitz linear convex combinations of state matrices, which reduce the scope of the obtained stability conditions.

The neutral-type time-delay model describing torsional dynamics of the drilling system (3.4) is considered a particular class of switched system since the nonlinear term of the TOB model involves the sign function:

$$T_{\mathrm{nl}}\left(z(t)\right) = W_{\mathrm{ob}} R_{\mathrm{b}} \left(\mu_{\mathrm{cb}} + (\mu_{\mathrm{sb}} - \mu_{\mathrm{cb}}) \mathrm{e}^{-\frac{\gamma_{\mathrm{b}}}{v_{\mathrm{f}}}|z(t)|}\right) \mathrm{sign}\left(z(t)\right).$$

Notice that the switching is autonomous and state-dependent.

In this section we investigate the stability of the drilling system subject to nonlinear perturbations bounded in magnitude. The proposal of an energy functional provides stability conditions stated in terms of the solution of a set of LMIs. The proposed approach avoids the use of convex combinations of system matrices and reduces the number of variables.

Consider a nonlinear neutral-type time-delay system with state-dependent switching of the form:

$$\begin{gathered} \dot{x}(t) - C_\sigma \dot{x}(t-\tau_1) = A_\sigma x(t) + B_\sigma x(t-\tau_1) + D_\sigma u(t) + f_{1\sigma}(t, x(t)) \\ + f_{2\sigma}(t, x(t-\tau_1)) \\ x(t_0+\theta) = \phi(\theta), \quad \forall \theta \in [-\tau_1, 0], \end{gathered} \tag{5.1}$$

where $x(t) \in \mathcal{R}^n$ is the state vector, $u(t) \in \mathcal{R}^m$ is the control input, $\tau_1$ is a positive constant time delay, $\phi$ is a continuously differentiable initial function and $\sigma \in \{1, 2, ..., N\}$ is a piecewise constant switching signal. The matrices $(A_\sigma, B_\sigma, C_\sigma)$ are allowed to take values, at an arbitrary time, in the finite set $(A_\sigma, B_\sigma, C_\sigma) \in \{(A_1, B_1, C_1), ..., (A_N, B_N, C_N)\}$.

We consider that the nonlinear functions $f_{1\sigma}(t, x(t))$, $f_{2\sigma}(t, x(t-\tau_1))$ are bounded in magnitude, i.e., there exist positive constants $\alpha_{1\sigma}$, $\alpha_{2\sigma}$ such that

$$\begin{aligned} \left\| f_{1\sigma}(t, x(t)) \right\| &\leq \alpha_{1\sigma} \left\| x(t) \right\|, \qquad \forall t \geq 0, \\ \left\| f_{2\sigma}(t, x(t-\tau_1)) \right\| &\leq \alpha_{2\sigma} \left\| x(t-\tau_1) \right\|, \ \sigma \in \{1, ..., N\}. \end{aligned} \tag{5.2}$$

Let $u(t)$ be a state-feedback controller in the form $u(t) = Kx(t-\tau_1)$. Substituting this control law into (5.1), we obtain the closed loop system:

$$\begin{gathered} \dot{x}(t) - C_\sigma \dot{x}(t-\tau_1) = A_\sigma x(t) + \bar{B}_\sigma x(t-\tau_1) + f_{1\sigma}(t, x_2(t)) \\ + f_{2\sigma}(t, x_2(t-\tau_1)) \\ x(t_0+\theta) = \phi(\theta), \quad \forall \theta \in [-\tau, 0], \end{gathered} \tag{5.3}$$

where $\bar{B}_\sigma = B_\sigma + D_\sigma K$.

In [121], asymptotic stability of switched neutral systems is analyzed. Here, following the proposed approach, we derive conditions for the exponential stability of nonlinear switched time-delay systems of neutral-type.

**Theorem 3 (Asymptotic stability)** *Given a gain matrix $K$, the switched neutral system (5.3) with $f_{1\sigma}(t,x(t))$ and $f_{2\sigma}(t,x(t-\tau_1))$ satisfying (5.2) is asymptotically stable if there are symmetric positive definite matrices $P, Q_1, Q_2, R_1$ such that the LMI*

$$\Psi_i = \begin{pmatrix} \Psi_{i11} & \sqrt{2}P & \sqrt{2}\alpha_{1i}W & \Psi_{i14} & 0 & \Psi_{i16} \\ * & -I & 0 & 0 & 0 & 0 \\ * & * & -I & 0 & 0 & 0 \\ * & * & * & \Psi_{i44} & \alpha_{2i}W & \Psi_{i46} \\ * & * & * & * & -I & 0 \\ * & * & * & * & * & \Psi_{i66} \end{pmatrix} < 0, \qquad (5.4)$$

*with*

$$\begin{aligned} \Psi_{i11} &= PA_i + A_i^T P + Q_1 + A_i^T W A_i - R_1 + \alpha_{1i}^2 I + \alpha_{1i}^2 W + 2A_i^T A_i \\ \Psi_{i14} &= P\bar{B}_i + A_i^T W \bar{B}_i + R_1 + 2A_i^T \bar{B}_i \\ \Psi_{i16} &= PC_i + A_i^T W C_i + 2A_i^T C_i \\ \Psi_{i44} &= -Q_1 + \bar{B}_i^T W \bar{B}_i - R_1 + 2\alpha_{2i}^2 I + \alpha_{2i}^2 W + 2\bar{B}_i^T \bar{B}_i \\ \Psi_{i46} &= \bar{B}_i^T W C_i + 2\bar{B}_i^T C_i \\ \Psi_{i66} &= -Q_2 + C_i^T W C_i + 2C_i^T C_i \\ \bar{B}_i &= B_i + D_i K \\ W &= Q_2 + \tau_1^2 R_1 \end{aligned}$$

*is feasible for all $i = 1, ..., N$.*

**Proof 4** *As in [121], we consider the energy functional*

$$\begin{aligned} V(x_t) &= x^T(t)Px(t) + \int_{t-\tau_1}^{t} x^T(s)Q_1x(s)ds + \int_{t-\tau_1}^{t} \dot{x}^T(s)Q_2\dot{x}(s)ds \qquad (5.5) \\ &\quad + \tau_1 \int_{-\tau_1}^{0} \int_{t+\theta}^{t} \dot{x}^T(s)R_1\dot{x}(s)dsd\theta. \end{aligned}$$

*Taking the derivative of $V(x_t)$ along the trajectories of any subsystem ith of (5.3), we have*

$$\begin{aligned}\dot{V}(x_t) &= 2x^T(t)P\dot{x}(t) - x^T(t-\tau_1)Q_1x(t-\tau_1) + x^T(t)Q_1x(t) \\ &\quad -\dot{x}^T(t-\tau_1)Q_2\dot{x}(t-\tau_1) + \dot{x}^T(t)\left(Q_2+\tau_1^2R_1\right)\dot{x}(t) \\ &\quad -\tau_1\int_{t-\tau_1}^{t}\dot{x}^T(s)R_1\dot{x}(s)ds.\end{aligned} \tag{5.6}$$

*Using the Jensen's inequality we can see that*

$$\begin{aligned}-\tau_1\int_{t-\tau_1}^{t}\dot{x}^T(s)R_1\dot{x}(s)ds &\leq -\int_{t-\tau_1}^{t}\dot{x}^T(s)ds R_1\int_{t-\tau_1}^{t}\dot{x}(s)ds \\ &= -(x(t)-x(t-\tau_1))^TR_1(x(t)-x(t-\tau_1)).\end{aligned} \tag{5.7}$$

*Then, substituting (5.7) into (5.6) gives*

$$\begin{aligned}\dot{V}(x_t) \leq\ & 2x^T(t)P\left[C_i\dot{x}(t-\tau_1)+A_ix(t)+\bar{B}_ix(t-\tau_1)\right] \\ & -x^T(t-\tau_1)Q_1x(t-\tau_1)+x^T(t)Q_1x(t) \\ & -\dot{x}^T(t-\tau_1)Q_2\dot{x}(t-\tau_1) \\ & +\left[C_i\dot{x}(t-\tau_1)+A_ix(t)+\bar{B}_ix(t-\tau_1)\right]^TW \\ & \left[C_i\dot{x}(t-\tau_1)+A_ix(t)+\bar{B}_ix(t-\tau_1)\right] \\ & -(x(t)-x(t-\tau_1))^TR_1(x(t)-x(t-\tau_1))+F_i,\end{aligned}$$

*where $W := Q_2+\tau_1^2R_1$, and*

$$\begin{aligned}F_i &= F_i(x_t,f_i) := 2x^T(t)P\left[f_{1i}(\cdot)+f_{2i}(\cdot)\right]+G_i^TW\left[f_{1i}(\cdot)+f_{2i}(\cdot)\right] \\ &\quad +\left[f_{1i}(\cdot)+f_{2i}(\cdot)\right]^TWG_i+\left[f_{1i}(\cdot)+f_{2i}(\cdot)\right]^TW\left[f_{1i}(\cdot)+f_{2i}(\cdot)\right],\end{aligned} \tag{5.8}$$

$$G_i = G_i(x_t) := \left[C_i\dot{x}(t-\tau_1)+A_ix(t)+\bar{B}_ix(t-\tau_1)\right].$$

*We look for an upper bound on $F_i$. Considering that for any vectors $a,b\in\mathcal{R}^n$, the inequality $2a^Tb\leq a^Ta+b^Tb$ is satisfied, and taking into account the bounds (5.2), we obtain*

$$2x^T(t)Pf_{1i}(\cdot)\leq x^T(t)PPx(t)+f_{1i}(\cdot)^Tf_{1i}(\cdot)\leq x^T(t)PPx(t)+\alpha_{1i}^2x^T(t)x(t),$$

$$2x^T(t)Pf_2(\cdot)\leq x^T(t)PPx(t)+f_{2i}(\cdot)^Tf_{2i}(\cdot)\leq x^T(t)PPx(t)+\alpha_{2i}^2x^T(t-\tau_1)x(t-\tau_1).$$

*Similarly,*

$$G_i^TWf_{1i}(\cdot)+f_{1i}^T(\cdot)WG\leq G_i^TG_i+f_{1i}^T(\cdot)WWf_{1i}(\cdot)\leq G_i^TG_i+\alpha_{1i}^2x^T(t)WWx(t),$$

$$\begin{aligned} G_i^T W f_{2i}(\cdot) + f_{2i}^T(\cdot) W G_i &\leq G_i^T G_i + f_{2i}^T(\cdot) W W f_{2i}(\cdot) \\ &\leq G_i^T G_i + \alpha_{2i}^2 x^T(t-\tau_1) W W x(t-\tau_1), \end{aligned}$$

*and*

$$\begin{aligned} [f_{1i}(\cdot) + f_{2i}(\cdot)]^T W [f_{1i}(\cdot) + f_{2i}(\cdot)] &= f_{1i}(\cdot)^T W f_{1i}(\cdot) + f_{2i}^T(\cdot) W f_{2i}(\cdot) \\ &\quad + f_{1i}(\cdot)^T W f_{2i}(\cdot) + f_{2i}(\cdot)^T W f_{1i}(\cdot) \\ &\leq \alpha_{1i}^2 x^T(t) W x(t) + \alpha_{2i}^2 x^T(t-\tau_1) W x(t-\tau_1) \\ &\quad + \alpha_{1i}^2 x^T(t) W W x(t) + \alpha_{2i}^2 x^T(t-\tau_1) x(t-\tau_1). \end{aligned}$$

*Substituting the above inequalities into (5.8) yields*

$$\begin{aligned} F_i \leq\ & 2x^T(t) P P x(t) + \alpha_{1i}^2 x^T(t) x(t) \\ & + 2\alpha_{2i}^2 x^T(t-\tau_1) x(t-\tau_1) + 2G_i^T G_i \\ & + 2\alpha_{1i}^2 x^T(t) W W x(t) + \alpha_{2i}^2 x^T(t-\tau_1) W W x(t-\tau_1) \\ & + \alpha_{1i}^2 x^T(t) W x(t) + \alpha_{2i}^2 x^T(t-\tau_1) W x(t-\tau_1). \end{aligned}$$

*Then, the derivative of $V(x_t)$ along the trajectories of any subsystem ith of (5.3) satisfies*

$$\begin{aligned} \dot{V}(x_t) \leq\ & 2x^T(t) P G_i - x^T(t-\tau_1) Q_1 x(t-\tau_1) + x^T(t) Q_1 x(t) \\ & - \dot{x}^T(t-\tau_1) Q_2 \dot{x}(t-\tau_1) + G_i^T W G_i \\ & - (x(t) - x(t-\tau_1))^T R_1 (x(t) - x(t-\tau_1)) \\ & + 2x^T(t) P P x(t) + \alpha_{1i}^2 x^T(t) x(t) \\ & + 2\alpha_{2i}^2 x^T(t-\tau_1) x(t-\tau_1) + 2G_i^T G_i + 2\alpha_{1i}^2 x^T(t) W W x(t) \\ & + \alpha_{2i}^2 x^T(t-\tau_1) W W x(t-\tau_1) \\ & + \alpha_{1i}^2 x^T(t) W x(t) + \alpha_{2i}^2 x^T(t-\tau_1) W x(t-\tau_1). \end{aligned}$$

*Setting $\xi(t) = (x^T(t) \quad x^T(t-\tau_1) \quad \dot{x}^T(t-\tau_1))$, the above inequality is written as*

$$\dot{V}(x_t) \leq \xi(t) \Phi_i(P, Q_1, Q_2, R_1) \xi^T(t), \tag{5.9}$$

*where*

$$\Phi_i = \begin{pmatrix} \Phi_{i11} & \Phi_{i12} & \Phi_{i13} \\ * & \Phi_{i22} & \Phi_{i23} \\ * & * & \Phi_{i33} \end{pmatrix}, \tag{5.10}$$

$$
\begin{aligned}
\Phi_{i11} &= PA_i + A_i^T P + Q_1 + A_i^T W A_i - R_1 + 2PP + \alpha_{1i}^2 I \\
&\quad +2\alpha_{1i}^2 WW + \alpha_{1i}^2 W + 2A_i^T A_i \\
\Phi_{i12} &= P\bar{B}_i + A_i^T W \bar{B}_i + R_1 + 2A_i^T \bar{B}_i \\
\Phi_{i13} &= PC_i + A_i^T W C_i + 2A_i^T C_i \\
\Phi_{i22} &= -Q_1 + \bar{B}_i^T W \bar{B}_i - R_1 + 2\alpha_{2i}^2 I + \alpha_{2i}^2 WW + \alpha_{2i}^2 W + 2\bar{B}_i^T \bar{B}_i \\
\Phi_{i23} &= \bar{B}_i^T W C_i + 2\bar{B}_i^T C_i \\
\Phi_{i33} &= -Q_2 + C_i^T W C_i + 2C_i^T C_i \\
\bar{B}_i &= B_i + D_i K \\
W = Q & \quad {}_2 + \tau_1^2 R_1.
\end{aligned}
$$

*By Schur's complements, it follows that* $\Phi_i < 0$ *in (5.10) is equivalent to* $\Psi_i < 0$ *in (5.4) and the result follows.*

### 5.2.1. Exponential stability conditions

The closed loop system (5.3) is said to be $\alpha-$stable or "exponentially stable" with decay rate $\alpha$ if there exists a scalar $\kappa \geq 1$ such that for any continuously differentiable initial condition $\phi$, the solution $x(t, t_0, \phi)$ satisfies:

$$|x(t, t_0, \phi)| \leq \kappa |\varphi| \, \mathrm{e}^{-\alpha(t-t_0)}.$$

Using the change of variable:

$$x^*(t) := \mathrm{e}^{\alpha t} x(t),$$

we can rewrite the system (5.3) as

$$
\begin{aligned}
\dot{x}^*(t) - C_\sigma \mathrm{e}^{\alpha\tau_1} \dot{x}^*(t-\tau_1) &= \bar{A}_\sigma x^*(t) + \mathrm{e}^{\alpha\tau_1} \bar{B}_\sigma x^*(t-\tau_1) \qquad (5.11) \\
&\quad - \alpha \mathrm{e}^{\alpha\tau_1} C_\sigma x^*(t-\tau_1) + f_{1\sigma}(t, x^*(t)) + f_{2\sigma}(t, x^*(t-\tau_1)), \\
x(t_0+\theta) &= \phi(\theta), \quad \forall \theta \in [-\tau, 0],
\end{aligned}
$$

where $\bar{A}_\sigma = A_\sigma + \alpha I$ and $\bar{B}_\sigma = B_\sigma + D_\sigma K$. Notice that the condition (5.2) imply

$$
\begin{aligned}
\|f_{1\sigma}(t, z(t))\| &\leq \alpha_{1\sigma} \|x^*(t)\|, \quad \forall t \geq 0, \\
\|f_{2\sigma}(t, z(t-\tau_1))\| &\leq \alpha_{2\sigma} \|x^*(t-\tau_1)\|, \quad \sigma \in \{1, ..., N\}.
\end{aligned}
$$

Our proposal is to find conditions for which the solution $x^* = 0$ of the transformed system (5.11) is stable. Clearly, these conditions will ensure the exponential stability of the system (5.3). The following result is based on Theorem 3.

**Theorem 4 (Exponential stability)** *Given a gain matrix $K$, the switched neutral system (5.3) with $f_{1\sigma}(t, x(t))$ and $f_{2\sigma}(t, x(t-\tau_1))$ satisfying (5.2) is exponentially stable if there are symmetric positive definite matrices $P, Q_1, Q_2, R_1$ such that the LMI*

$$\Psi_i = \begin{pmatrix} \Psi_{i11} & \sqrt{2}P & \sqrt{2}\alpha_{1i}W & \Psi_{i14} & 0 & \Psi_{i16} \\ * & -I & 0 & 0 & 0 & 0 \\ * & * & -I & 0 & 0 & 0 \\ * & * & * & \Psi_{i44} & \alpha_{2i}W & \Psi_{i46} \\ * & * & * & * & -I & 0 \\ * & * & * & * & * & \Psi_{i66} \end{pmatrix} < 0, \tag{5.12}$$

*with*

$$\begin{aligned}
\Psi_{i11} &= P\bar{A}_i + \bar{A}_i^T P + Q_1 + \bar{A}_i^T W \bar{A}_i - R_1 + \alpha_{1i}^2 I + \alpha_{1i}^2 W + 2\bar{A}_i^T \bar{A}_i \\
\Psi_{i14} &= e^{\alpha\tau_1} P\left(\bar{B}_i - \alpha C_i\right) + e^{\alpha\tau_1}\bar{A}_i^T W\left(\bar{B}_i - \alpha C_i\right) + R_1 + 2e^{\alpha\tau_1}\bar{A}_i^T\left(\bar{B}_i - \alpha C_i\right) \\
\Psi_{i16} &= e^{\alpha\tau_1} PC_i + e^{\alpha\tau_1}\bar{A}_i^T WC_i + 2e^{\alpha\tau_1}\bar{A}_i^T C_i \\
\Psi_{i44} &= -Q_1 + e^{2\alpha\tau_1}\left(\bar{B}_i - \alpha C_i\right)^T W\left(\bar{B}_i - \alpha C_i\right) - R_1 + 2\alpha_{2i}^2 I + \alpha_{2i}^2 W \\
&\quad + 2e^{2\alpha\tau_1}\left(\bar{B}_i - \alpha C_i\right)^T\left(\bar{B}_i - \alpha C_i\right) \\
\Psi_{i46} &= e^{2\alpha\tau_1}\left(\bar{B}_i - \alpha C_i\right)^T WC_i + 2e^{2\alpha\tau_1}\left(\bar{B}_i - \alpha C_i\right)^T C_i \\
\Psi_{i66} &= -Q_2 + e^{2\alpha\tau_1} C_i^T WC_i + 2e^{2\alpha\tau_1} C_i^T C_i \\
\bar{A}_i &= A_i + \alpha I \\
\bar{B}_i &= B_i + D_i K \\
W &= Q_2 + \tau_1^2 R_1
\end{aligned}$$

*is feasible for all $i = 1, ..., N$.*

The torsional drilling model (3.4) is represented as an autonomous state-dependent switching system as follows,

$$\begin{aligned}
\dot{z}(t) - \Upsilon\dot{z}(t-2\Gamma) = &\left(-\Psi - \frac{c_\mathrm{b}}{I_\mathrm{B}}\right) z(t) + \left(\frac{\Upsilon c_\mathrm{b}}{I_\mathrm{B}} - \Upsilon\Psi\right) z(t-2\Gamma) \\
&+ \Pi\Omega(t-\Gamma) + f_{1\sigma}\left(t, z(t)\right) + + f_{2\sigma}\left(t, z(t-2\Gamma)\right), \quad \sigma = 1, 2,
\end{aligned} \tag{5.13}$$

where the constants $\Upsilon$, $\Gamma$, $\Psi$ and $\Pi$ are defined in (2.10), the angular velocity coming from the rotary table is taken as the control input.

The functions $f_{1\sigma}$, $f_{2\sigma}$, $\sigma = 1, 2$ of system (5.13) are switched according to the following autonomous state-dependent rule:

$$\begin{cases} \text{for} \quad z(t) = 0 : \\ f_{11}(t, z(t)) = f_{21}(t, z(t - 2\Gamma)) = 0 \\ \\ \text{for} \quad z(t) > 0 : \\ f_{12}(t, z(t)) = -c_1 - c_2 \mathrm{e}^{-\frac{\gamma_b}{v_f} z(t)} \\ f_{22}(t, z(t - 2\Gamma)) = c_1 \Upsilon + c_2 \Upsilon \mathrm{e}^{-\frac{\gamma_b}{v_f} z(t-2\Gamma)}, \end{cases} \tag{5.14}$$

with $c_1 = \frac{W_{\mathrm{ob}} R_{\mathrm{b}}}{I_{\mathrm{B}}} \mu_{\mathrm{cb}}$, and $c_2 = \frac{W_{\mathrm{ob}} R_{\mathrm{b}}}{I_{\mathrm{B}}} (\mu_{\mathrm{sb}} - \mu_{\mathrm{cb}})$.

Notice that the switching depends on the angular velocity at the bottom end of the drillstring $z(t)$. If we approximate the switching rule (5.14) by the following one,

$$\begin{cases} \text{for} \quad 0 \leq z(t) < 0.1 : \\ f_{11}(t, z(t)) = f_{21}(t, z(t - 2\Gamma)) = 0 \\ \\ \text{for} \quad z(t) > 0.1 : \\ f_{12}(t, z(t)) = -c_1 - c_2 \mathrm{e}^{-\frac{\gamma_b}{v_f} z(t)} \\ f_{22}(t, z(t - 2\Gamma)) = c_1 \Upsilon + c_2 \Upsilon \mathrm{e}^{-\frac{\gamma_b}{v_f} z(t-2\Gamma)}, \end{cases} \tag{5.15}$$

then, the conditions (5.2) on $f_{12}(t, z(t))$ and $f_{22}(t, z(t - 2\Gamma))$ are satisfied for some relatively small constants $\alpha_1$, $\alpha_2$. The switching law (5.15) means that for small values of the angular velocity at the bottom end ($z < 0.1 \mathrm{rad\ s}^{-1}$) the nonlinear part of the TOB has no effect (this actually happens when $z = 0$). According to (5.15) we have that for $0 \leq z(t) < 0.1$:

$$\begin{aligned} \|f_{11}(t, z(t))\| &= 0 \leq \alpha_1 \|z(t)\| , \\ \|f_{21}(t, z(t - 2\Gamma))\| &= 0 \leq \alpha_2 \|z(t - 2\Gamma)\| , \end{aligned} \tag{5.16}$$

and for $z(t) \geq 0.1$:

$$\begin{aligned} \|f_{12}(t, z(t))\| &= \left\| -c_1 - c_2 \mathrm{e}^{-\frac{\gamma_b}{v_f} z(t)} \right\| \leq \alpha_1 \|z(t)\| , \\ \|f_{22}(t, z(t - 2\Gamma))\| &= \left\| c_1 \Upsilon + c_2 \Upsilon \mathrm{e}^{-\frac{\gamma_b}{v_f} z(t-2\Gamma)} \right\| \leq \alpha_2 \|z(t - 2\Gamma)\| . \end{aligned} \tag{5.17}$$

### 5.2.2. Numerical results

Using the model parameters given in (3.11), we obtain $\Gamma = 0.3719$, $c_1 = 85.0829$, $c_2 = 51.0498$. The conditions (5.16-5.17) are satisfied for all $\alpha_1 > 1317.1$, $\alpha_2 > 974.3$.

Figure 5.1 shows a simulation of the trajectory $z(t)$ of the drilling system (5.13-5.14) with $\Omega(t) = 15\text{rad s}^{-1}$.

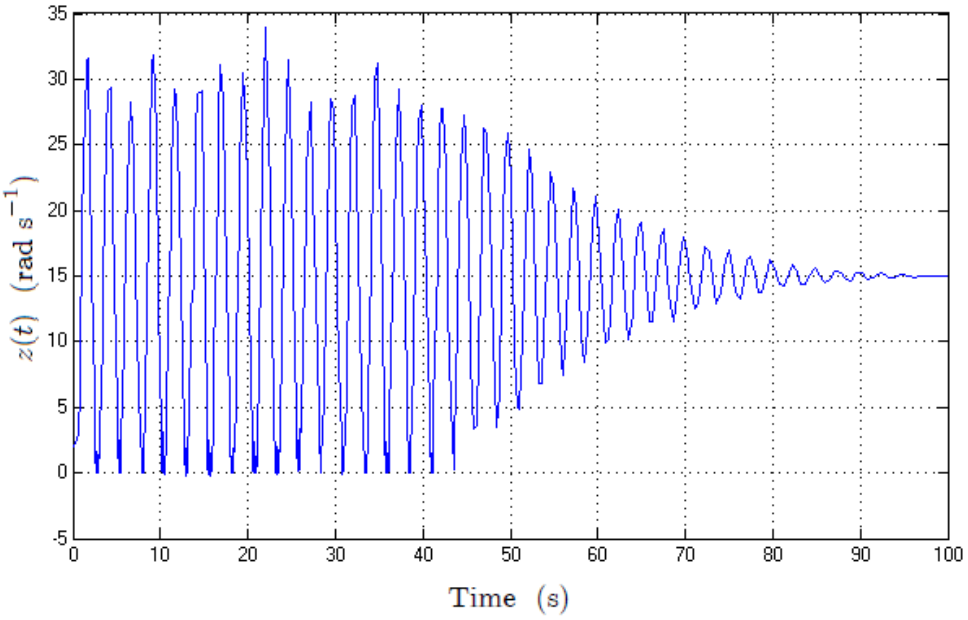


Figure 5.1: Angular velocity $z(t)$ of the drilling system described by (5.13-5.14) with $\Omega(t) = 15\text{rad s}^{-1}$.

Here, we propose a stabilizing control law that ensures the exponential convergence of the trajectory $x_1(t) = z(t) - \Omega_0$ and consequently the suppression of the stick-slip phenomenon. For stability issues the velocity at the bottom end must track the angular velocity at the upper part.

In order to achieve the velocity tracking we propose the control law

$$\Omega(t-\Gamma) = -\lambda_0 \dot{x_1}(t-2\Gamma) - \lambda_1 x_1(t-2\Gamma), \tag{5.18}$$

which according to (3.6), in terms of the bit speed, can be written as

$$\Omega(t-\Gamma) = -\lambda_0 \dot{z}(t-2\Gamma) - \lambda_1 z(t-2\Gamma) + \lambda_1 \Omega_0. \tag{5.19}$$

We apply the result of Theorem 4 to analyze the exponential stability of the drilling system subject to the switching rule (5.15) in closed loop with the controller (5.18). Notice that $\alpha_1$ and $\alpha_2$ satisfy (5.16-5.17).

After computing the LMIs stated in Theorem 4 with $\lambda_0 = 0.05$, $\lambda_1 = 0.36$, $\alpha_1 = 1320$, $\alpha_2 = 975$ and $\alpha = 0.6$ we conclude that the closed loop drilling system coupled to the switching law (5.15) where the functions $f_{1\sigma}(t, z(t))$, $f_{2\sigma}(t, z(t-2\Gamma))$ satisfy the conditions (5.16), (5.17) is exponentially stable.

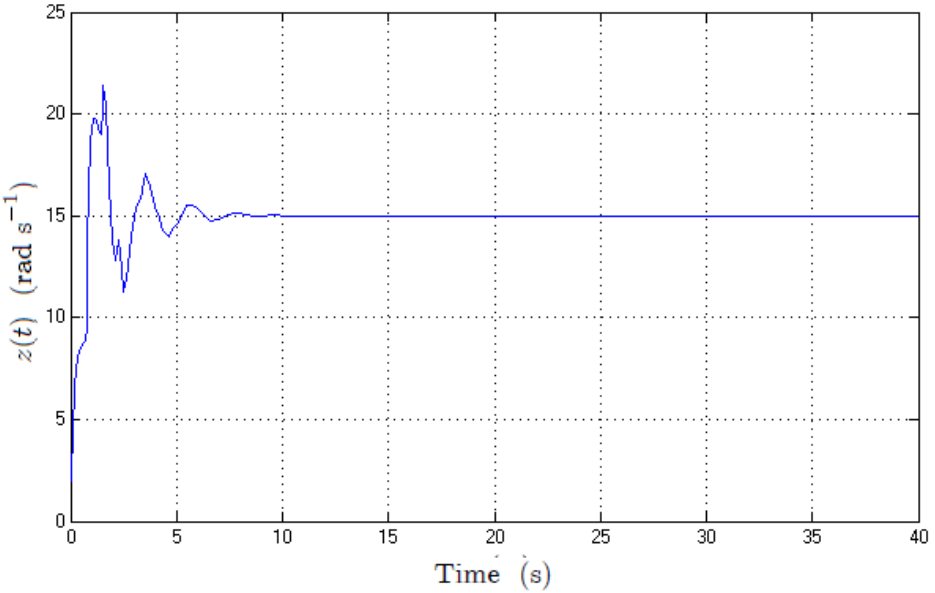


Figure 5.2: Angular velocity $z(t)$ of the drilling system described by (5.13-5.14) in closed loop with the control law (5.19) with $\Omega_0(t) = 15\text{rad s}^{-1}$.

The simulation results of Figure 5.2 show the stick-slip elimination by means of applying the controller (5.19).

## 5.3. Control of torsional vibrations: multimodel approximation approach

This section concerns the exponential stabilization of the class of nonlinear neutral type time-delay systems that can be transformed into a multi-model system. The approach introduced in [101], based on Lyapunov-Krasovskii techniques, allows to find an effective stabilizing controller for the suppression of the stick-slip in the oilwell drilling system described by (2.9-3.1). The

exponential stability properties are proved using an appropriate change of variables associated with a polytopic representation.

It is well known that nonlinear systems are indeed models closer to reality in the sense that their validity is not necessarily limited to an immediate neighborhood of an operating point or a reference trajectory.

In [108] the author presents stabilization results for nonlinear retarded type time-delay systems which can be represented in two different ways: as multi-model systems and as uncertain systems.

We investigate the stabilization of a class of nonlinear neutral type time-delay systems that can be transformed into a multi-model system, i.e., a set of linear models non-linearly weighted. A multi-model neutral type system can be represented as follows

$$\dot{x}(t) - D\dot{x}(t-\tau_1) = \sum_{i\in I^r} h_i(x_t)\left\{A_i x(t) + A_{i\tau_1} x(t-\tau_1) + Bu(t)\right\}, \qquad (5.20)$$

where $\tau_1 > 0$ is a constant time delay, the set $I^r$ is the set of integers $\{1, ..., r\}$, $r$ is the number of subsystems required to describe the multi-model system. The functions $h_i(\cdot)$ are scalar weighting functions satisfying the convexity conditions:

$$\sum_{i\in I^r} h_i(x_t) = 1 \quad \forall i = 1, ..., r, \quad h_i(x_t) \geq 0. \qquad (5.21)$$

First, we are going to analyze the $\alpha$-stability of the open loop system, i.e., the system:

$$\dot{x}(t) - D\dot{x}(t-\tau_1) = \sum_{i\in I^r} h_i(x_t)\left\{A_i x(t) + A_{i\tau_1} x(t-\tau_1)\right\}. \qquad (5.22)$$

To guarantee that the difference operator is stable we assume $|D| < 1$.

The change of variable $x_\alpha(t) = \mathrm{e}^{\alpha t} x(t)$ transforms the system (5.22) into:

$$\begin{aligned}\dot{x}_\alpha(t)D - \mathrm{e}^{\alpha\tau_1}\dot{x}_\alpha(t-\tau_1) = \sum_{i\in I^r} h_i(x_t)\left\{\left(A_i + \alpha I_n\right) x_\alpha(t)\right.\\ \left.+\mathrm{e}^{\alpha\tau_1}\left(A_{i\tau_1} - \alpha D\right) x_\alpha(t-\tau_1)\right\}. \qquad (5.23)\end{aligned}$$

The proposal is to find conditions for which the solution $x_\alpha = 0$ of the transformed system (5.23) is asymptotically stable. Clearly, these conditions will guarantee the exponential stability of system (5.22).

**Theorem 5** *The solution $x(t) = 0$ of the system (5.22) is $\alpha$-stable if there exist matrices $0 < P_1 = P_1^T$, $P_2$, $P_3$, $Q = Q^T$ and $R = R^T$, such that for all $i \in I^r$ the following LMI is satisfied*

$$\begin{pmatrix} \Psi_i & P^T \begin{pmatrix} 0 \\ e^{\alpha\tau_1}(A_{i\tau_1} - \alpha D) \end{pmatrix} & P^T \begin{pmatrix} 0 \\ e^{\alpha\tau_1} D \end{pmatrix} \\ * & -R/\tau_1 & 0 \\ * & * & -Q \end{pmatrix} < 0, \tag{5.24}$$

*where*

$$\begin{aligned} P &: = \begin{pmatrix} P_1 & 0 \\ P_2 & P_3 \end{pmatrix}, \quad P_1 = P_1^T > 0, \\ &, \\ \Psi_i &: = P^T \begin{pmatrix} 0 & I_n \\ \Lambda_i & -I_n \end{pmatrix} + \begin{pmatrix} 0 & I_n \\ \Lambda_i & -I_n \end{pmatrix}^T P + \begin{pmatrix} 0 & 0 \\ 0 & \tau_1 R + Q \end{pmatrix}, \\ \Lambda_i &: = A_i + \alpha I_n + e^{\alpha\tau_1}(A_{i\tau_1} - \alpha D). \end{aligned}$$

**Proof 5** *According to the Leibniz formula,*

$$x_\alpha(t - \tau_1) = x_\alpha(t) - \int_{t-\tau_1}^{t} \dot{x}_\alpha(s) ds,$$

*we can write the system (5.23) as*

$$\begin{aligned} &\dot{x}_\alpha(t) - D e^{\alpha\tau_1} \dot{x}_\alpha(t - \tau_1) = \\ &\sum_{i \in I^r} h_i(x_t) \left\{ [A_i + \alpha I_n + e^{\alpha\tau_1}(A_{i\tau_1} - \alpha D)] x_\alpha(t) - e^{\alpha\tau_1} [A_{i\tau_1} - \alpha D] \int_{t-\tau_1}^{t} \dot{x}_\alpha(s) ds \right\}. \end{aligned}$$

*Using the descriptor form introduced in [41] we have*

$$\begin{aligned} \dot{x}_\alpha(t) &= y(t), \\ y(t) &= \sum_{i \in I^r} h_i(x_t) \{ D e^{\alpha\tau_1} y(t - \tau_1) + \Lambda_i x_\alpha(t) \\ &\quad - e^{\alpha\tau_1}(A_{i\tau_1} - \alpha D) \int_{t-\tau_1}^{t} y(s) ds \Big\}, \end{aligned}$$

*where*

$$\Lambda_i := A_i + \alpha I_n + e^{\alpha\tau_1}(A_{i\tau_1} - \alpha D).$$

*Then, we can write*

$$E \begin{pmatrix} \dot{x}_\alpha(t) \\ \dot{y}(t) \end{pmatrix} = \begin{pmatrix} y(t) \\ \sum\limits_{i \in I^r} h_i(x_t) \cdot \lambda \end{pmatrix},$$

*where*

$$\begin{aligned} E &= diag\{I_n, 0\}, \\ \lambda &= -y(t) + De^{\alpha\tau_1}y(t-\tau_1) + \Lambda_i x_\alpha(t) - e^{\alpha\tau_1}(A_{i\tau_1} - \alpha D)\int_{t-\tau_1}^{t} y(s)ds. \end{aligned}$$

*Following [41], we use the Lyapunov-Krasovskii functional*

$$\begin{aligned} V_\alpha(t) = \begin{pmatrix} x_\alpha^T(t) & y^T(t) \end{pmatrix} EP \begin{pmatrix} x_\alpha(t) \\ y(t) \end{pmatrix} + \int_{-\tau_1}^{0}\int_{t+\theta}^{t} y^T(s)Ry(s)dsd\theta \\ + \int_{t-\tau_1}^{t} y^T(s)Qy(s)ds, \qquad (5.25) \\ P = \begin{pmatrix} P_1 & 0 \\ P_2 & P_3 \end{pmatrix},\ P_1 = P_1^T > 0,\ R > 0,\ Q > 0. \end{aligned}$$

*The functional $V_\alpha(t)$ is positive definite since*

$$\begin{pmatrix} x_\alpha^T(t) & y^T(t) \end{pmatrix} EP \begin{pmatrix} x_\alpha(t) \\ y(t) \end{pmatrix} = x_\alpha^T(t)P_1x_\alpha(t).$$

*Notice that $EP = P^TE$, taking the derivative in $t$ of $V_\alpha(t)$ we obtain*

$$\begin{aligned} \dot{V}_\alpha(t) = 2\begin{pmatrix} x_\alpha^T(t) & y^T(t) \end{pmatrix} P^T \begin{pmatrix} y(t) \\ \sum\limits_{i\in I^r} h_i(x_t)\cdot\lambda \end{pmatrix} + \tau_1 y^T(t)Ry(t) \\ - \int_{t-\tau_1}^{t} y^T(s)Ry(s)ds + y^T(t)Qy(t) - y^T(t-\tau_1)Qy(t-\tau_1). \end{aligned}$$

*Setting $\xi = \begin{pmatrix} x_\alpha(t) & y(t) & y(t-\tau_1) \end{pmatrix}$ we can write*

$$\begin{aligned} \dot{V}_\alpha(t) &= \xi^T \begin{pmatrix} \tilde{\Psi}_i & P^T \begin{pmatrix} 0 \\ e^{\alpha\tau_1}D \end{pmatrix} \\ \begin{pmatrix} 0 & e^{\alpha\tau_1}D^T \end{pmatrix} P & -Q \end{pmatrix} \xi + \Xi \\ &\quad - \int_{t-\tau_1}^{t} y^T(s)Ry(s)ds, \qquad (5.26) \end{aligned}$$

*where*

$$\begin{aligned} \Xi &= -2\int_{t-\tau_1}^{t} \begin{pmatrix} x_\alpha^T(t) & y^T(t) \end{pmatrix} P^T \begin{pmatrix} 0 \\ e^{\alpha\tau_1}(A_{i\tau_1} - \alpha D) \end{pmatrix} y(s)ds, \\ \tilde{\Psi}_i &: = \sum_{i\in I^r} h_i(x_t) \left\{ P^T \begin{pmatrix} 0 & I_n \\ \Lambda_i & -I_n \end{pmatrix} + \begin{pmatrix} 0 & I_n \\ \Lambda_i & -I_n \end{pmatrix}^T P + \begin{pmatrix} 0 & 0 \\ 0 & \tau_1 R + Q \end{pmatrix} \right\}. \end{aligned}$$

*In order to obtain an upper bound on* $\Xi$, *we use the following property.*

*For all vectors* $a,\ b \in \mathcal{R}^n$ *and positive definite matrix* $R \in \mathcal{R}^{n\times n}$, *the following inequality is satisfied*

$$\pm 2a^T b \leq a^T R^{-1} a + b^T R b.$$

*Then, we have*

$$\begin{aligned}\Xi \ \leq\ & \begin{pmatrix} x_\alpha^T(t) & y^T(t) \end{pmatrix} P^T \begin{pmatrix} 0 \\ e^{\alpha\tau_1}\left(A_{i\tau_1} - \alpha D\right) \end{pmatrix} \tau_1 R^{-1} \\ & \begin{pmatrix} 0 & e^{\alpha\tau_1}\left(A_{i\tau_1} - \alpha D\right)^T \end{pmatrix} P \begin{pmatrix} x_\alpha(t) \\ y(t) \end{pmatrix} \\ & + \int_{t-\tau_1}^{t} y^T(s) R y(s) ds. \end{aligned} \tag{5.27}$$

*From (5.26) and (5.27), it yields*

$$\begin{aligned}\dot{V}_\alpha(t) \leq \xi^T & \begin{pmatrix} \tilde{\Psi}_i & P^T \begin{pmatrix} 0 \\ e^{\alpha\tau_1} D \end{pmatrix} \\ \begin{pmatrix} 0 & e^{\alpha\tau_1} D^T \end{pmatrix} P & -Q \end{pmatrix} \xi \\ + \begin{pmatrix} x_\alpha^T(t) & y^T(t) \end{pmatrix} & P^T \begin{pmatrix} 0 \\ e^{\alpha\tau_1}\left(A_{i\tau_1} - \alpha D\right) \end{pmatrix} \left(\tau_1 R^{-1}\right) \\ & \begin{pmatrix} 0 & e^{\alpha\tau_1}\left(A_{i\tau_1} - \alpha D\right)^T \end{pmatrix} P \begin{pmatrix} x_\alpha(t) \\ y(t) \end{pmatrix}. \end{aligned}$$

*Finally, using Schur complements, the system (5.22) is asymptotically stable if every matrix,* $i \in I^r$

$$\begin{pmatrix} \Psi_i & P^T \begin{pmatrix} 0 \\ e^{\alpha\tau_1}\left(A_{i\tau_1} - \alpha D\right) \end{pmatrix} & P^T \begin{pmatrix} 0 \\ e^{\alpha\tau_1} D \end{pmatrix} \\ * & -R/\tau_1 & 0 \\ * & * & -Q \end{pmatrix},$$

*is negative definite, i.e., if the LMI condition (5.24) is satisfied.*

### 5.3.1. Exponential stabilization results

Having determined the criteria for exponential stability for the open loop system (5.22), the next step is to define an algorithm that allows the synthesis of a gain $K$ such that the feedback control law

$$u(t) = Kx(t - \tau_1) \tag{5.28}$$

exponentially stabilizes the closed loop system

$$\dot{x}(t) - D\dot{x}(t-\tau_1) = \sum_{i\in I^r} h_i(x_t)\left\{A_i x(t) + (A_{i\tau_1} + BK)\, x(t-\tau_1)\right\}, \qquad (5.29)$$

with a guaranteed decay rate $\alpha$.

By replacing the matrix $A_{i\tau_1}$ by the matrix $A_{i\tau_1} + BK$ in Theorem 5 we obtain that the solution $x(t) = 0$ of the system (5.29) is $\alpha$-stable if there exist matrices $0 < P_1 = P_1^T$, $P_2$, $P_3$, $Q = Q^T$, $R = R^T$ such that for all $i \in I^r$ the following BMI is satisfied

$$\begin{pmatrix} \Psi_i & P^T \begin{pmatrix} 0 \\ \mathrm{e}^{\alpha\tau_1}\chi \end{pmatrix} & P^T \begin{pmatrix} 0 \\ \mathrm{e}^{\alpha\tau_1} D \end{pmatrix} \\ * & -R/\tau_1 & 0 \\ * & * & -Q \end{pmatrix} < 0, \qquad (5.30)$$

where

$$\begin{aligned} P &: = \begin{pmatrix} P_1 & 0 \\ P_2 & P_3 \end{pmatrix}, \quad P_1 = P_1^T > 0, \\ \Psi_i &: = P^T \begin{pmatrix} 0 & I_n \\ \Lambda_i & -I_n \end{pmatrix} + \begin{pmatrix} 0 & I_n \\ \Lambda_i & -I_n \end{pmatrix}^T P + \begin{pmatrix} 0 & 0 \\ 0 & \tau_1 R + Q \end{pmatrix}, \\ \Lambda_i &: = A_i + \alpha I_n + \mathrm{e}^{\alpha\tau_1}\left(A_{i\tau_1} + BK - \alpha D\right), \\ \chi &: = \left(A_{i\tau_1} + BK - \alpha D\right). \end{aligned}$$

A well known synthesis gain technique which overcome the *bilinearity* of the conditions was introduced by [110]. It consists in to set

$$P_3 = \varepsilon P_2, \quad \varepsilon \in \mathcal{R},$$

where $P_2$ is a nonsingular matrix, and

$$\bar{P} = P_2^{-1}.$$

Define $\bar{P}_1 = \bar{P}^T P_1 \bar{P}$, $\bar{R} = \bar{P}^T R \bar{P}$, and $Y = K\bar{P}$. Multiplying the right side of (5.30) by $\Delta_3 = diag\left\{\bar{P}, \bar{P}, \bar{P}\right\}$ and the left side by $\Delta_3^T$ , we obtain the LMI stabilization condition stated in the following theorem.

**Theorem 6** *The system (5.29) is $\alpha$-stabilizable if there exist a real number $\varepsilon > 0$ and $n \times n$ matrices $\bar{P}_1 > 0$, $\bar{P}$, $\bar{Q} = \bar{Q}^T$, $\bar{R} = \bar{R}^T$, and $Y$ such that for all $i \in I^r$ the following LMI is satisfied*

$$\begin{pmatrix} \Phi_i & \begin{pmatrix} e^{\alpha\tau_1}\vartheta \\ \varepsilon e^{\alpha\tau_1}\vartheta \end{pmatrix} & \begin{pmatrix} e^{\alpha\tau_1} D\bar{P} \\ \varepsilon e^{\alpha\tau_1} D\bar{P} \end{pmatrix} \\ * & -\bar{R}/\tau_1 & 0 \\ * & * & -\bar{Q} \end{pmatrix} < 0,$$

*where*

$$\begin{aligned}\vartheta &: = (A_{i\tau_1} - \alpha D)\,\bar{P} + BY,\\ \Phi_i &= \begin{pmatrix} \Phi_{11} & \Phi_{12} \\ * & \Phi_{22} \end{pmatrix},\end{aligned}$$

$$\begin{aligned}\Phi_{11} &= (A_i + \alpha I_n + e^{\alpha\tau_1}(A_{i\tau_1} - \alpha D))\,\bar{P}\\ &\quad + \bar{P}^T(A_i + \alpha I_n + e^{\alpha\tau_1}(A_{i\tau_1} - \alpha D))^T + BY + Y^T B^T,\\ \Phi_{12} &= \bar{P}_1^T - \bar{P} + \varepsilon\bar{P}^T(A_i + \alpha I_n + e^{\alpha\tau_1}(A_{i\tau_1} - \alpha D))^T + \varepsilon Y^T B^T,\\ \Phi_{22} &= -\varepsilon\left(\bar{P} + \bar{P}^T\right) + \tau_1\bar{R} + \bar{Q}.\end{aligned}$$

*Moreover, the feedback gain is given by*

$$K = Y\bar{P}^{-1}.$$

In order to apply the above result to the drilling system, we obtain a polytopic representation of the nonlinear model (3.7). The following nonlinear expression to describe the drilling behavior at the ground level is obtained by considering $\mu_{\mathrm{cb}} = 0$,

$$\begin{aligned}\dot{x}_1(t) + d\dot{x}_1(t-2\Gamma) &= a_0x_1(t) + a_1x_1(t-2\Gamma) + bu(t-\Gamma)\\ &\quad - c_2\mathrm{e}^{-\frac{\gamma_{\mathrm{b}}}{v_{\mathrm{f}}}(x_1(t)+\Omega_0)}\mathrm{sign}\,(x_1(t)+\Omega_0)\\ &\quad + c_2\Upsilon\mathrm{e}^{-\frac{\gamma_{\mathrm{b}}}{v_{\mathrm{f}}}(x_1(t-2\Gamma)+\Omega_0)}\mathrm{sign}\,(x_1(t-2\Gamma)+\Omega_0),\end{aligned} \tag{5.31}$$

where $a_0 = -\Psi - \frac{c_{\mathrm{b}}}{I_{\mathrm{B}}}$, $a_1 = \frac{\Upsilon c_{\mathrm{b}}}{I_{\mathrm{B}}} - \Upsilon\Psi$, $d = -\Upsilon$, $b = \Pi$ and $c_2 = \frac{W_{\mathrm{ob}}R_{\mathrm{b}}\mu_{\mathrm{sb}}}{I_{\mathrm{B}}}$.

We choose the following change of variables:

$$\begin{cases}\varkappa_1(t) = x_1(t),\\ \varkappa_2(t) = \mathrm{e}^{-\frac{\gamma_{\mathrm{b}}}{v_{\mathrm{f}}}\varkappa_1(t)+\Omega_0},\end{cases}$$

therefore,

$$\begin{cases}\dot{\varkappa}_1(t) = \dot{x}_1(t),\\ \dot{\varkappa}_2(t) = -\frac{\gamma_{\mathrm{b}}}{v_{\mathrm{f}}}\dot{\varkappa}_1(t)\mathrm{e}^{-\frac{\gamma_{\mathrm{b}}}{v_{\mathrm{f}}}\varkappa_1(t)+\Omega_0} = -\frac{\gamma_{\mathrm{b}}}{v_{\mathrm{f}}}\dot{\varkappa}_1(t)\varkappa_2(t).\end{cases}$$

System (5.31) can be written as

$$\dot{x}(t) - D\dot{x}(t-2\Gamma) = A(x)x(t) + A_{2\Gamma}(x)x(t-2\Gamma) + B_\Gamma u(t-\Gamma), \tag{5.32}$$

where the control input $u(t)$ corresponds to the angular velocity provided by the rotary table and

$$x(t) = [\varkappa_1(t) \quad \varkappa_2(t)]^T$$

$$
\begin{aligned}
D &= \begin{pmatrix} \Upsilon & 0 \\ 0 & 0 \end{pmatrix}, \quad B_\Gamma = \begin{pmatrix} \Pi \\ 0 \end{pmatrix}, \\
A_{2\Gamma}(x) &= \begin{pmatrix} \Upsilon\left(\frac{c_\mathrm{b}}{I_\mathrm{B}} - \Psi\right) & c_2\Upsilon\mathrm{sign}(\varkappa_1(t-2\Gamma)+\Omega_0) \\ 0 & 0 \end{pmatrix}, \\
A(x) &= \begin{pmatrix} -\left(\Psi + \frac{c_\mathrm{b}}{I_\mathrm{B}}\right) & -c_2\mathrm{sign}\left(\varkappa_1(t)+\Omega_0\right) \\ 0 & -\frac{\gamma_\mathrm{b}}{v_\mathrm{f}}\dot{\varkappa}_1(t) \end{pmatrix}.
\end{aligned}
$$

Notice that the entries of the matrices $D$, $B_\Gamma$ are constant, and the entry $c_2\Upsilon\mathrm{sign}(\varkappa_1(t-2\Gamma)+\Omega_0)$ of the matrix $A_{2\Gamma}(x)$ is bounded. If we consider that $\dot{\varkappa}_1(t)$ is a bounded variable then, so is the matrix $A(x)$.

In this case, we can obtain a polytopic representation of the matrices $A(x)$, $A_{2\Gamma}(x)$ as:

$$
A(x)x(t) + A_{2\Gamma}(x)x(t-2\Gamma) = \sum_{i\in I^r} h_i(x_t)\left(A_i x(t) + A_{i2\Gamma}x(t-2\Gamma)\right), \quad (5.33)
$$

where $A_i$, $A_{i2\Gamma}$ have only constant coefficients [108]. The functions $h_i(x_t)$, $i \in I^r$ are scalar not necessarily known weighting functions satisfying the convexity property (5.21).

Clearly, the non-linear drilling system (5.31) can be written in the polytopic form (5.20) .

### 5.3.2. Numerical results

Using parameters given in (3.11), the matrices $A(x)$, $A_{2\Gamma}(x)$, $B_\Gamma$ and $D$ of the oilwell drilling model (5.32) take the following values:

$$
\begin{aligned}
D &= \begin{pmatrix} 0.7396 & 0 \\ 0 & 0 \end{pmatrix}, \; B_\Gamma = \begin{pmatrix} 5.8523 \\ 0 \end{pmatrix}, \\
A(x) &= \begin{pmatrix} -3.3645 & -136.1327\mathrm{sign}(\varkappa_1(t)+\Omega_0) \\ 0 & -0.9\dot{\varkappa}_1(t) \end{pmatrix}, \\
A_{2\Gamma}(x) &= \begin{pmatrix} -2.4878 & 100.6802\mathrm{sign}(\varkappa_1(t-2\Gamma)+\Omega_0) \\ 0 & 0 \end{pmatrix}.
\end{aligned}
$$

In order to obtain a polytopic representation of the system, $A(x)$ and $A_{2\Gamma}(x)$ must be bounded functions.

There are three independent functions involved: $\dot{\varkappa}_1(t)$, $\mathrm{sign}(\varkappa_1(t)+\Omega_0)$ and $\mathrm{sign}(\varkappa_1(t-2\Gamma)+\Omega_0)$.

According to (3.6), the variable $\dot{\varkappa}_1(t) = \dot{x}_1(t)$ represents the angular acceleration at the bottom end of the drillstring $\dot{z}(t)$, this is clearly a

bounded variable in real applications. The variables $\text{sign}(\varkappa_1(t)+\Omega_0)$ and $\text{sign}(\varkappa_1(t-2\Gamma)+\Omega_0)$ take only the values 1 and 0.

Under the assumption that $A(x)$ and $A_{2\Gamma}(x)$ are bounded, we can obtain a polytopic representation in the form (5.33), where $i \in I^r = 2^3 = 8$. For $A(x)$ we have

$$A_i(x) = \begin{pmatrix} -3.3645 & a_{23}^i(x) \\ 0 & a_{33}^i(x) \end{pmatrix},$$

with

$$\begin{aligned} -136.1327 &= a_{23}^1 \leq a_{23}^i(x) \leq a_{23}^2 = 0, \\ -0.9Acc_{\max} &= a_{33}^1 \leq a_{33}^i(x) \leq a_{33}^2 = -0.9Dec_{\max}, \end{aligned}$$

where $Acc_{\max}$ and $Dec_{\max}$ stand for the maximum acceleration and deceleration respectively. For $A_{2\Gamma}(x)$ we have

$$A_{i2\Gamma}(x) = \begin{pmatrix} -2.4878 & a_{2\Gamma 23}^i(x) \\ 0 & 0 \end{pmatrix},$$

with

$$0 = a_{2\Gamma 23}^1(x) \leq a_{2\Gamma 23}^i(x) \leq a_{2\Gamma 23}^2(x) = 100.6802.$$

Applying the result of Theorem 6 to the polytopic representation of the drilling system in closed loop with the control law

$$u(t) = Kx(t-\Gamma), \tag{5.34}$$

we obtain the feasible result:

$$K = Y\bar{P}^{-1} = \begin{pmatrix} 0.44 & -4.25 \end{pmatrix}.$$

Then, the stabilizing control law for the drilling system (5.31) is given by

$$u(t) = 0.44x_1(t-\Gamma) - 4.25\text{e}^{-\frac{\gamma_\text{b}}{v_\text{f}}x_1(t-\Gamma)+\Omega_0},$$

which according to (3.6), in terms of the bit speed, can be written as:

$$u(t) = 0.44z(t-\Gamma) - 4.25\text{e}^{-\frac{\gamma_\text{b}}{v_\text{f}}z(t-\Gamma)} - 0.44\Omega_0. \tag{5.35}$$

The simulation result of Figure 5.3 show an effective elimination of the stick-slip phenomenon by means of the application of the controller (5.35).

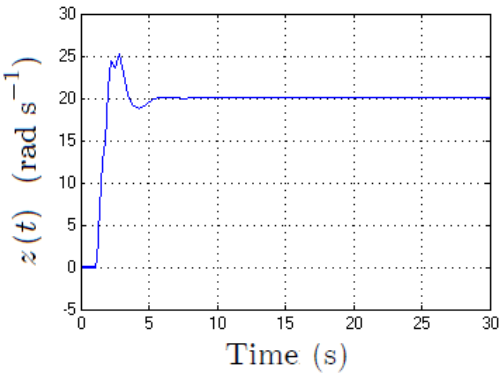


Figure 5.3: Angular velocity trajectory $z(t)$ of the drilling system (5.31) in closed loop with the control law (5.35) with $\Omega_0 = 20$rad s$^{-1}$.

## 5.4. Control of coupled vibrations: practical stability approach

In the real world, systems usually exhibit nonlinear characteristics and uncertainties for which the theoretical definitions of asymptotic or exponential stability can be too restrictive. Clearly, the state of a system may be mathematically unstable, but the response oscillates close enough to the equilibrium, to be considered as acceptable. In this situation, the notion of Lyapunov asymptotic or exponential stability is not appropriate. More suitable performance specifications, from an engineering point of view, are given by the he definition of practical stability, also refereed to as ultimate boundedness with a fixed bound [50]. These definition characterize the system transient behavior with estimates of the bounds on the system trajectories [4].

It is worthy of mention that the concept of practical stability is also referred to as dissipativeness in the sense of Levinson. This qualitative property is important in the theory of differential equations, especially in the study of self-sustained and forced nonlinear oscillations [96]. This notion, introduced in [71], was used in [8] to develop a basic theory of dissipative periodic processes on Banach spaces applied to retarded functional differential equations.

The dissipativeness definition is stated in [71] as follows:

**Définition 3** *The system*

$$\dot{x}(t) = f(t, x) \tag{5.36}$$

*is called dissipative if there exists some* $R > 0$ *such that*

$$\overline{\lim}_{t\to\infty} |x(t; t_0, x_0)| < R$$

*for any solution* $x(t; t_0, x_0)$ *of (5.36).*

This qualitative property, called also ultimate boundedness means that all systems trajectories will eventually enter into a ball of radius $R$ and will remain there. Various boundedness properties have been considered by Yoshizawa in [120] and their role in establishing existence of self-sustained and forced oscillations has been pointed out there. The basic results on dissipativeness in the sense of Levinson are also due to Yoshizawa [120]. In [96], some useful results on the study of systems dynamics are given; the author analyze three different concepts of dissipativeness: classical (standard) dissipativeness, dissipativeness in the sense of Levinson and dissipativeness in the sense of system theory. Criteria, applications and connections between these concepts are proved.

The following result highlight the fact that the knowledge of a Lyapunov function greatly simplifies the system analysis.

**Theorem 7 (Barbashin and Krasovskii)** *[7] Let* $V(x)$ *be a Lyapunov function defined for* $|x| \geq \rho_1$ *such that:*
*i) is radially unbounded i.e.*

$$\lim_{|x|\to\infty} V(x) = +\infty;$$

*ii) is non-increasing along those solutions such that* $|x(t)| \geq \rho_1$*;*
*iii)* $\dot{V}^*(t) = \frac{d}{dt}V(x(t)) \neq 0$ *for* $|x| \geq \rho$.
*Then system* $\dot{x} = f(x)$ *is dissipative in the sense of Levinson.*

In this section, based on the notion of dissipativeness in the sense of Levinson, we design a feedback controller ensuring the suppression of torsional drilling oscillations.

Using Lyapunov techniques and the descriptor approach introduced in [41], we design a stabilizing controller for a nonlinear neutral-type time-delay system subject to bounded perturbations. The proposed controller ensures the "practical stability" of the closed loop system. The result is applied to the torsional drillstring model to find the synthesis of a feedback controller which ensures the suppression of the stick-slip phenomenon. Due to the intimate coupling between the torsional and axial vibration, the elimination of the stick-slip vibration could give rise to the suppression of the bit bounce [29].

Consider the following time-delay system of neutral-type:

$$\begin{aligned} \dot{x}(t) + D\dot{x}(t-h) &= A_0 x(t) + A_1 x(t-h) + n(t), \\ x(\theta) &= \phi(\theta), \quad \theta \in [-h, 0]\,, \end{aligned} \tag{5.37}$$

where $h \geq 0$ is the time delay, $D \in \mathcal{R}^{n\times n}$ is Schur stable, $A_0$, $A_1 \in \mathcal{R}^{n\times n}$, $n(t)$ satisfies $\|n(t)\| \leq \zeta$, $\zeta > 0$, $t \geq 0$.

**Definition 3** *(Practical stability or ultimate boundedness with a fixed bound) The system is $\varepsilon$-practically stable if for some $\varepsilon > 0$ there exists $0 < T(\varepsilon, \varphi) < \infty$ such that $\|x(t, \varphi)\| \leq \varepsilon$ for all $t \geq T$.*

Following the ideas introduced in [117], we derive the following result:

**Lemma 5** *Consider a time-delay system of the form (5.37). If there exists a functional $V(x_t)$ satisfying:*

$$\alpha_1 \|x(t)\|^2 \leq V(x_t) \leq \alpha_2 \|x_t\|_h^2\,, \quad \forall t \geq 0, \tag{5.38}$$

*and*

$$\frac{\mathrm{d}}{\mathrm{d}t} V(x_t) + \sigma V(x_t) \leq \beta, \quad \forall t \geq 0, \tag{5.39}$$

*where $\alpha_1$, $\alpha_2$, $\sigma$ and $\beta$ are positive constants, then, for any initial condition $\phi$ the following "practical" exponential estimate of the response holds:*

$$\|x(t)\|^2 \leq \mathrm{e}^{-\sigma t} \left( \frac{\alpha_2}{\alpha_1} \|\phi\|_h^2 - \frac{\beta}{\alpha_1 \sigma} \right) + \frac{\beta}{\alpha_1 \sigma}, \tag{5.40}$$

*and the system (5.37) is $\mu$-practically stable with $\mu > \frac{\beta}{\alpha_1 \sigma}$ for all $t \geq T(\mu, \phi)$, where*

$$T(\mu, \phi) = \begin{cases} 0, & \text{if } \|\phi\|_h \leq \sqrt{\frac{\beta}{\alpha_2 \sigma}}; \\ \frac{1}{\sigma} \ln \left( \frac{\alpha_2 \sigma \|\phi\|_h^2 - \beta}{\alpha_1 \sigma \mu - \beta} \right), & \text{elsewhere.} \end{cases} \tag{5.41}$$

**Proof 6** *Premultiplication of (5.39) by $e^{\sigma\theta}$ yields*

$$\frac{d}{d\theta} \left( e^{\sigma\theta} V(x_t) \right) \leq \beta e^{\sigma\theta}.$$

*Integration from 0 to $t$ gives*

$$\int_0^t \frac{d}{d\theta} \left( e^{\sigma\theta} V(x_t) \right) d\theta \leq \int_0^t \beta\, e^{\sigma\theta} d\theta,$$

*equivalently,*

$$e^{\sigma t}V(x_t) - V(0,x_0) \leq \frac{\beta}{\sigma}\left(e^{\sigma t}-1\right),$$

*or*

$$V(x_t) \leq e^{-\sigma t}V(0,x_0) + \frac{\beta}{\sigma}\left(1-e^{-\sigma t}\right).$$

*It follows from (5.38) that*

$$\alpha_1 \|x(t)\|^2 \leq e^{-\sigma t}V(0,x_0) + \frac{\beta}{\sigma}\left(1-e^{-\sigma t}\right) \leq \alpha_2 e^{-\sigma t}\|\phi\|_h^2 + \frac{\beta}{\sigma}\left(1-e^{-\sigma t}\right).$$

*Then, we have*

$$\|x(t)\|^2 \leq \frac{\alpha_2}{\alpha_1}e^{-\sigma t}\|\phi\|_h^2 + \frac{\beta}{\alpha_1\sigma}\left(1-e^{-\sigma t}\right),$$

*equivalently,*

$$\|x(t)\|^2 \leq e^{-\sigma t}\left(\frac{\alpha_2}{\alpha_1}\|\phi\|_h^2 - \frac{\beta}{\alpha_1\sigma}\right) + \frac{\beta}{\alpha_1\sigma}. \tag{5.42}$$

*Observe that for all initial conditions satisfying*

$$\frac{\alpha_2}{\alpha_1}\|\phi\|_h^2 \leq \frac{\beta}{\alpha_1\sigma},$$

*or* $\|\phi\|_h \leq \sqrt{\frac{\beta}{\alpha_2\sigma}}$, *the inequality*

$$\|x(t)\|^2 \leq \frac{\beta}{\alpha_1\sigma} \quad \forall t \geq 0,$$

*is satisfied, i.e.,* $\|x(t)\| \leq \sqrt{\frac{\beta}{\alpha_1\sigma}} \quad \forall t \geq 0.$

*Otherwise, if*

$$\frac{\alpha_2}{\alpha_1}\|\phi\|_h^2 > \frac{\beta}{\alpha_1\sigma}, \tag{5.43}$$

*or* $\|\phi\|_h > \sqrt{\frac{\beta}{\alpha_2\sigma}}$, *it follows that*

$$\|x(t)\|^2 \leq \mu, \quad \forall t \geq T(\mu,\phi),$$

*where*

$$\mu > \frac{\beta}{\alpha_1\sigma}. \tag{5.44}$$

*In view of (5.42), $T(\mu,\phi)$ is obtained from:*

$$0 < e^{-\sigma t}\left(\frac{\alpha_2}{\alpha_1}\left\|\phi\right\|_h^2 - \frac{\beta}{\alpha_1\sigma}\right) \leq \mu - \frac{\beta}{\alpha_1\sigma}.$$

*With the following algebraic steps we get (5.41),*

$$\left(\frac{\alpha_2}{\alpha_1}\left\|\phi\right\|_h^2 - \frac{\beta}{\alpha_1\sigma}\right) \leq e^{\sigma t}\left(\mu - \frac{\beta}{\alpha_1\sigma}\right),$$

$$\left(\frac{\alpha_2\sigma\left\|\phi\right\|_h^2 - \beta}{\alpha_1\sigma}\right) \leq e^{\sigma t}\left(\frac{\alpha_1\sigma\mu - \beta}{\alpha_1\sigma}\right).$$

*Then,*

$$e^{\sigma T} \geq \frac{\alpha_2\sigma\left\|\phi\right\|_h^2 - \beta}{\alpha_1\sigma\mu - \beta},$$

$$\ln\left(e^{\sigma T}\right) \geq \ln\left(\frac{\alpha_2\sigma\left\|\phi\right\|_h^2 - \beta}{\alpha_1\sigma\mu - \beta}\right),$$

$$T \geq \frac{1}{\sigma}\ln\left(\frac{\alpha_2\sigma\left\|\phi\right\|_h^2 - \beta}{\alpha_1\sigma\mu - \beta}\right).$$

*Notice that conditions (5.43) and (5.44) imply that $\alpha_2\sigma\left\|\phi\right\|_h^2 - \beta > 0$, $\alpha_1\sigma\mu - \beta > 0$ and $\alpha_2\sigma\left\|\phi\right\|_h^2 - \beta > \alpha_1\sigma\mu - \beta$, hence $T$ exists.*

### 5.4.1. Practical stabilization conditions

The following result allows the "practical" stabilization of a class of a nonlinear neutral-type system.

**Theorem 8** *Let a neutral-type time-delay system of the form:*

$$\begin{aligned}\dot{x}(t) + D\dot{x}(t-2\tau) &= A_0x(t) + A_1x(t-2\tau) + Bu(t-\tau) + C_0f(x(t)) \\ &\quad + C_1f(x(t-2\tau)) + \omega,\end{aligned} \tag{5.45}$$

*where $\tau$ is a constant time delay, $D \in \mathcal{R}^{n\times n}$ is Schur stable, $A_0$, $A_1 \in \mathcal{R}^{n\times n}$, $B \in \mathcal{R}^{n\times m}$, $f$ satisfies $\left\|f(x(t))\right\| \leq \zeta$, $\zeta > 0$, $t \geq 0$, and $\omega$ is such that:*

$$\left\|\omega\right\|_{K_\omega} = \omega^T K_\omega \omega \leq 1, \qquad t \geq 0. \tag{5.46}$$

*Consider a control law of the form:*

$$u(t-\tau) = K_0\dot{x}(t-2\tau) + K_1 x(t-2\tau). \tag{5.47}$$

*If there exist positive definite matrices* $P$, $S$, $R \in \mathcal{R}^{n\times n}$, *and* $P_2$, $P_3$, $P_4$, $P_8 \in \mathcal{R}^{n\times n}$, $P_5$, $P_6$, $P_7 \in \mathcal{R}^{n\times m}$, $P_9 \in \mathcal{R}^{m\times m}$, $P_{10}$, $P_{11}$, $K_0$, $K_1 \in \mathcal{R}^{m\times n}$, *and* $\beta > 0$ *such that the BMI* $\Phi < 0$ *is feasible for some* $\sigma > 0$, *where*

$$\Phi = \begin{bmatrix} \Phi_{11} & \Phi_{12} & \Phi_{13} & \Phi_{14} & \Phi_{15} & P_2^TC_0 + A_0^TP_6 & P_2^TC_1 + A_0^TP_7 & \Phi_{18} \\ * & \Phi_{22} & A_1^TP_3 & \Phi_{24} & \Phi_{25} & A_1^TP_7 & A_1^TP_8 & A_1^TP_9 \\ * & * & \Phi_{33} & \Phi_{34} & \Phi_{35} & P_3^TC_0 - P_6 & P_3^TC_1 - P_7 & \Phi_{38} \\ * & * & * & \Phi_{44} & \Phi_{45} & P_4^TC_0 - D^TP_6 & P_4^TC_1 - D^TP_7 & \Phi_{48} \\ * & * & * & * & \Phi_{55} & P_5^TC_0 + B_1^TP_6 & P_5^TC_1 + B_1^TP_7 & \Phi_{58} \\ * & * & * & * & * & P_6^TC_0 + C_0^TP_6 & P_6^TC_1 + C_0^TP_7 & \Phi_{68} \\ * & * & * & * & * & * & P_7^TC_1 + C_1^TP_7 & \Phi_{78} \\ * & * & * & * & * & * & * & \Phi_{88} \end{bmatrix}, \tag{5.48}$$

*with*

$$\begin{aligned}
\Phi_{11} &= A_0^TP_2 + P_2^TA_0 + S - \mathrm{e}^{-\sigma 2\tau}R + \sigma P \\
\Phi_{12} &= \mathrm{e}^{-\sigma 2\tau}R + P_2^TA_1 \\
\Phi_{13} &= P - P_2^T + A_0^TP_3 \\
\Phi_{14} &= -P_2^TD + A_0^TP_4 \\
\Phi_{15} &= P_2^TB + A_0^TP_5 \\
\Phi_{18} &= P_2^T + A_0^TP_8 \\
\Phi_{22} &= -\mathrm{e}^{-\sigma 2\tau}(S+R) + P_{11}^TK_1 + K_1^TP_{11} \\
\Phi_{24} &= A_1^TP_4 + K_1^TP_{10} + P_{11}^TK_0 \\
\Phi_{25} &= A_1^TP_5 + K_1^TP_9 - P_{11}^T \\
\Phi_{33} &= 4\tau^2R - P_3 - P_3^T, \\
\Phi_{34} &= -P_3^TD - P_4 \\
\Phi_{35} &= P_3^TB_1 - P_5 \\
\Phi_{38} &= P_3^T - P_8 \\
\Phi_{44} &= -P_4^TD - D^TP_4 + P_{10}^TK_0 + K_0^TP_{10} \\
\Phi_{45} &= P_4^TB - D^TP_5 + K_0^TP_9 - P_{10}^T \\
\Phi_{48} &= P_4^T - D^TP_8 \\
\Phi_{55} &= P_5^TB_1 + B_1^TP_5 - P_9^T - P_9 \\
\Phi_{58} &= P_5^T + B_1^TP_8 \\
\Phi_{68} &= P_6^T + C_0^TP_8 \\
\Phi_{78} &= P_7^T + C_1^TP_8 \\
\Phi_{88} &= P_8^T + P_8 - \beta K_\omega
\end{aligned}$$

*then, for any initial condition* $\phi$, *the system (5.45) in closed loop with the control law (5.47) satisfies the "practical" exponential estimate (5.40) with*

$$\begin{aligned}
\alpha_1 &= \lambda_{\min}(P) \\
\alpha_2 &= \lambda_{\max}(P) + 2\tau\lambda_{\max}(S) + 4\tau^2\lambda_{\max}(R).
\end{aligned} \tag{5.49}$$

*In addition system (5.37) is* $\mu$*-practically stable for all* $t \geq T(\mu,\phi)$, *where* $T(\mu,\phi)$ *is given in (5.41).*

**Proof 7** *Let the functional*

$$\begin{aligned}
V(x_t) &= x^T(t)Px(t) + \int_{t-2\tau}^{t} e^{\sigma(s-t)}x^T(s)Sx(s)\,ds \\
&\quad + 2\tau\int_{-2\tau}^{0}\int_{t+\theta}^{t} e^{\sigma(s-t)}\dot{x}^T(s)R\dot{x}(s)\,ds\,d\theta.
\end{aligned} \tag{5.50}$$

*Notice that condition (5.38) of Lemma 5 is satisfied with $\alpha_1$ and $\alpha_2$defined in (5.49). The time derivative of (5.50) satisfies*

$$\begin{aligned}\frac{dV(x_t)}{dt} + \sigma V(x_t) \leq\ & 2x^T(t)P\dot{x}(t) + \sigma x^T(t)Px(t) \\ & + x^T(t)Sx(t) - e^{-\sigma 2\tau}x^T(t-2\tau)Sx(t-2\tau) \\ & - e^{-\sigma 2\tau}\left(x(t)-x(t-2\tau)\right)^T R\left(x(t)-x(t-2\tau)\right) \\ & + 4\tau^2\dot{x}^T(t)R\dot{x}(t).\end{aligned} \tag{5.51}$$

*Now, following the descriptor approach introduced in [41], we add to the right hand side of the inequality (5.51) two null terms derived from the system dynamic and the controller structure (5.47):*

$$\begin{aligned}0 \ =\ & 2[P_2x(t) + P_3\dot{x}(t) + P_4\dot{x}(t-2\tau) + P_5u(t-\tau) + P_6f(x(t)) \\ & + P_7f(x(t-2\tau)) + P_8\omega]^T[-\dot{x}(t) - D\dot{x}(t-2\tau) + A_0x(t) \\ & + A_1x(t-2\tau) + Bu(t-\tau) + C_0f(x(t)) + C_1f(x(t-2\tau)) + \omega],\end{aligned} \tag{5.52}$$

$$\begin{aligned}0 \ =\ & 2[P_9u(t-\tau) + P_{10}\dot{x}(t-2\tau) + P_{11}x(t-2\tau)]^T[-u(t-\tau) \\ & + K_0\dot{x}(t-2\tau) + K_1x(t-2\tau)],\end{aligned} \tag{5.53}$$

*where $P_2$, $P_3$, $P_4$, $P_8 \in \mathcal{R}^{n\times n}$, $P_5$, $P_6$, $P_7 \in \mathcal{R}^{n\times m}$, $P_9 \in \mathcal{R}^{m\times m}$, $P_{10}$, $P_{11}$, $K_0$, $K_1 \in \mathcal{R}^{m\times n}$. The condition (5.46) implies that $\omega^T K_\omega \omega - 1 \leq 0$, then for any $\beta > 0$, we have that $-\beta(\omega^T K_\omega \omega - 1) \geq 0$. In order to take into account the perturbation restriction we can add to (5.51) the term*

$$-\beta(\omega^T K_\omega \omega - 1). \tag{5.54}$$

*In view of (5.51-5.54), we obtain after symmetrization of cross terms,*

$$\frac{dV(x_t)}{dt} + \sigma V(x_t) - \beta \leq \eta^T \Phi \eta,$$

*where $\Phi$ is given in (5.48) and*

$$\eta = \begin{pmatrix} x(t) & x(t-2\tau) & \dot{x}(t) & \dot{x}(t-2\tau) & u(t-\tau) & f(t) & f(t-2\tau) & \omega \end{pmatrix}^T.$$

*If $\Phi < 0$ the condition (5.39) is satisfied and the result follows from Lemma 5.*

**Remark 2** *The synthesis of he controller (5.47) is directly obtained by solving the BMI $\Phi < 0$ with $\Phi$ given in Theorem 8.*

### 5.4.2. Numerical results

Next, we present simulation results of the torsional-axial coupled model (3.7-3.10). We apply the proposed strategy to find the synthesis of a stabilizing controller ensuring the suppression of the stick-slip oscillations and consequently the reduction of bit bouncing phenomenon.

Given that only the torsional model (3.7) is used to design the stabilizing controller, such methodology is reduced to the scalar case.

The resulting controller is applied to the coupled model to evaluate its performance, through simulations.

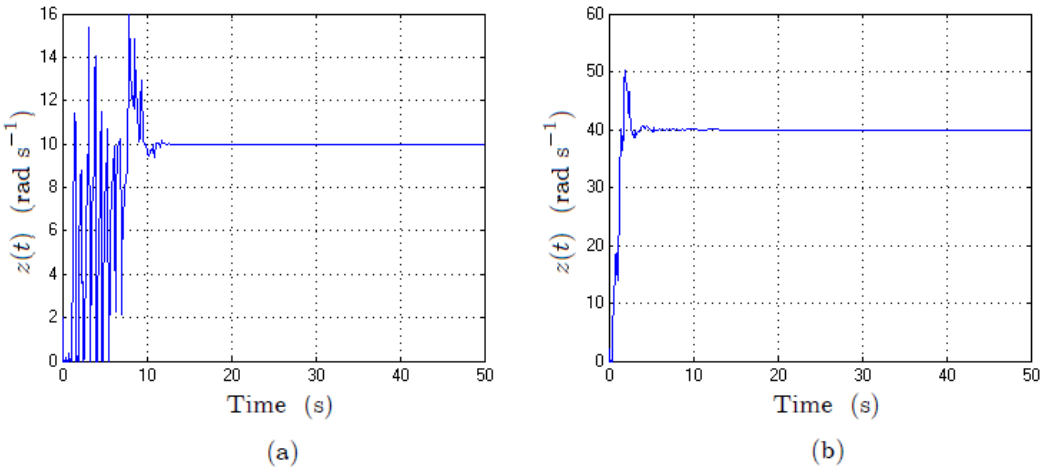


Figure 5.4: Angular velocity at the bottom extremity $z(t)$ of the drilling system in closed loop with the control law (5.56) with: (a) $\Omega_0 = 10\text{rad s}^{-1}$ (reduction of stick-slip), (b) $\Omega_0 = 40\text{rad s}^{-1}$ (elimination of stick-slip).

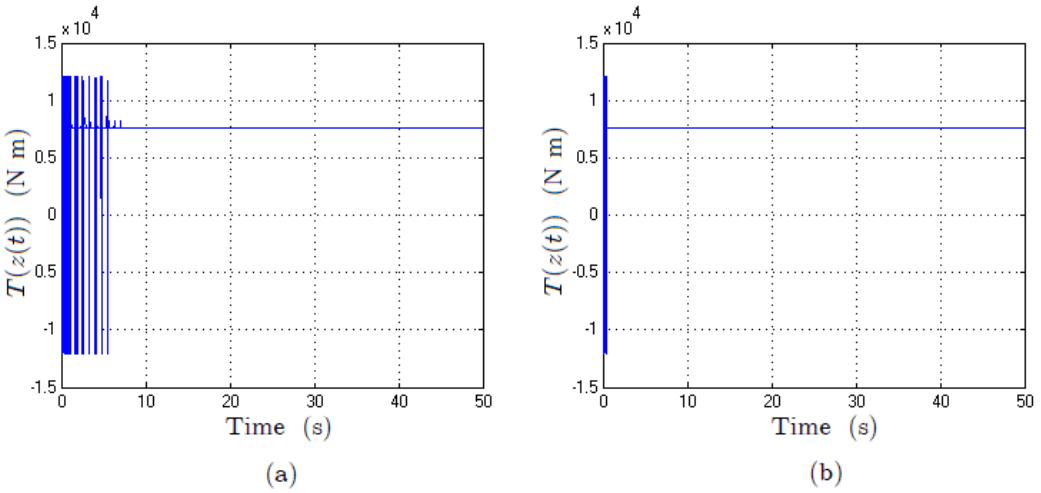


Figure 5.5: Torque on the bit $T(z(t))$ of the drilling system in closed loop with the control law (5.56) with: (a) $\Omega_0 = 10\text{rad s}^{-1}$, (b) $\Omega_0 = 40\text{rad s}^{-1}$.

Notice that the torsional drilling model (3.7) is a scalar representation of the system (5.45) with $x_1 = x$ and $\Gamma = \tau$. Using the model parameters given in (3.11), the constants $a_0$, $a_1$, $b$ and $d$ of the torsional drilling model (3.7) take the following values:

$$\begin{aligned} a_0 &= -3.3645, \quad & a_1 &= -2.4878, \\ d &= -0.7396, \quad & b &= 5.8523, \end{aligned}$$

the time delay is $\tau = 0.3719$, we assume that $\omega^2 \leq 0.8$.

Applying the result stated in Theorem 8, it is possible to obtain the synthesis of the controller (5.47) by means of the solution of the BMI $\Phi < 0$ by means of an appropriate computational tool such as the package "PENBMI" of MATLAB.

Choosing $\sigma = 1.5$ we find a feasible solution of the BMI $\Phi < 0$:

$$\begin{array}{llll} \beta = 1.3627, & K_0 = -0.1264, & P_4 = 4.9788, & P_8 = -97.8304, \\ S = 17.4167, & K_1 = 0.3984, & P_5 = 39.3970, & P_9 = 1.2411 \times 10^5, \\ R = 5.9585, & P_2 = 336.8970, & P_6 = 1.1003, & P_{10} = 1.5684 \times 10^4, \\ P = 7.9283, & P_3 = 100.1450, & P_7 = -0.8138, & P_{11} = -4.9447 \times 10^4. \end{array}$$

The controller that "practically" stabilizes the system (3.7) is given by:

$$u(t) = -0.1264\dot{x}(t-\tau) + 0.3984x(t-\tau). \tag{5.55}$$

Furthermore, the following "practical" exponential estimate is satisfied:

$$\|x(t)\|^2 \leq \mathrm{e}^{-1.5t}\left(3.0497\,\|\phi\|_h^2 - 0.1146\right) + 0.1146.$$

Regarding the change of variable (3.6), the controller (5.55) can be written in terms of the bit speed $z(t)$ as:

$$u(t) = -0.1264\dot{z}(t-\tau) + 0.3984z(t-\tau) - 0.3984\Omega_0. \tag{5.56}$$

Figures 5.4-5.7 show the response of the drilling system in colsed-loop with the control (5.56) involving downhole measurements.

With some initial transient behavior, all vibration amplitudes are reduced to acceptable levels. This result is remarkable considering the fact that only torsional motion is being directly controlled.

Clearly, the choice of the desired rotary table speed influences the system response. The axial vibrations are reduced since their sources of excitation are eliminated or the magnitudes of excitation inputs are lowered.

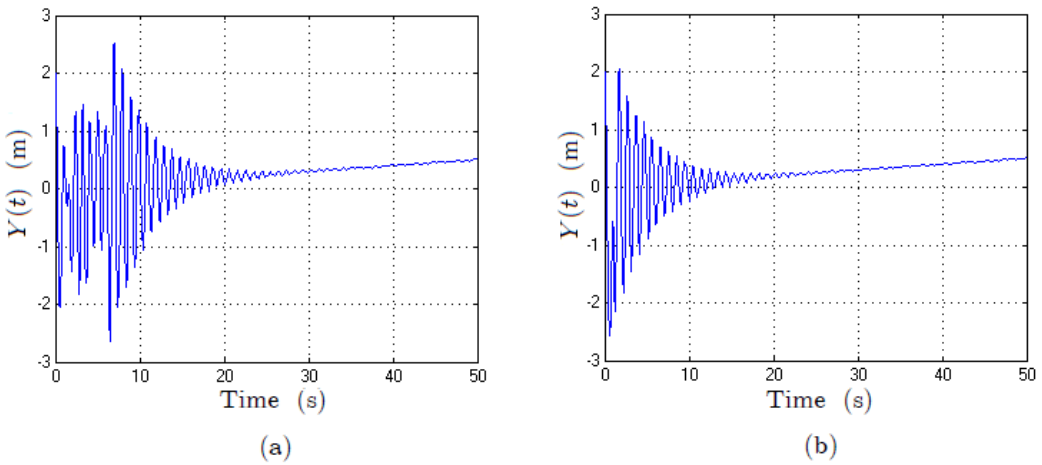


Figure 5.6: Axial displacement $Y(t)$ of the drilling system in closed loop with the control law (5.56) with: (a) $\Omega_0 = 10\text{rad s}^{-1}$, (b) $\Omega_0 = 40\text{rad s}^{-1}$.

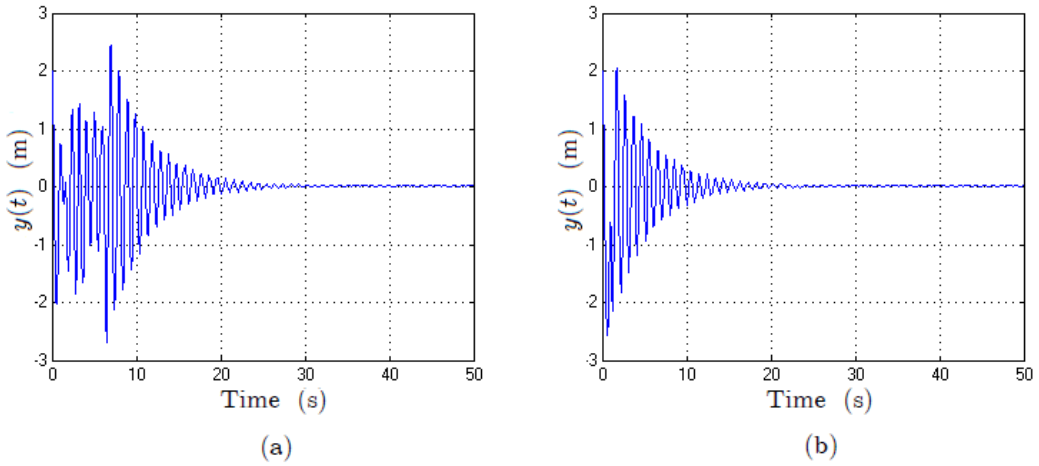


Figure 5.7: Axial displacement $Y(t)$ of the drilling system in closed loop with the control law (5.56) with: (a) $\Omega_0 = 10\text{rad s}^{-1}$, (b) $\Omega_0 = 40\text{rad s}^{-1}$.

The model (3.7-3.10) captures the basic characteristics of coupled drill-string dynamics. It is well known in the drilling industry, that what appears to be a smooth operation, sometimes unexpectedly results in catastrophic failure. This is due to lack of proper understanding of the coupled dynamics, or to changing conditions in the drilling environment.

## 5.5. Stick-slip and bit-bounce elimination: attractive ellipsoid method

Stability results of the previous section allow the elimination of torsional oscillations, which indirectly leads to the bit bounce reduction. Here, based on the aforementioned stability concepts, we design stabilizing controllers acting in both directions in which drilling vibrations appear.

Usually, the mathematical model of any physically motivated system is subject to perturbations due to uncertainties in the system parameters, measurement errors or external disturbances. In [13], [14] and [47] a control strategy allowing the system stability despite model perturbations is introduced; such strategy guarantees that the system trajectories are retained within a given domain (invariant set) and ensures the achievement of some target set. The relation of invariant sets with the Lyapunov theory studied in [20] raises

the possibility of using it for the control design of dynamic systems, robustness analysis, and suppression of disturbances.

In this section we address the problem of control design for the suppression of drilling vibrations via attractive ellipsoid method. Based on a combination of Lyapunov method and the principle of attractive sets, we develop an effective methodology allowing the control synthesis for the drilling system stabilization through the solution of an optimization problem subject to bilinear matrix constraints. The proposed strategy, guaranteeing the suppression of axial-torsional coupled oscillations, allows to determine the minimum attractive ellipsoid for the trajectories of the closed loop system.

**Lemma 6** *[92] Let $V(x_t)$ satisfying*

$$\frac{\mathsf{d}}{\mathsf{d}t}V(x_t) + \sigma V(x_t) \leq \beta, \quad \forall t \geq 0,\ \sigma > 0,\ \beta > 0,$$

*it follows that,*

$$\overline{\lim_{t\to\infty}} V(x_t) \leq \frac{\beta}{\sigma}.$$

*Notice that $V(x_t)$ defines an attractive set.*

**Definition 4** *[66] An ellipsoid centered at the origin is a set in $\mathcal{R}^n$ such that*

$$\mathcal{E}_M = \left\{x \in \mathcal{R}^n : x^T M x \leq 1\right\},$$

*where $M$ is a symmetric positive definite matrix.*

**Definition 5 (Invariant ellipsoid)** *[86] An ellipsoid $\mathcal{E}$ is positive invariant for the system (5.37) if $\phi(\theta) \in \mathcal{E}$, $\theta \in [-h, 0]$ implies that $x(t, \phi) \in \mathcal{E}$, $t \geq 0$ for every trajectory of the system.*

**Definition 6 (Attractive ellipsoid)** *[86] An ellipsoid $\mathcal{E}$ is an attractive domain for the system (5.37) if*
*1) $\phi(\theta) \in \mathcal{E}$, $\theta \in [-h, 0]$ implies that $x(t, \phi) \in \mathcal{E}$, $t \geq 0$,*
*2)$\phi(\theta) \in \mathcal{R}^n \backslash \mathcal{E}$, for some $\theta \in [-h, 0]$ implies that there exists $T_a$, $0 \leq T_a < \infty$, such that $x(t, \phi) \in \mathcal{E}$, $t \geq 0$.*

**Lemma 7** *Let the functional $V(x_t)$ satisfying*

$$x^T(t)Px(t) \leq V(x_t) \leq \alpha \|x_t\|_h^2, \tag{5.57}$$

*where $P$ is a symmetric positive definite matrix and*

$$\frac{\mathsf{d}}{\mathsf{d}t}V(x_t) + \sigma V(x_t) \leq \beta, \quad \forall t \geq 0, \quad \sigma > 0, \quad \beta > 0. \tag{5.58}$$

*Then for any initial function $\phi \in \mathcal{PC}([-h, 0], \mathcal{R}^n)$, the solution $x(t, \phi)$ is retained within the ellipsoid $\mathcal{E}_{\tilde{P}} = \left\{x \in \mathcal{R}^n : x^T \tilde{P} x \leq 1\right\}$, $\tilde{P} = \left(\frac{\sigma}{\beta} + \varsigma\right) P$, $\varsigma > 0$ for $t \geq T_a(\phi, \varsigma) > 0$ where*

$$T_a(\phi, \varsigma) = \frac{1}{\sigma} \ln \left( \frac{\alpha \|\phi\|_h^2}{\varsigma} - \frac{\beta}{\varsigma\sigma} \right).$$

**Proof 8** *Multiplying (5.58) by $e^{\sigma\theta}$ gives*

$$\frac{d}{d\theta}\left(e^{\sigma\theta}V(x_t)\right) \leq \beta e^{\sigma\theta}.$$

*Integrating the above expression from 0 to $t$ yields*

$$V(x_t) \leq e^{-\sigma t}V(0, x_0) + \frac{\beta}{\sigma}\left(1 - e^{-\sigma t}\right).$$

*It follows from (5.57) that*

$$x^T(t)Px(t) \leq e^{-\sigma t}V(0, x_0) + \frac{\beta}{\sigma}\left(1 - e^{-\sigma t}\right) \leq \alpha e^{-\sigma t}\|\phi\|_h^2 + \frac{\beta}{\sigma}\left(1 - e^{-\sigma t}\right).$$

*Then, we have*

$$x^T(t)Px(t) \leq e^{-\sigma t}\left(\alpha \|\phi\|_h^2 - \frac{\beta}{\sigma}\right) + \frac{\beta}{\sigma}. \tag{5.59}$$

*For the initial conditions fulfilling $\alpha \|\phi\|_h^2 \leq \frac{\beta}{\sigma}$, it yields*

$$x^T(t)Px(t) \leq \frac{\beta}{\sigma} \quad \forall t \geq 0,$$

*equivalently $x^T(t)\frac{\sigma}{\beta}Px(t) \leq 1$, for all $t \geq 0$. Otherwise, if*

$$\alpha \|\phi\|_h^2 > \frac{\beta}{\sigma},$$

*we look for the time instant* $T_a(\phi,\varsigma)$ *at which the solution* $x(t,\phi)$ *enters into the ellipsoid* $\mathcal{E}_{\tilde{P}}$. *In view of (5.59),* $T_a(\phi,\varsigma)$ *should guarantee*

$$x^T(t)Px(t) \leq \varsigma + \frac{\beta}{\sigma}$$

*for a small enough* $\varsigma > 0$, *i.e.,*

$$e^{-\sigma T_a}\left(\alpha \left\|\phi\right\|_h^2 - \frac{\beta}{\sigma}\right) = \varsigma.$$

*From the above expression we have*

$$\frac{1}{\varsigma}\left(\alpha \left\|\phi\right\|_h^2 - \frac{\beta}{\sigma}\right) = e^{\sigma T_a}$$

*and the result follows.*

### 5.5.1. Stabilization conditions: minimum attractive ellipsoid

Consider a neutral-type time-delay system of the form:

$$\begin{aligned}\dot{x}(t) + D\dot{x}(t-2\tau) &= A_0x(t) + A_1x(t-2\tau) + B_1u_1(t-\tau) \\ &\quad + B_2u_2(t) + C_0f(x(t)) + C_1f(x(t-2\tau)) + \omega,\end{aligned} \tag{5.60}$$

where $\omega$ satisfies (5.46). In view of the application under consideration, we propose the following structure for $u_1$:

$$u_1(t-\tau) = K_0\dot{x}(t-2\tau) + K_1x(t-2\tau), \tag{5.61}$$

and for $u_2(t)$ we use:

$$u_2(t) = K_2x(t). \tag{5.62}$$

Moreover, we assume that the control law $u_2$ is subject to the restriction:

$$|u_2(t)| \leq \bar{u}_2, \tag{5.63}$$

where $\bar{u}_2$ is the saturation level, i.e., the vector $u_2(t) = \text{col}\ \{u_2^1(t), ..., u_2^m(t)\}$ is subject to the following amplitude constraints:

$$\left|u_2^j(t)\right| \leq \bar{u}_2^j, \quad 0 < \bar{u}_2^j, \quad j = 1, ..., m.$$

Our aim is to find the conditions such that the ellipsoid

$$\mathcal{E}_{\tilde{P}} = \left\{ x \in \mathcal{R}^n : x^T \tilde{P} x \leq 1 \right\},$$

defines an attractive set for the trajectories of the system (5.60) in closed loop with (5.61-5.62), i.e.,

$$\overline{\lim_{t\to\infty}} x^T(t)\tilde{P}x(t) \leq 1.$$

Furthermore, the choice of the matrices $K_0$, $K_1$, $K_2 \in \mathcal{R}^{m\times n}$ and $\tilde{P}$ must guarantee the minimality of the ellipsoid $\mathcal{E}_{\tilde{P}}$. Given that the trace of the matrix $\tilde{P}$ is inversely related to the axes of the ellipsoid $\mathcal{E}_{\tilde{P}}$, the following optimization problem arises:

$$\begin{aligned} &\min \operatorname{tr}(\tilde{P}^{-1}) \\ &\text{subject to } \tilde{P} \in \Sigma_1, \quad K_0, K_1, K_2 \in \Sigma_2, \end{aligned} \tag{5.64}$$

where $\Sigma_1$, $\Sigma_2$, define the set of admissible matrices of dimension $n \times n$ and $m \times n$ respectively guaranteeing the invariance property of the ellipsoid $\mathcal{E}_{\tilde{P}}$.

Consider the functional $V(x_t)$ given in (5.50). Notice that condition (5.38) of Lemma 7 is satisfied with

$$\alpha = \lambda_{\max}(P) + 2\tau\lambda_{\max}(S) + 4\tau^2\lambda_{\max}(R).$$

The time derivative of $V(x_t)$ satisfies (5.51). Following the descriptor approach introduced in [41], we add to the right hand side of the inequality (5.51) the following null terms derived from the system dynamic and the controllers structure (5.61-5.62):

$$\begin{aligned} 0 \;=\; & 2[P_2x(t) + P_3\dot{x}(t) + P_4\dot{x}(t-2\tau) + P_5u_1(t-\tau) \\ & + P_6u_2(t) + P_7f(x(t)) + P_8f(x(t-2\tau)) + P_9\omega]^T \\ & [-\dot{x}(t) - D\dot{x}(t-2\tau) + A_0x(t) + A_1x(t-2\tau) + B_1u_1(t-\tau) \\ & + B_2u_2(t) + C_0f(x(t)) + C_1f(x(t-2\tau)) + \omega], \end{aligned} \tag{5.65}$$

$$\begin{aligned} 0 \;=\; & 2[P_{10}u_1(t-\tau) + P_{11}\dot{x}(t-2\tau) + P_{12}x(t-2\tau)]^T \\ & [-u_1(t-\tau) + K_0\dot{x}(t-2\tau) + K_1x(t-2\tau)], \end{aligned} \tag{5.66}$$

$$0 = 2[P_{13}u_2(t) + P_{14}x(t)]^T [-u_2(t) + K_2x(t)], \tag{5.67}$$

where $P_2$, $P_3$, $P_4$, $P_9 \in \mathcal{R}^{n\times n}$, $P_5$, $P_6$, $P_7$, $P_8 \in \mathcal{R}^{n\times m}$, $P_{10}$, $P_{13} \in \mathcal{R}^{m\times m}$, $P_{11}$, $P_{12}$, $P_{14}$, $K_0$, $K_1$, $K_2 \in \mathcal{R}^{m\times n}$.

In order to take into account the perturbation restriction, we add to (5.51) the term (5.54). Notice that condition (5.58) is fulfilled.

Finally, we obtain after symmetrization of the cross terms:

$$\frac{\mathrm{d}V(x_t)}{\mathrm{d}t} + \sigma V(x_t) - \beta \leq \eta^T \Phi \eta,$$

where

$$\eta = (x(t)\ x(t-2\tau)\ \dot{x}(t)\ \dot{x}(t-2\tau)\ u_1(t-\tau)\ u_2(t)\ f(x(t))\ f(x(t-2\tau))\ \omega)^T,$$

and $\Phi$ is a symmetric matrix with elements $\Phi_{ij}$, $i = 1, .., 9$, $j = 1, ..., 9$ defined as follows:

$$\begin{bmatrix}
\Phi_{11} & \Phi_{12} & \Phi_{13} & \Phi_{14} & \Phi_{15} & \Phi_{16} & \Phi_{17} & P_2^T C_1 + A_0^T P_8 & P_2^T + A_0^T P_9 \\
* & \Phi_{22} & A_1^T P_3 & \Phi_{24} & \Phi_{25} & A_1^T P_6 & A_1^T P_7 & A_1^T P_8 & A_1^T P_9 \\
* & * & \Phi_{33} & \Phi_{34} & \Phi_{35} & \Phi_{36} & \Phi_{37} & P_3^T C_1 - P_8 & P_3^T - P_9 \\
* & * & * & \Phi_{44} & \Phi_{45} & \Phi_{46} & \Phi_{47} & P_4^T C_1 - D^T P_8 & P_4^T - D^T P_9 \\
* & * & * & * & \Phi_{55} & \Phi_{56} & \Phi_{57} & P_5^T C_1 + B_1^T P_8 & P_5^T + B_1^T P_9 \\
* & * & * & * & * & \Phi_{66} & \Phi_{67} & P_6^T C_1 + B_2^T P_8 & P_6^T + B_2^T P_9 \\
* & * & * & * & * & * & \Phi_{77} & P_7^T C_1 + C_0^T P_8 & P_7^T + C_0^T P_9 \\
* & * & * & * & * & * & * & P_8^T C_1 + C_1^T P_8 & P_8^T + C_1^T P_9 \\
* & * & * & * & * & * & * & * & \Phi_{99}
\end{bmatrix},$$

where:

$$\begin{aligned}
\Phi_{11} &= A_0^T P_2 + P_2^T A_0 \\
&\quad + S + \sigma P - \mathrm{e}^{-\sigma 2\tau} R \\
&\quad + P_{14} K_2 + K_2^T P_{14} \\
\Phi_{12} &= \mathrm{e}^{-\sigma 2\tau} R + P_2^T A_1 \\
\Phi_{13} &= P - P_2^T + A_0^T P_3 \\
\Phi_{14} &= -P_2^T D + A_0^T P_4 \\
\Phi_{15} &= P_2^T B_1 + A_0^T P_5 \\
\Phi_{16} &= P_2^T B_2 + A_0^T P_6 \\
&\quad + K_2^T P_{13} - P_{14}^T \\
\Phi_{17} &= P_2^T C_0 + A_0^T P_7 \\
\Phi_{22} &= -\mathrm{e}^{-\sigma 2\tau}(S + R) \\
&\quad + P_{12}^T K_1 + K_1^T P_{12} \\
\Phi_{23} &= A_1^T P_3 \\
\Phi_{24} &= A_1^T P_4 + K_1^T P_{11} \\
&\quad + P_{12}^T K_0 \\
\Phi_{25} &= A_1^T P_5 + K_1^T P_{10} \\
&\quad - P_{12}^T \\
\Phi_{33} &= 4\tau^2 R - P_3 - P_3^T \\
\Phi_{34} &= -P_3^T D - P_4 \\
\Phi_{35} &= P_3^T B_1 - P_5 \\
\Phi_{36} &= P_3^T B_2 - P_6 \\
\Phi_{37} &= P_3^T C_0 - P_7 \\
\Phi_{44} &= -P_4^T D - D^T P_4 \\
&\quad + P_{11}^T K_0 + K_0^T P_{11} \\
\Phi_{45} &= P_4^T B - D^T P_5 \\
&\quad + K_0^T P_{10} - P_{11}^T \\
\Phi_{46} &= P_4^T B_2 - D^T P_6 \\
\Phi_{47} &= P_4^T C_0 - D^T P_7 \\
\Phi_{55} &= P_5^T B_1 + B_1^T P_5 \\
&\quad - P_{10}^T - P_{10} \\
\Phi_{56} &= P_5^T B_2 + B_1^T P_6 \\
\Phi_{57} &= P_5^T C_0 + B_1^T P_7 \\
\Phi_{66} &= P_6^T B_2 + B_2^T P_6 \\
&\quad - P_{13}^T - P_{13} \\
\Phi_{67} &= P_6^T C_0 + B_2^T P_7 \\
\Phi_{77} &= P_7^T C_0 + C_0^T P_7 \\
\Phi_{99} &= P_9^T + P_9 - \beta K_\omega
\end{aligned}$$

Clearly, if $\Phi < 0$, the condition (5.58) of Lemma 7 is satisfied.

The introduction of the additional inequality:

$$\mathcal{H} := \begin{bmatrix} H & I_n \\ I_n & P \end{bmatrix} > 0, \; H \geq P^{-1}$$

allows us to reduce the nonlinear optimization problem (5.64) to the linear problem min $\text{tr}(H)$. By Schur complements, the trace minimization of $H$ implies the the trace minimization of $P^{-1}$ [48].

To address the presence of physical constraints on the control inputs, for example, limits in force, torque, current, flow rate, etc., we combine the ideas introduced in [38] and [42] with the attractive ellipsoid properties as follows. From (5.62-5.63) we get the inequality $k_2^j x \leq \bar{u}_2^j$, $j = 1, ..., m$, then for all $x \in \mathcal{E}_{\tilde{P}}$, $\mathcal{E}_{\tilde{P}} = \left\{ x \in \mathcal{R}^n : x^T \left( \frac{\sigma}{\beta} + \varsigma \right) Px \leq 1 \right\}$ we have that:

$$2\left|k_2^j x\right| \leq \bar{u}_2^j \left[ 1 + \left( \frac{\sigma}{\beta} + \varsigma \right) x^T P x \right] \leq 2\bar{u}_2^j \quad j = 1, ..., m \tag{5.68}$$

we can write (5.68) as

$$\begin{pmatrix} 1 & \pm x^T \end{pmatrix} \begin{pmatrix} \bar{u}_2^j & k_2^j \\ * & \left( \frac{\sigma}{\beta} + \varsigma \right) \bar{u}_2^j P \end{pmatrix} \begin{pmatrix} 1 \\ \pm x \end{pmatrix} \geq 0, \quad j = 1, ..., m,$$

by Schur complements, the latter inequalities are equivalent to the following ones:

$$\left( \frac{\sigma}{\beta} + \varsigma \right) \bar{u}_2^j P - k_2^{jT} (\bar{u}_2^j)^{-1} k_2^j \geq 0,$$

$$\mathcal{I}_j := \begin{pmatrix} \left( \frac{\sigma}{\beta} + \varsigma \right) \bar{u}_2^j P & k_2^{jT} \\ * & \bar{u}_2^j \end{pmatrix} \geq 0 \quad j = 1, ..., m,$$

where $k_2^j$ is the $j$-th row of the matrix $K_2$.

Summarizing the above ideas, the result on the minimum attractive ellipsoid for system (5.60) is stated as follows:

**Theorem 9** *Let the optimization problem*

$$\min \; tr(H)$$

*subject to*

$$\begin{cases} \Lambda := \{H, P, S, R, K_0, K_1, K_2, P_k, \beta\}, \quad k = 1, ..., 14, \\ \Phi < 0, \\ \mathcal{H} > 0, \\ \mathcal{I}_j \geq 0 \quad j = 1, ..., m, \\ P > 0, \; S > 0, \; R > 0, \; \beta > 0, \; \sigma > 0, \; \varsigma > 0, \end{cases}$$

*with optimal solution* $\hat{\Lambda} := \left\{\hat{H}, \hat{P}, \hat{S}, \hat{R}, \hat{K}_0, \hat{K}_1, \hat{K}_2, \hat{P}_k, \hat{\beta}\right\}$, $k = 1, ..., 14$. *The ellipsoid* $\mathcal{E}(0, \tilde{P})$ *determined by the matrix* $\left(\frac{\sigma}{\hat{\beta}} + \varsigma\right)\hat{P}$, *is a minimum attractive ellipsoid for system (5.60) in closed loop with the controllers (5.61-5.63) for* $t \geq T_a(\phi, \varsigma) = \frac{1}{\sigma}\ln\left(\frac{\alpha\|\phi\|_h^2}{\varsigma} - \frac{\beta}{\varsigma\sigma}\right)$.

Dynamic systems are usually subject to uncertain time-varying delays. In [43] an overview on this topic is given. Here we consider the stability of a neutral-type time delay system of the form:

$$\dot{x}(t) + D\dot{x}(t - g(t)) = A_0x(t) + A_1x(t - \tau(t)), \tag{5.69}$$

where $g(t)$ and $\tau(t)$ are uncertain time-varying delays such that

$$\tau(t) = h + \eta(t), \tag{5.70}$$

where $h > 0$ is a nominal constant value and $\eta$ is a time-varying perturbation. Following [58], system (5.69) is represented as:

$$\dot{x}(t) + D\dot{x}(t - g(t)) = A_0x(t) + A_1x(t - h) + A_1\left[x(t - h - \eta(t)) - x(t - h)\right],$$

which is equivalent to

$$\dot{x}(t) + D\dot{x}(t - g(t)) = A_0x(t) + A_1x(t - h) - A_1\int_{t-h-\eta(t)}^{t-h}\dot{x}(s)ds. \tag{5.71}$$

In [43], two delay perturbation cases are considered:

- *Case 1.-* $\eta(t)$ is a sign-varying piecewise-continuous function satisfying $|\eta(t)| \leq \mu < h$ with known upper-bounds $\mu$, i.e.,

$$\tau(t) \in [h - \mu,\ h + \mu].$$

- *Case 2.-* $\eta(t)$ is a non-negative piecewise-continuous function such that $\eta(t) \leq \mu$, and thus,

$$\tau(t) \in [h,\ h + \mu].$$

The main idea for the stability analysis of (5.71) is to consider a Lyapunov function of the form: $V = V_n + V_a$, where $V_n$ is a nominal Lyapunov function from which the stability conditions of the nominal system ($\eta = 0$) are derived, and $V_a$ consists of an additional term depending on $\mu$.

Following these ideas, it is possible to determine additional conditions under which $\mathcal{E}(0,\tilde{P})$ is the minimum attractive ellipsoid for system (5.60-5.63) subject to uncertain time varying state delay of the form (5.70). In this case we might choose $V_n$ as in (5.50) with $2\tau = h$. For $V_a$ we would consider

$$V_a = (h+\mu)\int_{-\mu}^{\mu}\int_{t+\theta-h}^{t} \mathrm{e}^{\sigma(s-t)}\dot{x}^T(s)R_a\dot{x}(s)\mathrm{d}s\mathrm{d}\theta, \quad R_a > 0,$$

for the Case 1; for the Case 2:

$$V_a = (h+\mu)\int_{-\mu}^{0}\int_{t+\theta-h}^{t} \mathrm{e}^{\sigma(s-t)}\dot{x}^T(s)R_a\dot{x}(s)\mathrm{d}s\mathrm{d}\theta, \quad R_a > 0.$$

Note that for $\mu \to 0$ we have $V_a \to 0$ and thus $V \to V_n$. The latter will guarantee that if the conditions for the stability of the nominal system are feasible, then the stability conditions for the perturbed system will be feasible for small enough $\mu$. The additional stability conditions will be derived according to the choice of $V_a$ and to the system representation similar to (5.71).

## 5.5.2. Numerical results

In view of the models (3.7) and (3.10), the torsional-axial coupled dynamics of the drillstring can be described by the following equation:

$$\begin{aligned}\dot{x}(t) + D\dot{x}(t-2\Gamma) = {} & A_0x(t) + A_1x(t-2\Gamma) + B_1u_1(t-\Gamma) + B_2u_2(t) \\ & + C_0f(x_1(t)+\Omega_0) + C_1f(x_1(t-2\Gamma)+\Omega_0) + \omega, \end{aligned} \tag{5.72}$$

where $x(t) = \begin{bmatrix} x_1(t) & x_2(t) & x_3(t) \end{bmatrix}^T$,

$$x_1(t) = z(t) - \Omega_0, \qquad x_2(t) = y(t) = Y(t) - \mathrm{ROP}t, \qquad x_3(t) = \dot{y}(t),$$

$$A_0 = \begin{bmatrix} -\Psi - \frac{c_\mathrm{b}}{I_\mathrm{B}} & 0 & 0 \\ 0 & 0 & 1 \\ -\frac{\mu_1 c_\mathrm{b}}{m_0} & -\frac{k_0}{m_0} & -\frac{c_0}{m_0} \end{bmatrix}, \; A_1 = \begin{bmatrix} \frac{\Upsilon c_\mathrm{b}}{I_\mathrm{B}} - \Upsilon\Psi & 0 & 0 \\ 0 & 0 & 0 \\ \frac{\mu_1 c_\mathrm{b}}{m_0} & 0 & 0 \end{bmatrix}, \; B_1 = \begin{bmatrix} \Pi \\ 0 \\ 0 \end{bmatrix}$$

$$B_2 = \begin{bmatrix} 0 \\ 0 \\ -\frac{c_0}{m_0} \end{bmatrix}, \; C_0 = \begin{bmatrix} -\frac{1}{I_\mathrm{B}} \\ 0 \\ -\frac{\mu_1}{m_0} \end{bmatrix}, \; C_1 = \begin{bmatrix} \frac{\Upsilon}{I_\mathrm{B}} \\ 0 \\ 0 \end{bmatrix}, \; D = \begin{bmatrix} -\Upsilon & 0 & 0 \\ 0 & 0 & 0 \\ 0 & 0 & 0 \end{bmatrix},$$

the time delay is given by $\Gamma = \sqrt{\frac{I}{GJ}}L$, the control inputs $u_1$ and $u_2$ corresponds to the angular velocity at the surface $\Omega(t)$ and the ROP respectively, $f(\cdot)$ corresponds to the nonlinear term $T_\mathrm{nl}$ defined in (3.5).

The parameters used in the following simulations are given in (3.11). The trajectories of the open loop drilling model are shown in Figure 5.8.

We assume that due to the physical constraints of the drilling system, the control input $u_2(t)$ (corresponding to the ROP) is subject to the restriction $|u_2(t)| \leq \bar{u}_2$ where $\bar{u}_2 = 100$. We consider that the initial condition $\phi$ is such that $\|\phi\|_h = 2$. Using Theorem 9 we obtain the synthesis of the controllers (5.61-5.62) by means of an appropriate computational tool such as the package "PENBMI" of MATLAB.

The maximum exponential decay rate for which the conditions given in Theorem 9 are satisfied is $\sigma = 1.5$. The solution of the optimization problem is:

$$P = \begin{bmatrix} 6.1522 & 2.5914 & 0.2713 \\ 2.5914 & 13.0989 & 3.4865 \\ 0.2713 & 3.4865 & 1.4203 \end{bmatrix}, \quad \text{eig}(P) = \begin{Bmatrix} 0.4238 \\ 5.4240 \\ 14.8236 \end{Bmatrix},$$

$$\lambda_{\max}(S) = 318.9226, \ \lambda_{\max}(R) = 3.9407, \ \beta = 1.3620, \ \alpha = 254.1923,$$

$$K_0 = \begin{bmatrix} -0.1272 & 0 & 0 \end{bmatrix}, \quad K_1 = \begin{bmatrix} 0.4429 & 0.0196 & 0.0088 \end{bmatrix}, \quad (5.73)$$

$$K_2 = \begin{bmatrix} 24.3378 & 305.7411 & 120.3589 \end{bmatrix}.$$

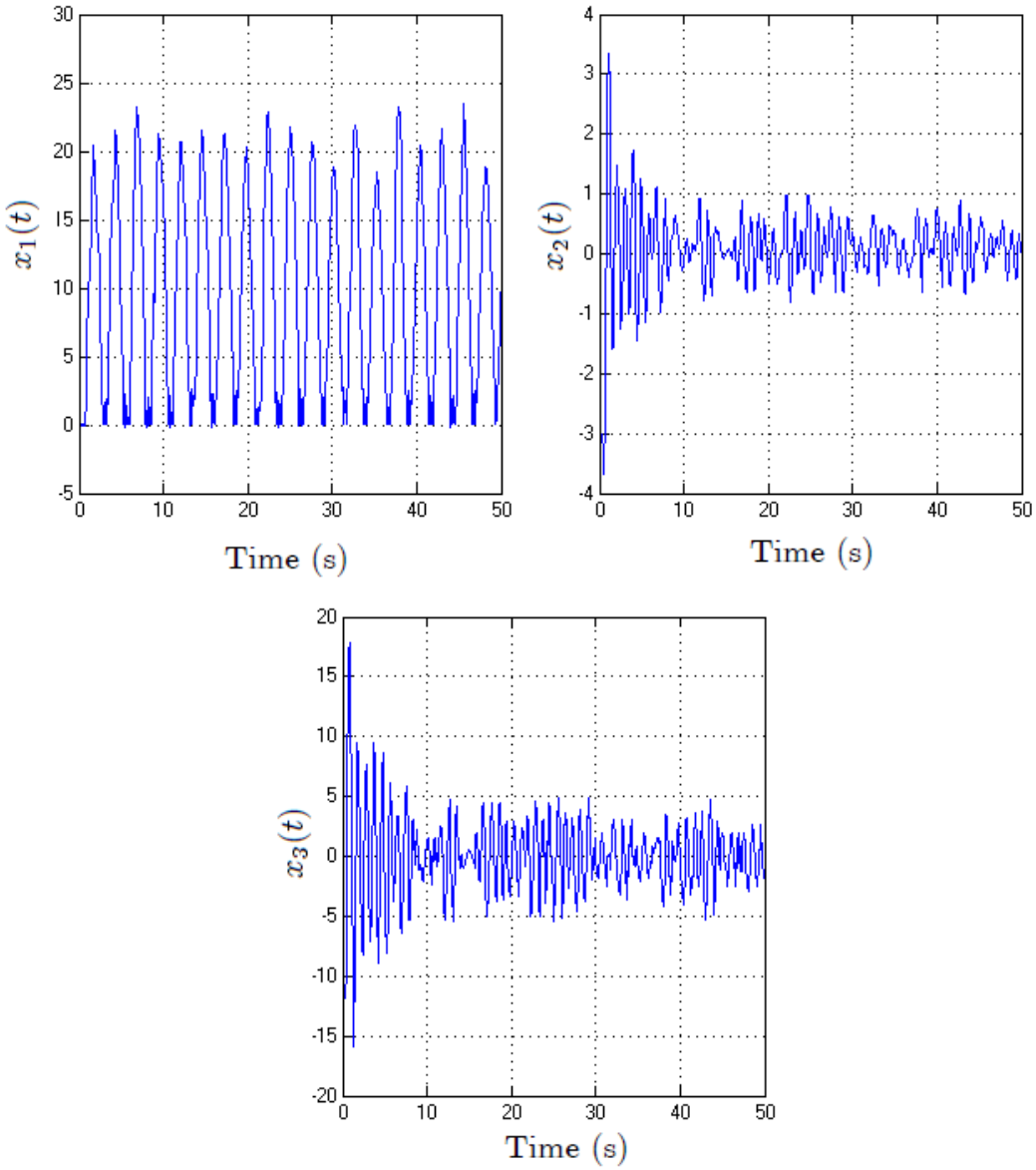


Figure 5.8: Trajectories $x_1(t)$, $x_2(t)$, $x_3(t)$ of the open loop system (5.72).

The resulting control input $u_2(t)$ is shown in Figure 5.9.

The trajectories of the drilling system (5.72) in closed loop with the controllers (5.61-5.62) with $K_0$, $K_1$, $K_2$ given in (5.73) are shown in Figure 5.10.

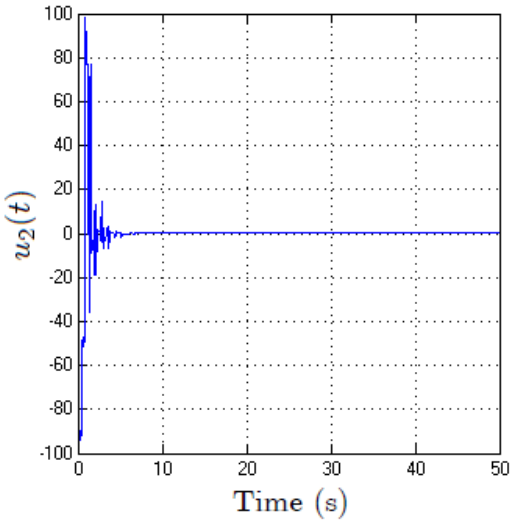


Figure 5.9: Controller $u_2$ given in (5.62).

For $\varsigma = 0.1$, the trajectories of the drilling system are retained into the ellipsoid $\mathcal{E}_{\tilde{P}} = \left\{x \in \mathcal{R}^n : x^T \tilde{P} x \leq 1\right\}$ where

$$\tilde{P} = \begin{bmatrix} 7.3906 & 3.1130 & 0.3259 \\ 3.1130 & 15.7357 & 4.1883 \\ 0.3259 & 4.1883 & 1.7062 \end{bmatrix},$$

for $t \geq T_a(\phi, \varsigma) = 0.6667 \ln\left(2541.9 \|\phi\|_h^2 - 9.0800\right) = 6.1510$s. The minimum attractive ellipsoid obtained for the drilling system (5.72) is shown in Figure 5.11.

The following table shows a comparative analysis of the obtained results for the drilling example for the case in which the control input is subject to the restriction $|u_2(t)| \leq 100$ and when there are no constraints on the controllers. Clearly, the absence of restrictions on $u_2$ gives a better performance.

| control input | $u_{2_{\max}}(t)$ | $\sigma$ | $\alpha$ | $\beta$ | $T_a(\phi, \varsigma)$ |
|---|---|---|---|---|---|
| restriction on $u_2(t)$ | 100 | 1.5 | 254.1923 | 1.3620 | 6.1510s |
| no restriction on $u_2(t)$ | 159 | 1.6 | 123.4176 | 1.6227 | 5.3140s |

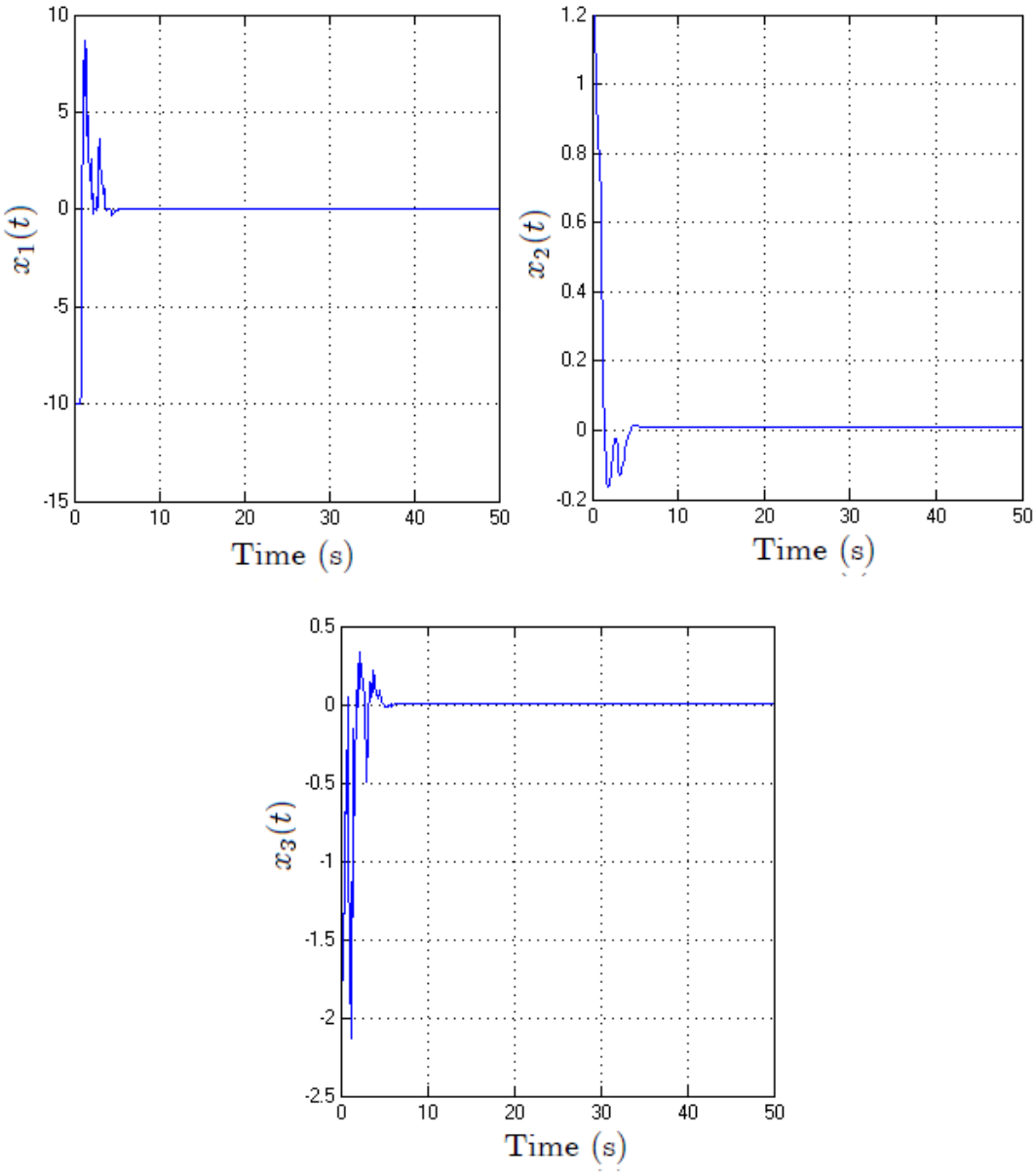


Figure 5.10: Trajectories $x_1(t)$, $x_2(t)$, $x_3(t)$ of the system (5.72) in closed loop with the controllers (5.61-5.62).

**Remark 3** *Nowadays there are diverse tools allowing the drilling downhole measurements in real time like the Drill String Acceleration Tool (DSA) developed by the Borehole Research Group - Lamont-Doherty Earth Observatory (BRG-LDEO) or the Measurement While Drilling (MWD) tool developed by the Esso Research Company which allows to measure axial, torsional and bending forces and moments; axial, lateral and angular accelerations; internal and*

*external pressure etc. Therefore the proposed controllers given in (5.61-5.62) are suitable to be applied regardless of the use of a state observer or estimator.*

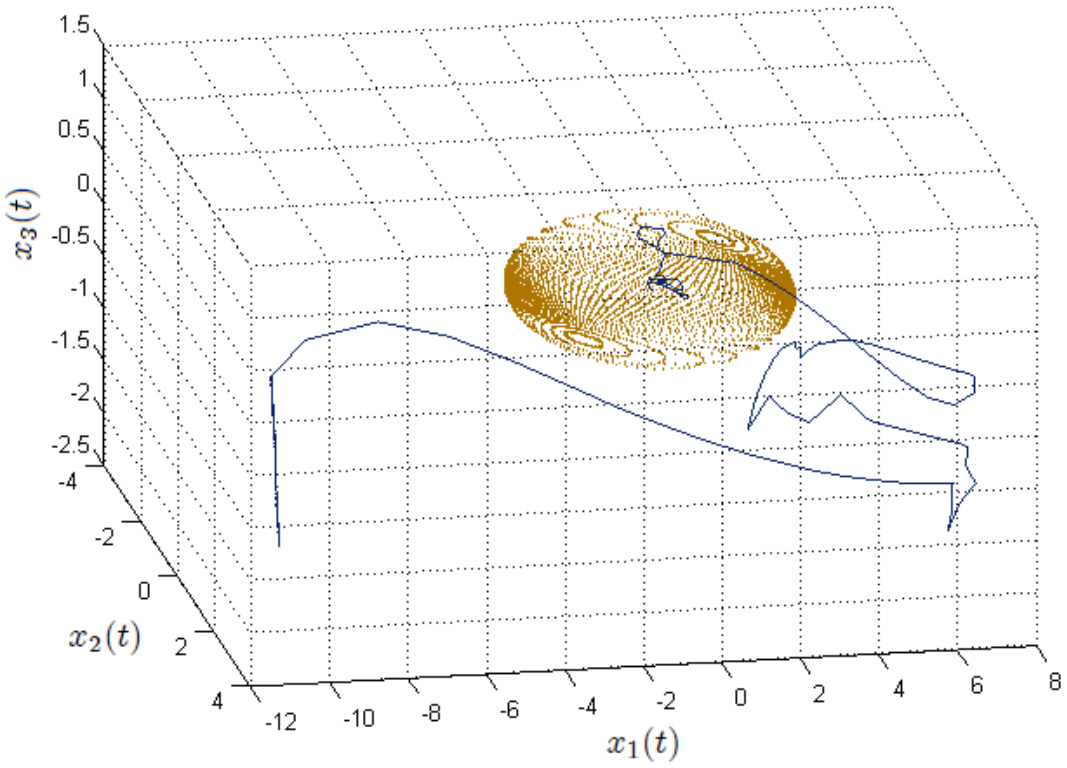


Figure 5.11: $x_1(t)$ vs. $x_2(t)$ vs. $x_3(t)$ converging to the ellipsoid $\mathcal{E}(0, \tilde{P})$.

## 5.6. Conclusion

Stability analysis and control of drilling vibrations were addressed within the framework of time-delay systems. Based on diverse analysis approaches, feedback control solutions have been proposed. The presented control strategies are derived through Lyapunov theory yielding stability and stabilization conditions in terms of matrix inequalities.

The analyses outlined in this chapter arise from three Lyapunov functionals suitable for each approach. Exponential stability of the drilling system, represented as an autonomous switching system, is investigated through

the functional given in (5.5), LMI-type conditions have been derived. The Lyapunov-Krasovskii functional stated in (5.25) is appropriate to deal with the descriptor form of the considered neutral-type system, stabilization conditions in terms of BMIs have been obtained. It was shown that under adequate manipulations, the bilinearity can be overcome to get linear constraints. For the practical stability analysis developed in Sections 5.4 and 5.5, the proposed functional (5.50) involves exponential terms allowing the achievement of the condition (5.39) stated in Lemma 5. In addition, the strategy of adding null terms derived from the system dynamics and controllers structure leads BMI type stability conditions that can be handled using an appropriate computational tool such as the package "PENBMI" of MATLAB.

The control strategies presented in the first three sections of this chapter are aimed at the suppressing torsional drilling behavior. To this end, diverse control structures have been proposed; the control law given in (5.19), chosen for the stability analysis in the framework of switched systems, and the controller stated in (5.56), arising from the practical stabilization approach, are state-feedback controllers involving the angular velocity and acceleration measured at the bit level. Nowadays, in practice, these variables are available in real time due to the acquired advanced technology. In Section 5.3 the nonlinear feedback controller (5.35), proposed to tackle the problem of stick-slip suppression, involves only the rotary speed at the bottom of the string.

In Section 5.4 we have analyzed the effect of applying the controller (5.56) on the bit-bounce. It was shown that the suppression of the stick-slip give rise to the reduction of axial oscillations. In Section 5.5 a comprehensive analysis of coupled vibrations has been carried out, the linear feedback controllers (5.61-5.62), involving the measurement of axial and torsional variables, have been proposed to simultaneously suppress the stick-slip and the bit bounce.

Simulation results show a satisfactory performance of all the proposed controllers, however, regarding the oscillating response of the closed loop trajectories, the time taken to suppress the stick-slip and the complexity involved in the solution of matrix inequalities, we can conclude that the nonlinear controller (5.35) which is derived from the multimodel approximation approach is the best solution to suppress torsional drilling oscillations. Nevertheless, the attractive ellipsoid method, albeit involving conservatism and complexity derived from the introduction of free weighting variables of the descriptor approach, provides an integral solution to the problem of coupled drilling oscillations. This strategy allows the synthesis of stabilizing feedback controllers guaranteeing the elimination of axial and torsional vibrations, even in pres-

ence of saturation restrictions on the control input. The arising optimization problem leads to find a minimal attractive set for the system trajectories.

# Chapter 6

# General conclusions and future work

This thesis summarizes the main contributions derived from an exhaustive research on modeling, analysis and control of vibrations occurring during the drilling process.

Stick-slip phenomenon consisting in torsional vibration of the drillstring has been the focal point of this research project since it constitutes the major source of failures in drilling operations. The occurrence of torsional vibrations contributes to the excitation of axial oscillations which greatly affect the drilling structure components; special attention has been paid to the vibrations coupling.

Torsional dynamics of the drilling system are modeled by the unidimensional wave equation subject to mixed boundary conditions. The sick-slip behavior is approximated by a nonlinear friction model reproducing the bit-rock interaction. By means of a direct transformation, a time-delay equation, representing a simplified input-output model of the system, was derived. In order to validate the proposed modeling strategy, system simulations in close agreement with field observations with regards to the stick-slip and bit-bounce, were developed. The main empirical practices to tackle the problem were investigated and tested. Increasing the angular velocity at the top extremity and reducing the WOB are the most common strategies used in practice to avoid torsional vibrations; however raising the angular speed provided by the rotary table may lead to lateral vibrations and lowering the weight on the cutting device may preclude an adequate penetration rate or even stop the drilling operation, these shortcomings requires us to develop effective control solutions.

On the basis of the different modeling strategies proposed to describe drill-string torsional dynamics, stability and stabilization analyses were carried out. Certainly, the wave equation model constitute the closest description to reality since it reproduces the distributed behavior of the system. However, the complexity involved in simulations make us prefer the simplified model constituting a reliable representation of the system and allowing to exploit techniques of the broad control theory for time-delay systems.

Just a few works of the available literature have provided a stability analysis of their proposed methods to treat the drilling vibration problem. Our control solution proposals are based on Lyapunov techniques and they guarantee the closed loop system stability.

Matrix-inequality approach derived from Lyapunov theory is shown to be a powerful and efficient tool to stability and control of dynamic systems. In this framework, the oilwell drilling system under consideration was studied highlighting that this approach is valid in both partial differential and time delay models. LMI approach for the analysis of distributed parameter models is an interesting area just opening up for research. Through this methodology, we have presented a comprehensive analysis of torsional drilling vibrations described by the wave equation. Ultimate bounds on the system response were found and a controller derived from the energy dissipation of the system was designed. In addition, a novel strategy to tackle the problem of boundary control of coupled wave-ODE systems, was introduced.

Based on the neutral-type time-delay model, we have proposed both linear and nonlinear controllers to overcome the drilling vibration problem involving the measurement of variables at the bit level which are readily accessible by the implementation of real time devices currently available. A significant advantage was proved for the nonlinear controller whose implementation entails a successful attenuation of torsional oscillations within a few seconds. We have also introduced an integral solution to the coupled vibration problem. This particular topic has been poorly studied, in fact, authors generally study the vibration modes individually. We have designed here, control laws to simultaneously suppress stick-slip and bit-bounce.

An important tool we have used, combined to the matrix inequality methodology, is the descriptor approach which albeit involving the introduction of free weighting variables, leading to an increase of the matrix inequalities size, significantly reduces the overdesign and conservatism entailed in the existing methods.

The obtained LMI-type conditions can be handled by using diverse computational tools such as the LMI toolbox of Matlab or the Sedumi and Yalmip packages. To solve problems stated in terms of BMIs, specific numerical solvers such as TOMLAB/PENBMI are required.

This research project has addressed several important topics of the control theory: robustness against perturbations, practical stability and stabilization of the drilling system subject to additive disturbances was proved; optimization problem, a set of conditions ensuring the minimization of the attractive set retaining the system trajectories were given; control input saturation, additional stability conditions to address the presence of physical constraints on the control inputs arising from limits in force, torque, current, flow rate, etc. were provided.

We can conclude that the proposed time-delay model constitutes a simple and reliable representation of the drilling dynamics. Furthermore, the suggested control techniques to suppress oilwell drilling oscillations are novel, simple and efficient compared to the existing ones. They lead to drill at lower speeds, which is, impossible without control. The presented strategies have a wide domain of application since they can be easily generalized to treat a broad range of other engineering, physical and biological problems.

## 6.1. Perspectives

The wave equation model accurately reproduce the propagation of coupled axial and torsional waves in the rod. Further analyses will be based on this modeling strategy; the boundary control of coupled PDE-PDE systems is an interesting and poorly explored topic to be addressed.

To fully describe the rod behavior during the drilling process, the future work must include a proper model for the lateral dynamics; Euler-Bernoulli and Timoshenko beam theory could lead to the development of the mathematical description of transversal drillstring motion. The inclusion of models for the diverse actuators involved in the system (rotary table motor, mud pump motor and winch motor for pulling/dragging drill pipes and drill collars) would be convenient. In addition, one should take into consideration the many unknown and varying parameters arising from the fact that drillstring characteristics change as the drilling operation makes progress such as the length of the rod and the weight supported by the cutting device.

Further research on control design to avoid drilling vibrations will be conducted through trajectory tracking control techniques. The controllers structure should be determined in agreement with the existing saturation levels of the control inputs, unlike the control laws proposed in this work whose structure is fixed a priori. Supplementary control inputs (WOB, motor power supply) and input saturations (constraints in motor torque and power, speed, acceleration and jerk) should be contemplated. A comparison study on effectiveness and robustness of the control strategies is another particular objective to be pursued.

On the other hand, the analysis of the drilling process considering different operating conditions is a particularly important research subject. For instance, we can refer the drilling operation conducted through the seabed (offshore drilling), in which additional characteristics must be considered: the depth of water, climatic conditions, the remoteness from the logistical base, etc.

A wide range of research lines may emerge of this thesis project. It is well known that vibrations are normally unwanted phenomenal behavior frequently occurring in structures and machines leading fatigue, failure, unreliability and noise pollution. Although they may cause safety problems in engineered systems. The modeling, analysis and control methodologies introduced here, could be useful to treat the vibration problem in many others mechanisms. There exist a wide variety of examples in which the oscillation problem may cause catastrophic failures, one of them is the aircraft wing oscillation. When an aircraft wing vibrates excessively, passengers in the aircraft become uncomfortable especially when the frequencies of vibration correspond to natural frequencies of the human body and organs, in fact, the resonant frequency of the human intestinal tract should be avoided at all costs when designing high performance aircraft and reusable launch vehicles because sustained exposure can cause serious internal trauma. Furthermore, if an aircraft wing vibrates at large amplitudes for an extended period of time, the wing will eventually experience a fatigue failure of some kind, which would potentially cause the aircraft to crash resulting in injuries and/or fatalities. The vibration treatments found in the specialized literature can be separated into two categories, passive and active, passive treatments include resilient materials and Tuned Vibration Absorbers (TVA), active solutions require controllers implementation, three main types can be distinguished: Active Isolation Control (AIC), Active Noise Control (ANC), Active Structural Control (ASC) [82]. Vibrational problems require continuous research in accordance with the growing technology.

# Bibliography


[1] Aarrestad, T.V., Kyllingstad, A. (1988). An experimental and theoretical study of a coupling mechanism between longitudinal and torsional drillstring vibrations at the bit. *SPE Drilling Engineering*, 3(1), 12–18. (Cited on page 68.)

[2] Abdulgalil, F., Siguerdidjane, H. (2004). Nonlinear control design for suppressing stick-slip in oil well drillstrings. *Proceedings of the 5th Asian Control Conference*, 1276–1281. (Cited on page 71.)

[3] Abolinia, V.E., Myshkis, A.D. (1960) A mixed problem for an almost linear hyperbolic system in the plane. *Matematicheskii Sbornik*, 50(92), 423–442. (Cited on pages 7, 39 and 78.)

[4] Anabtawi, M. (2011) Practical stability of nonlinear stochastic hybrid parabolic systems of ito-type: vector Lyapunov functions approach. *Nonlinear Analysis: Real World Applications*, 12(1), 1386–1400. (Cited on page 153.)

[5] Balanov, A.G., Janson, N.B., McClintock, P.V.E., Wang, C.H.T. (2002). Bifurcation analysis of a neutral delay differential equation modelling the torsional motion of a driven drill-string. *Chaos, Solitons and Fractals*, 15(2), 381–394. (Cited on pages 7, 39 and 78.)

[6] Bailey, J.J., Finnie, I. (1960). An analytical study of drillstring vibration. *Journal of Engineering for Industry, Transactions of the ASME*, 82(2), 122–128. (Cited on pages 7, 39, 67 and 78.)

[7] Barbashin E.A., Krasovsky, N.N. (1952). On the stability of motion in the large. *Doklady Akademii Nauk, USSR*, 86(3), 453–456. (Russian) (Cited on page 154.)

[8] Billotti, J.E., Lasalle J.P. (1971). Dissipative periodic processesstring vibration. *Bulletin of the American Mathematical Society*, 77(6), 1082–1088. (Cited on page 153.)

[9] Barreto-Jijón, R., Canudas-de-Wit, C., Niculescu, S.I., Dumon, J. (2010). Adaptive observer design under low data rate transmission with applications to oil well drill-string. American Control Conference (ACC), 1973–1978 (Cited on page 71.)

[10] Barton, D.A.W., Krauskopf, B., Wilson, R.E. (2007). Homoclinic bifurcations in a neutral delay model of a transmission line oscillator. *Nonlinearity,* 20(4), 809–829. (Cited on pages 7, 39 and 78.)

[11] Bauer, A. (1996). Utilisation of chaotic signals for radar and sonar purposes. *Norwegian Signal Processing Society NORSIG*, 96, 33–6. (Cited on page 82.)

[12] Belokobyl'skii, S.V., Prokopov, V.K. (1982). Friction-induced self-exited vibrations of drill rig with exponential drag law. Soviet Applied Mechanics, 18(12), 1134–1138. (Cited on page 67.)

[13] Bertsekas, D.P., Rhodes, I.B. (1971). On the minmax reachability of target set and target tubes. *Automatica*, 7(2), 233–247. (Cited on page 163.)

[14] Bertsekas, D.P. (1972). Infinite-time reachability of state-space regions by using feedback control. *IEEE Transactions on Automatic Control*, 17(5), 604–613. (Cited on page 163.)

[15] Besaisow, A.A., Jan, Y.M., Schuh, F.J. (1985). Detection of various drilling phenomena utilizing high frequency surface measurements. Drilling Conference, Rogaland Research Institute, SPE 14327; SPE/IADC. (Cited on page 67.)

[16] Besaisow, A.A., Payne, M.L. (1988). A study of excitation mechanisms and resonance inducing bottomhole-assembly vibrations. SPEDE 93–110; SPE 15560. (Cited on page 67.)

[17] Besaisow, A.A., Ng, F.W., Close, D.A. (1990). Application of ADAMS (Advanced Drillstring Analysis and Measurement System) and Improved Drilling Performance. SPE 19998; SPE/IADC Drilling Conference. (Cited on page 67.)

[18] Bi, X.L., Wang, J., Wang, Z.L., Sun, S.H. (2011). Finite element analysis on axial-torsional coupled vibration of drill string. Advanced Materials Research, 291, 1952–1956. (Cited on page 71.)

[19] Blakely, J.N., Corron, N.J. (2004). Experimental observation of delay-induced radio frequency chaos in a transmission line oscillator. *Chaos*, 14(4), 1035–1041. (Cited on pages 7, 39 and 78.)

[20] Blanchini, F. (1999). Set invariance in control - a survey. *Automatica*, 35(11), 1747–1768. (Cited on page 163.)

[21] Boussaada, I., Mounier, H., Niculescu, S.I., Cela, A. (2012). Analysis of drilling vibrations: a time delay system approach. *20th Mediterranean Conference on Control and Automation MED*, Barcelona, Spain. (Cited on pages 7, 39, 71, 78, 79 and 98.)

[22] Boussaada, I., Cela, A., Mounier, H., Niculescu, S.I. (2013). Control of drilling vibrations: a time-delay system-based approach *11th Workshop on Time-Delay Systems Part of 2013 IFAC Joint Conference SSSC*, Grenoble, France. (Cited on pages 7, 39, 71, 78, 79 and 98.)

[23] Brayton R.K. (1966). Bifurcation of periodic solutions in a non-linear difference-differential equation of neutral type. *Quarterly of Applied Mathematics*, 24, 215–224. (Cited on page 82.)

[24] Brett, J.F. (1992). The genesis of torsional drillstring vibrations. SPE Drilling Engineering, 7(3), 168–174. (Cited on pages 69 and 78.)

[25] Byrnes, C.I., Spong, M.W., Tarn, T.J. (1984). A several complex variables approach to feedback stabilization of neutral delay-differential systems. *Mathematical Systems Theory*, 17(1), 97–133. (Cited on page 91.)

[26] Canudas-de-Wit, C., Aracil, J., Gordillo, F., Salas, F. (2005). The oscillations killer: a mechanism to eliminate undesired limit cycles in nonlinear systems. *44th IEEE Conference on Decision and Control, European Control Conference (CDC-ECC)*, Seville, Spain. (Cited on pages 4, 36 and 71.)

[27] Canudas-de-Wit, C., Rubio, F.R., Corchero, M.A. (2008). D-OSKIL: a new mechanism for controlling stick-slip oscillations in oil well drillstrings. IEEE Transactions on Control Systems Technology, 16(6), 1177–1191. (Cited on pages 4, 36, 71 and 78.)

[28] Challamel, N. (2000). Rock destruction effect on the stability of a drilling structure. *Journal of Sound and Vibration,* 233(2), 235–254. (Cited on pages 7, 10, 11, 39, 42, 43, 78, 79, 82, 97 and 99.)

[29] Christoforou, A.P., Yigit, A.S. (2003). Fully coupled vibrations of actively controlled drillstrings. *Journal of Sound and Vibration,* 267(5), 1029–1045. (Cited on pages 70, 102 and 154.)

[30] Cooke, K., Krumme, D. (1968). Differential-difference equations and nonlinear initial boundary value problems for linear hyperbolic partial differential equations. *Journal of Mathematical Analysis and Applications*, 24(2), 372–387. (Cited on pages 7, 39 and 78.)

[31] Cooke, R.L., Nicholson, J.W., Sheppard, M.C., Westlake, W. (1989). First real time measurements of downhole vibrations, forces, and pressures used to monitor directional drilling operations. SPE/IADC 18651 Drilling Conference. (Cited on page 68.)

[32] Cull, S.J., Tucker, R.W. (1999). On the modelling of Coulomb friction. *Journal of Physics A: Mathematical and General*, 32(11), 2103–2113. (Cited on page 80.)

[33] Dawson, R., Lyn, Y.Q., Spanos, P.D. (1987). Drill string stick slip oscllations. Spring Conference of the Society for Experimental Mechanics, 14–19. (Cited on page 68.)

[34] Deily, F.H., Dareing, D.W., Paff, G.H., Ortloff, J.E., Lynn, R.D. (1968). Downhole measurements of drillstring forces and motions. Journal of Engineering for Industry, Transactions of the ASME, series B 90(2), 217–225. (Cited on page 67.)

[35] Dubinsky, V.S.H., Henneuse, H.P., Kirkman, M.A. (1992). Surface monitoring of downhole vibrations: russian, european, and american approaches European Petroleum Conference, 16–18, Cannes, France. (Cited on page 69.)

[36] Dufeyte, M.P., Henneuse, H. (1991). Detection and monitoring of the slip-stick motion: field experiments. SPE/IADC Drilling Conference, 11–14. (Cited on page 69.)

[37] Dunayevsky, V., Abbassian, F., Judzis, A. (1993). Dynamic stability of drillstrings under fluctuating weight on bit. SPE Drilling and Completion, 8(2), 84–92. (Cited on pages 1, 33 and 65.)

[38] Fang, H., Lin, Z., Hu, T. (2004). Analysis of linear systems in the presence of actuator saturation and $\mathcal{L}_2$-disturbances. *Automatica*, 40, 1229–1238. (Cited on page 169.)

[39] Finnie, I., Bailey, J.J. (1960). An experimental study of drill-string vibration. Journal of Engineering for Industry, Transactions of the ASME, 82(2), 129–135. (Cited on pages 7, 39, 67 and 78.)

[40] Fliess, M., Mounier, H., Rouchon, P., Rudolph, J. (1995). Controllability and motion planning for linear delay systems with an application to a flexible rod, *Proceedings of the 34th Conference on Decision & Control*, TA16 10:40 New Orleans, LA. (Cited on pages 7, 39 and 78.)

[41] Fridman, E. (2001). New Lyapunov–Krasovskii functionals for stability of linear retarded and neutral type systems. *Systems & Control Letters,* 43(4), 309–319. (Cited on pages 135, 146, 147, 154, 159 and 167.)

[42] Fridman, E., Pila, A., Shaked, U. (2003). Regional stabilization and $\mathcal{H}_\infty$ control of time-delay systems with saturating actuators. *International Journal of Robust and Nonlinear Control*, 13(9), 885–907. (Cited on page 169.)

[43] Fridman, E. (2005). A new Lyapunov technique for robust control of systems with uncertain non-small delays. *IMA Journal of Mathematical Control and Information*, 23(2), 165–179. (Cited on page 170.)

[44] Fridman E., Orlov, Y. (2009). An LMI approach to $\mathcal{H}_\infty$ boundary control of semilinear parabolic and hyperbolic systems. *Automatica*, 45(9), 2060–2066. (Cited on pages 110, 113, 114 and 116.)

[45] Fridman, E., Dambrine, M. (2009). Control under quantization, saturation and delay: a LMI approach. *Automatica*, 45(10), 2258–2264. (Cited on page 112.)

[46] Fridman, E., Mondié, S. Saldivar, M.B. (2010). Bounds on the response of a drilling pipe model. *Special issue on Time-Delay Systems in IMA Journal of Mathematical Control. & Information*, 27(4), 513–526. (Cited on pages 5, 7, 37, 39, 72 and 79.)

[47] Glover, D., Schweppe, F. (1971). Control of linear dynamic systems with set constrained disturbances. *IEEE Transactions on Automatic Control*, 16(5), 411–423. (Cited on page 163.)

[48] Gonzalez-Garcia, S., Polyakov, A.E., Poznyak, A.S. (2011). Using the method of invariant ellipsoids for linear robust output stabilization of spacecraft. *Automation and Remote Control*, 72(3), 540–555. (Cited on pages 27, 60 and 169.)

[49] Gulyaev, V.I., Glushakova, O.V., Khudolii, S.N. (2010). Quantized attractors in wave models of torsion vibrations of deep-hole drill strings. *Mechanics of Solids*, 45(2), 264–274. (Cited on pages 7, 39 and 78.)

[50] Hale, J.K., Verduyn-Lunel, S.M. (1993). Introduction to functional differential equations. Applied Mathematical Sciences, Vol. 99. New York: Springer. (Cited on pages 134 and 153.)

[51] Halsey, G.W., Kyllingstad, A., Kylling, A. (1988). Torque feedback used to cure slip-stick motion. *Proceedings of the 63rd Society of Petroleum Engineers Drilling Engineering*, Annual Technical Conference and Exhibition, Houston, TX, 277–282. (Cited on pages 3, 35, 68, 78 and 101.)

[52] Iserles, A. (1993). On the generalised pantograph functional–differential-equation. *European Journal of Applied Mathematics*, 4(1), 1–38. (Cited on page 82.)

[53] Jamaleddine, R., Vinet, A. (1999). Role of gap junction resistance in rate-induced delay in conduction in a cable model of the atrioventricular node. *Journal of Biological Systems*, 7(4), 475–490. (Cited on page 82.)

[54] Jansen, J.D. (1993). Nonlinear Dynamics of Oilwell Drillstrings. PhD dissertation Delft University of Technology, Delft University Press. (Cited on pages 1, 2, 3, 33, 34, 35, 66 and 70.)

[55] Jansen, J.D., van den Steen L. (1995). Active damping of self-excited torsional vibrations in oil well drillstrings. *Journal of Sound and Vibration,* 179(4), 647–668. (Cited on pages 3, 35, 65, 70, 78 and 97.)

[56] Khalil, H. (1992). Nonlinear Systems. New York: Macmillan Publishing Company. (Cited on page 110.)

[57] Kharitonov, V. (1998). Robust stability analysis of time delay systems: a survey. *Fourth IFAC Conference on System Structure and Control*, Nantes, France, plenary lecture, 1–12. (Cited on page 133.)

[58] Kharitonov, V.L., Niculescu, S.I. (2003). On the stability of linear systems with uncertain delay. *IEEE Transactions on Automatic Control*, 48(1), 127–132. (Cited on page 170.)

[59] Kim, S., Campbell, S.A., Liu, X. (2006). Stability of a class of linear switching systems with time delay. *IEEE Transactions on Circuits and Systems,* 53(2), 384–393. (Cited on page 135.)

[60] Kolmanovskii, V.B., Nosov, V.R. (1986). Stability of functional differential equations. London: Academic Press. (Cited on page 134.)

[61] Kolmanovskii, V. B., & Myshkis, A. (1992). Applied theory of functional differential equations. In Mathematics and Applications, Vol. 85. Dordrecht: Kluwer Academy. (Cited on page 134.)

[62] Kolmanovskii, V.B., Niculescu, S.I., Gu, K. (1999). Delay effects on stability: a survey. *38th IEEE Conference on Decision and Control (CDC)*, Phoenix, AZ, 1993–1998. (Cited on page 133.)

[63] Kreuzer, E., Steidl, M. (2012). Controlling torsional vibrations of drill strings via decomposition of traveling waves. Archive of Applied Mechanics, 82(4), 515–531. (Cited on page 71.)

[64] Kriesels, P.C., Keultjes, W.J.G., Dumont, P., Huneidi, I., Furat, A., Owoeye, O.O., Hartmann, R.A. (1999). Cost savings through an integrated approach to drillstring vibration control. SPE/IADC Middle East Driling Technology Conference, SPE/IADC 57555, Abu Dhabi. (Cited on pages 96 and 100.)

[65] Krstic, M. (2009). Delay compensation for nonlinear, adaptive, and PDE systems. Systems & Control: Foundations & Applications, Birkhäuser Boston, a part of Springer Science+Business Media, LLC. (Cited on page 134.)

[66] Kurzhanski, A.B., Veliov, V.M. (1994). Modeling techniques for uncertain systems. Progress in Systems and Control Theory, 18, BirghÄauser, Boston. (Cited on pages 25, 57 and 164.)

[67] Kyllingstad, A., Haisey, G.W. (1988). A study of slip/stick motion of the bit. SPE Drilling Engineering, 369–373. (Cited on pages 3, 35 and 68.)

[68] Leine, R.I. (1997). Literature survey on torsional drillstring vibrations. Report number: WFW 97.069, Division of Computational and Experimental Mechanics, Department of Mechanical Engineering Eindhoven University of Technology, The Netherlands. (Cited on page 67.)

[69] Leine, R.I. (1996). Nonlinear drillstring and thrasher dynamics. M. Sc. Thesis, Delft University of Technology, Faculty of Mechanical Engineering, The Netherlands. (Cited on page 69.)

[70] Leine, R.I., van Campen, D.H., Keultjes, W.J.G. (2002). Stick-slip whirl interaction in drillstring dynamics. *Journal of Vibration and Acoustics*, 124(2), 209–220. (Cited on page 97.)

[71] Levinson, N. (1944). Transformation theory of non-linear differential equations of the second order. *Annals of Mathematics*, 45(4), 723–737. (Cited on page 153.)

[72] Lin, Y., Wang, Y. (1990). New mechanism in drillstring vibration. 22nd Annual Offshore Technology Conference. (Cited on page 69.)

[73] Lin, Y., Wang, Y. (1991). Stick-slip vibration of drill strings. Transactions of ASME, 113, 38–43. (Cited on pages 69 and 78.)

[74] Liu, D.Y., Liu, X.Z., Zhong, S.M. (2008). Delay-dependent robust stability and control synthesis for uncertain switched neutral systems with mixed delays. *Applied Mathematics and Computation*, 202(2), 828–839. (Cited on page 135.)

[75] Loiseau, J.J. (1998). Algebraic tools for the control and stabilization of time-delay systems. *First IFAC Workshop on Linear Time Delay Systems*, Grenoble, France, plenary lecture, 234–249. (Cited on page 133.)

[76] Loiseau, J.J., Cardelli, M., Dusser, X. (2001). Neutral type time-delay systems that are not formally stable are not BIBO stabilizable. *IMA Journal of Mathematical Control and Information*, 19, 217–227. (Cited on page 91.)

[77] Lu, H., Dumon, J., Canudas-de-Wit, C. (2009). Experimental study of the D-OSKIL mechanism for controlling the stick-slip oscillations in a drilling laboratory testbed. IEEE Multi-conference on Systems and Control, Saint Petersburg: Russian Federation. (Cited on page 71.)

[78] Macpherson, J.D., Mason, J.S., Kingman, J.E.E. (1993). Surface measurement and analysis of drillstring vibrations while drilling. SPE/IADC 25777, Society of Petroleum Engineers. (Cited on pages 1, 33 and 65.)

[79] Mason, J.S., Sprawls, B.M. (1998). Addressing BHA whirl: the culprit in mobile bay. SPE Drilling and Completion, 13(4), 231–236. (Cited on pages 1, 33 and 65.)

[80] Michiels, W., Niculescu, S.I., Moreau L. (2004). Using delays and time-varying gains to improve the output feedback stabilizability of linear systems: a comparison. *IMA Journal of Mathematical Control and Information*, 21(4), 393–418. (Cited on page 134.)

[81] Miller, C.E., Rollins, H.M. (1968). Evaluation of a vibration damping tool and drill stem torque requirements from data recorded by an instrumented drill stem member. Journal of Engineering for Industry, Transactions of ASME, 226–230. (Cited on page 67.)

[82] Miller, L.R., Rossetti, D.J., Norris M.A. (1995). Passive, active and hybrid solutions for aircraft interior noise. Problems, LL-6007, Lord Corporation, November 1995. (Cited on page 182.)

[83] Mitchell, R.F., Allen, M.B. (1987). Case studies of BHA vibration failure. SPE 16675, Society of Petroleum Engineers, 1987. (Cited on pages 2, 34 and 66.)

[84] Navarro-López, E., Suárez, R. (2004). Practical approach to modelling and controlling stick-slip oscillations in oilwell drillstrings. *Proceedings of the 2004 IEEE International Conference on Control Applications*, 1454–1460. (Cited on pages 11, 13, 43, 45, 70, 78, 96, 97, 99, 106 and 107.)

[85] Navarro-López, E., Cortés, D. (2007). Sliding-mode of a multi-DOF oilwell drillstring with stick-slip oscillations. *Proceedings of the 2007 American Control Conference*. New York City, USA, 3837–3842. (Cited on pages 10, 42, 71, 78 and 79.)

[86] Nazin, A., Polyak, B. , Topunov M. (2007). Rejection of bounded exogenous disturbances by the method of invariant ellipsoids. *Automation and Remote Control*, 68(3), 467–486. (Cited on pages 25, 57 and 164.)

[87] Nicaise, S., Pignotti, C. (2008). Stabilization of the wave equations with variable coefficients and boundary conditions of memory type. *Asymptotic Analysis*. 50(1-2), 31–67. (Cited on page 113.)

[88] Ottesen, J.T. (1997). Modelling of the baroflex-feedback mechanism with time-delay. *Journal of Mathematical Biology*, 36, 41–63. (Cited on page 82.)

[89] Pavone, D.R., Desplans, J.P. (1994). Application of high sampling rate downhole measurements for analysis and cure of stick-slip in drilling. SPE Annual Technical Conference and Exhibition, SPE 28324, New Orleans, L.A., 335–345. (Cited on pages 3, 35 and 69.)

[90] Peltier, B.P., Cooper, G.A., Curry, D.A. (1987). Use of torque analysis to determine tri-cone bit failure. SPE 16698. Paper presented at the 62nd Annual Technical Conference and Exhibition of the Society of Petroleum Engineers, 27–30. (Cited on page 68.)

[91] Pontryagin, L.S. (1955). On the zeros of some elementary trascendental functions. *Transactions of the American Mathematical Society,* 2, 95–110. (Cited on page 91.)

[92] Poznyak, A.S. (2008). Advanced mathematical tools for automatic control engineers: deterministic techniques, Vol. 2. Elsevier. (Cited on page 164.)

[93] Puebla, H. Álvarez, J. (2008). Suppression of stick -slip in drillstrings: a control approach based on modeling error compensation. *Journal of Sound and Vibration* 310(4-5), 881–901. (Cited on pages 4, 37 and 71.)

[94] Rasvan, V. (1975). A method for distributed parameter control systems and electrical networks analysis, *Rev. Roumaine Sci. Techn. Serie Electrotechn. Energ.* 20, 561–566. (Cited on page 81.)

[95] Rasvan, V., Niculescu, S.I. (2002). Oscillations in lossless propagation models: a Lyapunov-Krasovskii approach, *IMA Journal of Mathematical Control and Information*, 19(1-2), 157–172. (Cited on page 81.)

[96] Rasvan, V. (2006). Three lectures on dissipativeness,*IEEE International Conference on Automation, Quality and Testing, Robotics*, 167–177. (Cited on pages 153 and 154.)

[97] Richard, J.P. (2003). Time-delay systems: an overview of some recent advances and open problems. *Automatica,* 39(10), 1667–1694. (Cited on pages 133 and 134.)

[98] Saldivar, M.B., Mondié, S., Loiseau, J.J. (2009). Reducing stick-slip oscillations in oilwell drillstrings. *6th International Conference on Electrical Engineering, Computing Science and Automatic Control (CCE)*, Toluca, México, 1–6. (Cited on pages 82 and 83.)

[99] Saldivar, M.B., Mondié, S., Loiseau, J.J., Rasvan, V. (2011). Stick-slip oscillations in oillwell drilstrings: distributed parameter and neutral type retarded model approaches. *18th IFAC World Congress* Milano, Italy, 284–289. (Cited on pages 5, 7, 8, 37, 39, 40, 72, 78, 80, 81 and 83.)

[100] Saldivar, M.B., Mondie, S., Loiseau, J.J., Rasvan, V. (2011). Exponential stability analysis of the drilling system described by a switched neutral type delay equation with nonlinear perturbations. *50th IEEE Conference on Decision and Control and European Control Conference (CDC-ECC)*, Orlando, FL, USA. (Cited on pages 5, 37 and 72.)

[101] Saldivar, M.B., Seuret A., Mondié, S. (2011). Exponential stabilization of a class of nonlinear neutral type time-delay systems, an oilwell drilling model example. *8th International Conference on Electrical Engineering, Computer Science and Automatic Control,* Mérida, Yucatan. (Cited on pages 5, 37, 72 and 144.)

[102] Saldivar, M.B., Mondié S., Drilling vibration reduction via attractive ellipsoid method.Accepted in *Journal of the Franklin Institute - Elsevier*, December 2012. (Cited on pages 5, 37 and 72.)

[103] Sananikone, P. (1993). Method and apparatus for determining the torque applied to a drillstring at the surface. U.S. Patent No. 5,205,163, Schlumberger Technology Co., Houston, Texas. (Cited on page 104.)

[104] Shyu, R.J. (1989). Bending vibration of rotating drill strings, Ph.D Thesis, Massachusetts Institute of Technology. (Cited on pages 2, 34 and 66.)

[105] Skaugen, E. (1987). The effects of quasi-random drill bit vibrations upon drillstring dynamic behavior. SPE 16660, Society of Petroleum Engineers. (Cited on pages 2, 34 and 65.)

[106] Seidel, H., Herzel, H. (1998). Bifurcations in a non-linear model of the baroreceptor-cardiac reflex. *Physica D: Nonlinear Phenomena*, 115, 145–160. (Cited on page 82.)

[107] Serrarens, A.F.A., van de Molengraft, M.J.G., Kok, J.J., van den Steeen, L. (1998). $\mathcal{H}_\infty$ control for suppressing stick-slip in oil well drillstrings. *IEEE Control Systems*, 18(2), 19–30. (Cited on pages 3, 36, 70, 78 and 97.)

[108] Seuret, A. (2006). Commande et observation des systèmes à retard variables, théorie et applications. Thesis PhD, Ecole Centrale de Lille, Univiersité des Sciences et Technologies de Lille, 57–94. (Cited on pages 23, 55, 145 and 151.)

[109] Sun, X.M., Fu, J., Sun, H.F., Zhao, J. (2005). Stability of linear switched neutral delay systems, *Proceedings of The Chinese Society for Electrical Engineering*, 25, 42–46. (Cited on page 135.)

[110] Suplin, V., Fridman, E., Shaked, U. (2006). $\mathcal{H}^\infty$ control of linear uncertain time-delay systems - a projection approach. *IEEE Transactions on Automatic Control*, 51(4), 680–685. (Cited on page 149.)

[111] Tucker, R.W., Wang, C. (1999a). On the effective control of torsional vibrations in drilling systems. *Journal of Sound and Vibration*, 224(1), 101–122. (Cited on pages 7, 39, 70, 78 and 79.)

[112] Tucker, R.W., Wang, C. (1999b). An integrated model for drill-string dynamics. *Journal of Sound and Vibration*, 224(1), 123–165. (Cited on pages 7, 39, 78 and 79.)

[113] Tucker, R.W., Wang, C. (2003). Torsional vibration control and Cosserat dynamics of a drill-rig assembly. *Mecanica*, 38(1), 145–161. (Cited on pages 7, 39, 78 and 79.)

[114] Van den Steen, L. (1997). Suppressing stick-slip-induced drillstring oscillations: a hyperstability approach. PhD Thesis, University of Twente, The Netherlands. (Cited on page 70.)

[115] Van der Heijden, G.H.M. (1994). Nonlinear drillstring dynamics. Ph.D Thesis, University of Utrecht. (Cited on pages 2, 34 and 66.)

[116] Vandiver, J.K., Nicholson, J.W., Shyu, R.J. (1990) Case studies of the bending vibration and whirling motion of drill collars. SPEDE, SPE 18652, 282–290. (Cited on pages 2, 34 and 66.)

[117] Villafuerte, R., Mondié, S., Poznyak, A. (2011). Practical stability of time delay systems: LMI´s approach. *European Journal of Control*, 17(2), 127–138. (Cited on page 155.)

[118] Wang, T. (1994). Stability in abstract functional-differential equations. II. Applications. *Journal of Mathematical Analysis and Applications*. 186, 835–861. (Cited on page 112.)

[119] Wang, C.H., Zhang, L.X., Gao, H.J., Wu, L.G. (2005). Delay-dependent stability and stabilization of a class of linear switched time-varying delay systems, *Proceeding of the Fourth ICMLC*, Guangzhou, 917–922. (Cited on page 135.)

[120] Yoshizawa T. (1966). Stability theory by Lyapunov´s second method, The Mathematical Society of Japan. (Cited on page 154.)

[121] Xiong, L., Zhong, S., Mao Ye (2009). New stability analysis for switched neutral systems, *2009 Second International Symposium on Computational Intelligence and Design*, 1, 180–183. (Cited on page 137.)

[122] Zamanian, M., Khadem, S.E., Ghazavi, M.R. (2007). Stick-slip oscillations of drag bits by considering damping of drilling mud and active damping system. Journal of Petroleum Science and Engineering, 59(3-4), 289–299. (Cited on pages 4, 36 and 71.)

[123] Zhang, Y., Liu, X., Zhu, H. (2007). Stability analysis and control synthesis for a class of switched neutral systems. *Applied Mathematics and Computation*, 190(2), 1258–1266. (Cited on page 135.)